Characterization of the Morphological and Cellular Effects of *Arabidopsis thaliana* Glutamate Receptor *AtGLR3.7* on Plant Growth and Physiology

Dissertation

zur

Erlangung des Doktorgrades (Dr. rer. nat.)

der

Mathematisch-Naturwissenschaftlichen Fakultät

der

Rheinischen Friedrich-Wilhelms-Universität Bonn

vorgelegt von

Matthias Weiland

aus

Pößneck

Bonn, August 2018

Angefertigt mit Genehmigung der Mathematisch-Naturwissenschaftlichen Fakultät der Rheinischen Friedrich-Wilhelms-Universität Bonn.

Erstgutachter:	PD. Dr. František Baluška
Zweitgutachter:	Prof. Dr. Lukas Schreiber
Tag der Promotion:	06. Dezember 2018
Erscheinungsjahr:	2019

Eidesstattliche Erklärung

Hiermit versichere ich, dass diese Dissertation von mir selbst und ohne unerlaubte Hilfe angefertigt wurde. Es wurden keine anderen als die angegebenen Hilfsmittel benutzt. Ferner erkläre ich, dass die vorliegende Arbeit an keiner anderen Universität als Dissertation eingereicht wurde.

Acknowledgement

I would like to express my sincere thanks to PD Dr. František Baluška at the University of Bonn and the research group of Prof. Dr. Stefano Mancuso at the University of Florence, Italy, where most of the laboratory work took place. Due to the support of both research groups, I was able to conduct all the experiments needed in order to obtain the data presented in this work.

A special thanks goes to Francesco Spinelli who is one of the best mentors I encountered. He was always willing to discuss the latest results and, thanks to his guidance, many obstacles were overcome much more easily. His critical comments helped me a lot to broaden my own perspective and to embed new data in a larger context. Together with Lucia Marti and Emily Rose Palm they formed a formidable group in which I was able to learn new techniques, expand my scientific knowledge and find innovative solutions. Our weekly journal club not only solidified and enhanced my academic skills but thanks to the freshly-provided sweets, it fuelled my cognitive processing unit again to tackle the problems at hand.

I also would like to express my very special thanks to my fiancée Lena who was supporting me during the whole duration of my PhD (as well as before and after that) in various ways. While the Journal Club Group supported me in a scientific way, she was the one who encouraged me the most on a personal level to uphold my tenacity during the more demanding periods of my PhD. My gratitude goes also to my friends and family who had to endure many complaints about the feasibility of my studies and the hardship of obtaining well-founded results.

Furthermore, I would like to thank the research group of Beáta Petrovská of the Institute of Experimental Botany in Prague, Czech Republic for their cooperation during the investigation of the endopolyploidy analyses and the Consiglio Nazionale delle Ricerche - Area di Ricerca di Firenze (CNR) for providing some of the facilities during the plant physiological experiments.

Ultimately, I would like to conclude my acknowledgements with a quote from Oscar Wilde which conveys a subtle sense of my experience during this work:

“Everything is going to be fine in the end. If it’s not fine, it’s not the end.”

Abstract

The ubiquitous involvement of glutamate receptor-like receptors (GLR) in all major physiological processes in plants as well as similar operating properties as in animal ionotropic glutamate receptors (iGluR), establish a profound basis for the investigations made on *AtGLR3.7* in *Arabidopsis thaliana* in the work presented here. This glutamate receptor shows a strong gene expression profile within the root tip and shoot apex, as well as in seeds, axillary shoots and buds. Its expression focus within the root apical meristem (RAM) makes it a reasonable candidate as an important regulator of plant growth and development in controlling DNA biosynthesis and cell proliferation. Furthermore, strong structural similarities between AtGLR3.7 and the glutamate receptor GluN1 of *Rattus norvegicus* indicate an involvement in plant calcium signalling since iGluRs as well as selected GLRs in *Arabidopsis thaliana* are known to form Ca^{2+}-permeable, amino acid-gated ion channels within cellular membranes (see Weiland *et al.*, 2015). Various involvements of GLRs in root growth have been found to affect the organization of the RAM and its meristematic activity in *Arabidopsis thaliana* as well as in *Oryza sativa* (Li *et al.*, 2006; Walch-Liu *et al.*, 2006). Knockouts and overexpressions of members of AtGLR clade III regulate cell division and expansion in primary and secondary root meristems where glutamate-induced changes in root architecture are likely transduced by mitogen-activated protein kinases (MAPK) (Forde *et al.*, 2013; Vincill *et al.*, 2013). In addition, GLRs are affecting calcium homeostasis by regulating Ca^{2+} fluxes across the plasma membrane (PM), and the plant's signal transduction capacities are at least partly dependent on GLR-mediated ion fluxes and PM depolarisations (Kim *et al.*, 2001; Mousavi *et al.*, 2013). Glutamate-induced variations in $[Ca^{2+}]_{cyt}$ and as well as GLR-induced protein and gene activations have also been found to play an important role in plant immunity and abiotic stress responses (Kwaaitaal *et al.*, 2011; Li *et al.*, 2013a; Singh *et al.*, 2014).

The aim of this work was to embed the glutamate receptor AtGLR3.7 within the plant physiology of *Arabidopsis thaliana*. To that end, *AtGLR3.7* overexpression plant lines were constructed, and their phenotypes compared to an *AtGLR3.7* knockout line and wildtype Arabidopsis plants (Col-0). Physiological studies concerning root, shoot and rosette growth as well as their modulation by the GLR agonist L-glutamate were conducted in order to assess a possible role for AtGLR3.7 as a regulator of plant growth. Morphological observations at the organ and cell level in combination with cell cycle gene expression analyses, protein quantification as well as qualification studies plus investigations of the nuclear DNA content aimed at explaining the measured deviations in plant growth and development in the transgenic

plant lines. In addition, the impact of AtGLR3.7 on plant stress tolerances were investigated by applications of abiotic (salinity) and biotic (*Pseudomonas syringae*) stresses.

Three different AtGLR3.7 overexpression lines were selected in order to create an *AtGLR3.7* gene expression gradient with increasing gene transcript levels. This gradient was reflected in the phenotypic deviations from Col-0 in most of the experiments. The knockout of *AtGLR3.7*, on the other hand, regularly displayed a phenotype contrary to those of the overexpression lines, even though this phenotype has been found to be much less pronounced in its divergence from Col-0. It was found that the seed size increased depending on the overexpression levels of *AtGLR3.7* whereas the knockout of *AtGLR3.7* led to smaller seeds. Even though the exact mechanism could not be determined, a possible explanation could potentially lie in an AtGLR3.7-mediated variation in Ca^{2+} fluxes affecting cell divisions either in the endosperm (possibly via IKU2/1 kinases) or the integument (via ARF2). Here, an involvement of an altered auxin distributions during seed development due to the misexpression of *AtGLR3.7* could be responsible for the changes in seed size.

The possibility of variations in auxin signalling and/or concentrations was also employed in other hypotheses regarding the observed deviations in plant growth. The overexpression of *AtGLR3.7* provoked a marked increase in root growth. Plants overexpressing this glutamate receptor were found to grow in general faster which was not only reflected by their accelerated development of the root architecture but also in their increased accumulation of above-ground tissue. The observed enlargement of the primary root was accompanied by a bigger rosette and enhanced inflorescence stem growth.

An explanation for the observed growth accelerations in the *AtGLR3.7* overexpression lines was found in an increased meristem size and an enhanced meristematic activity of the RAM while the knockout of *AtGLR3.7* caused a reduction in meristem activity and spatial expansion. Cell elongations have been excluded as a cause for the observed plant growth phenotype based on comparable mature cell morphologies and an equal hypocotyl elongation in darkness in all tested plant lines. AtGLR3.7 could be involved in a redistribution of the growth hormone auxin within the root tip. Here, the localization of auxin influx and efflux mediators such as PIN1 and AUX1/LAX, respectively, could have been affected potentially due to an altered Ca^{2+} signalling within the root apex in the transgenic *AtGLR3.7* plant lines. The change in auxin maxima within the root could directly affect the extension of the RAM. A similar mechanism could be active also in the above-ground tissue of the plants. Furthermore, it was found that L-glutamate, as an agonist of GLRs, strongly reduced root growth in the *AtGLR3.7* overexpression lines while it

had only a minor effect on wildtype plants. The *AtGLR3.7* knockout line, however, experienced a root growth acceleration. These data support a hypothesis in which AtGLR3.7 controls plant growth by varying, effective apoplastic glutamate concentrations where L-glutamate could function as a secondary messenger responsible for activating GLRs at the PM, which in turn transduce cellular Ca^{2+} variations as part of the Ca^{2+} signalling network.

Gene expression data for selected key regulators of the plant's cell cycle were also collected by RT-PCR and revealed a tendency for all transgenic plant lines to upregulate S-phase genes as well as adjust M-phase regulator gene expressions. The accelerated growth in the *AtGLR3.7* overexpressing plants appeared to be based on an increase in DNA replication and cell proliferation which was reflected by enhanced gene transcript levels of elements of the E2F-DP pathway as well as various other cyclins (CYC) and cyclin-dependent kinases (CDK). An explanation for similar upregulations in atglr3.7, which exhibited fewer cell divisions and therefore should not have displayed an increase in DNA biosynthesis, was found by measuring the transgenic plant lines' nuclear DNA content. Cells of *AtGLR3.7* knockout and overexpression lines exhibited an increase in their endopolyploidy levels represented by an elevation of nuclear DNA contents. It is notable that, these augmentations were much more pronounced in atglr3.7. The knockout and overexpression of AtGLR3.7 seems to affect regulators of the cell cycle S-phase in a similar way by enhancing relevant gene expressions and causing an increase in DNA biosynthesis. However, key regulators of the M-phase could be affected in opposite ways in the transgenic plant lines. The knockout of *AtGLR3.7* could lead to a reduction of gene transcripts/protein activities essential for the M-phase of the cell cycle. This would cause a reduction in the number of cytokinetic events and promote several endoreduplication rounds in RAM cells due to an alternation of S-phases and cell cycle gaps which are required for cellular adjustments. In contrast, an overexpression of *AtGLR3.7* could stimulate the activity of M-phase CDKs and/or associated proteins inciting additional cell divisions and, in this way, cause both a minor increase in endopolyploidy levels and a significant boost in plant growth/biomass production.

The plant's biotic and abiotic stress tolerances were also affected by an overexpression or knockout of *AtGLR3.7*. Probably due to altered glutamate receptor concentrations at the PM of root cells, the uptake of Na^+ from the medium was significantly increased in *AtGLR3.7* overexpressing lines whereas the Na^+ content in atglr3.7 was markedly reduced. In connection with the observed changes in the ionic content, the modified Na^+ uptake capacities of the transgenic plant lines were presumably responsible for the measured elevated salt tolerance of

atglr3.7 against mild and moderate salt stress. The observed enhanced resistance of the transgenic plant lines against *Pseudomonas syringae* likely had its origin in the increased endopolyploidy levels. The protection against Pto DC3000 (but not against its non-virulent version Pto DC3000 (hrcC)) was much stronger in atglr3.7 plants than in the *AtGLR3.7* overexpression lines where still an *AtGLR3.7* expression-dependent reduction of bacterial growth could be detected. A hypothesis for the measured positive correlation between endoreduplication events and the plant's defence capabilities is based on a derivation of the 'gene-balance-hypothesis' established by Birchler and Veitia (2010). Hence, increased levels of nuclear DNA within the all transgenic *AtGLR3.7* plant lines would create a multiplication of potential DNA targets for various pathogen effectors and the augmented chromatin quantities could also lead to an enhanced proteinogenesis, raising the possibility of triggering R gene/protein-mediated effector-triggered immunity (ETI) within the affected plant cells.

Considering all the collected data of this work, the glutamate receptor AtGLR3.7 emerges as an important regulator of plant growth, development and physiology. Its subtle influences on meristematic activities and the plant cell cycle appear to affect and fine-tune responses to environmental cues as well as to intrinsic plant growth features while the amino acid L-glutamate as an agonist of GLRs seems to function as an activator of these AtGLR3.7-mediated effects.

Abbreviations

ABA	Abscisic acid
ADR	Average cell division rate
AMPA	α-amino-3-hydroxy-5-methyl-4-isoxazolepropionic acid
AP-5	2-amino-5-phosphonopentanoic acid
AtGLR	Arabidopsis thaliana glutamate receptor-like receptor
ATP	Adenosine triphosphate
bp	DNA base pair
CCD	(Theoretical) cell cycle duration
CDK	Cyclin-dependent kinase
CFU	Colony-forming units
CI	Individual cell value based on root cell morphology
CL	Cell length
CL_{mat}	Mature cell length
CLSM	Confocal laser scanning microscopy
CN	Number of preceding cells
CNGC	Cyclic-nucleotide-gated channel
CPM	Cell production rate of the meristem
CR	Ratio cell length:width
CS	Cell size
CW	Cell width
CWr	Radial CW
CW_t	Tangential CW
CYC	Cyclin
$[Ca^{2+}]_{cyt}$	Cytosolic calcium cation concentration
DAI	Days after imbibition
DNA	Deoxyribonucleic acid
DNQX	6,7-dinitroquinoxaline-2,3-dione
DQ	Cell distance from QC
DW	Plant dry weight
DZ	Differentiation root zone
EGTA	Ethylene glycol-bis(β-aminoethyl ether)-N,N,N',N'-tetraacetic acid
ER	Endoplasmic reticulum
ETI	Effector-triggered immunity
EZ	Elongation root zone
FW	Plant fresh weight
GFP	Green fluorescent protein
GLR	Glutamate receptor-like receptor

GOI	Gene of interest
HKT	High-affinity K^+ transporter
iGluR	Ionotropic glutamate receptors
MAMP	Microbial-associated molecular pattern
MAPK	Mitogen-activated protein kinase
mRNA	Messenger RNA
MZ	Meristematic root zone
NMDA	N-methyl-D-aspartate
NSCC	Non-selective cation channels
PAMP	Pathogen-associated molecular pattern
PCR	Polymerase chain reaction
PM	Plasma membrane
PRR	Pattern-recognition receptor
PTI	Pattern-triggered immunity
QC	Quiescence centre of the RAM
qRT-PCR	Quantitative RT-PCR
RAM	Root apical meristem
RNA	Ribonucleic acid
RT-PCR	Real time PCR
RWC	Relative water content of the plant
SAM	Shoot apical meristem
SDS-PAGE	Sodium dodecyl sulfate-polyacrylamide gel electrophoresis
sqRT-PCR	Semi-quantitative RT-PCR
T3SS	Type III twin-arginine transport secretion system of Pseudomonas
TF	Transcription factor
TZ	Transition root zone

List of Figures

List of Tables

Table of Contents

1 Introduction

1.1 Glutamate Receptor-Like Receptors in Plants

In 1998, gene sequences similar to animal iGluRs were discovered in the genome of *Arabidopsis thaliana* (Lam *et al.*, 1998). The theoretical plant protein sequences had a strong structural resemblance to these animal glutamate receptors that are involved in fast synaptic responses in neuronal structures. Here, they participate in a broad spectrum of neuronal processes such as memory, but they are also involved in neuronal conditions like Alzheimer's or Parkinson's disease (Traynelis *et al.*, 2010). The genome of *Arabidopsis thaliana* contains 20 GLR genes that became thoroughly scrutinized within the last 20 years (Weiland *et al.*, 2015). Studies about their physiological function encompass, plant development and metabolism, photosynthesis, plant stress adaptation as well as abiotic and biotic and defence reactions (Forde *et al.*, 2013; Mousavi *et al.*, 2013; Vincill *et al.*, 2013). Their phylogenetic origin as well as their highly conserved protein structure allow for the assumption that their molecular activity comprises electrical long-distance and cell-to-cell signalling. GLRs are proposed to be integral transmembrane proteins that possess a ligand-gated ion channel enabling them to mediate Ca^{2+} fluxes across the PM of plant cells as well as across various endomembranes in mitochondria and chloroplasts (Price *et al.*, 2012).

GLRs can be found in every cell type and their ubiquitous presence prompts the idea of a family of universal sensors and mediators of a vast array of endogenous and exogenous stimuli not only in *Arabidopsis thaliana* but likely in all common plant species (Roy *et al.*, 2008). The GLR system appears to be highly regulated based on gene expression analysis under internal or external stress applications (Meyerhoff *et al.*, 2005). Their gene expression dynamics together with the occurrence of mRNA splice variants expand their potential to control various plant physiological pathways (Teardo *et al.*, 2015). Since a functional GLR complex presumably consists of four individual subunits and each subunit possesses two separate ligand-binding sites, the involvement of GLRs in the large number of physiological processes reported so far is highly conceivable (Acher and Bertrand, 2004). Precisely timed, local gene expressions within the plant body, as well as directed subcellular protein localizations, allow a fine-tuning of GLR activities on all possible regulatory levels in plant physiology.

1.1.1 Local Gene Expression of AtGLRs

The 20 GLRs of *Arabidopsis thaliana* (AtGLR) can be grouped into three clades based on DNA sequence similarities, while clades I and II are likely sister clades originating from gene duplication events (Chiu *et al.*, 2002). The possibility of multiplied gene sequences could explain the location of many GLR genes in tandems on single chromosomes (Singh *et al.*, 2014). The analysis of AtGLR gene expressions indicates that originally all GLRs were expressed in roots, leaves and reproductive organs where they would have fulfilled different functions (Chiu *et al.*, 2002).

Today, clade II is no longer expressed throughout the whole plant whereas members of clade I are is still expressed within various parts of the plant (Chiu *et al.*, 2002). It seems that clade I substituted the original functions of some of the proteins encoded in clade II. Genes of clade II are mostly expressed within the root and the majority of these proteins (five out of nine) can be found solely in this region (Chiu *et al.*, 2002). The expression patterns of the other clade II genes are restricted to the root and siliques while only AtGLR2.5 is expressed throughout the plant (Chiu *et al.*, 2002). There is the possibility of a developmental-dependent functional class within this clade since three genes are expressed only in eight-week-old plants (Chiu *et al.*, 2002). Unlike clade II, most genes of the other clades are expressed throughout the entire plant. It should be noted that, the highest expression levels were measured within roots indicating a focus of GLR activities in processes taking place in this particular tissue of the plant (Figure 1) (Chiu *et al.*, 2002).

In 2008, Roy *et al.* conducted a very elucidating study in which the expression patterns of individual GLRs could be separated on a single cell level and thereby distinguishing between different cell types. These investigations confirmed the expression of all 20 AtGLRs in the root and the restriction of most of the clade II genes on this region. Furthermore, there are some 16 - 18 GLRs expressed in stems, petioles and leaves, however, a continuous downregulation of clade II genes appears to occur during plant development with either very low levels such as in leaves or even a complete cessation of expression.

Shifting back to the cell level, it has been stated that there are five to six GLRs expressed simultaneously within one cell (Roy *et al.*, 2008). However, it was observed that a single GLR is expressed in different tissues in one individual seedling, but its expression varied greatly among different plants when considering a particular cell type. The fact that a certain set of AtGLRs seems to be active within a particular plant and that this group of genes is supposed to

vary among different individuals could either underline the redundancy of AtGLRs in general or account for a distinct physiology of individual plants of the same species.

Figure 1. **Gene Expression Analysis of All 20 AtGLRs in Different Plant Tissues and During Various Developmental Stages**. White: no expression, blue: high expression. Adapted data obtained from Genevestigator (Hruz *et al.*, 2008) and first published in Weiland *et al.* (2015).

Following the expression onset of GLRs during plant development, it was found that shortly after germination, first expressions are observed within the vascular tissue of cotyledons. GLR gene activations subsequently progress to the vasculature of other organs like the root and shoot until they are expressed also in flowers and siliques in later developmental stages (Chiu *et al.*, 2002). In these advanced plant development phases, the expression is no longer limited to the vascular tissue, but it can be detected in other cell types, too. About 5 out of 20 GLRs are likely expressed permanently in a single cell, which could be a reference to a potential ubiquitous need of these receptors (Roy *et al.*, 2008). Even their potential redundancy underlines their broad activity spectrum since the occurrence of GLR gene duplication events would allow a specialization of individual receptors without losing the original function. The presence of both redundancy and gene duplication apparently secured the functions of GLRs within the organism and enable enough possibilities to alter their role in different physiological processes. AtGLR clade II is exemplary for this scenario in which restricted gene expression to the root was only possible by a replacement of its activities in other regions with members of clade I.

Besides their ubiquitous expression, the highest expression levels were still measured within the plant root. Here, GLRs could be involved in the sensing of amino acids and facilitate the uptake or release of them within the xylem and phloem of the root as it is prompted by the presence of AtGLR-GFP-fusion proteins within this region (Vincill *et al.*, 2013). Another, possible function of GLRs in cells surrounding the vasculature could be in relaying information about various plant conditions or the environment such as salt content of the soil, exudates of other plants/species or the water status to more distant parts like the stem and leaves. Their involvement in these kinds of signalling events would enlarge the role of the vasculature from sole transportation pathways to a ‘signal transduction highway’ allowing a much faster communication between otherwise separated regions of the plant body. Indications supporting this hypothesis are found in the involvement of GLRs in transmitting wounding signals between different rosette leaves (Salvador-Recatalà *et al.*, 2014).

1.1.2 Origin of GLRs and Relation to Glutamate Receptors in other Kingdoms

An amino acid signalling seems to be an ancient feature of living organisms. Glutamate receptors and their related proteins can be found in miscellaneous bacteria, plants and animals where they are involved in the perception of amino acids. The currently prevalent conception of an origin of all existing glutamate receptors from an inverted prokaryotic potassium channel was first proposed by Davenport (2002). Underlining this theory, the bacterial glutamate receptor GluR0 from the cyanobacterium *Synechocystis* sp. PCC6803 is capable of binding L-serine and glycine, as well as L-glutamate, and it shows a similarity of about 20% to both a glutamate receptor of other cyanobacteria and AtGLRs (Chen *et al.*, 1999; Teardo *et al.*, 2011). Since GluR0 does not bind the iGluR agonists *N*-methyl-D-aspartate (NMDA) or α-amino-3-hydroxy-5-methyl-4-isoxazolepropionic acid (AMPA), a common ancestor for plant and animal glutamate receptors is likely to have existed even before the divergence of the iGluR subclasses into NMDA, AMPA and kainate receptors (Chiu *et al.*, 2002).

Phylogenetic studies attempting to elucidate the relationship between plant GLRs and animal iGluRs have been performed using different methods and software. Some authors suggest a strong relation of GLRs to non-NMDA receptors, namely kainate and AMPA receptors (Kim *et al.*, 2001; Nagata *et al.*, 2004) while others argue for the strongest analogy of GLRs to NMDA receptors, especially to the subunits GluN1 and GluN3 (Chiu *et al.*, 1999; Lacombe *et al.*, 2001; Dubos *et al.*, 2003). As reported in Weiland *et al.* (2015), based on a comparison of the amino acid sequences of all AtGLRs with iGluRs of rats, it seems plausible to assume the strongest relation of GLRs to AMPA and kainate receptors. Only NMDA receptor GluN1 appears to exceed all other iGluRs in terms of sequence conservation when comparing it with the AtGLRs. Considering the three GLR clades in *Arabidopsis thaliana*, the highest sequence similarity to animal iGluRs is found in clade II. Taken together, a conclusive explanation for the relationship of glutamate receptors from different kingdoms cannot be made currently.

Nonetheless, plant and animal glutamate receptors share both pore-forming transmembrane domains and external ligand-binding sites (Price *et al.*, 2012). These common features argue for an assembly of these domains before the divergence into animal and plant life as well as for a successive co-evolution in both kingdoms. Over this long period, only minor changes in the protein structure took place. The conservation of their function emphasizes an essential role of glutamate receptors in amino acid signalling and, based on this, in their involvement in a multitude of physiological processes.

Nowadays, glutamate receptors have been described in many different plant species including rice (Li *et al.*, 2006), wild grass (Li *et al.*, 2013b) and even long-distance relatives such as liverworts (Krol *et al.*, 2007). The genome of rice (*Oryza sativa*) contains 24 gene sequences closely related to AtGLRs which accounts for a divergence of both plant species relatively late in their phylogeny (Li *et al.*, 2006). Interestingly, the glutamate receptors of rice comprise an additional fifth transmembrane domain with a currently unknown function (Singh *et al.*, 2014). Speculations about an altered ion selectivity were made by the authors since changes in the amino acid sequence of the respective domains are known to affect the passage of cations in iGluRs (Nagata *et al.*, 2004). The glutamate receptors of tomato also contain signal sequences for the secretory pathway within their amino (N)-terminus, further supporting the idea of receptor insertions into cell membranes as a common trait for most of the GLRs (Aouini *et al.*, 2011). The majority of these tomato proteins are closely related to AtGLRs and only one out of three glutamate receptor clades appears to be unique in tomato one (Aouini *et al.*, 2011). The genome of the small radish *Raphanus sativus L.* encodes for several GLR-like proteins with a hydrophobic signal sequence as well as an endoplasmic reticulum (ER) retention signal in their carboxy (C)-terminus (Kang *et al.*, 2006). Both traits are indications of participation by these proteins in the secretory pathway aiming at an incorporation into cellular membranes (Kang *et al.*, 2006).

Interestingly, GLR-like proteins seem also to exist in the wild grass, *Echinochloa Crus-galli* (Li *et al.*, 2013b). However, their amino acid sequences display some considerable deviations. Although both common ligand-binding sites are present, they are located at opposing ends of the proteins where one binding site is exceptionally situated at the C-terminus while in all other GLRs the two ligand-binding sites are located at the N-terminus (Li *et al.*, 2013b). So far, it is not known if this accounts for an altered GLR function or that the relatively low degree of conservation gives reason to assume that these are completely different proteins.

Considering the potential omnipresence of GLR or GLR-like proteins in all plant species, it can be speculated if this type of receptor is present in all higher organisms. At least in *Arabidopsis thaliana*, it was shown that GLRs possess an ion channel-forming domain which is proposed to permit Ca^{2+} fluxes across the PM (Tapken and Hollmann, 2008). The provoked calcium signatures, which are essential parts of signal transduction events, could be easily controlled by the ligand-binding sites found in all GLRs.

1.1.3 Subcellular Localization of GLR Subunits

Most of the GLRs found in plants likely enter the secretory pathway and are transported to the PM. The respective signal peptides are mainly found within the N-terminal domain of these proteins (Lam *et al.*, 1998; Chiu *et al.*, 1999). Incorporation into different cell membrane types is most probable since various signal sequences have been detected which are known to cause not only to the inclusion into the PM but also into the inner membranes of mitochondria and chloroplasts (Teardo *et al.*, 2010; 2011). The location of GLRs in mitochondrial and plastid membranes could indicate an additional role for GLRs in mediating not only intercellular but also intracellular signals. This hypothesis is underlined by a study of Teardo *et al.* (2011) where a GFP-tagged version of AtGLR3.4 was found in both the PM and the outer or inner envelope of plastids.

The presence of several target sequences within one gene could enable a dynamic delivery of the respective GLRs depending on the actual cellular environment. Since this regulation takes place via mRNA splicing, alternative variants of the same gene could be translated and sent to different destinations. AtGLR3.5, for example, has a mitochondrial signal sequence within its N-terminus that when removed in one isoform causes a redirection of this GLR to the chloroplast membranes (Teardo *et al.*, 2015). Considering the possibility of a directed and modifiable targeting of GLRs to various cellular membranes, these receptors are prone to be highly flexible in terms of their field of operation in a temporal and spatial manner.

Looking at the glutamate receptors of clade III in *Arabidopsis thaliana*, AtGLR3.1, -3.2, -3.6 and -3.7 probably enter the secretory pathway and are incorporated into the PM while the others (AtGLR3.3, -3.4 and -3.5) contain sequences for multiple cellular targets (Teardo *et al.*, 2010; 2011). GFP-tagged versions of AtGLR3.2, -3.3 and -3.4 have been found scattered among all cell types within the root growth zone whereas a concentration at the PM of sieve plates within the phloem of the mature region of the root was observed (Turano *et al.*, 2001; Chiu *et al.*, 2002; Vincill *et al.*, 2013). The accumulation at the junction of phloem elements appears to be connected with the involvement of GLRs in long-distance wounding signal transduction as it is seen during an herbivore attack (Mousavi *et al.*, 2013).

1.1.4 Molecular Structure of Glutamate Receptors

1.1.4.1 Conserved GLR Domains in Different Plant Species

AtGLRs are 800 to 960 amino acids long and have a similar molecular weight of about 100 kDa. The GLR peptide folds into a six-domain structure with a strong homology to animal iGluRs (Lam *et al.*, 1998). Four transmembrane domains (M1-M4) anchor the protein in cellular membranes and form a channel through the phospholipid bilayer allowing for the passage of different ions. Additionally, the protein contains extracellular ligand-binding sites (S1 and S2) that are proposed to bind various ligands (Tapken *et al.*, 2013). Studies in animal cells show conformational changes in the ion pore-forming transmembrane domains upon binding of a ligand at the S1 and S2 domains (Sobolevsky *et al.*, 2009). These changes in the secondary structure presumably enable the ion fluxes across the respective membrane. Interestingly, AtGLRs like other plant GLRs accommodate an additional ligand-binding domain in its N-terminus which appears to bind a second ligand or a modulator in order to alter the receptor's sensitivity to further stimuli or modify its function (Price *et al.*, 2012).

There is a high likelihood that plant GLRs are operating as homo-/heterotetramers in which four subunits contribute individually to the final functionality of the receptor complex (Dubos *et al.*, 2003). Animal iGluRs also consist of four subunits, and the NMDA receptor family, which is closely related to AtGLRs, consists of three different types of NMDA subunits (NR-1, -2, and -3) (Ulbrich and Isacoff, 2008). The assembly of these receptors takes place within the ER and it is mediated by the N-terminal domains of the proteins leading to the formation of a dimer. Subsequently, this dimer interacts with another dimer and forms the final homo-/heterotetramer (Sobolevsky *et al.*, 2009; Traynelis *et al.*, 2010). The way in which the functional glutamate receptor is assembled could explain several described complications in early studies when trying to create a fluorescent fusion protein (see Davenport, 2002). The addition of GFP (238 amino acids) to a GLR subunit certainly hampers the subsequent assembly with the other three GLRs or it would at least limit the functionality of the ultimate GLR complex.

Various methods including sodium dodecyl sulfate-polyacrylamide gel electrophoresis (SDS-PAGE), fluorescence resonance energy transfer (FRET) and the mating-based split-ubiquitin system (mbSUS) provide evidence for the assembly of plant GLRs as multimeric complexes *in vivo* where interactions between different AtGLRs have also been observed at the PM (Turano *et al.*, 2001; Vincill *et al.*, 2012, 2013; Price *et al.*, 2013). In these studies, AtGLR2.9, -3.2 and -3.4 appear to be key subunits mediating the formation of a functional receptor complex.

Noteworthy, these complexes seem to include subunits of different clades that distinguishes them from their animal counterparts in which the constitution of a functional iGluR aggregate is restricted to members of only one class (Dingledine *et al.*, 1999). This flexibility of plant GLRs expands their dynamics and versatile area of operation.

1.1.4.2 Comparison of Amino Acid Sequences between Various Glutamate Receptors

The similar structure of glutamate receptors in plants and animals as well as recent findings in GLR function and involvements suggests a common functionality for most of these receptors. Besides the six homologue domains (M1-M4, S1-S2), iGluRs and GLRs share about 50-60% of their amino acid sequence indicating the possibility of a formation of glutamate receptors before the divergence of animals and plants (Chiu *et al.*, 2002; Nagata *et al.*, 2004). Similarities of the transmembrane and pore-forming domains M1-M4 can be found mainly in M1, M3 and M4 while M2 displays a rather low degree of conservation. Despite these deviations within the pore region, data obtained from iGluR research can be used to predict potential ion conductance properties of GLRs (Tapken *et al.*, 2013). Like the transmembrane domains, the ligand-binding sites S1 and S2 contain highly conserved residues in both animals and plants and a comparison of AtGLRs with their closest relative GluN1 reveals a similar structure of this region (Figure 2) (Chiu *et al.*, 1999; Weiland *et al.*, 2015).

The structural homology of AtGLRs shows only minor variations within the transmembrane domains underlining their potential ubiquitous role in mediating cation fluxes across membranes (Chiu *et al.*, 2002). However, the ligand-binding sites S1 and S2 vary significantly between different AtGLR clades (Chiu *et al.*, 2002). This finding accounts for a highly-selective receptor system where individually composed GLR complexes would be gated specifically by their respective ligands. Since a functional complex is likely made up of four single GLRs, each of them with its unique ligand-binding sites, and 20 different receptors are found in *Arabidopsis thaliana*, the GLR network could allow specialized Ca^{2+} signalling cascades for versatile and fine-tuned pathways involving particular ligands and/or stimuli.

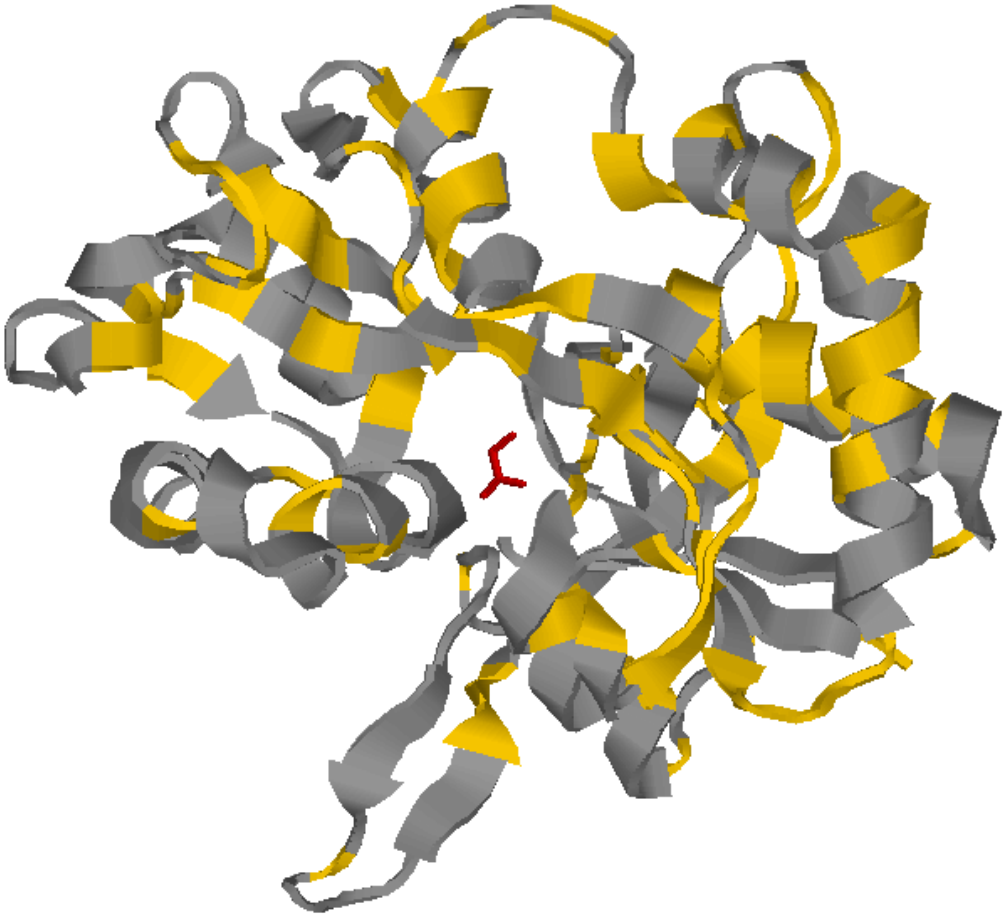

Figure 2. **Crystal Structure Homologies of the Ligand-Binding Domain of Glutamate Receptor GluN1 of *rattus norvegicus* and AtGLR3.7 of *Arabidopsis thaliana* when Complexed with the Agonist Glycine.** Identical or highly similar amino acids of GluN1 to AtGLR3.7 are highlighted in yellow. Glycine is depicted in red. Adapted crystal structure is based on an already described structure in Furukawa and Gouaux (2003). Displayed complex modified by 'RasMol' software (Sayle, 1995). Image first published in Weiland *et al.* (2015).

Besides the common architecture of animal and plant glutamate receptors, there are two distinct GLR structures found only in plants. One of them is a G-protein-coupled receptor-like domain that could be an evolutionary link to other kingdoms with other glutamate receptors than iGluRs (Chiu *et al.*, 1999; Turano *et al.*, 2001). The other structure is a long N-terminal region with a similarity to *γ*-aminobutyric acid (GABA) receptors and extracellular calcium sensors (Turano *et al.*, 2001). For five AtGLRs, GABA receptor activity has already been demonstrated hinting at a possible interaction between GLRs and the GABA signalling pathways (Roy and Mukherjee, 2017). Both unique GLR structures further substantiate a role for these receptors in mediating Ca^{2+} fluxes and their involvement in Ca^{2+} signalling.

1.1.5 Ligands and Ligand Binding

1.1.5.1 Ligands of GLRs

Although GLRs obtained their denotation from their similarity to animal glutamate receptors, for a long time it was not clear if GLRs were capable of binding glutamate at their ligand-binding sites. Sequence comparisons reveal some deviations in GLRs and in particular the substitution of the amino acid T655 for F655 in *Arabidopsis thaliana* was thought to prevent a proper glutamate binding (Dubos *et al.*, 2003). Since this threonine is strictly conserved in all iGluRs, glycine instead of glutamate was proposed as the main agonist for AtGLRs (Dubos *et al.*, 2003). However, there has been sufficient evidence collected up to now, which indicates an amino acid-triggered gating of GLRs involving various amino acids including glutamate and glycine but also serine, cysteine, glutathione and others (Weiland *et al.*, 2015). Glutathione appears to be rather unusual because it is a tripeptide made up of glutamate, cysteine and glycine but the presence of α-amino and β-carboxyl groups in this molecule seems to be sufficient to allow a binding at the S1 and S2 domains in GLRs similar to the binding of single amino acids.

Interestingly, classical iGluR agonists such as NMDA, AMPA or kainate seem to have no effect on GLRs which is reasonable since these substances are completely absent in plants (Vatsa *et al.*, 2011). Antagonists of iGluRs, on the other hand, appear to impede GLRs in plants, too. The inhibiting effects of agents such as 6,7-dinitroquinoxaline-2,3-dione (DNQX) and 2-amino-5-phosphonopentanoic acid (AP-5) are thought to rely on the binding of these chemicals inside of the ligand-binding sites S1 and S2, leading to the subsequent insensitivity of the receptor complex (Dubos *et al.*, 2003). General Ca^{2+} channel blockers like La^{3+} or Ga^{3+} are also effective in inhibiting Ca^{2+} currents in heterologous expression experiments of GLRs in *Xenopus* oocytes underlining the role of GLRs as true Ca^{2+} channels (Meyerhoff *et al.*, 2005; Vatsa *et al.*, 2011).

The finding that different amino acids activate various GLRs prompted a study of a concomitant application of several amino acids in order to determine a hierarchy of these agonists. It was found that the tested amino acids caused Ca^{2+} fluxes to variable degrees leading to a model in which three classes of receptor complexes display varying susceptibilities against particular amino acids (Stephens *et al.*, 2008). The current hypothesis of four GLRs forming a functional receptor complex is in accordance with these findings since each single GLR would have its own responsiveness against distinct amino acids and the whole receptor complex would comprise its individual agonist-dependent sensitivity.

1.1.5.2 Ligand Binding at Two Binding Sites

The ligand-binding sites S1 and S2 located at the N-terminus are a common feature of glutamate receptors in general. In addition, there is a second binding site in plant GLRs nearby which is thought to bind another ligand (Acher and Bertrand, 2004). The first pocket consisting of S1 and S2 forms a lysine/arginine/ornithine-binding protein (LAOBP)-like domain similar to the periplasmic binding protein-like II superfamily that is also found in iGluRs. This appears to be the main site for glutamate binding. The second ligand-binding site is characterized by a leucine/isoleucine/valine-binding protein (LIVBP)-like domain, and this region should be capable of binding either another amino acid or a completely different ligand (Acher and Bertrand, 2004).

In animal NMDA receptors binding of the respective ligand is accomplished by a 'Venus flytrap mechanism' consisting of two LIVBP-like domains (Traynelis *et al.*, 2010). Here, the composition of the receptor complex made up of either GluN2 or GluN1/GluN3 subunits determines its sensitivity against glutamate or glycine, respectively. It is highly likely, that a similar mechanism is responsible for the binding of ligands in GLRs, too, given that LIVBP and LAOBP domains are very much alike.

Upon binding of the respective ligand in the centre of the open-domain structure, conformational changes in the protein architecture lead to an opening of the ion pore within the membrane allowing for the passive passage of cations (Acher and Bertrand, 2004). At the same time, the ligand-binding sites close. In this process, the three amino acids D499, T501 and R506 are crucial for proper amino acid binding since point mutations at these sites cause strong impairments of the mediated ion fluxes or prevent them altogether (Tapken *et al.*, 2013). These amino acids are conserved in all AtGLRs, and further studies confirmed that the primary functional amino acid groups are critical for a binding of ligands to GLRs. These characteristics are already known for iGluRs where the ligand-binding site S1 recognizes the α-amino and β-carboxyl groups (Traynelis *et al.*, 2010).

1.1.6 GLR-Mediated Ion Conduction and Ion Flux Modulation

1.1.6.1 Ion Conduction across Cellular Membranes

In a study from 2000, Dennison and Spalding showed for the first time that an application of glutamate elicits an increase of the cytosolic calcium cation concentration ($[Ca^{2+}]_{cyt}$) which is accompanied by a PM depolarisation. Until then, it was not clear if glutamate receptors of plants are capable of conducting ion fluxes. Their animal homologs were long known for the mediation of ligand-gated influxes and effluxes of cations such as Na^+, K^+ and Ca^{2+} (Traynelis *et al.*, 2010). Their localization and function at the PM of neurons is the foundation for synaptic neurotransmission in most animals. Here, a signal is transduced by the activation of iGluRs in postsynaptic membranes upon binding of their respective ligands (for example NMDA, AMPA or kainate) that were released into the synaptic cleft. The binding of iGluRs' agonists causes membrane depolarisations and leads to vesicle fusions at the following presynaptic membrane allowing a propagation of the original signal.

In plant cells, glutamate induces dose-dependent electrical currents which can be prevented by an application of either Ca^{2+} chelators such as EGTA or universal ion channel blockers like La^{3+} and Ga^{3+} (Dennison and Spalding, 2000). The measured currents in plants cells can be explained by the 'Three-Plus-One' motif of GLRs which is also present in cyclic-nucleotide-gated channels (CNGC), voltage-gated $Na^+/K^+/Ca^{2+}$ channels and inward K^+ rectifiers where this motif is known to be responsible for the passage of ions across various cellular membranes (Chiu *et al.*, 1999). It is made up of the three membrane-spanning (M1, M3 and M4) domains and only one half of the membrane-spanning (M2) domain, which altogether assemble as a pore loop allowing the passage of sodium, calcium and potassium cations (Lam *et al.*, 1998; Tapken and Hollmann, 2008). This highly conserved structure among all GLRs is one of the reasons why they are considered as non-selective cation channels. In recent years, sufficient evidence has accumulated which shows that GLRs enable the passage of mono-and divalent cations including K^+, Na^+ and Ca^{2+} (Tapken and Hollmann, 2008; Vincill *et al.*, 2012, 2013; Tapken *et al.*, 2013; Ni *et al.*, 2016). However, difficulties in GLR research employing heterologous expression systems point to a requirement of auxiliary proteins to the functional GLR complex as is described for animal glutamate receptors (Tapken and Hollmann, 2008; Vincill *et al.*, 2013; Teardo *et al.*, 2015).

Interestingly, one of the pore-forming domains (M2) is prone to RNA editing (Chiu *et al.*, 1999), a feature shared with iGluRs where RNA editing is known to change the ion permeabilities of the channel (Traynelis *et al.*, 2010). It is highly probable that GLRs do not

possess the same ion conductivities as animal glutamate receptors. Amino acid deviations detected in the pore region of GLRs, along with a missing QRN-site which is essential for ion selectivities in iGluRs (i.e. the passage of Ca^{2+} and a Mg^{2+}-mediated channel blockage) hint at a reduced ion selectivity in plants (Nagata *et al.*, 2004; Tapken and Hollmann, 2008). Together with the phenomenon of alternative splicing of GLR transcripts, it is highly likely that the final plant receptor complex exhibits ion conductance characteristics that vary by the actual composition made up of the single GLR subunits. The modular structure of GLRs could allow not only a broader spectrum in ligand-binding but also in selective ion permeabilities.

Although most studies aimed at discovering the nature of GLR-mediated ion currents showed a rather non-selective transport of cations including Na^+, Ba^+ and K^+, plant glutamate receptors show a clear preference for Ca^{2+}. Two facts clarify the character of GLR-mediated currents at the PM level of plant cells. First, the reversal potential originating from Na^+ and K^+ fluxes after a glutamate-induced action potential is not affected by varying GLR agonist concentrations while the permeability of the PM for Ca^{2+} strongly depends on the initial dosage of GLR ligands (Tapken and Hollmann, 2008). Second, increasing Ca^{2+} concentrations within the culture medium cause a reduced selectivity for other ions (Vincill *et al.*, 2012). Both findings indicate a clear preference for Ca^{2+} over other cations.

In detail measurements concerning the process of the observed Ca^{2+} fluctuations show that only the initial transient Ca^{2+} influx into the cytoplasm is provoked by an activation of GLRs in the PM (Demidchik *et al.*, 2004). These first Ca^{2+} inward currents happen within seconds and they are accompanied by burst-like channel events which increase $[Ca^{2+}]_{cyt}$ to a level which is significantly higher than before the GLR activation (Vatsa *et al.*, 2011). However, several GLR activations either subsequently or simultaneously but spatially different are necessary to exceed a $[Ca^{2+}]_{cyt}$ threshold which activates other, secondary calcium channels (Meyerhoff *et al.*, 2005). Therefore, the strong $[Ca^{2+}]_{cyt}$ oscillations that are a part of Ca^{2+} signalling cascades leading to cellular responses appear to be mediated only partly by GLRs but they seem to rely on these secondary calcium channels, as well. Only those later calcium currents are responsible for the depolarisation of the PM that is characteristic of a cellular plant action potential. After the Ca^{2+} signalling takes place, the resting potential is restored by a repolarization of the membrane via ion channels, transporters and ATPase pumps (Meyerhoff *et al.*, 2005).

1.1.6.2 GLR Channel Activation and Modulation

Glutamate, glycine and other agonists/antagonists can bind to GLRs in their active state provoking a long-lasting insensitivity for more than 1 h against repeated ligand treatments (Meyerhoff *et al.*, 2005). This arises from the conformational changes happening close to the ion pore upon ligand-binding (Stephens *et al.*, 2008). In order to restore the GLR sensitivity, the receptor needs to either release its respective ligand or the receptor has to be removed from the membrane via endocytosis-mediated degradation. In animal cells, proper receptor degradation and biosynthesis is essential for the functionality of NMDA and kainate receptors which allows not only a fine-tuned temporal sensitivity but also an effective subcellular localization of the receptor complex (Kato *et al.*, 2005; Salinas *et al.*, 2006). *De novo* receptor biosynthesis likely also exists in plant cells. The application of translational inhibitors inhibits the restoration of the plant cell susceptibility to a subsequent agonist treatment and enhanced GLR gene upregulation is detected upon administrations of various stress stimuli (Meyerhoff *et al.*, 2005). The existence of an insensitive receptor state as well as its reconstitution potentially via protein biosynthesis, argues for an inducible and non-constitutive GLR system which supports a highly sensitive and versatile cellular signal perception.

Similarities of GLRs and iGluRs are not only implied by their activation through the amino acids glutamate and glycine but also by the effectiveness of known iGluR antagonists such as DNQX, AP-5 and dizocilpine (MK-801) on GLRs (Dubos *et al.*, 2003; Vatsa *et al.*, 2011). However, plant glutamate receptors are unique in terms of selective agonist/antagonist binding. The inhibitory effect of DNQX on glutamate-induced ion fluxes depends on the tested plant region since this antagonist appears to block Ca^{2+} fluxes only in above-ground tissues of *Arabidopsis thaliana* indicating the existence of different GLR receptor complexes within the plant body (Dubos *et al.*, 2003).

Another particular feature of plant glutamate receptors concerns the potency of varying amino acid concentrations ranging from 0.01 to 10 mM as well as the dose-dependent activation of GLRs by other amino acids than glutamate or glycine (Vincill *et al.*, 2012). For example, simultaneous application of glutamate and glycine is much more effective than the application of one of these amino acids alone and a treatment with synergistically-operating amino acids causes a saturation of the receptor complex at concentrations as low as 0.01 mM (Dubos *et al.*, 2003; Stephens *et al.*, 2008). These characteristics of GLRs illustrate the versatility of this receptor system in plants where a multitude of potential amino acid agonists activate different subsets of GLR complexes.

Besides the active and inactive state of GLRs upon ligand-binding, modifications at the N- and C-terminus of individual glutamate receptors allow for further adjustment of the GLR activities. Based on amino acid sequencing tools, several N-glycosylation, phosphorylation and myristoylation sites can be found in most of the plant glutamate receptors indicating elaborated involvements in exogenous and endogenous signal transduction events (Figure 3) (Roy and Mukherjee, 2017). For example, C-terminal modifications of iGluRs in animal cells are known to affect receptor subcellular localization, its intracellular trafficking and recycling properties as well as its membrane insertion capabilities (Traynelis *et al.*, 2010). Furthermore, 16 out of the 20 GLRs in *Arabidopsis thaliana* contain a 14-3-3 protein-binding motif, and binding of these proteins has been already confirmed for five AtGLRs (Chang *et al.*, 2009). Since 14-3-3 proteins are capable of distinguishing phosphorylated and dephosphorylated proteins, they are well-established mediators of the interactions of proteins with their respective kinases/phosphatases or with their target protein after phosphorylation/dephosphorylation (Fu *et al.*, 2000). It is highly likely that GLRs are subject to phosphorylation events and the presence of 14-3-3 protein-binding motif could connect them with the subsequent downstream processes such as receptor degradation, recycling or relocalization.

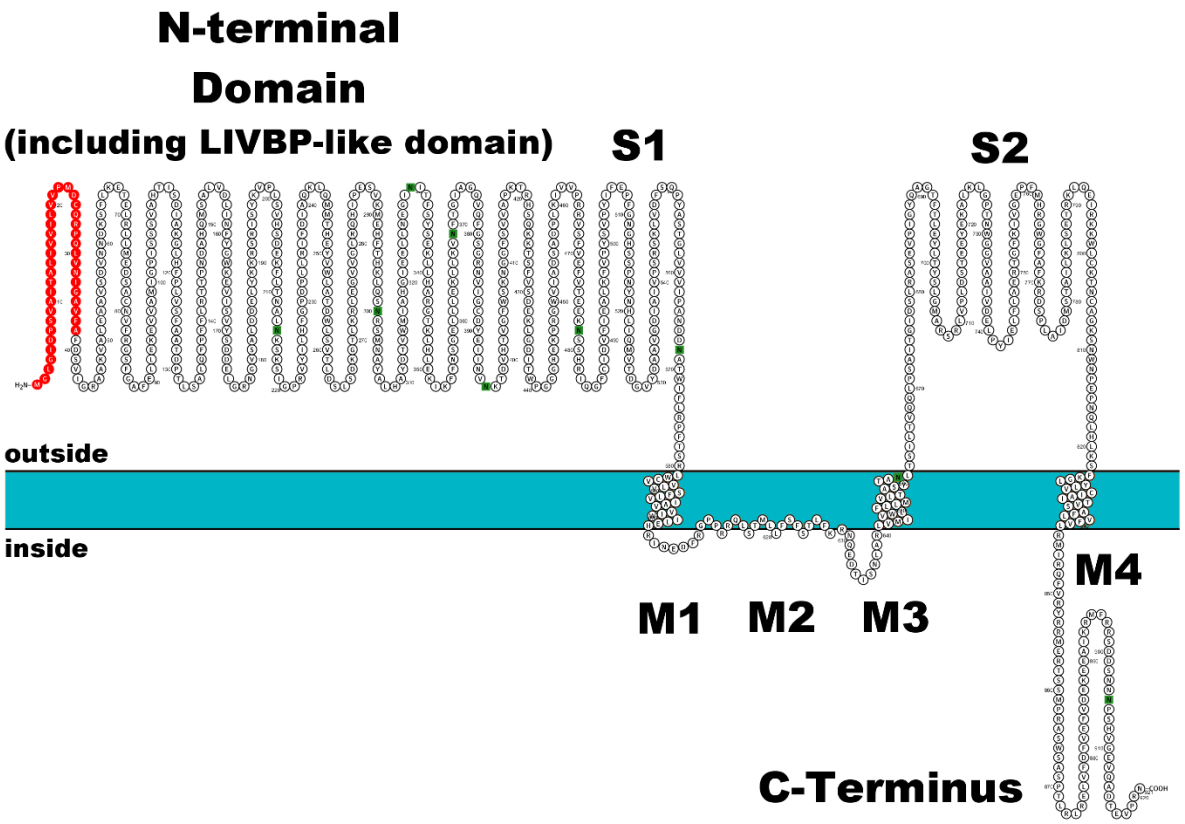

Figure 3. **Theoretical Incorporation of *Arabidopsis thaliana* Glutamate Receptor AtGLR3.7 into a Phospholipid Bilayer.** The signal sequence at N-terminus for the secretory pathway is marked in red. Possible N-glycosylation sites are marked in green. Transmembrane predictions were performed using 'Protter' software (Omasits *et al.*, 2014). Image first published in Weiland *et al.* (2015).

1.1.7 Involvements of GLRs in Plant Physiology

1.1.7.1 GLRs Affect Root Development

First studies of glutamate and its involvement in plant physiology were made on roots of *Arabidopsis thaliana*. It was shown that an application of L-glutamate but not its enantiomer D-glutamate leads to a dose-dependent growth arrest of the primary root while the growth of younger secondary roots up to a length of 10 mm was promoted (Walch-Liu *et al.*, 2006). The usage of very low amino acid concentrations and an application of glutamine and nitrogen as background resources for an exclusion of possible interferences with the amino acid metabolism to underline a true glutamate-triggered alteration of the root architecture (Walch-Liu *et al.*, 2006). The initial response to a glutamate treatment is a reduction of cell division activities in the root apex while prolonged exposures to glutamate also inhibit cell elongations in the root's elongation zone (Walch-Liu *et al.*, 2006). Since the observed effects are developmental-dependent and distinct Arabidopsis ecotypes show different sensitivities against glutamate, it

appears that GLR activities are defined temporally and spatially on the gene expression and/or protein level.

The role of certain GLRs in the organization and function of the RAM is further supported by a characterization of an *Oryza sativa* OsGLR3.1 knockout line where the whole root system, including lateral and adventitious roots, is affected (Li *et al.*, 2006). Here, apoptotic events in the elongation zone combined with inhibitions of radial cell expansion within the transition zone cause severe growth restrictions. In addition, the knockout of this GLR seems to disturb the overall organization of the RAM. The quiescence centre (QC) as well as root cell initials of the lateral roots display a higher mitotic activity whereas the root apex in general is characterized by a reduction of cell division events. Furthermore, cells along the root differentiate prematurely contributing to the dysfunctional root development.

The regulation of root growth by altered meristematic activities of the RAM was also shown for a member of clade III (AtGLR3.6) in *Arabidopsis thaliana* (Singh *et al.*, 2016). Here, it was speculated that the glutamate receptor AtGLR3.6 could affect gene expressions associated with the control of cell divisions within the root tip since its knockout negatively affects root growth parameters. There are also indications of the involvement of two other AtGLRs (AtGLR3.2 and AtGLR3.4) in root primordia initiation (Vincill *et al.*, 2013). The knockout of both receptors appears to negatively affect cell divisions in the bulging primordia which ultimately causes a cessation of the whole primordia's activity.

The GLR-mediated effects of glutamate are likely exerted via MAPKs. In a study by Forde *et al.* (2013), it was demonstrated that a chemical interfering with MAPK activities as well as the knockout of one particular kinase (MEKK1) prevent glutamate-mediated root growth arrest. It is noteworthy that, MEKK1 is also involved in plant immunity together with several GLRs as will be discussed further below.

1.1.7.2 Impacts of GLRs on Plant Development

The gene expression pattern of several GLRs in different plant species indicates an involvement in the onset and progression of the reproductive stage. During inflorescence formation, four glutamate receptors of *Oryza sativa* are upregulated while the gene expression of four others is reduced and there are six GLRs expressed in *Arabidopsis thaliana* pollen (Pina *et al.*, 2005; Singh *et al.*, 2014). Additionally, the knockout of two GLRs expressed in pollen (AtGLR1.2 and AtGLR3.7) leads to a lowered number of seeds per silique (Michard *et al.*, 2011). Partial

male sterility appears to have its origin in abnormal pollen tube growth, which is characterized by a reduced growth velocity and unusual tube morphology. Cellular investigations revealed significant alterations in Ca^{2+} oscillations during pollen tube growth that can be alleviated by an application of GLR antagonists (DNQX or AP-5) or the potential GLR agonist D-serine. In this case, the presumed GRL-mediated D-serine signalling during pollen tube growth apparently guides the pollen tube within the ovule (Michard *et al.*, 2011).

A wide range of developmental implications was shown for a small radish GLR when expressed in Arabidopsis plants. The functionality of a glutamate receptor from a different species in *Arabidopsis thaliana* as well as morphological similarities of Arabidopsis and small radish plants overexpressing AtGLR3.2 and RsGLR, respectively, suggest a high redundancy of plant GLRs (Kang *et al.*, 2006). The overexpression of each of these glutamate receptors leads to a retarded plant development and a dwarf phenotype with undeveloped lateral shoots as well as irregular-shaped leaves and flowers. The overexpression of RsGLR in Arabidopsis also causes an enhanced resistance to necrotrophic fungi due to upregulation of plant immune response genes involved in the jasmonic acid pathway. Additionally, genes involved in the abscisic acid (ABA) pathway, such as water stress response genes, are downregulated leading to a reduced drought tolerance of the GLR overexpression plants.

The glutamate receptor AtGLR3.5, on the other hand, affects aging in *Arabidopsis thaliana* (Teardo *et al.*, 2015). Plants lacking this receptor are characterized by a reduction in chlorophyll content within the leaves as well as a premature senescence. Together with the observation of AtGLR3.5 gene upregulations in five-week-old plants, it is assumed that GLRs are also involved in this concluding part of a plant's life cycle.

1.1.7.3 Calcium Homeostasis Mediated by GLRs

GLRs as potential calcium channels are not only involved in Ca^{2+} signatures but they are likely also responsible for ion uptake from the soil and the conveyance of the current Ca^{2+} status within the plant. An AtGLR3.2 overexpression line shows a reduced growth, a browning of the whole plant, necrotic areas at leaf tips and curled leaves, all of which are typical calcium deficiency symptoms (Kim *et al.*, 2001). Since the plant's total calcium content is comparable to wildtype plants, the calcium uptake from the soil appears to function properly. Therefore, perturbations of calcium distribution within the plant are more likely to be the effect of this GLR's overexpression. This idea is supported by the finding that an exogenous surplus of

calcium alleviates the deficiency symptoms, probably by balancing the plant's internal Ca^{2+} discrepancies (Kim *et al.*, 2001).

Furthermore, the overexpression of AtGLR3.2 causes hypersensitivity to Na^+ and K^+ associated with a reduced salt tolerance (Kim *et al.*, 2001). Here, an excess of the potential ion channel at the PM could be the reason for an uncontrolled influx of sodium and potassium cation. It is noteworthy that, the sensitivity to Ca^{2+} in this overexpression line is comparable to wildtype plants. Since GLRs are proposed to be cation channels for all three ions, an explanation could be that hypersensitivity to Ca^{2+} is not detectable only because of the surplus of external calcium which helps to counteract the observed Ca^{2+} imbalance within the plant.

The knockout of AtGLR3.1, on the other hand, causes a measurable increase in sensitivity to Ca^{2+} (Kang and Turano, 2003). In this case, plants are characterized by root growth inhibitions probably due to natural encounters with cations in the soil. The opposite reactions of the AtGLR3.2 overexpressing and the AtGLR1.1 knockout plant could be explained by diverging functions of the respective receptors. AtGLR3.2 may have an ion channel function at the PM of root cells in which it would mediate directly the passage of cations including Ca^{2+}, Na^+ and K^+ whereas AtGLR1.1 could be involved in the transmission of the actual calcium status of the plant in which case it would only relay that information. A disturbed signal transduction in the AtGLR1.1 knockout line would then lead to a premature onset of salt stress responses including the measured growth inhibitions.

1.1.7.4 GLR Signalling in Carbon Metabolism

There are indications that GLRs are involved in the communication of the carbon:nitrogen ratio within *Arabidopsis thaliana*. The knockout of AtGLR1.1 impairs seed germination on low sugar media while only the application of nitrate as an additional nitrogen source but not the increase of glucose as a carbon source, could alleviate the effects on seed dormancy (Kang and Turano, 2003). Furthermore, the knockout line exhibits a reduction in gene expression and protein activities of genes/proteins associated with carbon and nitrogen metabolism. These effects of AtGLR1.1 prompted the authors of the study to speculate about a role for AtGLR1.1 as a sensor of sucrose concentrations within the plant in which a knockout causes a higher sensitivity to sucrose derivatives due to an incorrect estimation of the true sucrose status. Ca^{2+} signalling within the vasculature could form the basis for this signal transduction pathway. Two GLRs (AtGLR3.2 and AtGLR3.4) are found at the sieve plates of the phloem and it is highly

likely that other GLRs are also involved in the long-distance transmission of various signals along the plant's vasculature (Vincill *et al.*, 2012, 2013). Since the amino acid concentration within the xylem correlates with the availability of carbon and nitrogen, GLRs could be candidates for the perception and transmission of the plant's carbon:nitrogen ratio by creating the respective Ca^{2+} signatures (Vincill *et al.*, 2013).

1.1.7.5 Influence of GLRs on Stomatal Movements and Photosynthesis

The regulation of stomata opening and closing is a strictly controlled process and different physiological pathways converge at the stomatal apparatus. While open stomata are essential for the photosynthetic process in terms of water evaporation, heat dissipation and gas exchange, a closure is often caused by a pathogen attack or drought stress in order to hamper bacterial entry into the plant or water loss from the leaves, respectively (Jia and Zhang, 2008).

Stomatal movements are encoded through Ca^{2+} signatures where a sudden increases in $[Ca^{2+}]_{cyt}$ accompanied by PM depolarisations are characteristic of a short-term closure, while Ca^{2+} oscillations are likely to program a long-term closing of the stomata (Allen *et al.*, 2001). The glutamate receptor AtGLR3.1 displays a comparatively strong gene expression within stomatal guard cells (Cho *et al.*, 2009). An overexpression of this GLR has implications on the long-term closure due to significant variations in Ca^{2+} oscillations and signatures leading to constantly open stomata (Cho *et al.*, 2009). The observed aberrant Ca^{2+} fluctuations probably still permit the burst-like calcium influxes characteristic of a short-term closure since the overexpression of this putative calcium channel would allow for typically massive Ca^{2+} influx. However, subtle Ca^{2+} oscillations that stimulate a long-term closure would no longer be attainable if this system is disturbed by an uncontrolled expression of AtGLR3.1.

The programming of the stomata apparatus likely involves amino acids as potential ligands for GLRs. In a study by Yoshida *et al.* (2016), it was shown for the first time that glutamate promotes stomatal closure in Arabidopsis, and that the effects of the glutamate could be prevented by a GLR antagonist (AP-5). Both actions strongly influenced the Ca^{2+} fluxes across the PM of the guard cells, implying that GLR-mediated Ca^{2+} signatures are a prerequisite for stomata closing. This hypothesis is supported by the fact that the knockout of AtGLR3.5 desensitises the plant against the activities of both glutamate and AP-5 (Yoshida *et al.*, 2016). However, a study by Kong *et al.* (2015) points to a methionine-gated GLR mediation of Ca^{2+} signatures essential for stomatal closing. Here, it could be shown that the amino acid L-

methionine also promotes an AtGLR3.1/-3.5-dependent Ca^{2+} influx that was significantly diminished in the respective AtGLR knockout lines (Kong *et al.*, 2016).

The knockout of another member of the same clade (AtGLR3.4) appears to affect the photosynthetic apparatus directly (Teardo *et al.*, 2010). In this plant line, photosystem II shows a decreased capacity for non-photochemical quenching and a reduction of the photosynthetic yield in general. Furthermore, applications of GLR antagonists significantly decrease, in a dose-dependent manner, oxygen production in spinach (Teardo *et al.*, 2011). Taken together, the involvement of several GLRs in photosynthesis expands the significance of GLR-mediated calcium signalling to this crucial metabolic plant pathway.

1.1.7.6 Transduction of Plant Stress Signalling by GLRs

Abiotic stresses including cold, touch and wounding are found to provoke an upregulation of GLR gene expression in *Arabidopsis thaliana* (Meyerhoff *et al.*, 2005). Cellular acidification and osmotic stress also lead to enhanced transcript levels of the glutamate receptor AtGLR3.4. Since these gene upregulations are prevented by an application of a nonspecific cation channel blocker (La^{3+}), it is conceivable that Ca^{2+} signatures encode a stress-triggered upregulation of GLR gene expressions which would then support computing of the actual stress responses. Observations made in *Oryza sativa* regarding a similar gene regulation of OsGLRs during cold, salt and drought stress, as well as the findings that the overexpression of a rice GLR in *Arabidopsis thaliana* confers enhanced salt tolerance, point to a universal feature of GLRs in mediating abiotic stress reactions in different plant species (Lu *et al.*, 2014; Singh *et al.*, 2014).

A sophisticated mechanism in which glutamate could fulfil the role of a second messenger by mediating Al^{3+}-induced stress responses during the experience of aluminium toxicity appears to exist in Arabidopsis, too (Sivaguru *et al.*, 2003). The Al^{3+}-induced root growth inhibition as well as PM depolarisations and microtubule depolymerisations can be suppressed by a treatment of the root with either an antagonist of GLRs or unspecific cation channel blockers such as Ga^{3+}. It is noteworthy that, blockage of aluminium channels by 5-nitro-2-(3-phenylpropylamino) benzoic acid prevents the effects of Al^{3+} within the plant cell but the application of glutamate still causes a PM depolarisation and microtubule disassembly. Sivaguru *et al.* (2003) stipulated the hypothesis that the actual response for aluminium toxicity originates from a glutamate-binding at the apoplastic ligand-binding domain of GLRs that in turn induces Ca^{2+} signatures decoding the actual Al^{3+} stress response. While Al^{3+} is likely

perceived by its respective receptors at the PM, this recognition appears to trigger only a release of glutamate out of the cell. This secreted apoplastic glutamate could function as a secondary messenger, activating the actual calcium channels. Verification of this hypothesis by other studies would indicate a role for glutamate as a releasable secondary messenger similar to its function in animal neurotransmission.

1.1.7.7 Abscisic Acid Pathways are Affected by GLR Activities

The plant hormone ABA and its signalling pathway are found to be targets of various GLRs in *Arabidopsis thaliana*. ABA is, among others, a mediator of seed dormancy and its levels are strongly increased in AtGLR1.1 knockout lines. This increase does not only cause prolonged seed dormancy but also delayed seed development and weakened root growth (Kang *et al.*, 2004). Furthermore, the transgenic plants are characterized by an elevated drought tolerance due to additional ABA-mediated stomatal closure. The increased hormone levels are likely caused by an elevation of ABA biosynthesis gene expression and a suppression of proteins involved in ABA desensitisation (Kang and Turano, 2003; Kang *et al.*, 2004). However, the exact pathway in which AtGLR1.1 could be regulating ABA production and plant responsiveness is still unknown.

Nonetheless, two more findings support the idea of a GLR-mediated transmission of ABA signals. First, a treatment with a GLR antagonist (DNQX) further increases the already elevated hormone levels in the AtGLR1.1 knockout line but it exerts no effects in wildtype plants (Kang and Turano, 2003). Second, a simultaneous application of glutamate mitigates both the effects of an AtGLR1.1 knockout and the antagonism of DNQX (Kang and Turano, 2003). The observed phenomena can be explained when assuming AtGLR1.1 as the common target for both ligands.

In accordance with this data, another GLR of clade III has been found to be part of ABA-mediated development processes in *Arabidopsis thaliana*. The knockout or overexpression of AtGLR3.5, which is predominantly in germinating seeds expressed, severely affects Ca^{2+} signatures involved in ABA-mediated seed germination (Kong *et al.*, 2015). Plants overexpressing AtGLR3.5 are less sensitive to ABA, while its knockout causes a hypersensitivity to this plant hormone. A measurable reduction of a Ca^{2+}-induced $[Ca^{2+}]_{cyt}$ increase in the AtGLR3.5 knockout line is accompanied by a reduction of transcript levels of Ca^{2+} sensing proteins (Kong *et al.*, 2015). Together with the fact that the exogenous application

of calcium counteracts the prolonged inhibition of seed germination in the knockout line, it appears that under normal conditions AtGLR3.5 mediates an increase in $[Ca^{2+}]_{cyt}$ which inhibits the plant's responsiveness to ABA during seed germination.

1.1.7.8 A Role for GLRs in Plant Immunity

First indications for an involvement of GLRs in the plant's immune system were based on the finding that an application of glutamate or asparagine desensitizes plants to a subsequent microbe-associated molecular pattern (MAMP) treatment (Kwaaitaal *et al.*, 2011). MAMP-triggered Ca^{2+} influxes are severely reduced in a dose-dependent manner after the amino acid treatment, indicating a preceding activation of the respective channels by the GLR agonists. A pretreatment with glutamate, furthermore, impaired a Ca^{2+} signature-dependent activation of defence genes by MAMPs. Apparently, glutamate acts downstream of pathogen-induced signalling cascades since not only MAMPs but also other pathogen-secreted molecules like cryptogein and residues of pathogen-induced cell wall degradation such as oligogalacturonides, are less effective in triggering an immune response if a previous application of glutamate occurs (Vatsa *et al.*, 2011; Manzoor *et al.*, 2013).

Cryptogein was also found to trigger a glutamate efflux into the apoplast and that this process is susceptible to exocytosis inhibitors (Vatsa *et al.*, 2011). Since these inhibitors reduced the cryptogein-induced $[Ca^{2+}]_{cyt}$ elevations, it is thought that, similar to the plant's response to aluminium toxicity (see Sivaguru *et al.*, 2003), glutamate could function as a secondary messenger to the actual stress stimulus. Anyway, the pathogen-triggered increases in $[Ca^{2+}]_{cyt}$ by cryptogein or oligogalacturonides, are greatly diminished after a previous application of glutamate which hints at a desensitisation of the respective calcium channels.

A treatment with GLR agonists alone appears to be sufficient to influence plant immune responses under certain conditions. Glutamate was found to activate MAPKs involved in plant immune responses (MAPK3, -4 and -6) while a treatment with GLR antagonists prevented the glutamate-induced MAPK activations (Kwaaitaal *et al.*, 2011). Furthermore, common GLR antagonists were also found to inhibit glutamate-induced Ca^{2+} variations as well as downstream immune responses such as the productions of reactive oxygen species or nitric oxide and the upregulation of defence genes (Vatsa *et al.*, 2011; Manzoor *et al.*, 2013). In addition, the plant's

defence capabilities against biotrophic and necrotrophic pathogens were severely hampered after a treatment with the GLR antagonist DNQX (Manzoor *et al.*, 2013).

The direct involvement of GLRs in plant immunity is also indicated by biotic stress-induced up- and downregulation of genes belonging to AtGLR clades I and III, respectively (Manzoor *et al.*, 2013; Roy and Mukherjee, 2017). In accordance with this data, a knockout of members of clade III amplifies the susceptibility to pathogens and downregulates the expression of plant defence genes (Manzoor *et al.*, 2013; Mousavi *et al.*, 2013). Besides a weakened immune response, the knockout of clade III genes causes reduced PM depolarisations associated with the transmission of wounding signals, indicating a role of the respective GLRs in biotic stress signal transduction (Mousavi *et al.*, 2013). The phloem-based forwarding of wounding signals from one leaf to another is severely impaired in AtGLR3.3 and -3.6 double knockout lines whereas AtGLR3.5 appears to be crucial for the propagation of signals from the wounding site to non-neighbouring leaves (Mousavi *et al.*, 2013; Salvador-Recatalà, 2016).

Taken together, GLRs seem to play a pivotal role in plant immune defence reactions and they are connected to various other processes of plant physiology, too. Their involvement is likely based on their function as amino acid-gated calcium channels. Glutamate receptors in plants could either operate as sensory proteins conveying only the plants actual amino acid status or they could function as transmembrane receptors evoking essential Ca^{2+} signatures through the secondary messenger-like activity of amino acids such as glutamate, interlacing them in the here-described physiological phenomena (Figure 4).

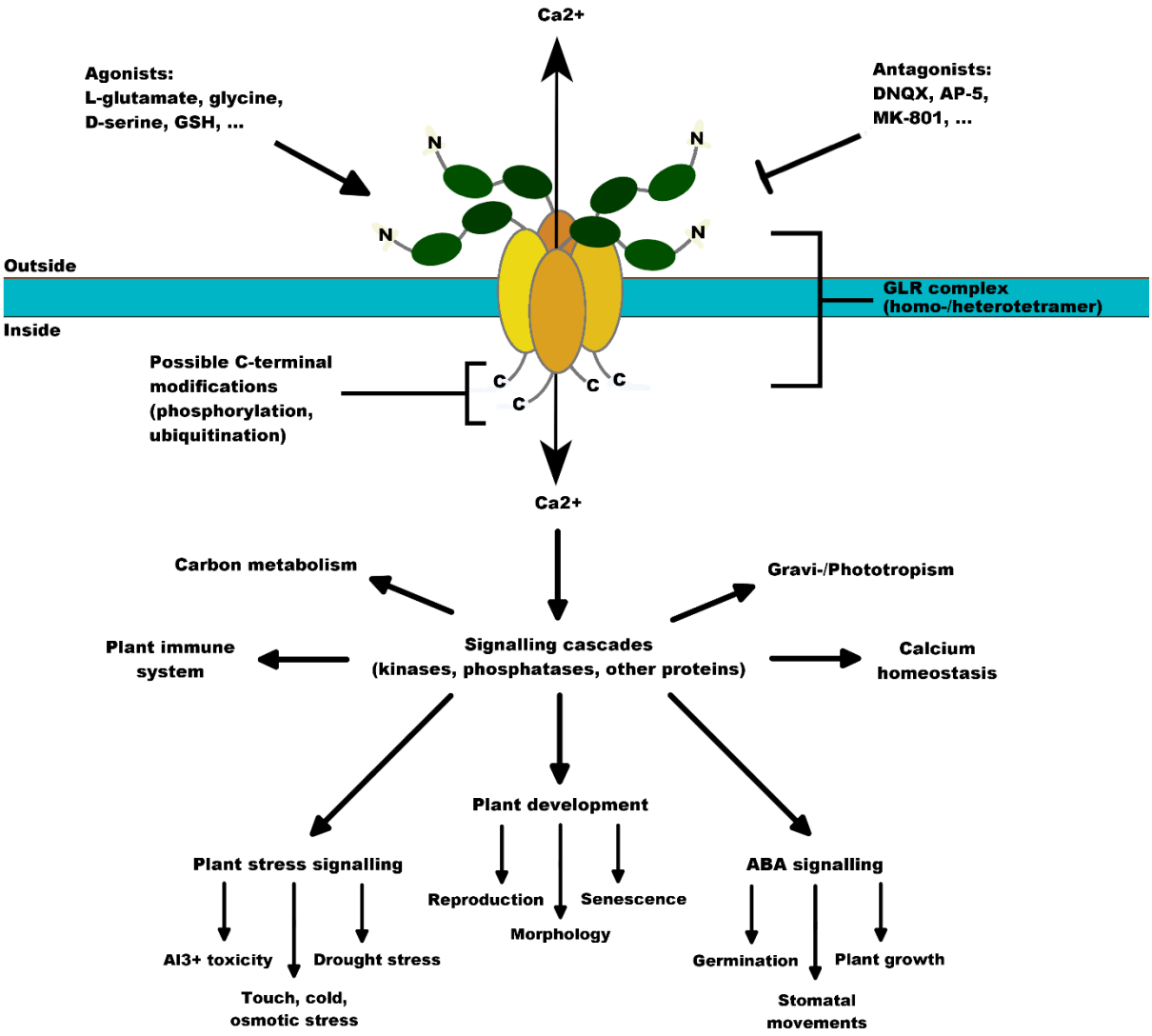

Figure 4. **Illustrated Overview of a Functional Transmembrane GLR Receptor Complex and its Potential Involvement in Plant Physiology.** The complex is depicted as four GLR subunits (yellow) with intracellular C-termini prone to cellular modifications (grey) and extracellular ligand-binding domains within the N-terminal region (green). GLRs are proposed to convey calcium fluxes across various cellular membranes (blue) i.e. the PM as well as mitochondrial and plastid membranes. The created Ca^{2+} signatures are proposed to be involved in a broad spectrum of physiological processes. Illustration first published in Weiland *et al.* (2015).

1.2 Physiology of *Arabidopsis thaliana*

1.2.1 Root System

1.2.1.1 Root Apical Meristem

The sessile nature of most plants implies the need to adapt growth and development during the plant's life cycle. A high degree of developmental flexibility is achieved by a coordinated and fine-tuned growth regulation at the shoot and root tips where the primary meristems are located, namely the shoot apical meristem (SAM) and RAM (Palmer *et al.*, 2012). Both apical meristems harbour pluripotent stem cells that are continuously producing new cells allowing for a post-embryonical supply of additional plant tissues. These new cells differentiate subsequently into all known cell types found in plants (Benfey and Scheres, 2000).

The QC is the region within the RAM that contains the only occasionally dividing stem cells which is made up of four cells in *Arabidopsis thaliana*. These four cells maintain the overall structure of the RAM by affecting the surrounding cells which are called stem cell initials, through gradients of phytohormones and transcription factors (TF) (Drisch and Stahl, 2015). Both the cells in the QC and the stem cell initials are essential for the consecutive, mitotic activity of the adjacent, shorter-lived stem cells. Asymmetrical divisions of these ephemeral cells produce daughter cells that maintain their cytokinetic state and form the proximal parts of the root tip while at the same time substitute stem cells close to the QC (van den Berg *et al.*, 1997).

1.2.1.2 Root Architecture

The root system is essential for most plant species since it fulfils the task of anchoring the organism in its current position and providing the possibility to acquire water and nutrients from the soil. The uptake of these compounds, including essential ions and other chemical substances, occurs mostly in this part of the plant either in an active or passive way. The arrangement of the roots differs significantly between monocotyl and dicotyl plants. While the first form a predominantly fibrous root system, the latter develop a tap root system like it is found in *Arabidopsis thaliana* (Hochholdinger *et al.*, 2004).

In the case of Arabidopsis, an embryonical-initiated primary root is accompanied by several lateral roots that are formed during post-embryo stages. Lateral roots are then produced by root primordia-forming secondary meristems within the primary root that emanate from pericycle cells that regain their cell division capabilities (Pacheco-Villalobos and Hardtke, 2012). The

shape and development of the root is affected by endogenous factors such as genetic programs and exogenous causes like the availability of nutrients (phosphorus, nitrogen, etc.) and ions (potassium, sodium, etc.) (Tian *et al.*, 2014).

Besides taking up essential compounds from the soil, the root enables communication to other organisms. Here, an information exchange is facilitated between the plant and beneficial or harmful bacteria and fungi as well as other plant species. In the latter case, plants have been found to be capable of differentiating between strangers and individuals from the same species, called Kin recognition (Baluška *et al.*, 2009). The structure and development of the root system, therefore, plays an important role in the plant's ability to grow and its capacity to endure competition with other organisms.

1.2.1.3 Partition of the Root into Different Zones

The root of *Arabidopsis thaliana* can be divided into four distinct zones (Verbelen *et al.*, 2006). The root apex contains mitotic cells whose cell division activity provides a permanent stock of new cells. This region is called the meristematic zone (MZ) and it can be categorized by radial-stretched and lengthwise-shortened cells. The slenderness of this cell type seen in images of longitudinal sections of the root, has its origin in ongoing symmetric cell divisions. The following region is called the transition zone (TZ) and it is characterized by square-shaped cells that undergo physiological changes in preparation for elongation. Cells in this part of the root have a strongly reduced mitotic activity and they start to develop a central vacuole and a polarized cytoskeleton. Furthermore, the cell wall is remodelled in order to stretch the cells longitudinally. Proximal to the TZ, cells begin to expand rapidly along the root axis within the elongation zone (EZ). These cells drastically alter their cell wall composition to enable fast, turgor-driven cell elongation. When they reach their final size, cells start to differentiate into the various cell types found within the root. This region is called the differentiation zone (DZ) and it is situated proximal to the EZ (Dolan *et al.*, 1993).

1.2.2 Shoot System

1.2.2.1 Shoot Apical Meristem

In plants, all aerial parts are produced by the SAM either directly by meristems located at the shoot apex or indirectly by secondary meristems situated at proximal parts of the shoot (Ha *et al.*, 2010). The SAM of *Arabidopsis thaliana* produces the stem which is characterized by theoretically indeterminate growth whereas the plant's leaves originate from descendants of the SAM (leaf primordia) which are defined by a limited growth capacity (Steeves and Sussex, 1989). The meristematic tissues of the above-ground plant organs contain pluripotent stem cells akin to those in animals. These cells provide a constant supply of new cells and renew themselves at the same time, which allows this region to operate throughout the plant's lifecycle (Aichinger *et al.*, 2012).

The SAM comprises three layers while the uppermost layers L1 and L2, called tunica, constitute the surface of the tissue, and the layer L3 forms the corpus of the meristem. Both L1 and L2 are clearly distinct from each other and their cells divide anticlinally. The organisation of L2, however, begins to fade and becomes more dispersed at the onset of organ formation. Viewing the SAM from a cell division rate perspective, the upper part of the meristem contains a small group of very slowly dividing cells called the central zone. This zone is responsible for meristem maintenance and it constitutes the actual stem cells similar to the QC in the root. On the opposite, cells at the periphery of the SAM are characterized by an increased cell division rate relative to the central zone, and it is this part of the meristem that effectively creates new plant organs such as leaves and additional plant tissues like the elongation of the stem.

A group of founder cells in this region form the outgrowing organ primordium and they are characterized by accelerated proliferation and cell expansion rates in order to allow a proper growth (Traas and Doonan, 2001). During the first period, cells in the organ primordium proliferate continuously and their cytoplasm remains densely packed. The steady cell divisions lead also to a constant cell size in this tissue (Schopfer *et al.*, 2006). Cells farther way from the meristem cease to proliferate at a distinct range and enter a phase of cell elongation. In this phase, their vacuole increases in size and cell wall modifications occur in order to enable cellular expansion (Cosgrove, 2005). Here, in addition to the cell enlargement, their DNA content usually starts to increase due to endoreduplication events, completing the final stage of cell maturation in the newly formed plant organ (Donnelly *et al.*, 1999). The shift from cell division to cell elongation (and finally maturation) is often described as an arrest front moving from the tip of the developing organ to the base of the primordium (White, 2006).

The initial cell division activity strongly influences the ultimate size of the organ and, therefore, the duration of cell proliferation events is spatially as well as temporally strictly-controlled since these early events determine the final cell number of the plant organ. An example of such a connection between cell number/initial cell divisions and terminal organ size can be found in the formation of leaves. There, the spatial extension of the cell proliferation area at the base of the primordium, as well as the velocity of cell cycling, greatly affect the final leaf size (Rojas *et al.*, 2009; Ichihashi *et al.*, 2010).

1.2.2.2 Rosette and Inflorescence Stem

The SAM produces all the plant's above-ground tissue, including the rosette. Most of the rosette growth occurs during the vegetative phase in *Arabidopsis thaliana*. During that growth period, the plant stem remains strongly reduced and newly formed rosette leaves are spirally-arranged at very short internodes. The planar disposition of the leaves optimizes the available photosynthetic plane around the plant while minimizing an overlap in order to avoid shading of the underlying leaves (Rodriguez *et al.*, 2014). During the vegetative growth period, Arabidopsis plants are rather two-dimensional structures aiming for the highest possible photosynthetic yield just above the soil surface.

The transition from a vegetative state to the reproductive state is characterized by the onset of elongation of the plant shoot system. Here, the SAM changes its character to become an inflorescence meristem, producing the main stem as well as lateral side bolts (Alvarez-Buylla *et al.*, 2010). These reproductive processes lead to a loss of the almost two-dimensional character of the plant by an emergence of the long, vertically-extending stem from the horizontally-orientated rosette. Furthermore, cauline leaves are formed from pre-existing leaf primordia underneath the lateral inflorescence stems and flowers, as the principal inflorescence organs, originate at the respective shoot apices which later on harbour the plant siliques and its developing seeds (Hempel and Feldman, 1995).

1.2.3 Salt Stress and Tolerance

1.2.3.1 Perception of Salt Stress

Salt stress is a major factor impeding plant growth and survival. Elevated levels of sodium chloride within the soil pose a severe challenge to plant fitness due to a twin effect. First, the heightened ionic concentration causes an osmotic stress and it impairs the plant's water uptake capabilities. Second, the accumulation of Na^+ and Cl^- ions originating from an augmented ion gradient within the plant, disrupts metabolic processes and negatively affects photosynthetic yields (Sahi *et al.*, 2006; Teakle and Tyerman, 2010). Several strategies have been evolved in plants to counteract these effects. Plants can (I) try to prevent ion uptake, (II) produce osmotically active particles, called osmolytes, such as organic compounds (proline, sugar alcohols, polyamines, etc.) belonging to the late embryogenesis abundant (LEA) superfamily, (III) take up inorganic ions to counterbalance or compartmentalize Na^+ in vacuoles or (IV) exclude Na^+ from photosynthetic tissues (Tarczynski *et al.*, 1993; Blumwald, 2000).

The perception of a hyperosmotic environment or elevated Na^+ concentrations is not yet fully understood in detail. However, there is sufficient evidence to suggest that plants can sense and distinguish osmotic and ionic stress (Kumar *et al.*, 2013). Whatever the actual sensor might be, alterations of cellular Ca^{2+} concentrations are a clear response of the plant when dealing with salt stress (Knight *et al.*, 1997). Plants naturally encounter elevated salt concentrations within the soil and several studies have confirmed the role of the root system in producing the associated Ca^{2+} signatures (Tracy *et al.*, 2008). Therefore, a role for this part of the plant as a point of origin for salt stress perception and early responses connected with $[Ca^{2+}]_{cyt}$ variations is highly likely. Furthermore, most of the relaying molecules such as annexins or reactive oxygen species (ROS) are part of a broader Ca^{2+} signalling network (Laohavisit *et al.*, 2012; Jiang *et al.*, 2013).

There is evidence for the activation of calcium-dependent protein kinases (CDPK), calcineurin B-like proteins (CBL) and CBL-interacting protein kinases (CIPK) during an encounter with high concentrations of Na^+ (Harmon *et al.*, 2000; Weinl and Kudla, 2009). The progression of Ca^{2+} signals associated with salt stress could activate TFs like calmodulin-binding transcription activators (CAMTA), GT element-binding-like proteins (GTL) and TFs of the myeloblastosis (MYB) family (Yoo *et al.*, 2005; Weng *et al.*, 2012; Pandey *et al.*, 2013). These TFs are transcriptionally regulated within the root cortex cells upon triggering a salt stress response and they themselves alter expression levels and patterns of salt stress-associated genes (Geng *et al.*, 2013).

1.2.3.2 Salt Tolerance

Salt tolerance in plants is mainly conferred by the sequestration and transportation of Na^+ within the plant body or by balancing the Na^+-induced ionic stress by a reallocation of K^+ ions (Schroeder *et al.*, 2013). The PM of root cells is one of the principal entry points for Na^+. Here, ion channels such as CNGCs and GLRs could allow the passage of monovalent sodium cations (Hua *et al.*, 2003; Tapken and Hollmann, 2008). Another possibility is the flow of Na^+ into the root through anti-/transporters comparable to the rice transporter OsHKT2;1 which mediates Na^+ influxes under K^+ starvation or the *Arabidopsis thaliana* cation/H^+ antiporter AtCHX21 which carries Na^+ from endodermal cells into the root stele (Hall *et al.*, 2006; Horie *et al.*, 2007). Both strategies aim at maintaining biologically active Na^+ concentrations as low as possible.

A similar method is employed during sequestration of sodium ions into the vacuole. The tonoplast-localized Na^+/H^+ exchanger, NHX1, and the PM-localized Na^+/H^+ antiporter, NHX7, are examples of transporters involved in this crucial task. NHX1 sequesters Na^+ out of the cytosol and stores the ion within the vacuole where it can no longer disrupt vital cellular processes (Blumwald and Poole, 1985). However, the antiporter NHX7 becomes active when Na^+ ions have already entered the cell, after which it mediates Na^+ flux back out of the cell (Qiu *et al.*, 2002). The establishment of a high potassium:sodium ratio in leaves is another way to counteract salt stress. A special family of passive Na^+ transporters (HKT class I) removes Na^+ from the xylem vessels and translocates the ions into xylem parenchyma cells while simultaneously stimulating a K^+ flux in the opposite direction via K^+ outward-rectifying channels (Sunarpi *et al.*, 2005). In this way, the redistribution of K^+ allows to counterbalance the ionic disproportion (Schroeder *et al.*, 1994). Further examples include inward- and outward-rectifying K^+ channels and the rice K^+ transporter OsHAK5 that confers a relatively high salt tolerance when expressed in BY2 tobacco cells (Schroeder *et al.*, 1987; Horie *et al.*, 2011).

1.2.4 Plant Immune System

Plants are continuously attacked by microbial or viral pathogens and they had to develop an adequate immune system in order to defend themselves properly. The first barrier that must be overcome by pathogens is the cuticle on top of the epidermal cells. However, there are more obvious entry points for bacteria and viruses through stomata, hydathodes or wounds. Since plant cells lack the mobile defender cells common in animals, each plant cell is required to provoke its own defence reactions while systemic signalling from wounding/infection sites to adjacent and distant parts of the plant must be active throughout the plant body (Dangl and Jones, 2001).

1.2.4.1 Pattern-Triggered Immunity (PTI) and Pattern-Recognition Receptors (PRR)

Currently, it is stated that plant cells possess at least two different mechanisms to recognize a pathogen attack. Pathogen perception can occur through high-affinity transmembrane pattern-recognition receptors (PRR) on the surface of the plant cell where these receptors bind distinct microbial-/pathogen-associated molecular patterns (MAMP/PAMP) (Monaghan and Zipfel, 2012). MAMPs/PAMPs are slowly evolving structures that recognize common pathogen patterns such as bacterial flagellins or the elongation factor Tu (EF-Tu) (Zipfel and Felix, 2005; Zipfel *et al.*, 2006).

Most of the PRRs are leucine-rich repeat (LRR) receptor kinases or lysine motif (LysM) kinases that become active upon binding of specific MAMPs/PAMPs. However, there are also some PRRs that lack a kinase domain and therefore need a co-receptor to transduce the perceived signals properly. In any case, the recognition of pathogens by PRRs triggers an immunity response (PTI) which leads to variations in gene expressions, mostly through transcriptional regulations that inhibit pathogenic infection (Monaghan and Zipfel, 2012).

1.2.4.2 Effector-Triggered Immunity (ETI) and Nucleotide-Binding(NB)-LRR proteins

Pathogens, on the other hand, attempt to suppress the plant's immune responses by releasing their own molecules to block intracellular signalling or to inactivate associated genes/proteins within the host. Extracellular bacteria like *Pseudomonas syringae* can use their type III secretion system to inject type III pathogen effectors into the host cell. These effectors impede a proper vesicle trafficking, block RNA pathways or change the function of specific organelles (Block and Alfano, 2011). Another system to infiltrate the host is employed by fungi and

oomycetes. These organisms develop infectious hyphae or haustoria to connect with the host cell in order to obtain nutrients as well as to supress simultaneously the host's immune response by releasing their own pathogen effectors (Mendgen and Hahn, 2002). Aphids and nematodes, on the other hand, use their corrosive salivary to penetrate the cuticle and to digest parts of the plant cell wall while concurrently silencing the plant's immune system (Bos *et al.*, 2010).

As a response to these rather sophisticated strategies employed by the pathogens, plants have developed their own polymorphic receptors that are capable of detecting those pathogen effectors. These plant receptors are encoded by disease resistance genes organized in multigene clusters (R genes). The translated proteins are called NLR proteins since they contain a characteristic nucleotide-binding(NB)-LRR protein domain. However, NLR proteins are only effective against biotrophic or hemi-biotrophic pathogens but they are useless against a necrotrophic attack (Glazebrook, 2005).

NLR proteins become selectively activated depending on the used effector and the attacking pathogen (Chae *et al.*, 2016). The perception of effectors is kingdom-independent since pathogens employ similar strategies and cause comparable defence reactions in various hosts. The ETI and activation of NLR proteins occurs either via direct binding of the pathogen effector or by recognition of an effector-altered cellular target within the host cell (Dodds *et al.*, 2006; van der Hoorn *et al.*, 2008). Upon activation, other proteins and cofactors such as TFs are recruited through the N-terminal region of NRL proteins in order to elicit consecutive gene upregulations or protein modifications (Chang *et al.*, 2013).

1.2.4.3 Plant Immune Responses

Upon triggering PTI or ETI, there are several ways in which plants can respond to a pathogen attack. One way is an enhanced production and relocation of specific receptor-like kinases (RLK) or receptor-like proteins (RLP) to the PM to further specify the recognition of the pathogen on the basis of its PAMPs/MAMPs. The intracellular kinase domain of these receptors phosphorylates their respective substrates and transduces the signal further downstream (Macho and Zipfel, 2015). Three different classes of molecules can be recognized by such receptors: (I) proteins/molecules specific to the pathogen comprising distinct groups of the bacterial cell wall polysaccharides or cell wall chitins of fungi (Miya *et al.*, 2007; Macho and Zipfel, 2015), (II) enzymes released by the pathogen in order to disrupt the cuticle (cutinases) or cell wall (cellulases, xylanases, pectin lyases) (Boller and Felix, 2009) and (III) molecules that originate

from the pathogen-induced breakdown of the cell wall (oligogalacturonides) or the PM (membrane lipids) (Galletti *et al.*, 2008; Ruelland *et al.*, 2015).

The stimulation of immunity-related RLKs often leads to an activation of the phytohormones salicylic acid, ethylene and jasmonic acid which cause an upregulation of R gene expression through TFs or the various cofactors of RLKs (Lumba *et al.*, 2010). Salicylic acid is mostly involved in biotrophic pathogen responses and it is perceived by the TF NPR1 that translocates into the nucleus after the binding of this phytohormone (Furniss and Spoel, 2015). Jasmonic acid and ethylene mainly take part in necrotrophic pathogen attacks and their pathways can lead to an increase in cell wall thickness (Lloyd *et al.*, 2011).

MAPKs play a pivotal role in immune response-related signal transduction. Their main function lies in mediating signals from the perceiving receptors further downstream where they can cause a change in gene expression patterns or an altered cellular organisation. MAPKs belong to the family of serine/threonine protein kinases and they often form a cascade of at least three different enzymes which phosphorylate/activate another sequentially (Colcombet and Hirt, 2008). The progression of a specific MAPK cascade often results in an activation of TFs, phospholipases or cytoskeletal proteins that in turn activate distinct sets of genes. Involvements of MAPKs in various plant processes such as cell proliferation, plant development, stress and immune signalling have been confirmed over the past several years (Taj *et al.*, 2010). The immune response of *Arabidopsis thaliana* against *Pseudomonas syringae,* for instance, involves the phosphorylation of MAPK4 and a subsequent release of the TF WRKY33 in order to induce the biosynthesis of the phytoalexin camalexin (Rushton *et al.*, 2010).

WRKY33 is only one example for various other TFs that are involved in plant immunity. These protein types are responsible for the controlled expression of R genes that can translate metabolites that are that are then used against a vast array of pathogens (Alves *et al.*, 2014). Those metabolites and proteins may be antimicrobial like phytoalexins (pathogen-induced expression) and phytoanticipins (constitutive expression) or they function as detoxifiers and eliminate toxins and other virulence factors (Ahuja *et al.*, 2012; Nawrot *et al.*, 2014). There are also other protein conjugates which impair pathogen progress by reinforcing cell walls via the deposition of callose or phenolic compounds (Yogendra *et al.*, 2014). The delivery of such metabolites in *Arabidopsis thaliana* takes place via vesicle trafficking at the pathogen infection

site and it encompasses penetration resistance 3 (PEN3) or ATP-binding cassette (ABC) transporters (Frescatada-Rosa *et al.*, 2015).

1.2.5 The Plant Cell Cycle and Endoreduplications

The cell cycle is a universal feature of all eukaryotic cells. It comprises a phase of DNA synthesis (S-phase) as well as a mitotic phase (M-phase). Both phases are separated by gaps (G) in which G1 occurs after the M-phase and G2 happens after the S-phase. The mitotic phase is furthermore divided into four major stages (prophase, metaphase, anaphase and telophase) and it is followed by the subsequent cytokinesis. Cells can also exit the cell cycle by entering a phase of cell maintenance (G0) after the S-phase (Bray, 1987).

The cell cycle is crucial for proper plant development since plants need to adapt their growth in response to a constantly changing environment. This can be achieved by regulating the mitotic activities of the various plant meristems. A stimulation of cell divisions enables phylogenetic development or the renewal of lost parts like leaves, branches or roots. On the other hand, a downregulation of cell mitosis occurs when plants need to enforce innate processes such as defence reactions or an enhanced metabolism in order to prepare for dormancy. The control of cell division/differentiation is achieved through both endogenous signals including phytohormones and other regulating proteins as well as exogenous stimuli such as temperature, light intensity and wounding (Polyn *et al.*, 2015).

1.2.5.1 Cell Cycle Regulation

The mitotic cell cycle as a sequence of transitions through DNA synthesis (S), cytokinesis (M) and the respective gaps in between them (G1 and G2), is strictly governed by an array of key enzymes and their cofactors. CDKs and CYCs as their coactivators, play a fundamental role in the passage from one phase to another. There are several ways in which CDKs can be regulated and fine-tuned: (I) phosphorylation events on CDKs, (II) biosynthesis and degradation of CYCs, (III) interactions of CDK-inhibiting proteins with their respective CDK and (IV) dis-/assembly of CYC complexes (Scofield *et al.*, 2014).

Activated CDKs, in turn, phosphorylate a vast array of substrates essential for cell cycle progression and it was found that CDK activities oscillate over the course of the cell cycle in which they are reduced in G1 and reach a peak during the M-phase (Coudreuse and Nurse, 2010).

Cyclin-dependent kinases and cyclins

Two major classes of CDKs have been well described in plants: A-type CDKs (CDKA) and the plant-specific B-type CDKs (CDKB) (Veylder *et al.*, 2007). CDKAs are highly conserved serine/threonine-specific kinases having homologues in all kingdoms of life. In Arabidopsis, CDKA is encoded by only one gene (*CDKA;1*) whose expression level appears to be constant during the cell cycle. CDKBs of *Arabidopsis thaliana* are encoded by four different genes (*CDKB1;1*, *CDKB1;2*, *CDKB2;1* and *CDKB2;2*) and unlike CDKA;1, their gene expression is strictly regulated in mitotic cells. CDKB1s are upregulated starting from the S-phase and peaking in G2, whereas CDKB2s are progressively expressed from G2 to the M-phase (Sorrell *et al.*, 2001).

Translated CDKs, however, must be activated by the binding of their respective CYCs. The genome of *Arabidopsis thaliana* encodes for about 32 different CYCs but A- (CYCA), B- (CYCB) and D-type cyclins (CYCD) are the best studied and their involvement in the plant cell cycle is well understood (Wang *et al.*, 2004). CYCBs are tightly associated with CDKBs governing G2-to-M transitions and the M-phase whereas CYCDs are involved in G1-to-S transitions. CYCAs, on the other hand, control the progression from the S-phase to the M-phase.

Besides the binding of cyclins, CDKs are also regulated by various protein modifications such as the phosphorylation of a threonine residue within the T-loop region of CDKs by CDK-activating kinases which stimulates CDK functionality or phosphorylations of Tyr-14 or Tyr-15 by members of the WEE1 kinase family causing a deactivation of CDKs by blocking their ATP-binding site (Shimotohno *et al.*, 2004; Schutter *et al.*, 2007).

Progression from one phase of the cell cycle to another does not only require an expression/activation of new CDKs and their cofactors but also a deactivation of the now obsolete but still present CDK complexes. This can be achieved by proteasome-mediated degradation. Here, the anaphase-promoting complex (APC) and the SKP1/Cullin/F-box (SCF)-related complex are known for a direct degradation of CYCs and CDKs (Vodermaier, 2004). Another possibility of silencing CDKs is a termination of their activity by CDK inhibitors. Two major classes of CDK inhibitors exist in plants: The SIAMESE/SIAMESE-related (SIM/SMR) family and KIP-related proteins/interactors of CDKs (KRP/ICK) (van Leene *et al.*, 2010). While KRPs bind both CYCDs and CDKA;1 activated during the S-phase, SIM/SMRs inhibit not only CDKA;1 complexes but also the M-phase CDKB1;1 (Veylder *et al.*, 2001; Churchman *et al.*, 2006).

E2 promoter-binding factors (E2F), dimerization partners (DP) and 3-Myb-repeats (MYB3R)

Besides CDKs and their interaction partners, there are other important players in the plant cell cycle such as the adenovirus E2 promoter-binding factors (E2F) and their dimerization partners (DP), both representing crucial families of TFs. There are six E2Fs (E2Fa, E2Fb, E2Fc, E2Fd, E2Fe and E2Ff) present in *Arabidopsis thaliana*. E2Fa, E2Fb and E2Fc are positive regulators of genes active during the S-phase and they are only effective when bound as a dimer with one of the two DPs (DPa and DPb). E2Fd, E2Fe and E2Ff seem to be involved in a negative feedback loop that represses promoters formerly activated by E2Fa, E2Fb or E2Fc. These three repressing E2Fs lack a transactivation domain but they possess two DNA-binding domains in order to function as monomers, contrary to E2Fa, E2Fb and E2Fc which contain only one DNA-binding site, and therefore require DPs (Mariconti *et al.*, 2002).

The G1-to-S phase transition is characterized by an upregulation of S-phase-specific genes that were formerly suppressed by an E2Fc-DP dimer complex. This complex loses its inhibiting function due to phosphorylation events on E2Fc. At the same time, the transcriptional activator dimers E2Fa-DP and E2Fb-DP become phosphorylated, too, leading to a release of the bound retinoblastema-related protein (RBR1) that kept them in an inactive state. This relief, in turn, activates those protein complexes participating in the gene upregulations (Wildwater *et al.*, 2005).

The genome of *Arabidopsis thaliana* also encodes five TFs of the three-Myb-repeat family (MYB3R1 to MYB3R5). These transcriptional regulators of key genes of the G2-to-M-phase transition are thought to function either as repressors (MYB3R3 and MYB3R5 as well as MYB3R1 but only when in complex with MYB3R3 or MYB3R5) or activators (MYB3R1 (alone) and MYB3R4) of M-phase genes (Haga *et al.*, 2011; Kobayashi *et al.*, 2015). MYB3R proteins likely interact with the E2F-DP-RBR1 pathway and it appears that they bind to either transcription-activating E2Fs including E2Fb or gene-repressing E2Fs such as E2Fc (Kobayashi *et al.*, 2015). Interestingly, single as well as multiple gene knockouts of MYB3R family members cause deviations in plant organ growth as well as distortions in plant development. In addition, DNA damage responses appear to rely at least in part on the activity of the repressing MYB3Rs (Chen *et al.*, 2017).

Histone modifications

Changing chromatin accessibility for transcription is another way of up- or downregulating several genes/proteins at the same time. Histone modifications are known to cause an exposure or covering of DNA regions and their respective genes. This greatly affects the binding capabilities of TFs and other DNA-associated proteins.

Methylation events on lysine residues at the N-terminus of histone H3 are known to either supress or activate gene expressions depending on the position and quantity of the attached methyl groups. Tri-methylations at Lys-4 have been shown to coincide with a gene upregulation whereas tri-methylations at Lys-27 cause a repression of gene expressions (Zhang *et al.*, 2009; Roudier *et al.*, 2011). In this respect, gene suppression is achieved through a network of tri-methylated Lys-27 and other protein complexes. This network allows for stable gene repression in mitotically active cells maintaining an undifferentiated state. The affected gene expression includes members of auxin-related proteins (i.e. auxin transporters and receptors) and it therefore likely involved in the distribution of auxin maxima (Lafos *et al.*, 2011). Interfering with the correct methylation of Lys-4, on the other hand, can cause plant developmental defects such as a reduced leaf size or weakened root growth due to inadequate cellular differentiation (Guo *et al.*, 2010; Yao *et al.*, 2013).

Histone modifications are also crucial for DNA synthesis during the S-phase of the cell cycle where the chromatin needs to be uncoiled in order to have its replication origins accessible for DNA replication polymerases (Desvoyes *et al.*, 2014). In this way, sequential alterations of the histone structure are a part of complex series of cell cycle transitions, but they are also needed for a proper cell maintenance and differentiation.

1.2.5.2 Endocycle: DNA Endoreduplication during the Cell Cycle

Polyploidy as a state in which more than two paired chromosomes are present within the cell, can be found in various plant tissues such as the seed endosperm, fruits, roots, leaves and the hypocotyl. Leaf cells of *Arabidopsis thaliana*, for example, can reach a polyploidy level of 32C (32-fold increase of its genomic DNA copies). It is known that the level of polyploidy is linked to cell growth/elongation and it contributes to a correct leaf development (Melaragno *et al.*, 1993). The increased DNA content in polyploid cells could be a necessity for large cells in order to function on an elevated metabolic level. Furthermore, the surplus of chromatin could

have also a protective effect against DNA-damaging radiation or agents since additional gene copies would substitute the disrupted ones.

The evolution of polyploidy in *Arabidopsis thaliana* could also be involved in a compensatory cell growth to counterbalance a decrease in cell numbers or an impaired meristematic activity. It was shown that the effect of a reduced cell number in Arabidopsis leaves due to a diminution in cell divisions is alleviated by an increase in cell size. These larger cells exhibit a higher DNA content because of an augmentation of endoreduplication events (Skirycz *et al.*, 2011).

In general, endoreduplications/endocycles are cell cycles in which the M-phase is bypassed as a result of a continuing alternation of S-phase and G1. Here, nuclear breakdown, chromosome condensation and spindle formation are partially or completely skipped. Since chromosome separation does not occur due to the absent cytokinesis, various rounds of endoreduplication cause the polyploid state of the cell, which is often permanent. Therefore, high polyploidy levels are most often connected to cell differentiation/maturation.

The cell cycle machinery employed in endocycling cells is similar to the one present in mitotically dividing cells. However, there is a need for the repression of the majority of proteins essential for chromosome separation and cell division active during the G2 and M-phase (Fox and Duronio, 2013). Here, M-phase CDKs must be downregulated or deactivated while CDKs imperative for the S-phase must remain switched on to keep the endocycle running (Nowack *et al.*, 2012). These regulations are controlled mainly either by CDK-inhibiting proteins including KRPs or CDK-activating cofactors like CYCs. Furthermore, TFs such as E2Fs are likely involved in the endocycle control, too (Veylder *et al.*, 2012). An oscillating gene expression of these TFs allows a cycling between the various S-phases, where the activity of E2Fs promotes genome replication by stimulating the expression of S-phase-promoting CYCs (Zielke *et al.*, 2011).

2 Material and Methods

2.1 Generation of Transgenic *Arabidopsis thaliana*

2.1.1 Vector Construction

2.1.1.1 pBI-AtGLR3.7

The full-length coding sequence of *AtGLR3.7* (TAIR accession: AT2G32400.1) was obtained by PCR amplification from a cDNA of *Arabidopsis thaliana* ecotype Columbia (Col-0) using forward (5' – CGA TAT CCC GGG ATG GGA CTG GGC ATT GAC – 3' including SmaI restriction site) and reverse (5' – CAT CGC TTA ATT AAT CAA TTT CGT GGT ACC TCA GTA TCA G – 3' including PacI restriction site) primer. The PCR product was cloned into a modified version of pBI121 containing an additional PacI restriction site within its multiple cloning sites. Expression of *AtGLR3.7* was controlled by the 35S promoter of the pBI121 vector.

2.1.1.2 pMDC7-AtGLR3.7

The full-length coding sequence of *AtGLR3.7* was obtained by PCR amplification from a cDNA of *Arabidopsis thaliana* (Col-0) using forward (5' – CGA TAT GGC GCG CCA TGG GAC TGG GCA TTG - 3' including SgsI restriction site) and reverse (5' – CAT CGC TTA ATT AAT CAA TTT CGT GGT ACC TCA GTA TCA G – 3' including PacI restriction site) primer. The PCR product was cloned into the vector pMDC7. The 17-β-estradiol inducible expression of the insert was under control of the XVE inducible promoter of the pMDC7 vector.

2.1.2 Bacterial Transformation via Electroporation

The constructed pBI-AtGLR3.7 and pMDC7-AtGLR3.7 vectors were transformed into *Escherichia coli* strain MC1061 via electroporation (2.5 kV; 200 Ω; 25 µF). Resistant colonies were selected on lysogeny broth (LB) agar plates containing streptomycin (100 µg mL^{-1}; *Escherichia coli* MC1061 selection) and either kanamycin (50 µg mL^{-1}; pBI-AtGLR3.7 selection) or spectinomycin (100 µg mL^{-1}; pMDC7-AtGLR3.7 selection). Positive clones were verified by colony PCR covering the border of the respective promoter and the beginning of the inserted *AtGLR3.7* sequence as well as by plasmid digestion using SmaI/PacI (pBI-AtGLR3.7) or SgsI/PacI (pMDC7-AtGLR3.7) restriction enzymes. Correct base pair (bp) sequences of the *AtGLR3.7* inserts were verified by DNA sequencing (Centro Interdipartimentale di servizi per

le biotechnologie die interesse agrario, chimico, industrial (CIBIACI) - Via Romana 25-29/Rosso, 50125 Firenze, Italy).

Both vectors were further transformed into *Agrobacterium tumefaciens* strain GV3101 via electroporation (2.5 kV; 200 Ω; 25 µF) and resistant colonies were selected on yeast extract broth (YEB) agar plates containing rifampicin (10 µg mL^{-1}) and gentamicin (30 µg mL^{-1}) for *Agrobacterium tumefaciens* GV3101 selection as well as either kanamycin (50 µg mL^{-1}; pBI-AtGLR3.7 selection) or spectinomycin (100 µg mL^{-1}; pMDC7-AtGLR3.7 selection).

LB Medium

Tryptone	10 g
Yeast extract	5 g
NaCl	10 g
(Agarose)	(15 g)
ddH_2O	Added up to a final volume of 1 L

LB medium's pH was adjusted to 7.0 before autoclaving for 20 min at 121°C, 103.421 kPa. Antibiotics were added when the medium had cooled down to about 60°C after autoclaving. Agarose (15 g) was added before autoclaving when solid medium was required.

YEB Medium

Beef extract	5 g
Yeast extract	1 g
Peptone	5 g
Sucrose	5 g
$MgSO_4$	0.3 g
(Bacto agar)	(20 g)
ddH_2O	Added up to a final volume of 1 L

YEB medium's pH was adjusted to 7.0 before autoclaving for 20 min at 121°C, 103.421 kPa. Antibiotics were added when the medium had cooled down to about 60°C after autoclaving. Bacto agar (20 g) was added before autoclaving when solid medium was required.

2.1.3 Transformation of *Arabidopsis thaliana* (Col-0) via Floral Dip

The pBI-AtGLR3.7 and pMDC7-AtGLR3.7 vectors in *Agrobacterium tumefaciens* GV3101 were transformed into *Arabidopsis thaliana* (Col-0) using the floral dip method by Clough and Bent (1998). Plants at the flowering stage were dipped into a solution of Agrobacteria harbouring the respective vector. Collected seeds were surface sterilized and selected on Murashige-Skoog (MS) agar plates containing kanamycin (50 µg mL^{-1}; plant selection for pBI-AtGLR3.7) or hygromycin B (10 µg mL^{-1}; plant selection for pMDC7-AtGLR3.7). Homozygous plants harbouring either pBI-AtGLR3.7 (designated OE:AtGLR3.7(1), -(2) and -(3)) or pMDC7-AtGLR3.7 (designated I:AtGLR3.7(1) and -(2)) were obtained in the T3 generation using segregation assays.

MS Medium

MS salt	4.3 g
Sucrose	10 g
MES	0.5 g
(Phytagel)	(4 g)
ddH_2O	Added up to a final volume of 1 L

MS medium's pH was adjusted to 5.7 before autoclaving for 20 min at 121°C, 103.421 kPa. Antibiotics were added when the medium had cooled down to about 60°C after autoclaving. Phytagel (4 g) was added before autoclaving when solid medium was required.

2.2 Plant Growth Conditions and Plant Development Evaluations

2.2.1 Standard Plant Growth Conditions

All plant genotypes used in this study had the background of *Arabidopsis thaliana* Col-0. The *AtGLR3.7* knockout line, atglr3.7, was kindly provided by Prof. Lai-Hua Liu (China Agriculture University Beijing, China). Different plant genotypes and growth conditions were used depending on the experiment. If not explicitly mentioned, the standard growth conditions that followed were applied.

Sterile growth conditions were maintained by surface sterilization of Arabidopsis seeds. Rough sterilization was done in 70% ethanol for 1 min, followed by a thorough sterilization in a sterilization solution for 10 min. Seeds were washed at least five times in sterile ddH_2O.

Sterilized seeds were either (I) plated on sterile filter paper in a petri dish and stored at 4°C in darkness, (II) plated directly on sterile ½ MS-agar medium in round (90 mm) or square-shaped (120x120 mm) petri dishes or (III) put in liquid, sterile MS-medium for hydroponic growth.

Sterilization Solution

Bleach	50%
ddH_2O	50%
Polysorbate 20 (Tween-20)	0.05%

Plants were always stratified for 3 d at 4°C in darkness before they were transferred to controlled growth chambers (temperature: 22°C; light intensity: 110 mmol m^{-2} s^{-1}; photoperiod: 16 h light/8 h dark; humidity: 70%).

The plant age was calculated based on seed imbibition and therefore included the stratification period of 3 d (DAI: days after imbibition).

2.2.2 Plant Image Analysis

Rough measurements were done observing plants by eye (e.g. stage of development) or measuring crude growth parameters such as stem growth using a flexible ruler. For a more detailed analysis, individual plants or parts of them were digitalized with either a scanner or a camera. The acquisition of microscopic images was accomplished using three different microscope types: a stereomicroscope 'SteREO Lumar.V12' ('AxioCam MRm Rev.3') (Carl Zeiss), an inverted fluorescence microscope 'AxioObserver Z1' ('AxioCam MR3') (Carl Zeiss) and confocal laser scanning microscope (CLSM) 'Confocal Leica TCS SP5' (Leica). Analysis of the obtained images/videos was done with the respective manufacturer software. Additional image analysis was conducted with the free, open-source software 'ImageJ' (https://imagej.nih.gov/ij/) and 'GIMP' (https://www.gimp.org/).

2.2.3 Evaluation of Plant Growth in Darkness (Skotomorphogenesis)

Arabidopsis seeds were sown on square-shaped ½ MS agar plates. After stratification, petri dishes were wrapped in aluminium foil and transferred to growth chambers. Seedlings were grown in a vertical position for ten days. At the end of the experiment, plates were digitalized with a scanner and hypocotyl elongation as well as primary root length measured with 'ImageJ' software.

2.2.4 Interpretation of Root Growth

Root growth measurements were done using sterilized Arabidopsis seeds sown on ½ MS agar in petri dishes. After stratification, plants were transferred to a growth chamber and root growth was marked with a pen on the petri dish in distinct time periods ranging from one to three days. At the end of the desired growth period, petri dishes were digitalized using a scanner and evaluated using 'ImageJ' and 'GIMP' image-analysing software. Depending on the experiment, the MS agar may have contained specific chemicals (e.g. amino acids, 17-β-estradiol, etc.) that were sterile-filtered and added to tepid MS medium/agar after autoclaving.

The inducible expression of *AtGLR3.7* in I:AtGLR3.7(1) and I:AtGLR3.7(2) was initiated by growing these plants and Col-0 as a control on ½ MS agar containing 5 µM 17-β-estradiol. The effect of glutamate on plant growth was observed by growing Col-0, atglr3.7 and OE:AtGLR3.7(2) on ½ MS agar containing 50, 250 or 1,000 µM L-glutamate (D-glutamate served as a negative control). Mock treatments were performed using standard ½ MS agar.

2.2.5 Analyses of Rosette Growth and Stem Development

Plants were grown in soil under standard conditions. Pictures with a reference marker were taken with a camera. Photographing continued daily for six days after the rosette reached its final size, about 35 DAI. Image analysis was performed with 'ImageJ' software.

Stem growth was measured with a flexible ruler starting about 23 DAI when the inflorescence stems emerged. The number of side bolts and branches on the main stem were counted by eye. All measurements were recorded at intervals of every two to three days.

2.2.6 Plant Biomass and Relative Water Content Assays

Plants were grown in soil or sterile on petri dishes and harvested at distinct time points with a minimum growth period of three weeks. Fresh weight (FW) was measured by directly weighing the plant material on a precision micro scale immediately after collecting the plants. The plant material was then transferred into a beaker filled with water. After 3 h, the weight of the plant material was measured again and recorded as turgid weight (TW). The plant material was then put in a drying oven at 70°C overnight. The dried material was removed from the oven and permitted to adjust to room temperature and humidity for about 24 h before it was again measured, and the new weight recorded as dry weight (DW). The following formula was used to calculate the relative water content of the plant material (RWC):

Equation 1. $$\mathrm{RWC} = \frac{\mathrm{FW}-\mathrm{DW}}{\mathrm{TW}-\mathrm{DW}} * 100$$

2.3 Characterization of the Root Apical Meristem

2.3.1 Visual Observations of Roots Using CLSM

All observed plant lines were grown under sterile standard conditions. Root growth was measured daily, and a root length of 2.5 cm was selected as a time point for marking detailed observations of the RAM. This approach was used to circumvent any possible developmental variations among the different genotypes which could have affected the formation and therefore the size and characteristics of the meristem. By using the primary root length as a reference instead of the plant age, the focus was placed only on root development. The reference root length of 2.5 cm was reached at the earliest on 8 DAI, allowing the primary root to grow for at least five days. This growth period is considered to be sufficient to finalize the RAM formation (Perilli *et al.*, 2012).

After reaching the selected root length, plants were removed from the ½ MS agar plate and stained with 50 µM propidium iodide in order to visualize the cell wall. This staining allowed for the mapping of root tip cells by CLSM. Z-stacks composed of 20 slices with an average step size of 3 µm were created near the root tip to capture the three-dimensional structure of the root.

2.3.2 Kinematic Analyses of Root Growth and the Characterization of the RAM

Kinematic analyses are based on the concept of the single root row as a continuum of several cell development stages that can be observed simultaneously in one image of the root tip (Erickson and Silk, 1980). In short, cells of the root emanate from cell division events close to the QC and progress along the root axis, i.e. they remain in their position and change only in size while the root conducts distal elongation/growth. Cells that keep dividing are located within the meristem, while cells that cease to divide and start to reprogram their cell cycle are found in the TZ. Afterwards, cells begin to elongate within the EZ until they reach their final cell size in the DZ. These zones can be roughly distinguished from each other by the cell shape and size within them, with respect to their progenitors and successors within the cell row.

2.3.2.1 Determining the Extension of the Meristematic Zone

In this work, the MZ comprises the meristem and the TZ, and its extension was estimated by mapping the distribution of cells on the basis of their individual cell morphology along the root axis starting from the QC. Cells within the meristem as distal parts of the MZ are characterized by a low cell length(CL):cell width(CW) ratio (CR). CR approaches '1' in the TZ as the proximal part of the MZ and increases significantly in the EZ. Combining these features with a general comparison of cell size (CS) and CL, as well as its distance from the QC (DQ), allows for the characterization of individual cells within a single cell row. A unique value for each individual cell (CI) can be calculated based on CL and the position of the cell within the root as a combination of DQ and the number of its preceding cells (CN):

Equation 2. $$\mathrm{CI} = \frac{\mathrm{CL}}{\mathrm{CN} * \mathrm{DQ}}$$

The comparison of CI values allows an estimation of cell characteristics and together with the aforementioned features it enables a reasonable evaluation of the end of the MZ and the beginning of the EZ. The border between these zones can be determined by a particular 'jump' of the respective cell morphology from one profile to another. These 'jumps' can be measured and each investigated trait (CR, CL, CS, and CI) may supply several 'jumps' to the total characterisation of a single cell. Only cells that were characterized by multiple 'jumps' were

considered possible border cells. Only such cells were employed for a determination of the MZ extension.

Since the plant root is made of several cell rows and each row has a different distribution of meristematic cells, MZ length can vary in one individual root from one cell row to another. Therefore, four cortical and four epidermal cell rows were mapped for one single plant while two of each originated from a tangential section plane and two from a radial section plane. CL does not differ within the different planes. On the other hand, CW exists in two different dimensions (tangential: CW_t; radial: CW_r). All three parameters together allowed a calculation of the total cell volume/CS:

Equation 3. $$\mathrm{CS} = \mathrm{CL} * \mathrm{CW_t} * \mathrm{CW_r}$$

2.3.2.2 Computing the Meristematic Activity of the RAM

The quantitative and qualitative analysis of dividing cells within the RAM was based on a study of Fioriani and Beemster (2006). The following formulas were taken from that study and adapted to calculate the following features for single cell rows and the meristem as a whole:

Equation 4. Cell production rate of the meristem (CPM):

$$\mathrm{CPM} = \frac{\mathrm{E}}{\mathrm{CL_{mat}}}$$

where E is the elongation rate of the root [µm h^{-1}] and CL_{mat} is the mature cell length [µm].

Equation 5. Average cell division rate (ADR):

$$\mathrm{ADR} = \frac{\mathrm{CPM}}{\mathrm{N_{div}}}$$

where N_{div} is the number of dividing cells.

Equation 6. Theoretical cell cycle duration (CCD):

$$\mathrm{CCD} = \frac{\ln(2)}{\mathrm{ADR}}$$

Equation 7. Residence time within the RAM of progenitor cells (RTP) emanating from stem cell initials:

$$RTP = log_2(N_{div}) * CCD$$

2.4 Molecular Analyses

2.4.1 Gene Expression Analyses in *Arabidopsis thaliana*

Arabidopsis thaliana was grown under standard conditions either in soil or sterile in hydroponics as a bulk of seedlings. Plants were harvested after two to three weeks or on 14 DAI, respectively. The plant material was immediately frozen in liquid nitrogen and used for RNA purification or stored at -80°C for later use. The frozen tissue was homogenized in plastic tubes with tungsten carbide beads using a bed mill 'TissueLyser II' (Qiagen). RNA extraction was done with 'Trizol Reagent' (Invitrogen, Cat No. 15596026) according to the manufacturer's instructions. Transcription of RNA from transgenic and wildtype plants into cDNA was done using 'QuantiTect Reverse Transcription Kit' (Qiagen, Cat No. 205311). Primer pairs for the genes of interest (GOI) were designed with the free-available software 'NCBI/Primer-BLAST' (https://www.ncbi.nlm.nih.gov/tools/primer-blast/) to choose an optimal annealing temperature (T_m) and a PCR product length of about 100-150 bp for each GOI. A detailed list of the used primer pairs and RT-PCR conditions can be found in section 7.1 'List of Primer and PCR Conditions for RT-PCRs'.

Semi-quantitative RT-PCR (sqRT-PCR) analyses were conducted using 'DreamTaq DNA Polymerase' (Thermo Fisher Scientific, Cat. No. EP0703). Quantitative RT-PCR (qRT-PCR) was conducted using 'SsoAdvanced™ Universal SYBR® Green Supermix' (Bio-Rad Laboratories, Cat. No. 1725270) employing a 'Rotor-Gene Q 5plex HRM' (Qiagen, Cat. No. 9001580) thermocycler. Image analysis of sqRT-PCR data was done with the free-available software 'GelAnalyzer 2010' (http://www.gelanalyzer.com/) which allowed a precise band detection and background subtraction.

2.4.2 Measurement of the Nuclear DNA Content

Arabidopsis thaliana was grown under sterile conditions and seedlings were harvested 14 DAI. Plants were prepared following established protocols (see Otto, 1990; Dolezel and Göhde, 1995). Briefly, about 20 mg of plant tissue was chopped with a razor blade in 500 µL of ice-cold Otto I buffer. The suspension of released nuclei was filtered over a 42 µm nylon mesh and resuspended in 2 mL of Otto II buffer containing 4 µg mL^{-1}. The nuclei were analysed with 'CyFlow® Space' (Sysmex, Cat. No. CY-S-3001) (30 nuclei per second; about 4,000 nuclei in total). Data were analysed with the manufacturer software 'FloMax'. All experiments regarding an estimation of the nuclear DNA content were done in collaboration with Dr. Beáta Petrovská (Institute of Experimental Botany AS CR, Olomouc, Czech Republic).

Otto Buffer I

Citric acid monohydrate (100 mM)	4.2 g
Tween 20 (0.5%; v/v)	1 mL
ddH_2O	Added up to a final volume of 200 mL

Otto Buffer II

Na_2HPO_4	28.75 g
ddH_2O	Added up to a final volume of 200 mL

2.4.3 Quantitative and Qualitative Protein Analyses

2.4.3.1 Protein Extraction and SDS-PAGE

Total protein extraction for AtMAPK3/-6

Arabidopsis thaliana was grown under sterile standard conditions in hydroponics and harvested on 14 DAI. Plants were immediately frozen in liquid nitrogen and ground with a bed mill 'TissueLyser II' (Qiagen). Proteins were extracted in 'Total Protein Extraction Buffer'. Proteins were purified via centrifugation at 12,000 g at 4°C for 20 min. Protein quantitates were calculated using 'Bio-Rad Protein Assay Kit I' (Bio-Rad, Cat. No. 5000001) following the manufacturer's instructions. Samples (15 mg) were separated by SDS-PAGE in a 10% separating gel.

Total Protein Extraction Buffer

Tris-HCl (pH 7.5)	50 mM
NaCl	200 mM
Ethylenediaminetetraacetic acid (EDTA)	1 mM
NaF	10 mM
Sodium orthovanadate	2 mM
Sodium molybdate	1 mM
Glycerol	10% (v/v)
Tween20	0.1%
Phenylmethylsulfonyl fluoride (PMSF)	1 mM
Dithiothreitol (DTT)	1 mM
13-protease-inhibitor cocktail P9599 (Sigma-Aldrich, Cat. No. 00677817)	µL per 15 mg FW

SDS-PAGE	Separation Gel	Stacking Gel
ddH_2O	4.1 mL	6.1 mL
Acrylamide/bis (30%; 37.5:1)	3.3 mL	1.3 mL
Tris–HCl (1.5 M; pH 8.8)	2.5 mL	2.5 mL
SDS (10%)	100 µL	100 µL
Tetramethylethylenediamine (TEMED)	10 µL	10 µL
Ammonium persulfate (APS) (10%)	32 µL	100 µL

Histone H3: Membrane-bound protein extraction

The extraction of membrane-bound proteins followed the protocol of Abas and Luschnig (2010). Briefly, *Arabidopsis thaliana* was grown under sterile standard conditions in hydroponics and harvested on 14 DAI. Plant material (150 mg FW) were immediately frozen in liquid nitrogen and ground with a bed mill 'TissueLyser II' (Qiagen). A clear homogenate was prepared by suspension of the plant material in 'Membrane-Bound Protein Extraction Buffer'. The homogenate was mixed with 5% polyvinylpolypyrrolidone (PVPP) (based on plant FW) and centrifuged at 600 g for 3 min at 22°C. The supernatant was diluted with water and centrifuged at 18,000 g for 3 h at 4°C. The supernatant was discarded, and the membrane pellet was washed twice with 'Wash Buffer' followed by a centrifugation step at 18,000 g for 1.5 h. Protein quantities were calculated by using 'Bio-Rad Protein Assay Kit I' following the manufacturer's instructions. Samples (15 mg) were separated by SDS-PAGE in a 12% separating gel.

Membrane-Bound Protein Extraction Buffer

Tris–HCl (pH 7.5, 20°C)	100 mM
Sucrose	25% (w/w; 0.81 M)
Glycerol	5% (v/v)
EDTA (pH 8.0)	10 mM
EGTA (pH 8.0)	10 mM
KCl	5 mM
Dithioerythritol (DTE)	1 mM
Casein	0.2-0.5% (w/v)
Benzamidine HCl	5 mM
Phenylmethylsulfonyl fluoride (PMSF)	1 mM
E-64 protease inhibitor (Sigma-Aldrich, Cat. No. E3132)	2 µg mL^{-1}
Pepstatin A	0.7 µg mL^{-1}
Aprotinin	1 µg mL^{-1}
Leupeptin	1 µg mL^{-1}
Pefabloc-SC	1 mM
Disodium β-glycerophosphate	20 mM
NaF	50 mM
Na_2MoO_4	2 mM
Na_3VO_4	0.2 mM
Okadaic acid	2 nM

Wash Buffer

Tris-HCl (pH 7.5)	20 mM
EDTA	5 mM
EGTA	5 mM
Phenylmethylsulfonyl fluoride (PMSF)	1 mM

2.4.3.2 Coomassie Brilliant Blue R-250 Protein Staining

Polyacrylamide gels were treated with 'Fixing Solution' on a shaker overnight and subsequently put in 'Staining Solution' where they were kept on a shaker for 2-4 h. Gels were then destained in 'Clearing Solution' for 24 h with regular changes of the medium. Destained gels were scanned and digitally analysed using 'ImageJ' software.

	Fixing Solution	Staining Solution	Clearing Solution
Methanol	50 %	50 %	5 %
Acetic acid	10 %	10 %	7.5 %
Coomassie Brilliant Blue R-250	---	0.25 %	---
ddH_2O	40 %	40 %	87.5 %

2.4.3.3 Immunoblotting

Separated proteins by SDS-PAGE were blotted on a 0.1 um pore nitrocellulose membrane and dried. Plots were Ponceau-stained (0.2% w/v Ponceau S, 5% glacial acetic acid) in order to verify protein transfer. Plots were then washed three times for 5 min with 'Washing Solution' and incubated in 'Blocking Solution' for 1 h. After the blocking, plots were washed three times for 5 min in 'Washing Solution' and transferred to 'Primary Antibody Solution' consisting of TBST and the respective antibody overnight (for further details see section 7.2 'Antibodies for Protein Quantification and Qualification'). Subsequently, plots were washed three times for 5 min in 'Washing Solution' and transferred to 'Secondary Antibody Solution' consisting of TBST and the respective antibody for 3 h. Plots were washed three times for 5 min in 'Washing Solution' before they were developed using 'SuperSignal™ West Pico PLUS Chemiluminescent Substrate' (Thermo Fisher Scientific, Cat. No. 34080). Visualization was done by exposure on 'CL-XPosure™ Film' (Thermo Fisher Scientific, Cat. No. 34090). Exposed films were digitized, and the intensity was evaluated using ImageJ software.

Solutions	Blocking	Washing
Tris–HCl (pH 7.5)	20 mM	20 mM
NaCl	150 mM	150 mM
Tween20	0.1%	0.1%
Bovine serum albumin (BSA)	3%	---

2.5 Determination of Plant Physiology Parameters

2.5.1 Ion Content Assay of *Arabidopsis thaliana*

Arabidopsis plants were grown under standard conditions in soil for three weeks. Plants were harvested and dried in an oven at 60°C for 24 h. The dried tissue was ground with a mortar and pestle, and digested in a volume of 0.5 M HNO_3 depending on the amount of plant FW (2.5 mL per < 20 mg; 5 mL per 20-50 mg, 10 mL per 50-100 mg) at room temperature on a shaker for 48 h in darkness. Samples were diluted with ddH_2O and analysed with a photoelectric flame photometer 'Digiflame 2000 DV710' (Sarin). Standard curves were calculated based on known concentrations of sodium, potassium and calcium ions ranging from 0 to 100 ppm in standard solutions containing either NaCl for Na^+, KCl for K^+ or $CaCl_2$ for Ca^{2+}. The final ion concentration was given in mmol mg^{-1} plant DW.

2.5.2 Identification of Plant Salt Stress Tolerance

Salt stress tolerance was investigated by using sterile Arabidopsis seedling grown under standard conditions and transferred to ½ MS agar plates containing NaCl concentrations of 50, 250 or 1,000 mM as well as agar plates without salt (mock treatment) on 7 DAI. After transferring, plants were grown for further seven days under salt stress conditions in a growth chamber under standard conditions. Root growth was marked daily with a marker on the bottom of the petri dish. At the end of the experiment, plates were digitalized with a scanner and daily root growth was analysed using 'ImageJ' software.

2.5.3 *Pseudomonas syringae* Pathogenicity Assays in *Arabidopsis thaliana*

Transgenic and wildtype *Arabidopsis thaliana* were grown under standard conditions in soil for four to five weeks. *Pseudomonas syringae* strain pv. tomato DC3000 (Pto DC3000) and a non-virulent version named Pto DC3000 hrcC (kindly provided by Kenichi Tsuda, Max Planck Institute for Plant Breeding Research, Cologne, Germany) were used to test the plants' immune response capabilities against Pseudomonas. Bacteria were grown overnight at 23°C in nutrient-yeast-glycerol (NYG) medium containing 25 µg mL^{-1} rifampicin for bacterial selection. Upon reaching an OD_{600} < 2, bacteria were harvested by centrifugation at 6,000 rpm for 3 min and washed twice in 5 mM $MgSO_4$. Bacterial dilutions with an OD_{600} of 0.0002 were prepared in 5 mM $MgSO_4$ and infiltrated into two leaves (number 6 and 7) of the *Arabidopsis thaliana* rosette using a needleless syringe. Thus, inoculated bacteria had a density of 10^4 CFU mL^{-1}. All assays were repeated at least four times on leaves from different plants and the full experiment was conducted twice.

Bacterial growth was investigated 48 h after infection by excising two leaf discs (0.5652 mm^2 in total) from each infected leaf using a circular cutter. Both discs were transferred into 400 µL 5 mM $MgSO_4$ buffer and the tissue was ground in a bed mill 'TissueLyser II' (Qiagen, Cat. No. 85300). The homogenate was diluted (10^{-1}, 10^{-10} and 10^{-100} for Pto DC3000; 10^{-10}, 10^{-100} and 10^{-1000} for Pto DC3000 hrcC) and plated on NYG plates containing 25 µg mL^{-1} rifampicin. After 48 h at 28°C, the plates were digitalized, and the colonies were counted using 'ImageJ' software.

NYG Medium

Peptone	5 g
Yeast extract	3 g
Glycerol	20 g
ddH_2O	Added up to a final volume of 1 L

NYG medium's pH was adjusted to 7.0 before autoclaving for 20 min at 121°C, 103.421 kPa. Antibiotics were added when the medium had cooled down to about 60°C after autoclaving.

3 Results

3.1 *AtGLR3.7* Expression Levels

Arabidopsis thaliana (Col-0) was transformed with the constructed vector pBI-AtGLR3.7 via floral dip. The expression level of *AtGLR3.7* in three different overexpression lines (OE:AtGLR3.7(1), -(2) and -(3)), an *AtGLR3.7* knockout line (atglr3.7) and Col-0 were roughly determined by sqRT-PCR (Figure 5B). Primers for only a short fragment of the original 2,766 bp gene length of *AtGLR3.7* were used to estimate its mRNA levels after transcription into cDNA. A very faint band was amplified in the sample containing cDNA of atglr3.7. The sample of Col-0 produced a distinct bright band at a height of about 450 bp. Samples with cDNA from OE:AtGLR3.7(1), OE:AtGLR3.7(2) and OE:AtGLR3.7(3) produced markedly brighter bands on the agarose gel. The highest intensity was observed for OE:AtGLR3.7(3) followed by OE:AtGLR3.7(2). OE:AtGLR3.7(1) showed the lowest intensity band of all overexpression lines.

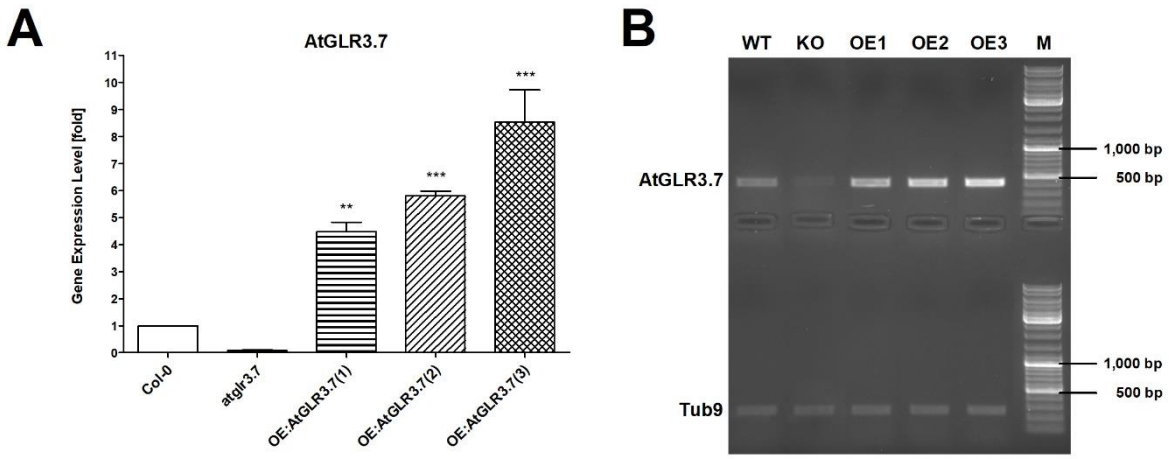

Figure 5. **Gene Expression Levels of *AtGLR3.7*.** Data was obtained from three different overexpression lines OE:AtGLR3.7(1) (OE1), OE:AtGLR3.7(2) (OE2) and OE:AtGLR3.7(3) (OE3) as well as in the knockout line atglr3.7 (KO) and Col-0 (WT) *Arabidopsis thaliana* by qRT-PCR (A) and sqRT-PCR (B). Plants were grown sterile in hydroponics and harvested on 14 DAI. *Tubulin beta 9 chain* (*Tub9*) served as a reference gene. qRT-PCR data were related to *Tub9* expression and normalized to Col-0. PCR products represent a unique segment of the respective gene sequence with a length of 150 and 450 bp for *Tub9* and *AtGLR3.7*, respectively. Statistical analyses among genotypes were conducted using a one-way ANOVA and Dunnett's *post hoc* test; $n = 3$. Asterisks indicate significant deviations from Col-0 with $^{**}\rho < 0.01$ and $^{***}\rho < 0.001$. Error bars indicate SE. Marker (M; 'GeneRuler DNA Ladder Mix', Thermo Fisher Scientific; Cat. No. SM0331).

In order to verify and determine the exact *AtGLR3.7* expression levels in all five plant lines, qRT-PCR was conducted on three individual sets of about ten Arabidopsis plants for each genotype grown in hydroponics (Figure 5A). The highest expression of *AtGLR3.7* was confirmed for OE:AtGLR3.7(3) with a highly significant fold expression of 8.54±2.06 when compared to Col-0. Similarly, OE:AtGLR3.7(2) showed a highly significant fold expression of 5.81±0.31. OE:AtGLR3.7(1) was characterized by a lower but still significant fold expression of 4.47±0.62. The knockout line atglr3.7 exhibited a fold expression of 0.08±0.04.

3.2 Plant Growth

3.2.1 Characterization of Seeds

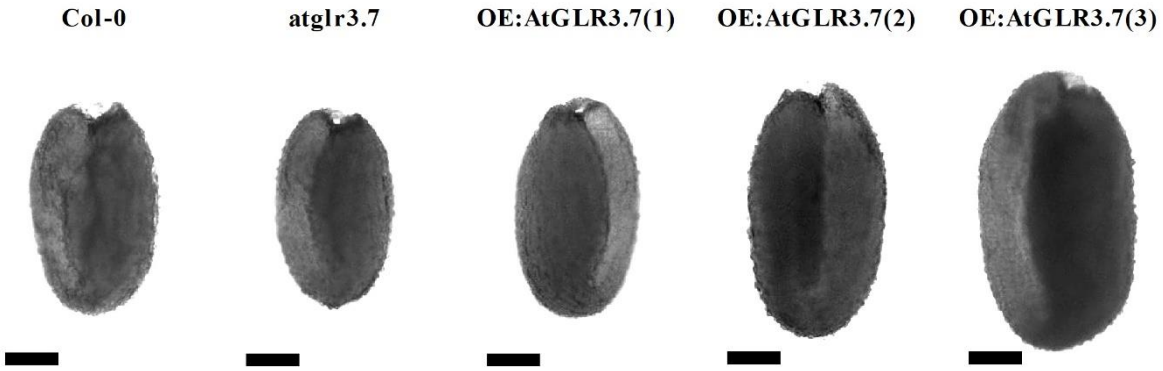

Figure 6. **Morphological Comparison of Seeds.** Seeds of Col-0, atglr3.7, OE:AtGLR3.7(1), OE:AtGLR3.7(2) and OE:AtGLR3.7(3) serving as examples for the respective *Arabidopsis thaliana* line. Siliques containing the displayed seeds were harvested from ten-week-old plants. Black bars represent 100 µm.

An investigation of the different plant phenotypes began with observations regarding the seeds of Col-0 and the transgenic plant lines atglr3.7, OE:AtGLR3.7(1), OE:AtGLR3.7(2) and OE:AtGLR3.7(3). An increase in total seed size was noted for all *AtGLR3.7* overexpression lines whereas the knockout line exhibited a slightly reduced seed size (Figure 6).

More in-depth measurements revealed highly significant variations among all plant lines in the four tested parameters (seed area, perimeter, major and minor axis) (one-way ANOVA, $\rho < 0.0001$, n = 68-108). The overexpression lines were generally characterized by an increase in the observed seed characteristics when compared to Col-0 (Table 1). OE:AtGLR3.7(3) showed the strongest increase in seed area (37.36%), perimeter (20.46%) as well as major (12.22 %) and minor (13.09%) seed axis. Similarly, OE:AtGLR3.7(2) was also characterized by an overall

enlargement of its seed size (seed area: 22.06%, perimeter: 6.76%, major axis: 7.86% and minor axis: 16.56%). OE:AtGLR3.7(1) exhibited only a minor increase of its seed area (6.48%). A significant reduction in seed size was observed for atglr3.7, leading to a slight decrease of its seed area (-4.63%) and perimeter (-7.48%).

Table 1. **Detailed Characteristics of Seeds from Transgenic and Wildtype *Arabidopsis thaliana*.**

Plant line	**Seed area (mm^2 ± SD)**	**Seed perimeter (mm ± SD)**	**Seed major axis (mm ± SD)**	**Seed minor axis (mm ± SD)**
Col-0	0.108 ± 0.014	1.47 ± 0.12	0.502 ± 0.033	0.269 ± 0.022
atglr3.7	0.103 ± 0.014	1.36 ± 0.11 (***)	0.471 ± 0.035 (***)	0.281 ± 0.021 (**)
OE:AtGLR3.7(1)	0.115 ± 0.016 (*)	1.43 ± 0.12	0.491 ± 0.040	0.294 ± 0.022 (***)
OE:AtGLR3.7(2)	0.133 ± 0.016 (***)	1.56 ± 0.12 (***)	0.542 ± 0.032 (***)	0.314 ± 0.022 (***)
OE:AtGLR3.7(3)	0.149 ± 0.027 (***)	1.64 ± 0.17 (***)	0.568 ± 0.056 (***)	0.324 ± 0.030 (***)

Statistical analyses were conducted using a one-way ANOVA and Dunnett's *post hoc* test, n = 68-108; *$\rho < 0.05$, **$\rho < 0.01$ and ***$\rho < 0.001$.

3.2.2 Root Development

An observation of the plant root system and its development in transgenic and wildtype *Arabidopsis thaliana* aimed at investigating the effects of AtGLR3.7 on growth characteristics of the plants' underground tissue. The development of the root system on 14 DAI differed visually among the tested genotypes (Figure 7).

Continuous measurements over a period of 14 d allowed for a development-dependent characterisation of the plant's primary root length and its daily root growth. The root length of OE:AtGLR3.7(2) and -(3) showed a constant surplus compared to Col-0 while the root of atglr3.7 continued to be shorter than in wildtype plants (Figure 8A). A look on the daily root growth rate showed a significant, additional growth up to 41% on 7 DAI for OE:AtGLR3.7(3) compared to Col-0 (Figure 8B). This boost in root growth abated down to 30% on 9 DAI and only 6% on 13 DAI. The knockout of *AtGLR3.7* led to a constantly diminished daily growth compared to Col-0 down to -33% on 7 DAI and about -15% during later growth stages.

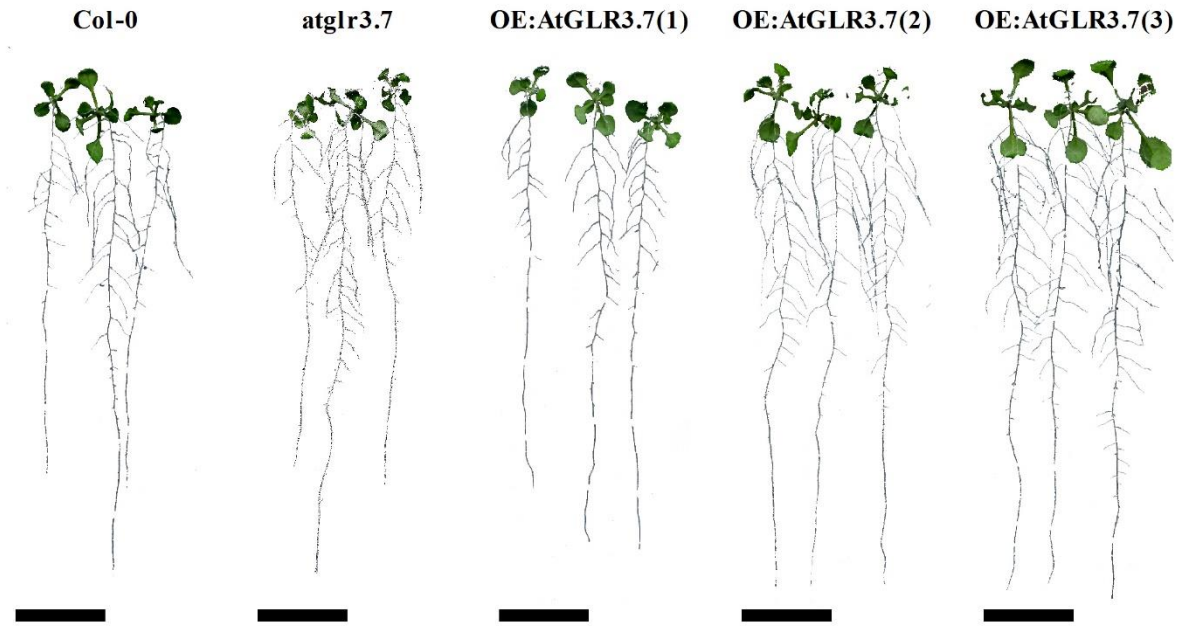

Figure 7. **Developed Root System on 14 DAI.** Seedlings serving as examples for the respective Arabidopsis plant line. Wildtype and transgenic *Arabidopsis thaliana* were grown in ½ MS agar for two weeks. Black bars represent 20 mm.

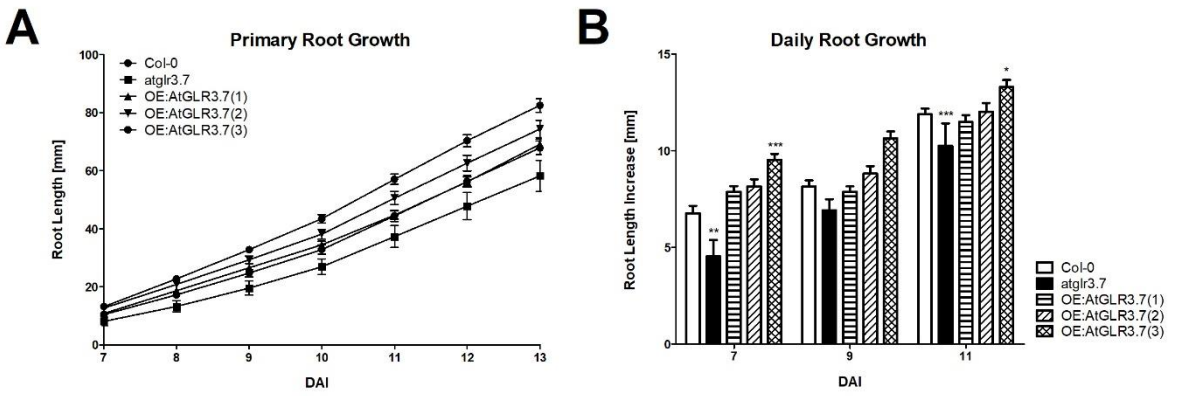

Figure 8. **Primary Root Length and Daily Root Growth.** Primary root length (A) and daily root growth (B) of wildtype and transgenic *Arabidopsis thaliana* grown on ½ MS agar were measured regularly for two weeks. Daily measurements started from 7 DAI onwards. The *AtGLR3.7* overexpression lines showed an increase in primary root length whereas atglr3.7 was characterized by a reduction in primary root development. Statistical analyses among genotypes were conducted using a one-way ANOVA and Dunnett's *post hoc* test; n = 11-19. Asterisks indicate significant deviations from Col-0 with *$\rho < 0.05$, **$\rho < 0.01$ and ***$\rho < 0.001$. Error bars indicate SE.

An investigation of the root architecture showed no significant quantitative or qualitative deviations in lateral root development among the tested plant lines (Table 2). However, atglr3.7 exhibited a slight increase in secondary root density of about 11.65% while its final primary root length showed a reduction of -14.20% compared to Col-0. OE:AtGLR3.7(3) had a significantly higher-developed root architecture than wildtype plants with an increase of 17.96% in primary root length and 11.53% in root diameter. OE:AtGLR3.7(2) was also characterized by a longer primary root (9.65%) and a significantly wider root diameter (8.23%). OE:AtGLR3.7(1) showed a root phenotype similar to Col-0. Determinations of the beginning of the root hair zone showed no deviations among the plant lines. First root hairs emerged at a distance of 1.25 ± 0.02 mm from the root tip in all tested Arabidopsis genotypes.

Table 2. **Root Architecture of Transgenic and Wildtype *Arabidopsis thaliana* on 14 DAI.**

Plant line	**1° root length (mm ± SD)**	**1° root diameter (µm ± SD)**	**Start of root hair zone (mm ± SD)**	**2° roots per cm (# ± SD)**
Col-0	67.88 ± 10.04	154.4 ± 6.4	1.23 ± 0.09	3.69 ± 0.82
atglr3.7	58.24 ± 17.76	153.5 ± 9.8	1.27 ± 0.14	4.12 ± 1.32
OE:AtGLR3.7(1)	69.18 ± 5.49	156.7 ± 5.6	1.27 ± 0.04	3.60 ± 0.25
OE:AtGLR3.7(2)	74.43 ± 12.17	167.1 ± 12.9 (*)	1.25 ± 0.13	3.73 ± 0.66
OE:AtGLR3.7(3)	80.07 ± 7.69 (*)	172.2 ± 5.8 (**)	1.23 ± 0.09	3.73 ± 0.42

Statistical analyses were conducted using a one-way ANOVA and Dunnett's *post hoc* test, n = 9-19; *$\rho < 0.05$, **$\rho < 0.01$.

3.2.3 Aerial Tissue

3.2.3.1 Rosette Growth

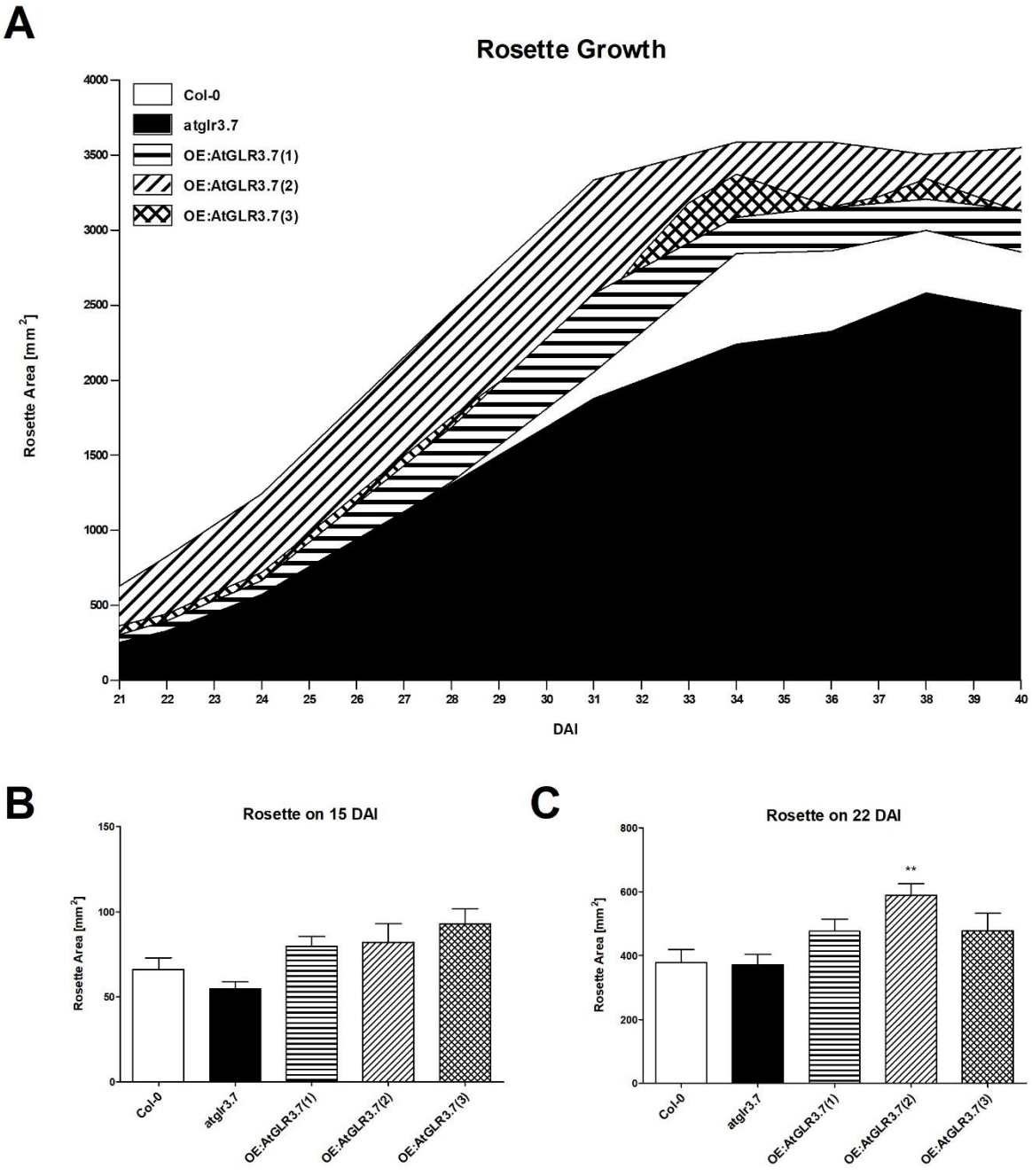

Figure 9. **Rosette Growth and Size at Different Developmental Stages.** Rosette area of wildtype and transgenic *Arabidopsis thaliana* grown in soil was measured daily during a plant life cycle until 40 DAI (A). Rosette size of plants grown on ½ MS agar on 15 DAI (B) and plants grown in soil at the beginning of the reproductive stage (C) serve as reference marker for specific plant development stages. The *AtGLR3.7* overexpression lines were characterized by a tendency of increased rosette growth which was especially prominent in OE:AtGLR3.7(2). Statistical analyses among genotypes were conducted using a one-way ANOVA and Dunnett's *post hoc* test; *n* = 5-18. Asterisks indicate significant deviations from Col-0 with **$\rho < 0.01$. Error bars indicate SE.

An investigation of the rosette growth revealed variations among transgenic and wildtype plants grown in soil (Figure 9A). Following the rosette development over a period of about 40 d, atglr3.7 showed the least rosette growth with a decrease in rosette size of -14% compared to Col-0. OE:AtGLR3.7(1) and OE:AtGLR3.7(2) showed an overall increase in their rosette size of 11 and 28%, respectively. The deviations were especially prominent in early plant development stages as it can be seen for plants grown in petri dishes on 15 DAI (Figure 9B). At this stage, OE:AtGLR3.7(3) grew bigger than OE:AtGLR3.7(2) while atglr3.7 exhibited clearly a smaller rosette. When reaching the reproductive stage, OE:AtGLR3.7(2) showed a significant increase of about 56% in rosette area compared to Col-0 whereas OE:AtGLR3.7(3) exhibited only a minor increase similar to OE:AtGLR3.7(1) in comparison to wildtype plants (Figure 9C).

A detailed comparison of rosette parameters revealed a constant and significant increase in rosette area and expansion (major and minor radius) only for OE:AtGLR3.7(2) (Table 3). OE:AtGLR3.7(1) and OE:AtGLR3.7(3) also showed increases in their rosette dimensions but to a lesser extent. Furthermore, the initial growth boost in these latter plant lines was less stable throughout the plant's life cycle (Figure 9A).

Table 3. **Rosette Characteristics of Transgenic and Wildtype *Arabidopsis thaliana* Grown in Soil on 22 DAI.**

Plant line	**Rosette area (mm^2 ± SD)**	**Rosette perimeter (mm ± SD)**	**Rosette major radius (mm ± SD)**	**Rosette minor radius (mm ± SD)**
Col-0	378.04 ± 92.22	250.72 ± 46.13	24.28 ± 2.83	19.53 ± 2.81
atglr3.7	371.38 ± 72.83	251.53 ± 43.45	23.49 ± 1.85	19.95 ± 2.46
OE:AtGLR3.7(1)	420.00 ± 126.76	266.70 ± 71.82	25.57 ± 2.77	20.48 ± 4.61
OE:AtGLR3.7(2)	588.80 ± 80.86 (**)	334.96 ± 60.79	29.11 ± 1.54 (*)	25.65 ± 2.33 (*)
OE:AtGLR3.7(3)	477.47 ± 109.39	259.76 ± 56.03	25.93 ± 3.69	23.14 ± 2.19

Statistical analyses were conducted using a one-way ANOVA and Dunnett's *post hoc* test, n = 5-6; *$\rho < 0.05$, **$\rho < 0.01$.

3.2.3.2 Shoot Growth

Starting from the onset of the reproductive stage of *Arabidopsis thaliana*, the shoot transforms into an inflorescence stem while side bolts emerge from the rosette. An investigation of the stem in transgenic and wildtype Arabidopsis plants showed a significant and constant increase in growth for OE:AtGLR3.7(2) (Figure 10). OE:AtGLR3.7(1) and OE:AtGLR3.7(3) exhibited an initial boost in stem growth similar to OE:AtGLR3.7(2) until 31 DAI. However, this growth acceleration abated until it was comparable to Col-0 and atglr3.7 during the final stages of stem growth/development.

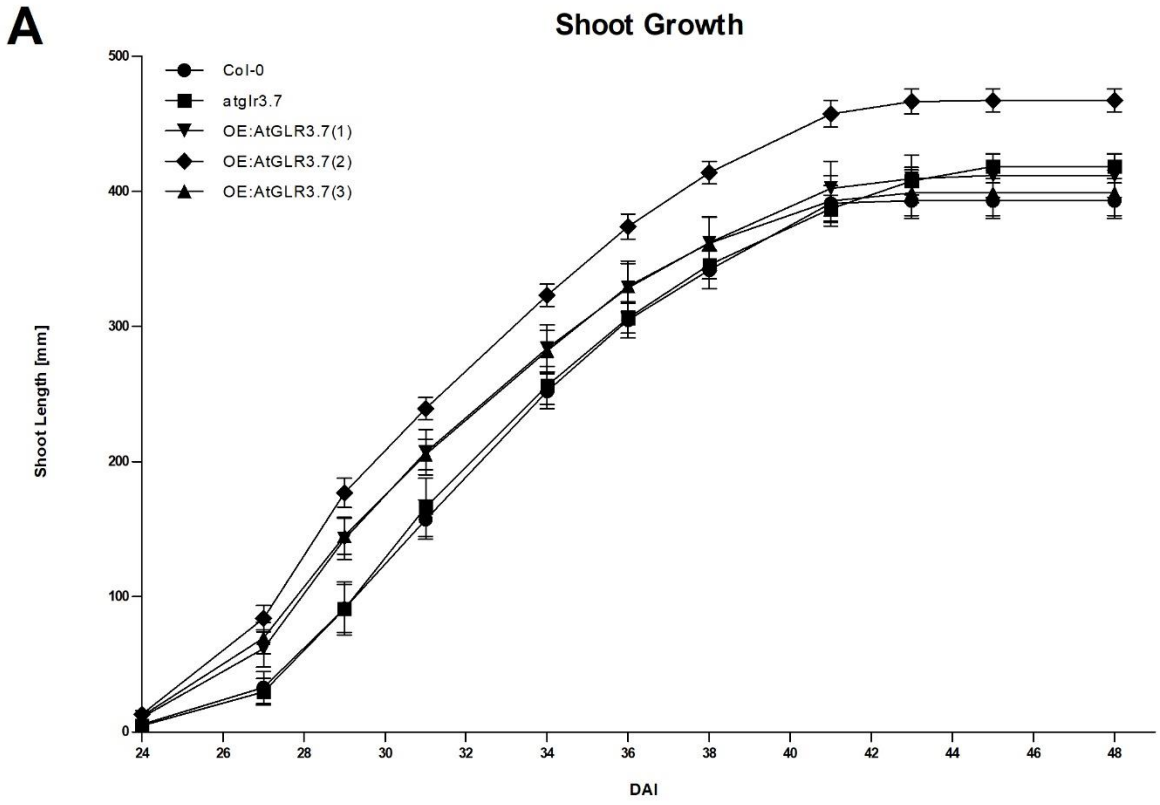

Figure 10. **Shoot Growth During the Reproductive Stage.** Shoot length of wildtype and transgenic *Arabidopsis thaliana* grown in soil was measured every two to three days. All *AtGLR3.7* overexpression lines showed an initial boost in stem growth while only OE:AtGLR3.7(2) exhibited a constant growth acceleration. OE:AtGLR3.7(1) and -(3) displayed a reduction in daily stem growth starting from 34 DAI. The *AtGLR3.7* knockout line was characterized by a stem growth comparable to Col-0. Error bars indicate SE, n = 5-6.

The morphology of the stem including the side branches was similar among all tested plant lines that were characterized by 2.8 ± 0.2 branches on the main stem (Table 4). The number of side bolts emerging from the rosette increased about 21 and 9% in OE:AtGLR3.7(2) and OE:AtGLR3.7(3), respectively. The *AtGLR3.7* knockout line showed a minor reduction of about -12% compared to Col-0 while OE:AtGLR3.7(1) exhibited no deviations from wildtype plants. OE:AtGLR3.7(2) was the only transgenic plant line which showed a strong increase in final stem length of about 19% compared to Col-0.

Table 4. **Stem and Side Bolt Growth in Transgenic and Wildtype *Arabidopsis thaliana* on 48 DAI.**

Plant line	**Final stem length (mm ± SD)**	**Branches on main stem (# ± SD)**	**Side bolts (# ± SD)**
Col-0	404.60 ± 16.50	3.0 ± 0.6	5.7 ± 1.0
atglr3.7	418.30 ± 21.92	3.0 ± 0.6	5.0 ± 0.6
OE:AtGLR3.7(1)	411.60 ± 35.93	2.6 ± 0.5	5.8 ± 1.3
OE:AtGLR3.7(2)	467.20 ± 20.89 (**)	2.7 ± 0.5	6.6 ± 0.9
OE:AtGLR3.7(3)	398.80 ± 37.80	2.6 ± 0.5	6.2 ± 1.1

Statistical analyses were conducted using a one-way ANOVA and Dunnett's *post hoc* test, n = 5-6; **$\rho < 0.01$.

3.2.3.3 Plant Biomass Accumulation and Relative Water Content

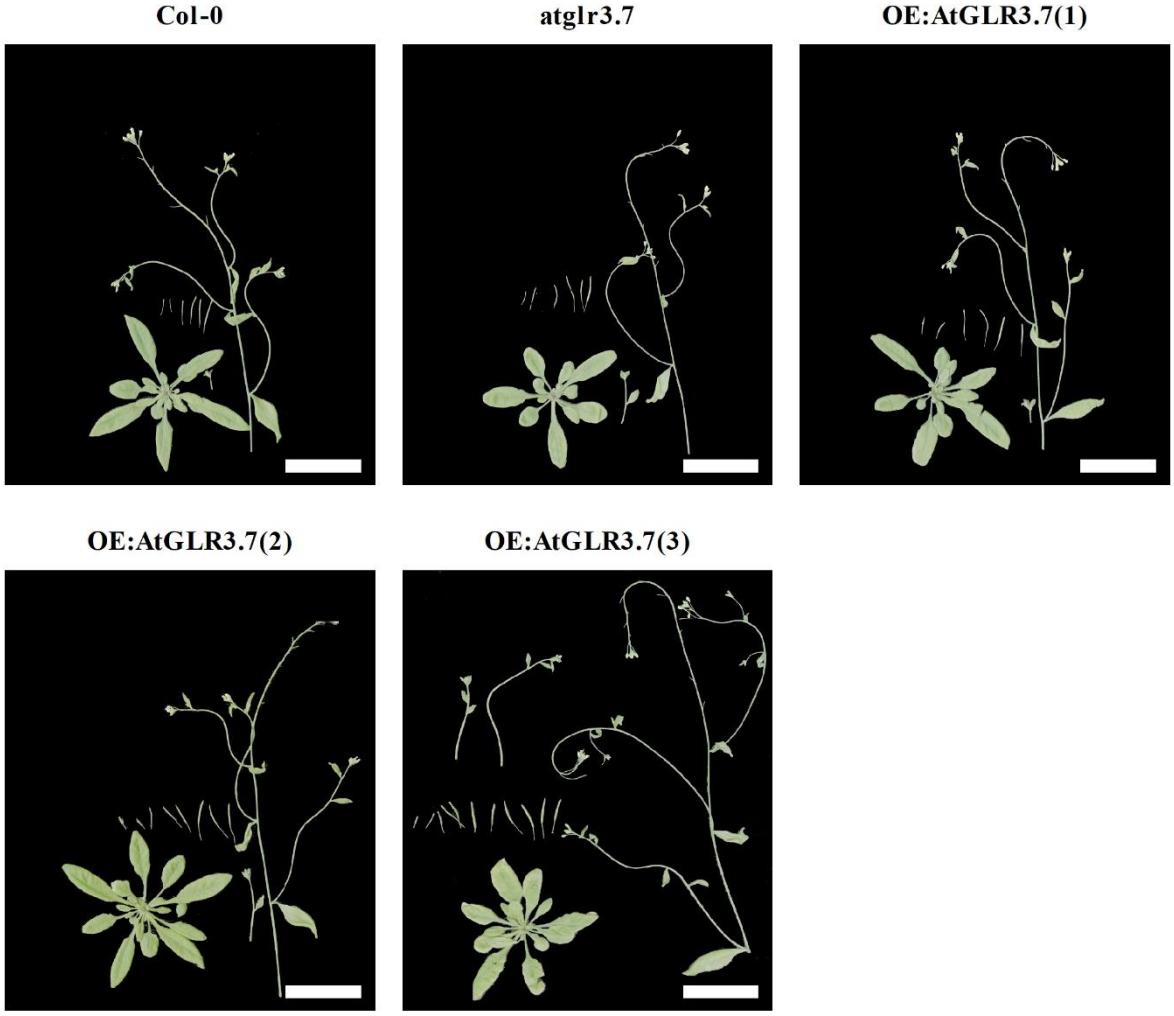

Figure 11. **Produced Above-Ground Tissue on 31 DAI.** Wildtype and transgenic *Arabidopsis thaliana* were grown in soil and harvested after they entered the reproductive stage in which they started to produce flowers and siliques. White bars represent 40 mm.

Measurements on the plants' above-ground tissue was done on 31 DAI from transgenic and wildtype *Arabidopsis thaliana* grown in soil. This time point allowed an estimation of the produced biomass at a stage in which the rosette growth was completed, and first inflorescence tissues emerged (Figure 11). The increase in produced above-ground tissue (FW) is highly significant for OE:AtGLR3.7(3) and (2) with 21 and 15%, respectively, compared to Col-0 (Figure 12A). OE:AtGLR3.7(1) exhibited a weaker but still significant increase in accumulated biomass of about 7%. On the other hand, atglr3.7 produced less above-ground tissue as indicated by a FW reduction of -15%.

Since variations of the measured FW in the transgenic and wildtype plants could be affected by the plants' water status, the RWC of all tested plant lines was calculated based on FW, TW and DW of the collected material. There were no major deviations detectable and all plant lines had an average RWC of 88.25 ± 0.39% (Figure 12B).

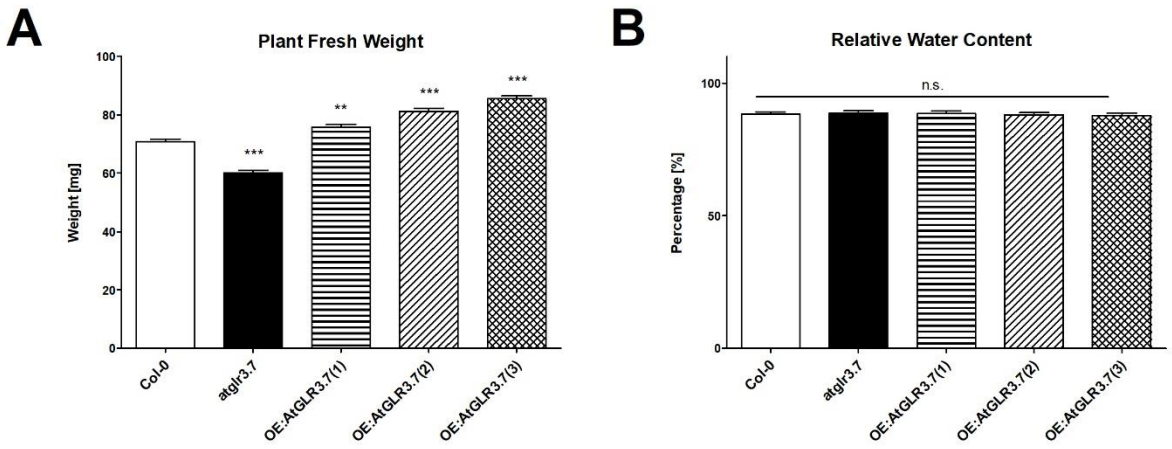

Figure 12. **Fresh Weight and Relative Water Content on 20 DAI.** The *AtGLR3.7* overexpression lines showed an *AtGLR3.7* expression-dependent increase in FW while atglr3.7 showed a reduction in above-ground tissue production (A). All tested plant lines displayed a similar RWC (B). Wildtype and transgenic *Arabidopsis thaliana* were grown under sterile conditions and harvested on 20 DAI. Statistical analyses among genotypes were conducted using a one-way ANOVA and Dunnett's *post hoc* test; n = 16-18. Asterisks indicate significant deviations from Col-0 with **$\rho < 0.01$ and ***$\rho < 0.001$. Error bars indicate SD.

3.2.4 Plant Growth Alterations

3.2.4.1 Growth in Darkness

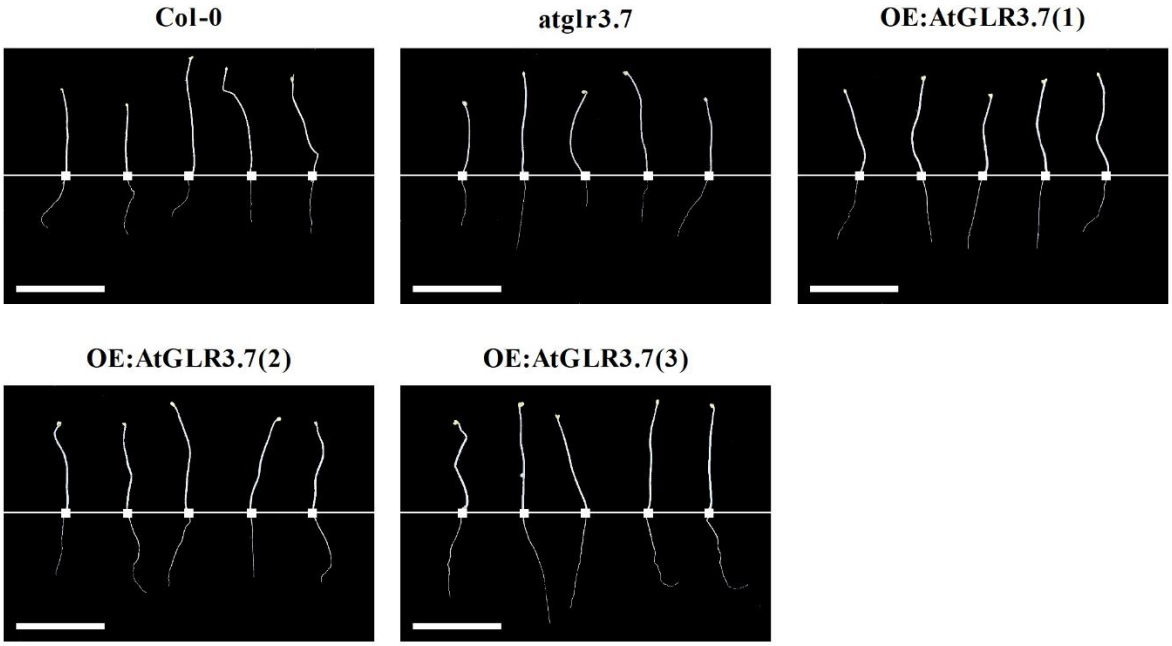

Figure 13. **Growth of Seedlings in Darkness on 10 DAI.** Wildtype and transgenic *Arabidopsis thaliana* were grown on ½ MS agar in petri dishes covered with aluminium foil under otherwise standard conditions. Seedlings were removed from petri dishes and digitalized on 10 DAI. White bars represent 20 mm.

Since hypocotyl growth in darkness is solely a process of cell elongation without cell division, the experimental setup was designed to reveal the role of cell elongation in the observed growth acceleration/decrease of the transgenic *Arabidopsis thaliana*. Plants were germinated and grown under sterile conditions in darkness for ten days, a condition that promoted strong hypocotyl elongation with no deviations in hypocotyl length among the tested plant lines (Figure 13).

Comparisons among the different plant genotypes regarding their hypocotyl elongation showed no significant variations (Figure 14A). The average elongation rate was 16.04 ± 0.76 mm on 10 DAI. However, the primary root length showed significant differences when comparing among the overexpression lines with Col-0 (Figure 14B). Here, the final root length of OE:AtGLR3.7(3) and OE:AtGLR3.7(2) was significantly higher with 13.78 ± 3.50 and 11.90 ± 1.90 mm compared to 9.48 ± 1.58 mm in Col-0, which equals an increase of 45 and 26%, respectively. OE:AtGLR3.7(1) exhibited an only slightly longer root (10.98 ± 2.18 mm) with an increase of about 16% compared to wildtype plants. The *AtGLR3.7* knockout line was characterized by an average root length of 9.51 ± 2.95 mm, similar to that of Col-0.

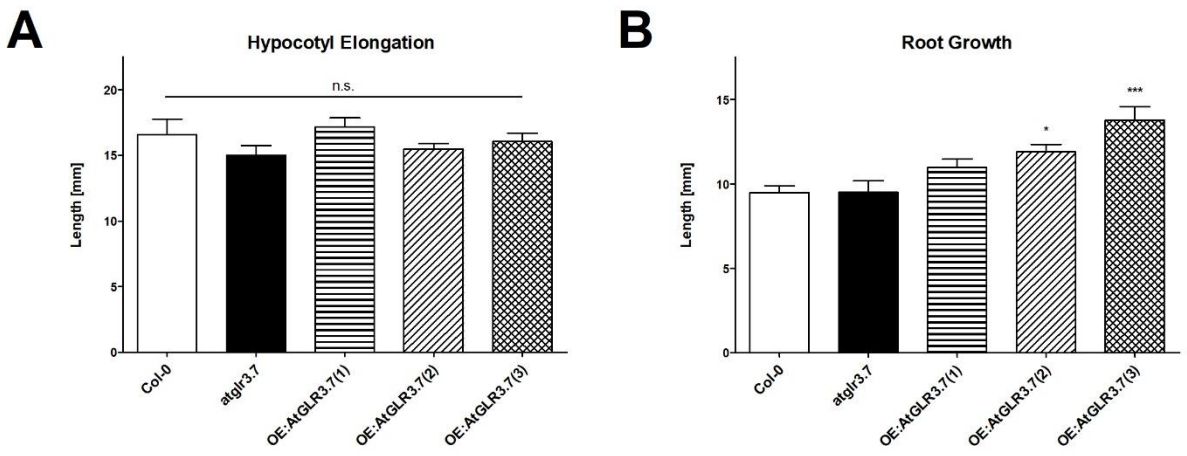

Figure 14. **Hypocotyl Elongation and Primary Root Length in Darkness on 10 DAI.** Wildtype and transgenic *Arabidopsis thaliana* were grown under sterile conditions on ½ MS agar in darkness. The hypocotyl elongation was comparable among all tested plant lines (A). Primary root length was significantly increased in the two *AtGLR3.7* overexpression lines with the highest *AtGLR3.7* expression levels (B). Measurements were done after removing the seedlings from the petri dishes wrapped in aluminium foil. Statistical analyses among genotypes were conducted using a one-way ANOVA and Dunnett's *post hoc* test; n = 16-20. Asterisks indicate significant deviations from Col-0 with *$\rho < 0.05$ and ***$\rho < 0.001$. Error bars indicate SE.

3.2.4.2 Controlled Induction of AtGLR3.7 *Gene Overexpression*

A triggered induction of an *AtGLR3.7* overexpression was achieved in plants carrying the gene sequence of *AtGLR3.7* under control of a 17-β-estradiol inducible promoter. The overexpression could be prompted by a growth of the seedlings on agar plates containing 17-β-estradiol. The application of this chemical caused a significant increase in rosette growth in both transgenic plant lines while one of the two inducible overexpression lines exhibited also a significant augmentation in its root development (Figure 15A).

The plant lines I:AtGLR3.7(1) and (2) showed a significant increase in rosette size of about 81.83 and 20.49% (70.94 ± 22.61 and 47.01 ± 14.83 mm^2), respectively, compared to Col-0 (39.02 ± 17.09 mm^2) when roots grew inside the estradiol-containing ½ MS agar (Figure 15B). Plants grown on the agar surface showed a smaller increase in rosette size of about 36.66 and 13.91% (54.11 ± 10.74 and 45.10 ± 21.92 mm^2), respectively, compared to Col-0 (39.59 ± 8.71 mm^2). Studying plants of the same genotype grown either on the agar surface or within the agar, only I:AtGLR3.7(1) showed a significant increase in rosette size when its roots grew within the estradiol-containing agar (31.11%).

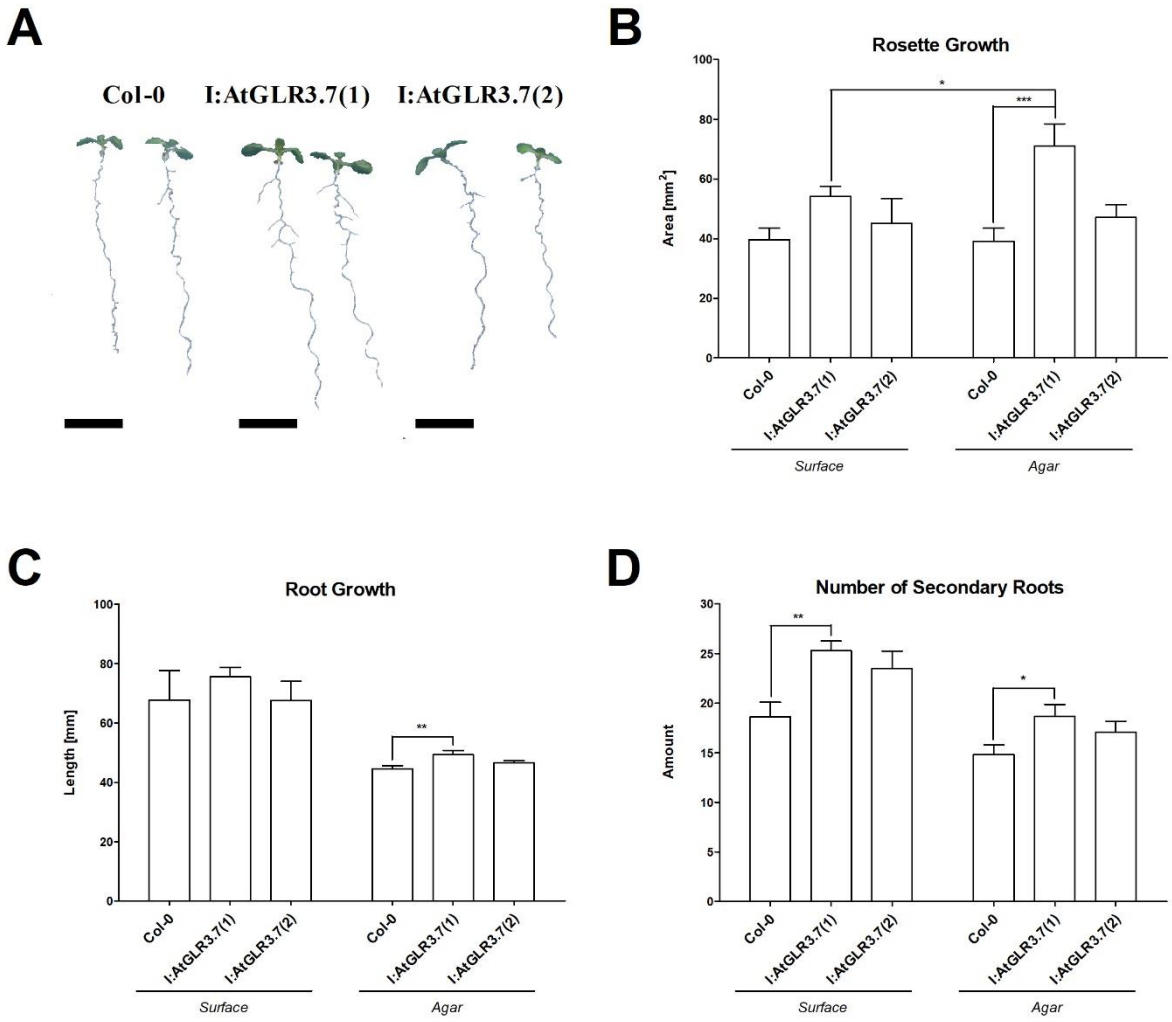

Figure 15. **Phenotype of Inducible *AtGLR3.7* Overexpression Lines.** Wildtype and transgenic *Arabidopsis thaliana* were grown in ½ MS agar containing 5 µM 17-β-estradiol and visualized on 10 DAI (A). Both transgenic plant lines exhibited an increase in rosette size (B). Only I:AtGLR3.7(1) showed a significant increase in primary root length when plants grew within the estradiol-containing agar (C). The number of secondary roots was elevated in both transgenic plant lines compared to Col-0 (D). Measurements for (B-C) were done on 13 DAI. Experiments were done also with plants grown on ½ MS agar without the addition of 17-β-estradiol and no deviations were detected (see section Supplemental 7.4 'Mock Treatment of AtGLR3.7 Inducible Overexpression Plants'). Statistical analyses among genotypes were conducted using a one-way ANOVA and Dunnett's *post hoc* test; n = 5-14. Asterisks indicate significant deviations from Col-0 with *$\rho < 0.05$ and ***$\rho < 0.001$. Error bars indicate SE. Black bars represent 10 mm.

I:AtGLR3.7(1) was characterized by an increase in root length, too, when grown on 17-β-estradiol (Figure 15C). However, only roots grown within the agar were characterized by a significant increase of 10.48% (49.27 ± 4.56 mm) compared to Col-0 (44.60 ± 3.60 mm). I:AtGLR3.7(2) showed a root length similar to wildtype plants.

However, the number of lateral roots was increased in both transgenic plant lines after the induction of *AtGLR3.7* by 17-β-estradiol (Figure 15D). Here, secondary root emergence was elevated when plants were grown on the agar surface in I:AtGLR3.7(1) and (2) with an increase in lateral roots of about 36.02 and 26.34% (25.3 ± 3.0 and 23.5 ± 4.3), respectively, compared to Col-0 (18.6 ± 3.4). A similar but weakened increase in root emergence was observed for both transgenic plant lines when plants were grown within the agar. Here I:AtGLR3.7(1) and -(2) exhibited an augmentation of 26.25 and 15.54% (18.7 ± 3.5 and 17.1 ± 3.8), respectively, compared to Col-0 (14.8 ± 3.7).

3.2.4.3 Effect of L-Glutamate on Primary Root Growth

The effect of L-glutamate as a potential ligand and activator of GLRs was investigated at three different concentrations (50, 250 and 1,000 µM; plus control) on *Arabidopsis thaliana* Col-0, atglr3.7 and OE:AtGLR3.7(2). Significant variations between the different plant lines were detected depending on the applied L-glutamate concentrations. A strong root growth reduction was observed at the highest concentration of 1,000 µM L-glutamate in OE:AtGLR3.7(2) whereas atglr3.7 experienced a notably boost in root growth (Figure 16A). The experiments were also conducted with the enantiomer D-glutamate, which served as a negative control, but no major deviations between different concentrations or genotypes could be observed (see section 7.5 'D-Glutamate Treatment of Transgenic and Wildtype *Arabidopsis thaliana*').

Varying L-glutamate concentration had only minor effects on the final primary root length of Col-0 (Figure 16B). Comparing the final root length of the three different plant lines at the varying amino acid concentrations, a highly significant growth boost of OE:AtGLR3.7 against Col-0 during a mock treatment abated already at 50 µM L-glutamate and was no longer detected at higher concentrations (Figure 16B). On the other hand, the *AtGLR3.7* knockout line was characterized by a highly significant increase in primary root length at 1,000 µM L-glutamate compared to the other plant lines (Figure 16B).

Figure 16. **Effect of L-Glutamate on Root Development on 14 DAI.** Wildtype and transgenic *Arabidopsis thaliana* were grown on ½ MS agar containing different L-glutamate concentrations (50, 250 and 1,000 µM). Plant growth in response to 1,000 µM L-glutamate (A). Primary root growth was reduced in an amino acid concentration-dependent manner in OE:AtGLR3.7(2) whereas atglr3.7 responded to increasing L-glutamate concentrations with an accelerated root growth (B). Statistical analyses among genotypes were conducted using a one-way ANOVA and Dunnett's *post hoc* test; n = 7-9. Asterisks indicate significant deviations from Col-0 with $^{**}\rho < 0.01$. Error bars indicate SE. Black bars represent 10 mm.

The initial root length measured on plants before they were transferred to new, glutamate-containing plates on 7 DAI served as a reference marker for the relative root growth during the amino acid treatment. This relative root growth allowed an accurate estimation of the effect of L-glutamate on the plant root system (Figure 17). L-glutamate had minor effects on root growth in wildtype *Arabidopsis thaliana* (Figure 17A). Only a high concentration of 1,000 µM L-glutamate led to an insignificant reduction in primary root length in Col-0. The *AtGLR3.7* knockout line experienced a constant and significant boost in root growth at L-glutamate concentrations of 250 and 1,000 µM equalling an additional growth of about 19 and 26%, respectively (Figure 17C). The opposite effect was observed for OE:AtGLR3.7(2) in which increasing concentrations of L-glutamate caused continuing, highly significant root growth reductions especially at the highest amino acid concentrations of 250 and 1,000 µM (Figure 17E). Here, the primary root was about -25 and -44% shorter, respectively, than in the mock treatment.

An investigation of the daily root growth helps to illustrate the temporal process of an exposure to glutamate. The daily increase in root length fluctuated around 9.14 ± 1.79 mm in Col-0 with only minor deviations occurring at a L-glutamate concentration of 1,000 µM where plants responded with a significant reduction down to 7.35 ± 1.87 mm during advanced exposure

periods on 13 and 14 DAI (Figure 17B). However, the daily root growth of 8.77 ± 1.42 mm in atglr3.7 during a mock treatment was significantly increased starting from a L-glutamate concentration of 250 µM on upwards and peaked with an average daily root growth of 13.32 ± 0.22 mm at a concentration of 1,000 µM L-glutamate (Figure 17D). Contrary, a highly significant decrease in daily root growth was observed in OE:AtGLR3.7(2) where an average growth of about 13.64 ± 1.20 mm during a mock treatment was diminished in an amino acid concentration-dependent manner down to 4.48 ± 1.41 mm at 1,000 µM L-glutamate (Figure 17F).

Comparing the root growth of Col-0, atglr3.7 and OE:AtGLR3.7(2) at particular L-glutamate concentrations, previous results concerning the root growth were reiterated in the mock treatment of all three plant lines where OE:AtGLR3.7(2) experienced a primary root growth boost while atglr3.7 showed a slightly reduced root growth compared to Col-0 (Figure 18A). Looking at the deviation in primary root growth in atglr3.7's and OE:AtGLR3.7(2) from wildtype plants, it was shown that the overexpression line displayed a steady increase in root length of about 45% while the *AtGLR3.7* knockout line was characterized by an ongoing reduction in root length of about -5% compared to Col-0 (Figure 18B). A minor L-glutamate concentration of 50 µM reduced the additional root growth in OE:AtGLR3.7(2) slightly during early exposure periods where its root length was only about 32% longer than Col-0 (Figure 18C, D). The *AtGLR3.7* knockout line showed under the same conditions a minor but steady alleviation of its growth reductions (Figure 18C, D). However, a concentration of 250 µM L-glutamate led to a highly significant reduction in primary root length in OE:AtGLR3.7(2) which caused a similar root length to Col-0 after one week of amino acid treatment (Figure 18E, F). A strong and highly significant increase in primary root length in atglr3.7 was caused by the same amino acid concentration leading to a root length likewise to Col-0 after one week (Figure 18E, F). The highest tested concentration of 1,000 µM L-glutamate provoked a severe growth reduction on the *AtGLR3.7* overexpression line already early during the amino acid treatment which continued over the time course of the experiment while atglr3.7 matched the root length of Col-0 three days after the beginning of an L-glutamate application and excelled the primary root length of wildtype plants with an additional increase of about 35% at the end of the experiment (Figure 18G, H).

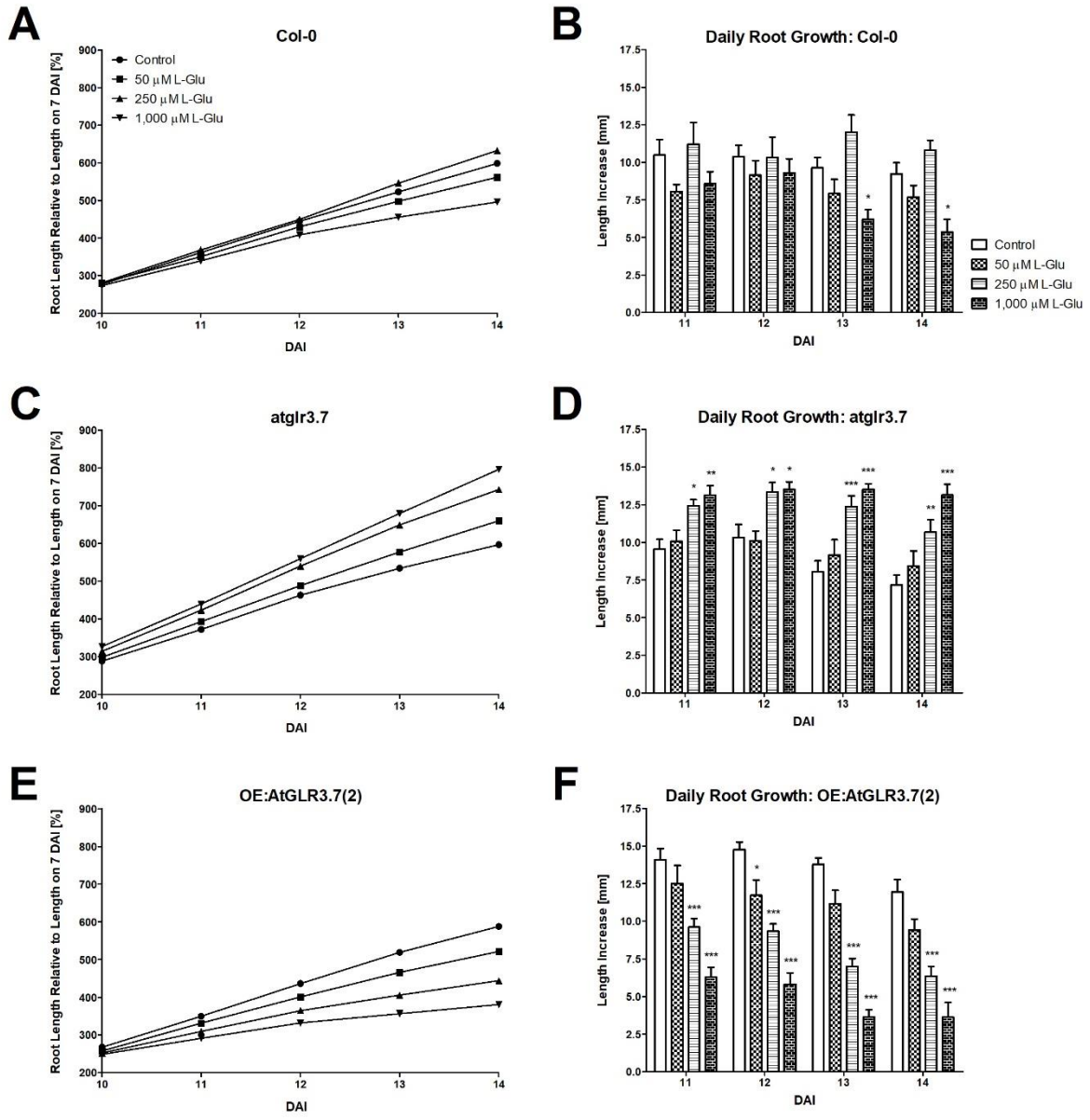

Figure 17. **Relative and Daily Root Growth in Response to Rising L-Glutamate Concentrations.** Wildtype and transgenic *Arabidopsis thaliana* were grown under standard conditions on ½ MS agar and transferred to L-glutamate-containing agar plates (0, 50, 250 and 1,000 µM) on 7 DAI. Relative root growth refers to the initial root length at the beginning of the exposure to L-glutamate where atglr3.7 responded with a continuing increase in its primary root growth depending on increasing L-glutamate concentrations while OE:AtGLR3.7(2) exhibited the opposite phenotype (A), (C) and (E). Daily root growth is depicted during an advanced exposure to L-glutamate (11-14 DAI) (B), (D) and (F). Statistical analyses among genotypes were conducted using a two-way ANOVA and Bonferroni's *post hoc* test; n = 7-9. Asterisks indicate significant deviations from Col-0 with *$\rho < 0.05$, **$\rho < 0.01$ and ***$\rho < 0.001$. Error bars indicate SE.

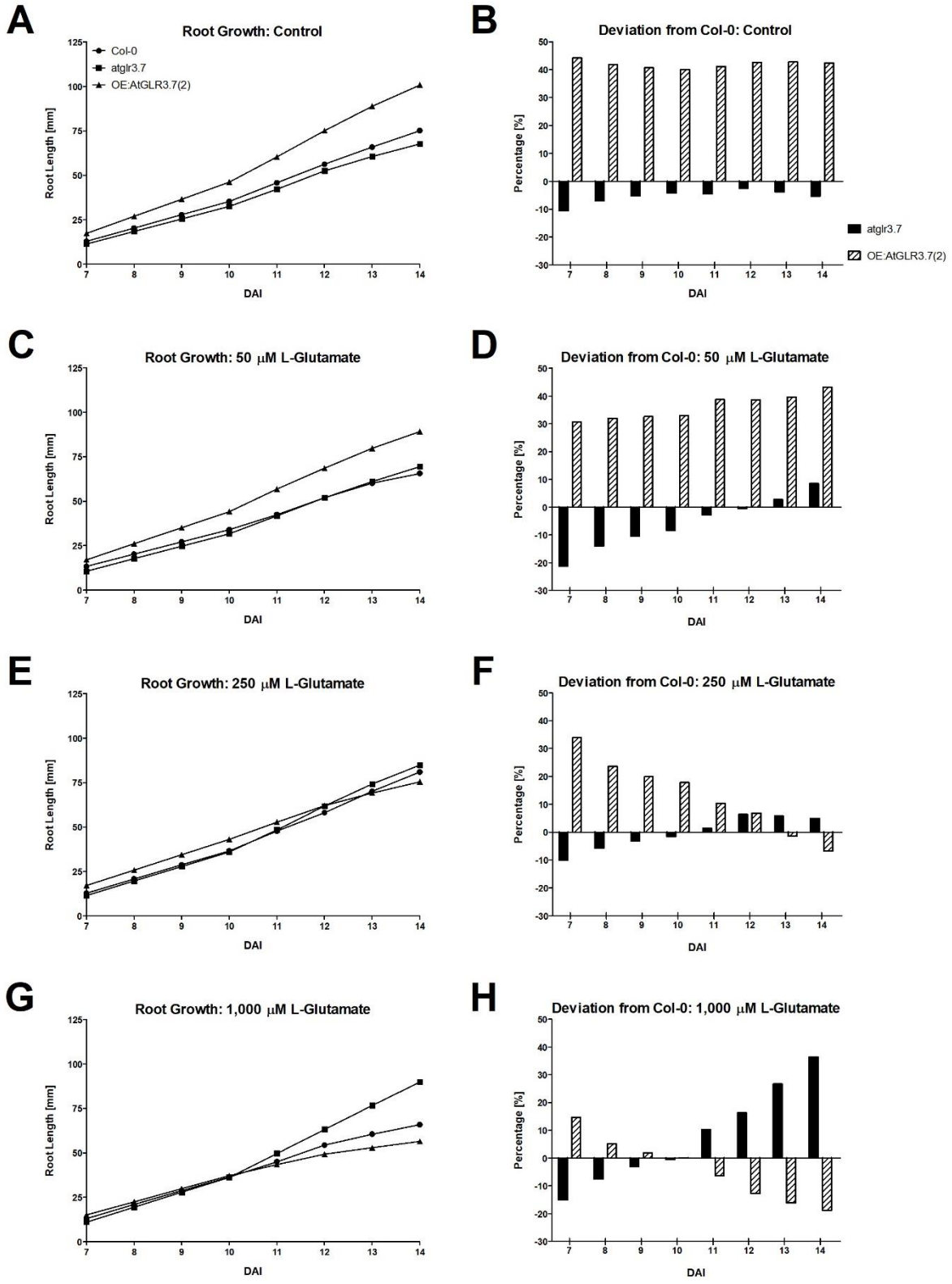

Figure 18. **Root Growth and Deviation from Col-0 in Response to Increasing L-Glutamate Concentrations.** Wildtype and transgenic *Arabidopsis thaliana* were grown under standard conditions on ½ MS agar and transferred to L-glutamate-containing agar plates (0, 50, 250 and 1,000 µM) on 7 DAI. Root length was measured daily and plotted for Col-0, atglr3.7 and OE:AtGLR3.7(2) for the respective L-glutamate concentrations (A), (C), (E) and (G). Root growth deviations of atglr3.7 and OE:AtGLR3.7(2) from Col-0 displayed for each day over a period of one week (B), (D), (F) and (H).

3.3 Characterization of the Root Apical Meristem

3.3.1 Meristem Size

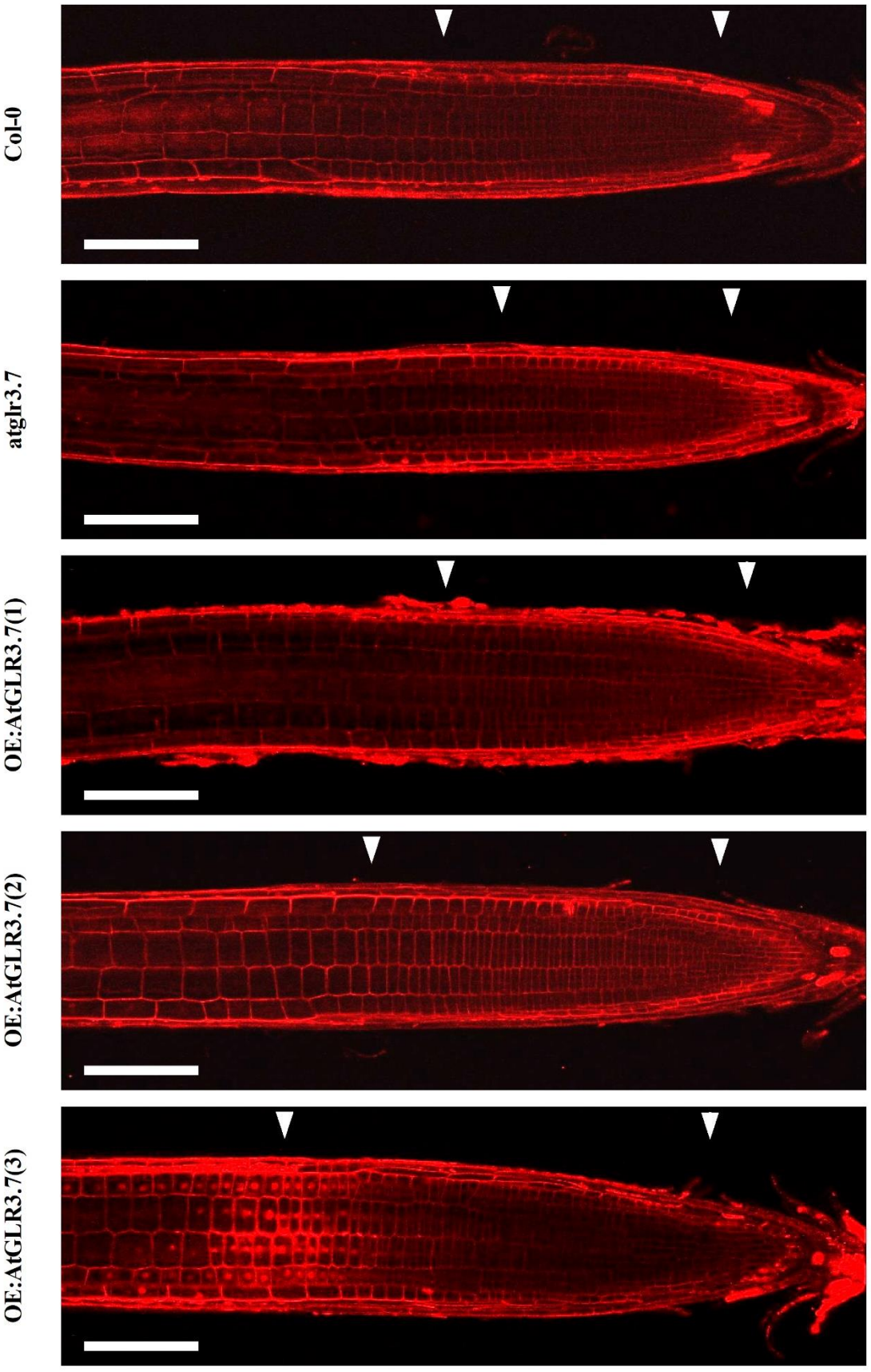

Figure 19. **Meristematic Zone Extension within the Root Tip.** Close-up images of the primary root apex were obtained by staining the plant root with 50 µM propidium iodide and cutting the root axis optically by CLSM. White arrows indicate quiescent centre (QC) (right arrow) and the beginning of the elongation zone (EZ) (left arrow). Wildtype and transgenic *Arabidopsis thaliana* were grown under standard conditions on ½ MS agar and observed at various plant ages ranging from 8-10 DAI. White bars represent 100 µm.

The mapping of the RAM required staining and locating all cells within the root tip. The extension of the MZ was calculated based on the event of distinctive, abrupt changes in cell morphology within single cell rows (for a detailed description see section 2.3.2.1 'Determining the Extension of the Meristematic Zone'). Measurements were conducted on plants with a similar root length in order to avoid any possible interference due to the developmental stage of meristem formations. Therefore, plants were surveyed when they reached a primary root length of 2.50 cm. The plant age varied slightly among the tested plant lines with an average of 9.25 ± 0.50, 9.75 ± 0.50, 8.75 ± 0.50, 8.25 ± 0.50 and 8.00 DAI for Col-0, atglr3.7, OE:AtGLR3.7(1), -(2) and -(3), respectively.

A first visual estimation of the MZ revealed strong variations of its extension among transgenic and wildtype *Arabidopsis thaliana* (Figure 19). The shortest MZ length was observed for atglr3.7, which were close to those of Col-0. The *AtGLR3.7* overexpression lines exhibited overall larger MZ extensions than wildtype plants. Here, OE:AtGLR3.7(3) was characterized by the longest MZ followed by OE:AtGLR3.7(2) and OE:AtGLR3.7(1).

A more accurate survey permitted a differentiation between the epidermal layer and the cortex of the root apex. The cortical MZ stretched farther from the QC than the epidermal MZ with distances in Col-0 of 329.1 ± 10.8 and 237.7 ± 18.2 µm, respectively (Figure 20). However, the cortical and the epidermal MZs were significantly extended in OE:AtGLR3.7(3) with 449.5 ± 17.2 and 272.7 ± 16.5 µm, respectively, which amounted to an increase of about 15 % for both tissues compared to Col-0. In a similar but less pronounced manner, OE:AtGLR3.7(2) showed an increase 436.9 ± 33.4 and 264.8 ± 15.8 µm of its cortical and epidermal MZ, respectively. Both MZ regions exhibited an additional extension of about 11%. A slight, but not significant increase of about 3% was measured for OE:AtGLR3.7(1) with 403.7 ± 23.2 and 244.2 ± 20.7 µm for the cortical and epidermal MZ, respectively. The knockout line atglr3.7 showed a minor decrease in its MZ length down to 372.0 ± 29.46 and 227.9 ± 13.6 µm for its cortical and epidermal tissues which resulted in a reduction of about 4.5% compared to Col-0.

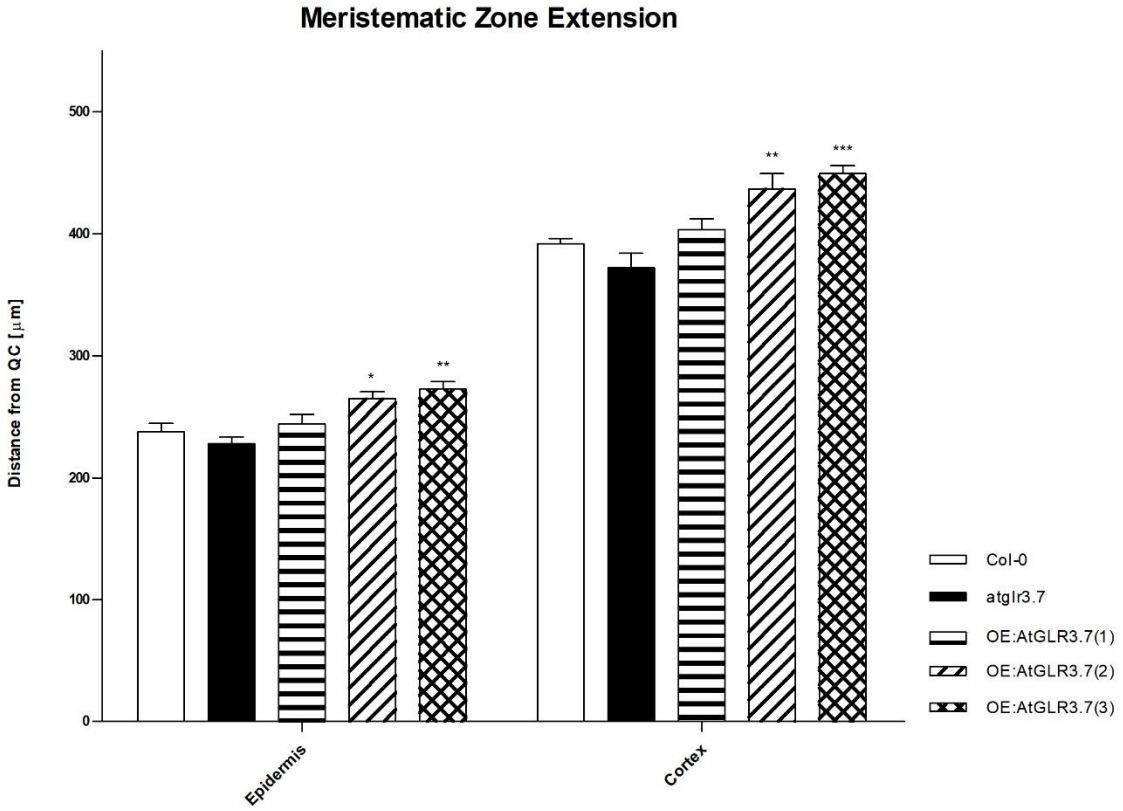

Figure 20. **Extension of the Epidermal and Cortical Meristematic Zone within the Root Tip.** *AtGLR3.7* overexpressions lines OE:AtGLR3.7(2) and -(3) showed a significant enlargement of their meristematic zone (MZ) while atglr3.7 was characterized by a minor reduction in MZ expansion. The length of the MZ was measured as the mean distance of the farthest dividing cells from the quiescent centre (QC). Wildtype and transgenic *Arabidopsis thaliana* were grown under standard conditions on ½ MS agar and observed at variable plant ages ranging from 8-10 DAI. Statistical analyses among genotypes were conducted using a one-way ANOVA and Dunnett's *post hoc* test; n = 6-7. Asterisks indicate significant deviations from Col-0 with *$\rho < 0.05$, **$\rho < 0.01$ and ***$\rho < 0.001$. Error bars indicate SE.

3.3.2 Cell Morphology within the Meristematic and Differentiation Zone

3.3.2.1 Meristematic Zone

The delimitation of the MZ allowed a morphological characterization of the cells located within this region. Aside from the CN within the meristem, definitions of the average CD, CL, CW_r/CW_t and CS were achievable based on the exact measurements of single cells within the root tip. Strong variations in cell morphology and structure were found among the transgenic and wildtype *Arabidopsis thaliana*.

CN and CS varied significantly, while CD and CL were comparable among the tested plant lines (Table 5 and Table 6). The most significant deviations were found in OE:AtGLR3.7(3) where the MZ was characterized by an increase in CN of 21 and 18% within the epidermal and cortical layer, respectively, compared to Col-0. Furthermore, both CW_r and CW_t were raised within the epidermal (14 and 10%) as well as cortical layers (22 and 14%), respectively. Therefore, the CS within the MZ in OE:AtGLR3.7(3) was affected by an increase of 20 and 30% in the epidermal and cortical layer, respectively. However, all overexpression lines showed elevations of their mean CS to varying degrees when compared to wildtype plants.

OE:AtGLR3.7(2) showed a significant increase in CN of 12 and 15% for the epidermal and cortical layer, respectively, whereas OE:AtGLR3.7(1) displayed comparable cell morphologies and characteristics to Col-0. The *AtGLR3.7* knockout line was characterized by a reduction in CN of -7 and -5% in the epidermal and cortical layer, respectively, while the CL of epidermal cells within the MZ was reduced about -11%.

Table 5. **Cell Morphology of the Epidermal Meristematic Zone within the Roots of Transgenic and Wildtype *Arabidopsis thaliana* about 8-10 DAI.**

Plant line	**Cell number (# ± SD)**	**Cell density (# per 100 µm ± SD)**	**Cell length (µm ± SD)**	**Cell width$_{(t)}$ (µm ± SD)**	**Cell width$_{(r)}$ (µm ± SD)**	**Cell size (µm^3 ± SD)**
Col-0	37.9 ± 5.5	8.9 ± 1.4	11.9 ± 1.6	14.7 ± 1.1	18.2 ± 0.9	3,178 ± 276
atglr3.7	35.3 ± 5.3	9.8 ± 1.5	10.6 ± 1.5 (*)	15.4 ± 0.9	17.8 ± 0.8	2,918 ± 248
OE:AtGLR3.7(1)	36.2 ± 3.4	9.0 ± 1.3	11.8 ± 1.8	16.2 ± 2.4	18.5 ± 0.7	3,590 ± 948
OE:AtGLR3.7(2)	42.6 ± 3.7 (*)	8.9 ± 1.1	12.0 ± 1.4	15.4 ± 0.8	19.2 ± 1.9	3,573 ± 812
OE:AtGLR3.7(3)	45.9 ± 5.9 (***)	9.3 ± 1.6	11.5 ± 1.7	16.1 ± 2.0	20.7 ± 1.4 (*)	3,818 ± 561 (*)

Statistical analyses were conducted using a one-way ANOVA and Dunnett's *post hoc* test, n = 4-16; *$\rho < 0.05$ and ***$\rho < 0.001$.

Table 6. **Cell Morphology of the Cortical Meristematic Zone within the Roots of Transgenic and Wildtype *Arabidopsis thaliana* about 8-10 DAI.**

Plant line	**Cell number (# ± SD)**	**Cell density (# per 100 µm ± SD)**	**Cell length (µm ± SD)**	**Cell width$_{(t)}$ (µm ± SD)**	**Cell width$_{(r)}$ (µm ± SD)**	**Cell size (µm^3 ± SD)**
Col-0	60.2 ± 7.1	12.9 ± 2.2	8.3 ± 1.2	30.0 ± 2.2	18.0 ± 0.9	4,461 ± 608
atglr3.7	57.5 ± 5.0	12.3 ± 2.0	8.2 ± 0.9	29.2 ± 3.3	18.5 ± 1.3	4,618 ± 875
OE:AtGLR3.7(1)	60.0 ± 4.5	12.1 ± 1.7	8.8 ± 1.1	29.5 ± 2.0	19.5 ± 1.9	5,081 ± 608
OE:AtGLR3.7(2)	68.9 ± 8.0 (***)	12.0 ± 1.1	9.0 ± 0.6	31.4 ± 4.4	19.6 ± 3.5	5,519 ± 572
OE:AtGLR3.7(3)	71.3 ± 3.1 (***)	12.8 ± 1.0	8.3 ± 0.6	34.3 ± 3.9 (**)	21.9 ± 2.5 (***)	5,790 ± 746 (*)

Statistical analyses were conducted using a one-way ANOVA and Dunnett's *post hoc* test, n = 4-16; *$\rho < 0.05$, **$\rho < 0.01$ and ***$\rho < 0.001$.

3.3.2.2 Differentiation Zone

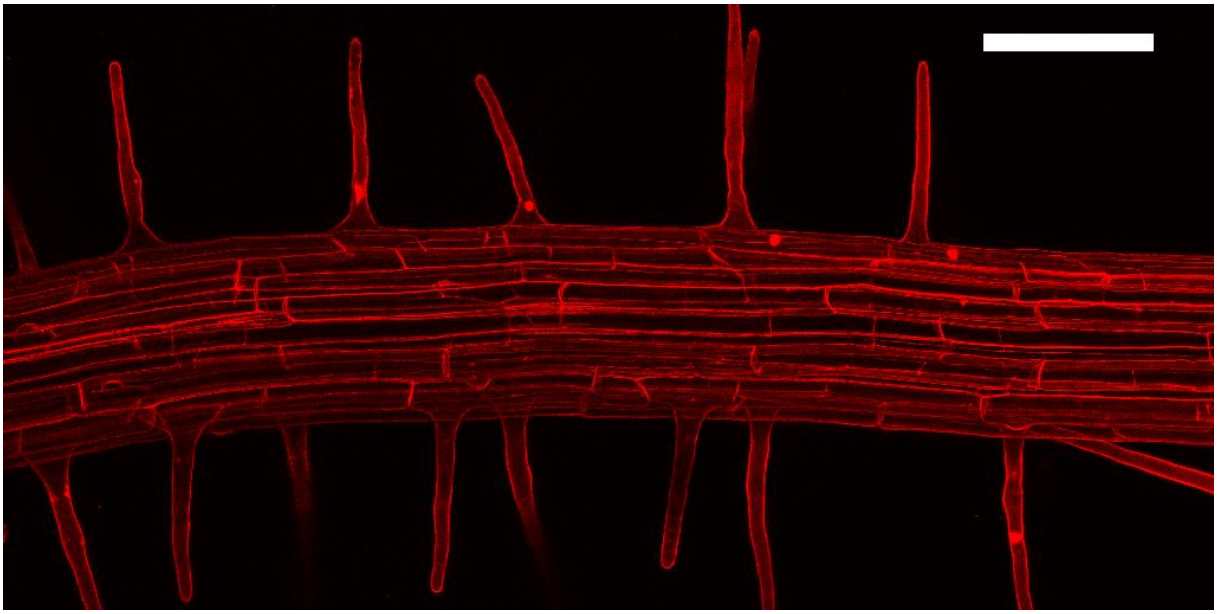

Figure 21. **General Overview of the Differentiation Zone/Root Hair Zone.** The image represents a Z-stack overlay of the root hair zone of the primary root of *Arabidopsis thaliana* (Col-0) in which roots were stained with 50 µM propidium iodide and observed with CLSM. Wildtype and transgenic *Arabidopsis thaliana* were grown under standard conditions on ½ MS agar and observed on 9 DAI. White bar represents 100 µm.

The morphological characterization of mature root cells within the differentiation/root hair zone was conducted on cells of the epidermis and cortex of transgenic and wildtype *Arabidopsis thaliana* (Figure 21). All tested plant lines showed a similar CL value of 226.22 ± 12.17 and 192.07 ± 11.34 µm in the epidermis and cortex, respectively (Table 7 and Table 8). There were, however, minor but significant deviations of CW_t and CW_r in OE:AtGLR3.7(3) detected. Here, CW_t increased about 14 and 9% whereas CW_r increased about 5 and 17% compared to Col-0 in the epidermal and cortical layer, respectively. This caused an increase in CS of mature root cells of about 15 and 21 % in the epidermis and cortex, respectively, in OE:AtGLR3.7(3). OE:AtGLR3.7(1), -(2) and atglr3.7 were characterized by only minor and non-significant variations. Although, taken together, the deviations in cell morphology among the tested plant lines were negligible.

Table 7. **Cell Morphology of Mature Epidermal Cells within the Root Hair Zones of Transgenic and Wildtype *Arabidopsis thaliana* about 8-10 DAI.**

Plant line	**Cell length (µm ± SD)**	**Cell width$_{(t)}$ (µm ± SD)**	**Cell width$_{(r)}$ (µm ± SD)**	**Cell size (µm^3 ± SD)**
Col-0	244.95 ± 16.53	15.67 ± 1.14	18.53 ± 1.20	68,163 ± 7,428
atglr3.7	214.52 ± 15.13	16.24 ± 1.28	16.67 ± 0.53	58,081 ± 6,171
OE:AtGLR3.7(1)	211.47 ± 9.51	18.04 ± 0.42 (*)	17.36 ± 3.04	71,600 ± 8,040
OE:AtGLR3.7(2)	231.77 ± 40.41	15.89 ± 1.46	17.73 ± 1.03	64,670 ± 8,833
OE:AtGLR3.7(3)	228.39 ± 7.94	17.79 ± 0.55 (*)	19.46 ± 0.53	78,233 ± 5.993

Statistical analyses were conducted using a one-way ANOVA and Dunnett's *post hoc* test, n = 4-16; *$\rho < 0.05$.

Table 8. **Cell Morphology of Mature Cortex Cells within the Roots of Transgenic and Wildtype *Arabidopsis thaliana* about 8-10 DAI.**

Plant line	**Cell length (µm ± SD)**	**Cell width$_{(t)}$ (µm ± SD)**	**Cell width$_{(r)}$ (µm ± SD)**	**Cell size (µm^3 ± SD)**
Col-0	193.93 ± 4.82	26.13 ± 1.38	23.26 ± 2.08	117,920 ± 13,171
atglr3.7	209.25 ± 18.53	24.68 ± 1.64	22.37 ± 2.24	106,559 ± 6,920
OE:AtGLR3.7(1)	183.54 ± 33.07	25.97 ± 1.51	24.10 ± 2.19	115,854 ± 28,302
OE:AtGLR3.7(2)	176.40 ± 13.92	26.18 ± 0.59	23.19 ± 1.14	109,650 ± 11,665
OE:AtGLR3.7(3)	197.23 ± 8.04	28.52 ± 0.92 (**)	26.43 ± 2.37 (*)	142,811 ± 12,867

Statistical analyses were conducted using a one-way ANOVA and Dunnett's *post hoc* test, n = 4-16; *$\rho < 0.05$ and **$\rho < 0.01$.

3.3.3 Meristematic Activity and Cell Cycle Progression

Following the study of Fioriani and Beemster (2006), it was possible to calculate the major characteristics of the meristematic activity of the RAM in transgenic and wildtype *Arabidopsis thaliana*. Significant variations occurred in all tested parameters among the different plant lines (Figure 22).

The average CPM was significantly elevated by 23% in OE:AtGLR3.7(3) (1.94 ± 0.19 cells row^{-1} h^{-1}) compared to Col-0 (1.58 ± 0.08 cells row^{-1} h^{-1}) whereas the *AtGLR3.7* knockout line showed a reduction of -18% in its CPM (1.29 ± 0.06 cells row^{-1} h^{-1}) (Figure 22A). OE:AtGLR3.7(2) and -(1) showed only a slight increase in their CPM of 7 and 3% (1.69 ± 0.18 and 1.63 ± 0.10 cells row^{-1} h^{-1}), respectively.

The ADR within the RAM of atglr3.7 was significantly reduced by -17% down to 0.03088 ± 0.00061 cells $cell^{-1}$ h^{-1} compared to Col-0 with 0.03729 ± 0.00113 cells $cell^{-1}$ h^{-1} (Figure 22B). The *AtGLR3.7* overexpression lines did not show any significant deviations from Col-0 with 0.03808 ± 0.00151, 0.03475 ± 0.00162 and 0.03743 ± 0.00274 cells $cell^{-1}$ h^{-1} for OE:AtGLR3.7(1), -(2) and -(3), respectively.

The theoretical CCD was prolonged in atglr3.7 by 21% up to 22.5 ± 0.4 h compared to Col-0 with 18.6 ± 0.6 h (Figure 22C). OE:AtGLR3.7(1) and -(3) showed CCDs similar to Col-0 with 18.2 ± 0.7 and 18.6 ± 1.3 h, respectively. OE:AtGLR3.7(2) exhibited a minor but not significant prolongation of its cell cycle up to 20.0 ± 0.9 h.

Considering RTP, atlgr3.7 was characterized by a highly significant increase of 20% to 121 ± 2 h compared to Col-0 with 101 ± 5 h (Figure 22D). Meristematic cells of OE:AtGLR3.7(1) remained for 99 ± 4 h within the RAM similar to cells of the wildtype. However, OE:AtGLR3.7(2) and -(3) also displayed minor increases in RTP of 11 and 5% (112 ± 5 h and 106 ± 7 h), respectively.

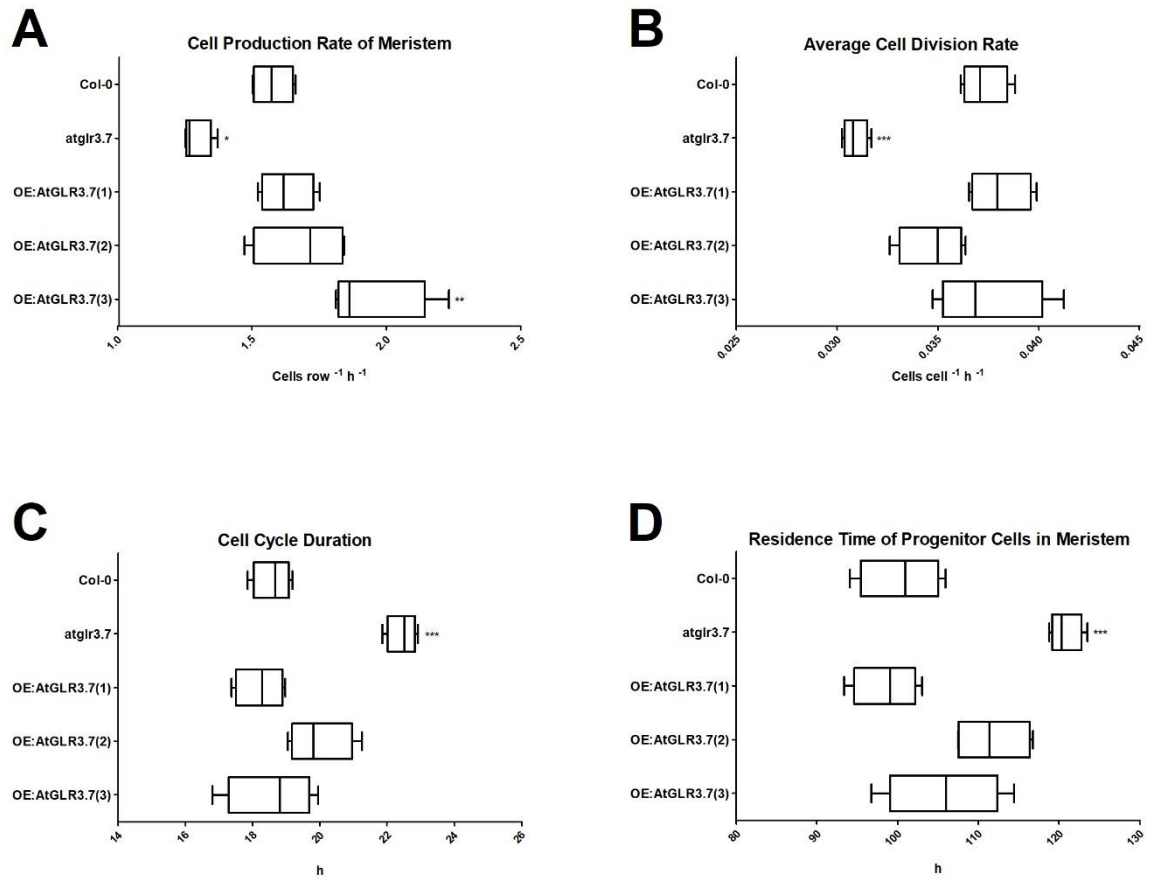

Figure 22. **Activity and Features of the Root Apical Meristem.** Kinematic analyses combined with measurements of total root growth rates as well as of meristematic and mature cell morphologies allowed the calculation of the meristematic cell production rate (CPM) which was significantly elevated in OE:AtGLR3.7(3) and significantly reduced in atglr3.7 (A). The average cell division rate (ADR) of the RAM was significantly reduced in atglr3.7 (B) while the average cell cycle duration time (CCD) showed a prolongation in the *AtGLR3.7* knockout line (C). The period progenitor cells emanating from the stem cell initials near the QC reside within the meristem (RTP) was also extended in atglr3.7 (D). Calculations were based on the work of Fiorani and Beemster (2006). Wildtype and transgenic *Arabidopsis thaliana* were grown under standard conditions on ½ MS agar and observed at various plant ages ranging from 8-10 DAI. Statistical analyses among genotypes were conducted using a one-way ANOVA and Dunnett's *post hoc* test; $n = 4$. Asterisks indicate significant deviations from Col-0 with $*\rho < 0.05$, $**\rho < 0.01$ and $***\rho < 0.001$. Bars indicate the minimal and maximal values of the population.

3.4 Molecular Analyses

3.4.1 Cell Cycle Gene Expression

3.4.1.1 Semi-Quantitative RT-PCR

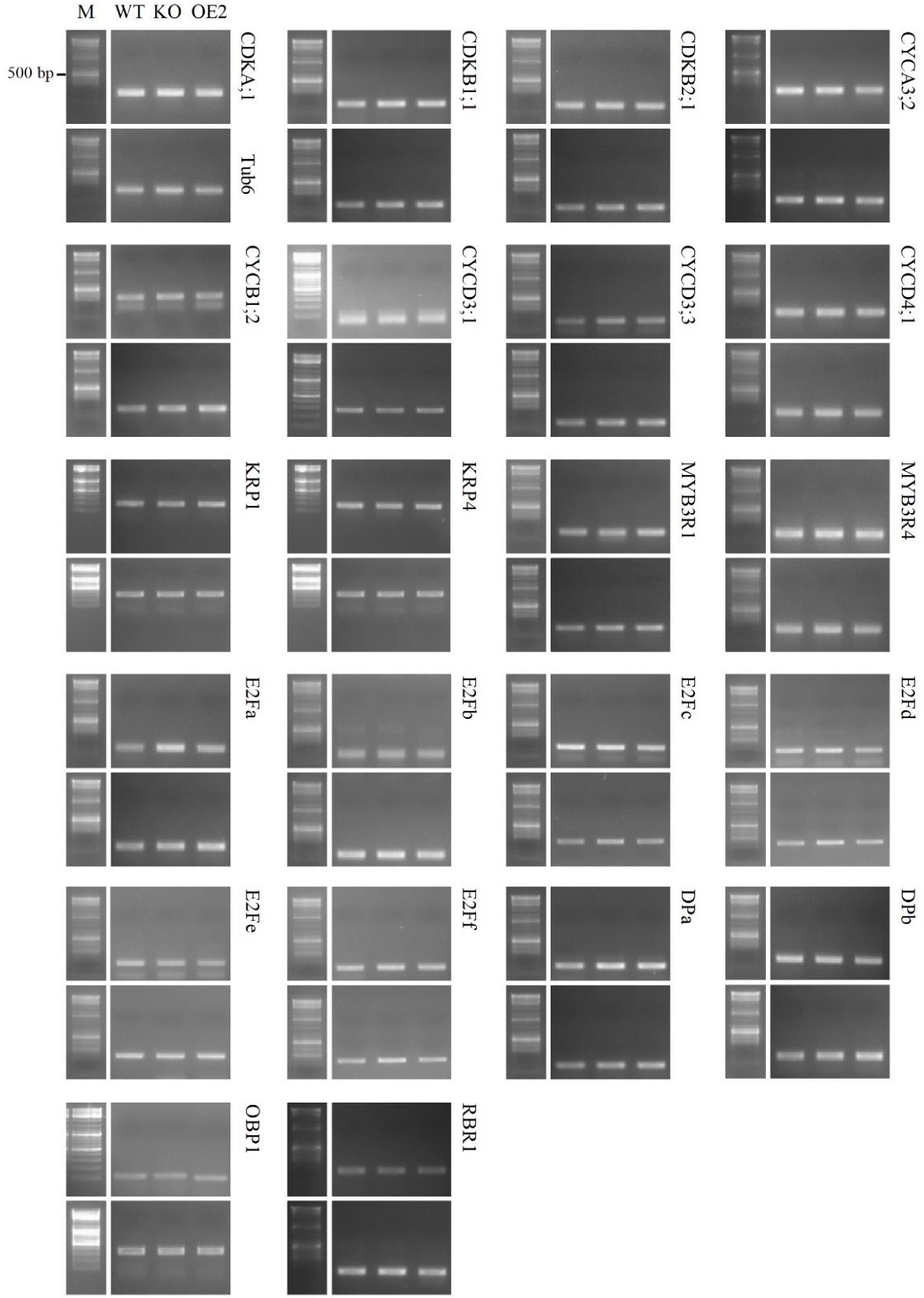

Figure 23. **Gene Expression of Cell Cycle Regulators.** Wildtype and transgenic *Arabidopsis thaliana* were grown hydroponically in sterile conditions and harvested on 14 DAI. Bulk RNA extractions and transcription into cDNA was followed by sqRT-PCR. Displayed images are representative for one to two RT-PCR repetitions. *Tubulin alpha-6 chain* (*Tub6*) served as a reference gene on which GOI expression was qualified. M: DNA ladder 'GeneRuler DNA Ladder Mix' (Thermo Fisher Scientific); WT: Col-0; KO: atglr3.7; OE2: OE:AtGLR3.7(2).

The gene expression of 22 cell cycle regulators was observed via sqRT-PCR in Col-0, atglr3.7 and OE:AtGLR3.7(2) (Figure 23). OE:AtGLR3.7(2) was chosen as a representative for an *AtGLR3.7* overexpression since this plant line exhibited a moderate overexpression of the glutamate receptor and its phenotype was the most stable of all three *AtGLR3.7* overexpression lines. Analyses of agarose gel band intensities revealed several gene upregulations in the transgenic plant lines compared to the wildtype (Table 9). GOI expression level deviations from Col-0 were categorized as negligible (0-50%), medium (50-100%) and high (> 100%).

The *AtGLR3.7* knockout line showed for 11 out of 22 tested genes moderate or high upregulations. The seven moderately upregulated genes comprised the cyclin-dependent proteins kinases CDKA;1, CDKB1;1 and CDKB2;1, cyclin CYCD4;1 as well as the transcription factors MYB3R1, E2Fd and E2Ff. A high upregulation was detected for the two cyclins CYCB1;2 and CYCD3;3 as well as for the transcription factors E2Fa and DPa while no considerable downregulation was observed for the tested cell cycle regulators.

The overexpression line OE:AtGLR3.7(2) displayed three moderate gene upregulations for the two cyclin-dependent kinases CDKB1;1 and CDKB2;1 as well as for cyclin CYCB1;2. Furthermore, four genes were highly upregulated comprising cyclin CYCD3;3 and the three transcription factors MYB3R1, E2Fa and DPa. There was no substantive gene downregulation observed in OE:AtGLR3.7(2).

Seven genes were alike upregulated in both the *AtGLR3.7* knockout and overexpression line encompassing the two cyclin-dependent kinases CDKB1;1 and CDKB2;1, the two cyclins CYCB1;2 and CYCD3;3 as well as the three transcription factors MYB3R1, E2Fa and DPa. Four genes were upregulated only in atglr3.7 but not in OE:AtGLR3.7(2), namely, cyclin-dependent protein kinase CDKA;1, cyclin CYCD4;1 as well as the two transcription factors E2Fd and E2Ff. Only transcription factor MYB3R4 was modestly upregulated in atglr3.7 and slightly downregulated in OE:AtGLR3.7(2).

Table 9. **Semi-Quantitative Analysis of 22 Cell Cycle Regulator Genes in Two-Week-Old Transgenic and Wildtype *Arabidopsis thaliana*.**

	Gel band intensity			**Deviation from Col-0 (%)**	
Gene	**Col-0**	**atglr3.7**	**OE(2)**	**atglr3.7**	**OE(2)**
CDKA;1	906	1,679	922	+ (85.31)*	+ (1.82)
CDKB1;1	549	962	1,043	+ (75.16)*	+ (90.01)*
CDKB2;1	561	1,012	995	+ (80.41)*	+ (77.37)*
CYCA3;2	1,062	1,315	1,062	+ (23.79)	+ (0.04)
CYCB1;2	312	638	572	+ (104.36)**	+ (83.17)*
CYCD3;1	674	579	681	- (14.10)	+ (1.01)
CYCD3;3	224	543	539	+ (142.41)**	+ (140.48)**
CYCD4;1	800	1,356	777	+ (69.56)*	- (2.83)
KRP1	465	484	585	+ (4.04)	+ (25.83)
KRP4	567	595	552	+ (4.92)	- (2.69)
MYB3R1	553	1,059	1,160	+ (91.43)*	+ (109.78)**
MYB3R4	1,105	1,601	937	+ (44.91)	- (15.25)
E2Fa	411	1,108	921	+ (169.61)**	+ (124.13)**
E2Fb	439	581	423	+ (32.34)	- (3.69)
E2Fc	656	902	584	+ (37.55)	- (10.96)
E2Fd	381	728	325	+ (91.17)*	- (14.77)
E2Fe	369	317	282	- (14.04)	- (23.60)
E2Ff	415	766	456	+ (84.47)*	+ (9.92)
DPa	591	1,212	1,308	+ (105.02)**	+ (121.36)**
DPb	838	1,098	1,084	+ (30.98)	+ (29.41)
OBP1	188	189	220	+ (0.53)	+ (16.94)
RBR1	309	320	297	+ (3.62)	- (3.85)

Gel band intensity is measured as counted pixel above background; * medium and ** high deviations from Col-0.

3.4.1.2 Quantitative RT-PCR

The three transcription factors MYB3R4, DPa and E2Fa as well as the cyclin-dependent kinase CDKB1;1 were selected for a quantification of their gene expression level in Col-0, atglr3.7 and OE:AtGLR3.7(2) employing qRT-PCR (Figure 24). The transcription factor MYB3R4 showed a slight upregulation in atglr3.7 (1.23 ± 0.41 fold change) and a minor downregulation in OE:AtGLR3.7(2) (0.73 ± 0.36 fold change). The cyclin-dependent kinase CDKB1;1 was significantly upregulated in atglr3.7 (1.66 ± 0.22 fold change) and to a lesser extent in OE:AtGLR3.7(2) (1.28 ± 0.19 fold change). The upregulation of the transcription factor DPa, however, was more intense in the *AtGLR3.7* overexpression line (1.80 ± 0.25 fold change) than in the knockout line (1.48 ± 0.21 fold change) compared to Col-0. The transcription factor E2Fa was similarly regulated in both transgenic plant lines showing a highly significant upregulation of 2.16 ± 0.12 and 1.57 ± 0.08 fold change in atglr3.7 and OE:AtGLR3.7(2), respectively.

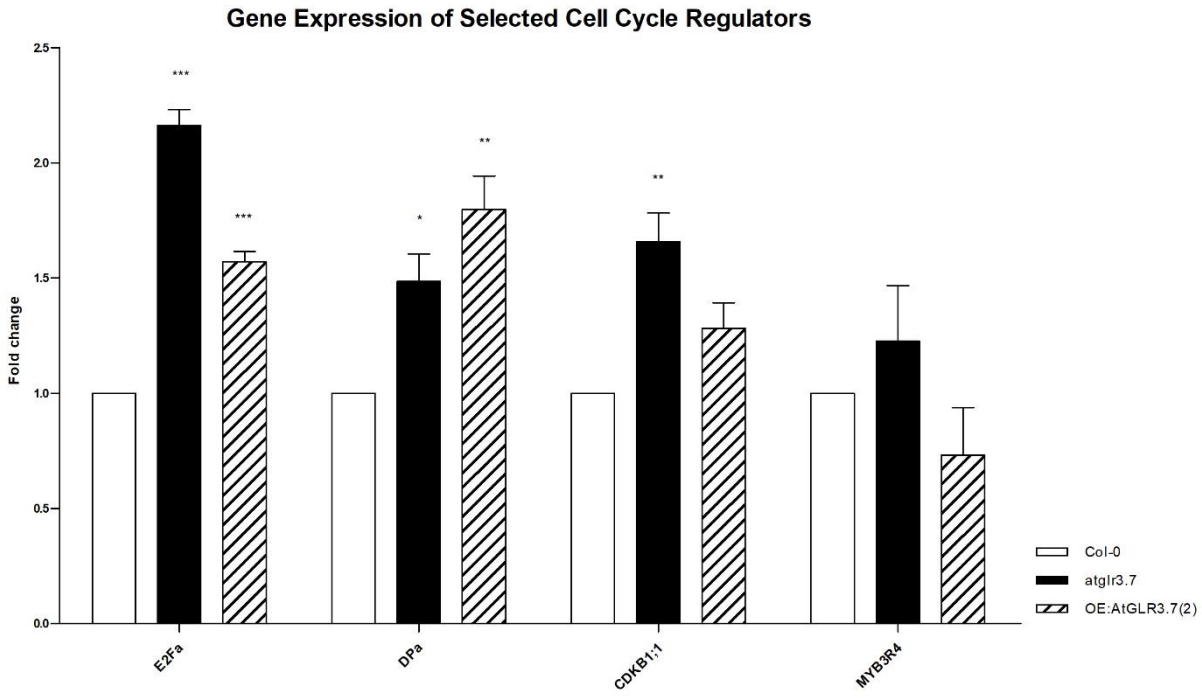

Figure 24. **Quantitative RT-PCR for Four Selected Cell Cycle Regulators.** Wildtype and transgenic *Arabidopsis thaliana* were grown hydroponically in sterile conditions and harvested on 14 DAI. Bulk RNA extractions and transcription into cDNA was followed by qRT-PCR. OE:AtGLR3.7(2) was characterized by upregulations of E2Fa, DPa and CDKB1;1 and a minor downregulation of MYB3R4, whereas the *AtGLR3.7* knockout line showed upregulations in all four genes. Data was normalized to *tubulin alpha-6 chain* (*Tub6*) and compared to Col-0. Statistical analyses among genotypes were conducted using a one-way ANOVA and Dunnett's *post hoc* test; $n = 3$. Asterisks indicate significant deviations from Col-0 with *$\rho < 0.05$, **$\rho < 0.01$ and ***$\rho < 0.001$. Error bars indicate SE.

3.4.2 Endoreduplication: Nuclear DNA Content

Endoreduplication events affecting the nuclear DNA content were measured by flow cytometry of DAPI-labelled nuclei from transgenic and wildtype *Arabidopsis thaliana*. The analysis of relative fluorescence intensities presented a unique pattern for each tested plant line (Figure 25). Peaks of fluorescence intensities represent the plant line's nuclear DNA content (C-value) that indicates the actual cellular chromosome quantity in which a genome duplication causes a two-fold increase of the C value.

Cells of the *AtGLR3.7* knockout line were generally characterized by a shift to a higher nuclear DNA content than in Col-0. An increase of 8C-, 16C- and 32C-values was detected at the expense of cells with 2C- and 4C-values. The overexpression lines OE:AtGLR3.7(1), -(2) and -(3) exhibited also an increase of cells with higher C-values. However, the quantity of cells with an elevated nuclear DNA content relative to Col-0 was much lower than in atglr3.7. A reduction of cells with a 2C-value and a pronounced increase of cells with a 4C-value was characteristic for all *AtGLR3.7* overexpression lines while this feature was most developed in OE:AtGLR3.7(2). Cells with a C-value higher than 4 were only slightly more frequent in the *AtGLR3.7* overexpression lines than in wildtype plants.

The percent distribution of all C-values in one plant line varied notably among the tested Arabidopsis genotypes (Figure 26A). The number of cells with a 2C-value was markedly reduced in both the *AtGLR3.7* knockout and overexpression lines which was indicated by the 4C:2C ratio (Figure 26B). This ratio considered cells which were in the process of cell proliferation or their first round of endoreduplication (4C) and related them to the number of cells which predated DNA synthesis, or which reached a mature cell state without endoreduplication events (2C). However, only the proportion of cells with a 4C-value was reduced in atglr3.7 while it was comparable in the *AtGLR3.7* overexpression lines and Col-0.

The proportion of cells with an 8C-value was elevated in all four transgenic plant lines. A moderate increase in the relative 8C-value was detected in the *AtGLR3.7* overexpression lines. The highest increase in the relative 8C-value was measured in atglr3.7.

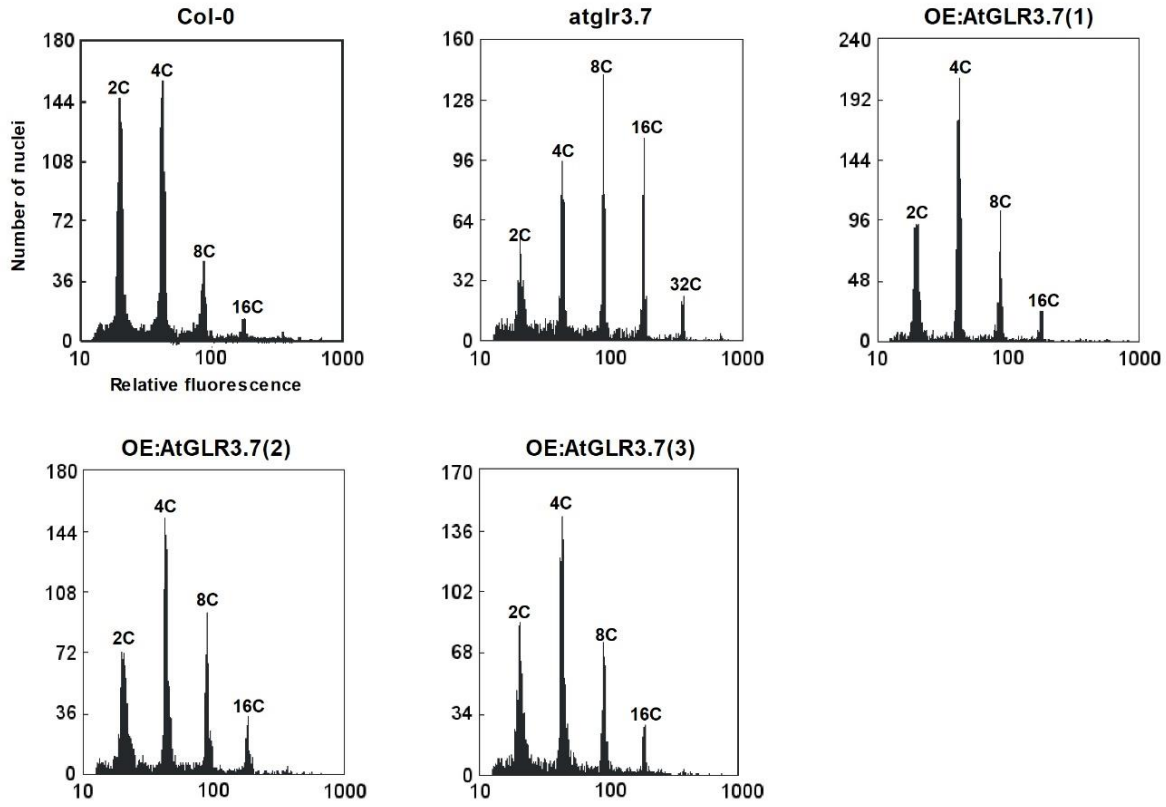

Figure 25. **Nuclear DNA Content Linked to Endopolyploidy Levels.** The respective nuclear DNA content is represented as a histogram of relative fluorescence intensities of isolated plant nuclei. All transgenic plant lines showed a reduction of cell with a 2C-value and an increase of cells with a >4C-value. Wildtype and transgenic *Arabidopsis thaliana* were sterile grown in ½ MS agar and harvested on 14 DAI. About 4,000 nuclei were counted for each plant line. Relative fluorescence is given in a logarithmic scale.

The relative amount of cells with a 16C-value was also elevated in atglr3.7 but only slightly increased in OE:AtGLR3.7(1), -(2) and -(3) compared to Col-0. The *AtGLR3.7* knockout line was, furthermore, the only tested plant line which displayed cells with a 32C-value.

Considering different groups of cells based on their C-values, the >2C:2C ratio was markedly elevated in the *AtGLR3.7* knockout line with a ratio of 4 but only half as much in the three overexpression lines which showed a ratio of 2 compared to a ratio of 1 in Col-0 (Figure 26C). This ratio considered all cells which were proliferating, in the process of endoreduplication or having reached a mature cell state with previous endoreduplication events (>2C) and related them to the number of cells which predated DNA synthesis, or which reached the mature cell state without endoreduplication events (2C).

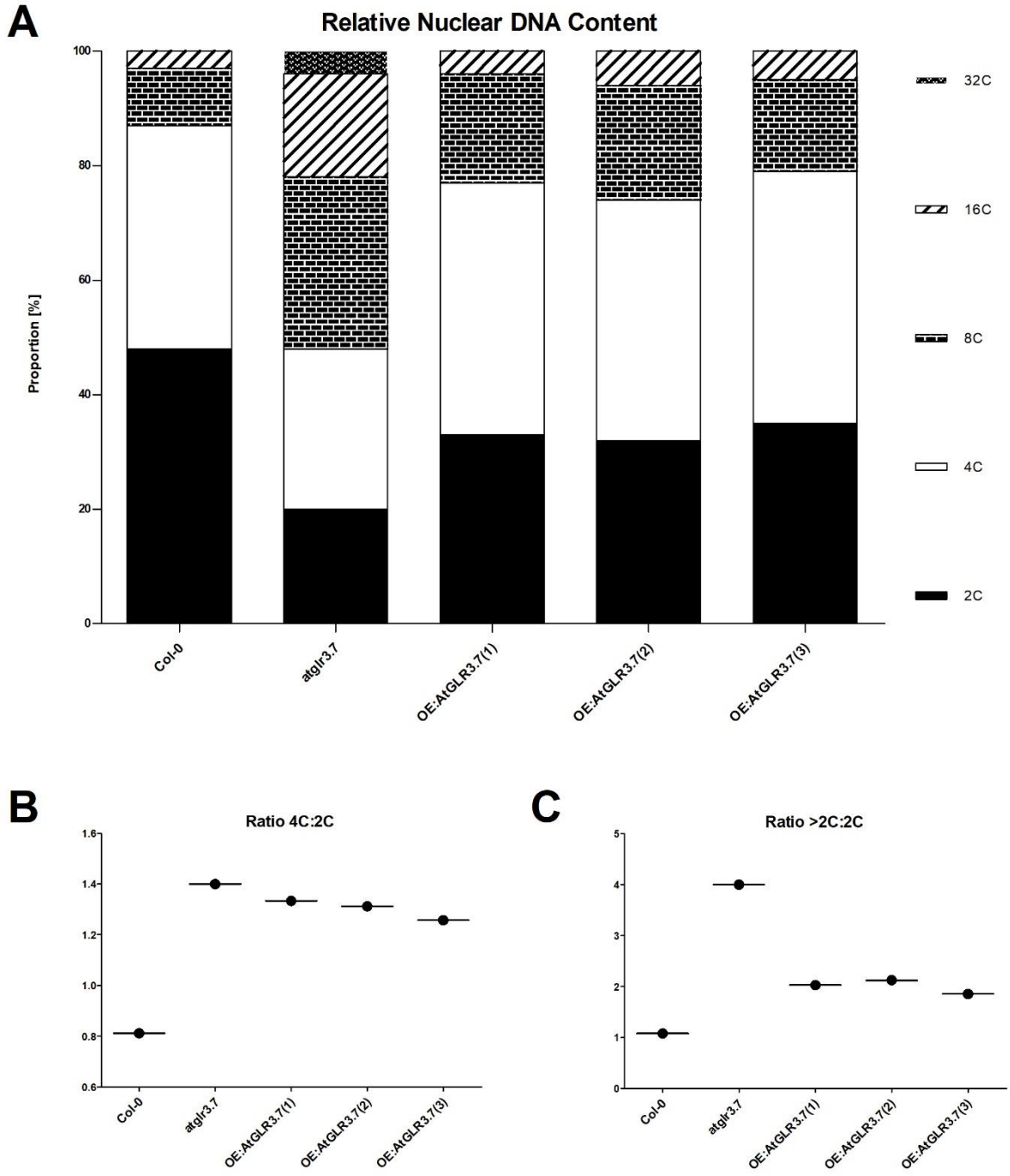

Figure 26. **Relative Nuclear DNA Content Linked to Endopolyploidy Levels.** Proportion of cells with a different C-value/DNA content ranging from 2C to 32C showed a strong increase of cells with a >4C-value in the *AtGLR3.7* knockout line and to a lesser degree also in the *AtGLR3.7* overexpression lines (A). The 4C:2C ratio was similarly elevated in all transgenic plant lines compared to Col-0 (B) whereas the ratio >2C:2C was quadrupled in atglr3.7 and doubled in all three *AtGLR3.7*overexpression lines (C). Wildtype and transgenic *Arabidopsis thaliana* were sterile grown on ½ MS agar and harvested on 14 DAI.

3.4.3 Protein Modification: AtMAPK3/-6 and Histone H3

3.4.3.1 Phosphorylation Status of AtMAPK3/-6

Total protein quantities and the amount of phosphorylated AtMAPK3/-6 were investigated in transgenic and wildtype *Arabidopsis thaliana* in order to determine the activation status of this protein kinase. Total protein extractions were made from seedlings for immunoblotting of AtMAPK3/-6.

A Coomassie Brilliant Blue staining verified an equal amount of extracted protein in all three samples (Figure 27A). Antibody labelling against the C-terminus of AtMAPK3/-6 led to two prominent bands on the immunoblot at a height of 42 and 44 kDa as well as to several unspecific bindings. There were no major deviations observed in the absolute protein quantity between Col-0, atglr3.7 and OE:AtGLR3.7(2) (Figure 27B).

An antibody labelling against only mono- and diphosphorylated AtMAPK3/-6 showed fainter bands on the immunoblot at similar heights of 42 and 44 kDa (Figure 27C). The intensity of these bands was comparable among all three plant lines.

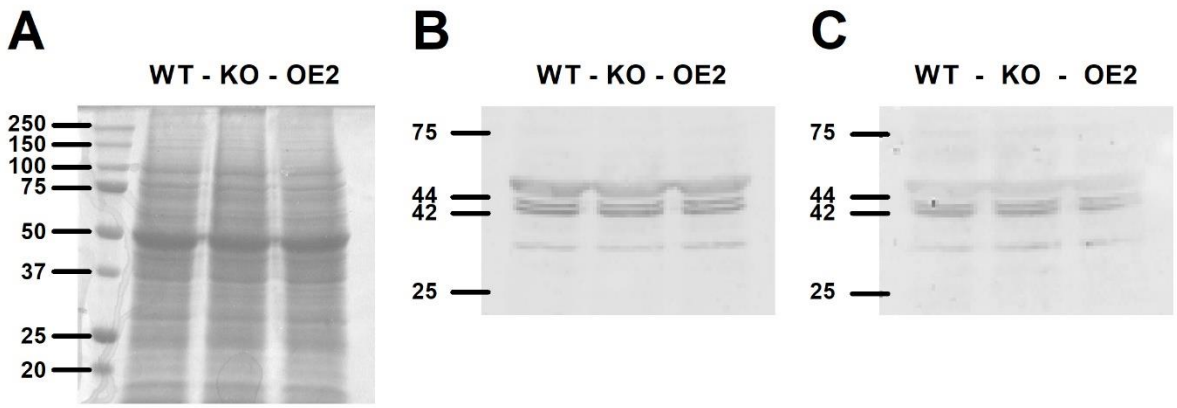

Figure 27. **Protein Quantities of AtMAPK3/-6 and Phosphorylated Isoforms.** Wildtype and transgenic *Arabidopsis thaliana* were sterile grown in ½ MS agar and harvested on 14 DAI. Equal protein loadings were indicated by Coomassie Brilliant Blue staining (A). Detection of AtMAPK3 and AtMAPK6 by anti-AtMAPK3 (42 kDa) and anti-AtMAPK6 (44 kDa), respectively, showed similar protein quantities in all tested plant lines (B). Phosphorylated AtMAPK3/-6 labelling by a phospho-p44/42 MAPK (Erk1/2) (Thr202/Tyr204) antibody revealed no deviations among wildtype and transgenic plant lines (C). WT – Col-0; KO – atglr3.7; OE2 – OE:AtGLR3.7(2). Molecular mass indications to the left of the gels in kDa.

3.4.3.2 Methylation Status of Histone H3

Investigations of the total amount of histone H3 and its methylation status were performed using transgenic and wildtype *Arabidopsis thaliana* plant extracts of only membrane-bound protein fractions. The loading control with Coomassie Brilliant Blue staining showed similar protein quantities in the samples of Col-0, atglr3.7 and OE:AtGLR3.7(2) (Figure 28A).

Antibody labelling with anti-histone H3 antibodies showed one strong band at a height of 16 kDa (Figure 28B). The band's intensity was comparable among all tested plant lines. An investigation of the methylation status of histone H3 by using a specific antibody against tri-methylated histone H3 at K27 led to the appearance of one prominent band at a height of 16 kDa (Figure 28C). The intensity of the band was comparable among the tested plant lines.

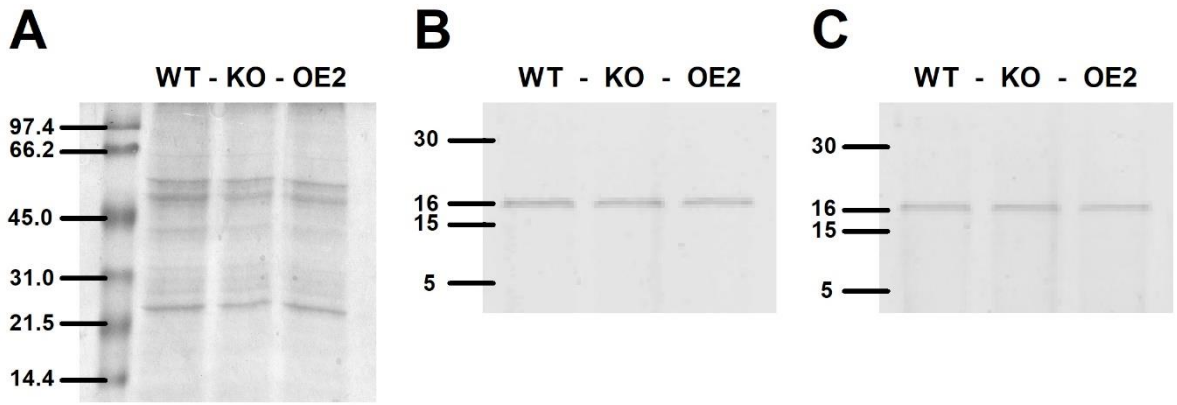

Figure 28. **Protein Quantities of Histone H3 and Its Methylated Isoform.** Wildtype and transgenic *Arabidopsis thaliana* were sterile grown in ½ MS agar and harvested on 14 DAI. Protein loadings are indicated by Coomassie Brilliant Blue staining (A). Detection of histone H3 by an anti-histone H3 antibody showed similar protein quantities in all tested plant lines (B). Tri-methylated histone H3 labelled by an anti-histone H3 (tri-methyl K27) antibody revealed no deviations among wildtype and transgenic plant lines (C). WT – Col-0; KO – atglr3.7; OE2 – OE:AtGLR3.7(2). Molecular mass indications to the left of the gels in kDa.

3.5 Plant Physiology

3.5.1 Evaluation of Sodium, Potassium and Calcium Ion Content

The knockout or overexpression of *AtGLR3.7* could have had an effect on the cellular ion uptake/loss. In order to investigate this possibility, wildtype and transgenic *Arabidopsis thaliana* were grown in soil and harvested three weeks after germination. Their total Na^+, K^+ and Ca^{2+} content was determined by photoelectric flame photometry and compared between Col-0, atglr3.7 and OE:AtGLR3.7(2) (Figure 29).

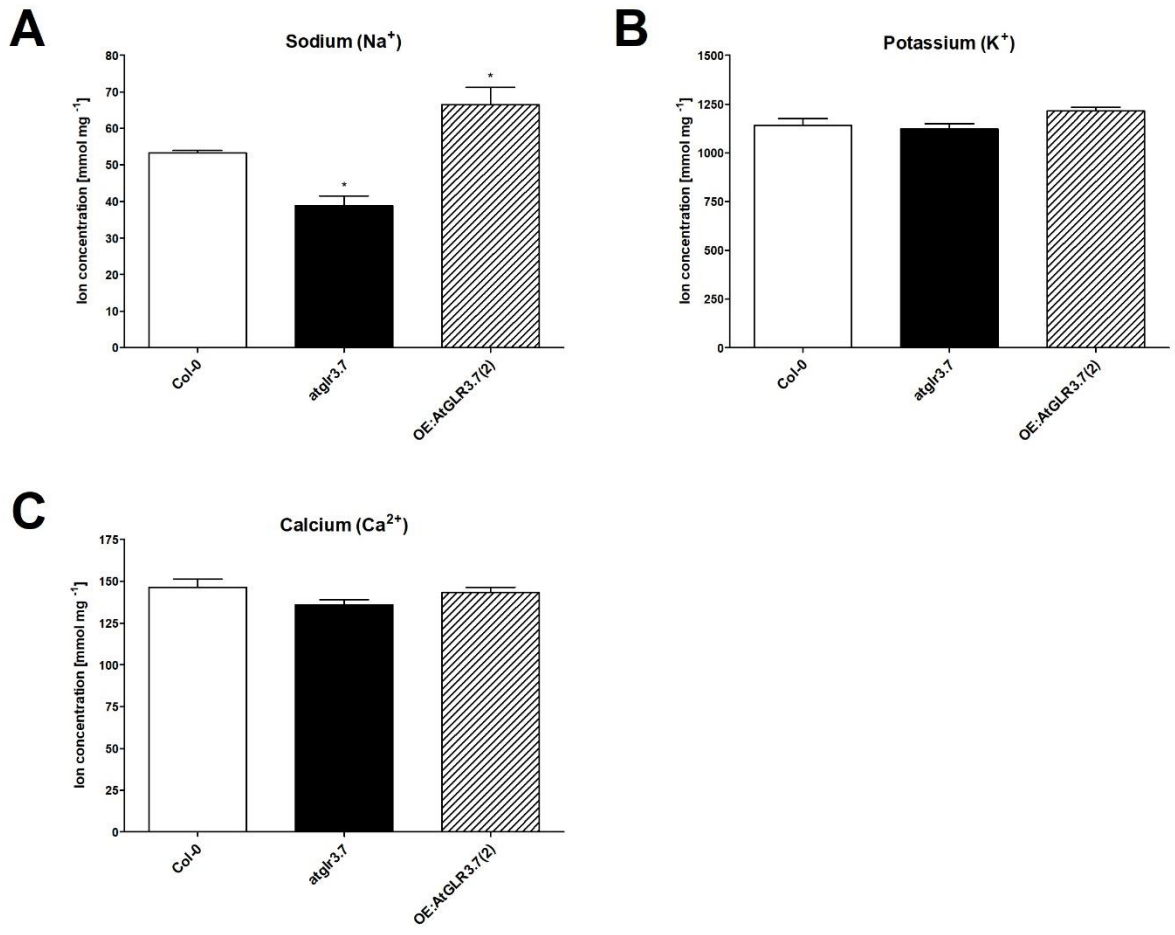

Figure 29. **Ion Concentration of Sodium, Potassium and Calcium in Three-Week-Old Arabidopsis Plants.** The sodium ion content was significantly increased in OE:AtGLR3.7(2) whereas atglr3.7 displayed a significantly lower sodium concentration than Col-0 (A). Concentrations of potassium (B) and calcium ions (C) were comparable among the tested plant lines. Wildtype and transgenic *Arabidopsis thaliana* were grown for three weeks in soil. Digested plant material was analysed using a flame photometer. Statistical analyses among genotypes were conducted using a one-way ANOVA and Dunnett's *post hoc* test; n = 6-7. Asterisks indicate significant deviations from Col-0 with *$\rho < 0.05$. Error bars indicate SD.

The concentration of K^+ did not vary significantly among the three tested genotypes with 1140 ± 35, 1121 ± 28 and 1213 ± 19 mmol mg^{-1} for Col-0, atglr3.7 and OE:AtGLR3.7(2), respectively. Similarly, concentrations of Ca^{2+} showed only minor variations with 146.4 ± 4.9, 135.9 ± 3.2 and 143.2 ± 3.3 mmol mg^{-1} for Col-0, atglr3.7 and OE:AtGLR3.7(2), respectively. However, the amount of Na^+ was significantly reduced in atglr3.7 by 73% (38.81 ± 6.10 mmol mg^{-1}) whereas OE:AtGLR3.7(2) showed a significantly increased concentration of Na^+ up to 125% (66.40 ± 11.78 mmol mg^{-1}) compared to the amount of Na^+ in Col-0 (53.24 ± 1.55 mmol mg^{-1}).

3.5.2 Response to Elevated Salinity

Alterations in the transgenic plant lines' ion content (see section 3.5.1 'Evaluation of Sodium, Potassium and Calcium Ion Content') prompted an investigation of the salt tolerances of wildtype and transgenic *Arabidopsis thaliana*. Therefore, the plant lines were exposed to three different salt concentrations (0, 50, 75 and 100 mM NaCl). Plants grown under sterile standard conditions were transferred to NaCl-containing ½ MS agar plates on 7 DAI and their root growth was measured daily (Figure 30A-C). The highest tested NaCl concentration (100 mM) caused similar growth reductions of -54.4 ± 0.3% in all tested plant lines compared to the mock treatment (Figure 30D).

However, significant variations in the plants' responses against mild (50 mM) and medium (75 mM) salt stress were detected among the different Arabidopsis genotypes. A relatively low concentration of 50 mM NaCl reduced the root growth of both Col-0 and OE:AtGLR3.7(2) by about -35% compared to untreated plants. Similarly, a medium salt concentration of 75 mM NaCl had a comparable effect on both plant lines which led to a root growth reduction of about -45%. On the other hand, the *AtGLR3.7* knockout line experienced a reduction of only -29 and -38% at low and medium salt concentrations, respectively.

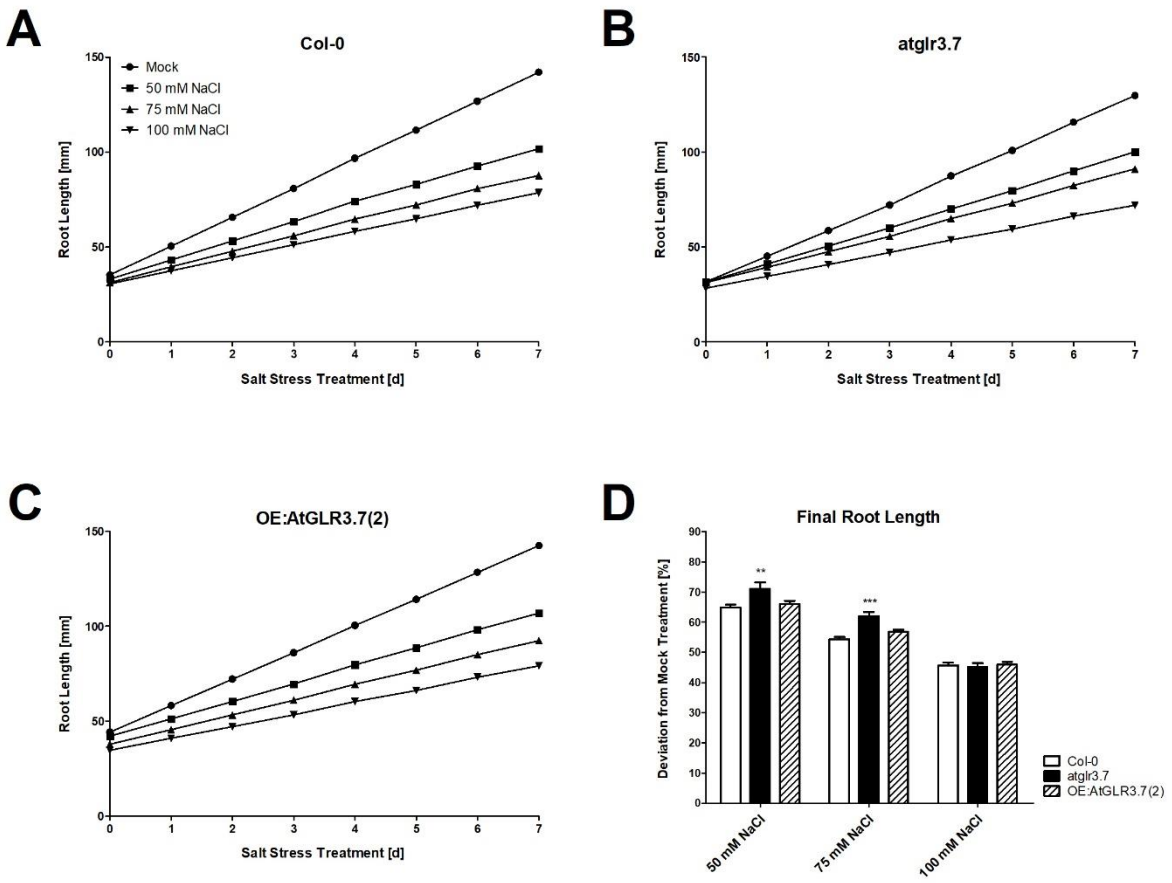

Figure 30. **Primary Root Growth in Response to Elevated NaCl Concentrations.** Wildtype and transgenic *Arabidopsis thaliana* were germinated on ½ MS agar and transferred to new ½ MS agar plates containing various NaCl concentrations (0, 50, 75 and 100 mM NaCl) on 7 DAI. Primary root growth was measured daily during the seven days of salt stress treatment (7-14 DAI) which caused comparable reductions in root growth in Col-0 and OE:AtGLR3.7(2) whereas atglr3.7 experienced less severe growth impairments at mild and medium salt concentrations (A)-(C). Comparisons of the final primary root length relative to a mock treatment in the respective genotype on 14 DAI showed highly significant deviations in atglr3.7 at 50 and 75 mM NaCl concentrations (D). Statistical analyses among genotypes were conducted using a one-way ANOVA and Dunnett's *post hoc* test; n = 11-18. Asterisks indicate significant deviations from Col-0 with $^{**}\rho < 0.01$ and $^{***}\rho < 0.001$. Error bars indicate SE.

3.5.3 Pathogenicity of *Pseudomonas syringae* in *Arabidopsis thaliana*

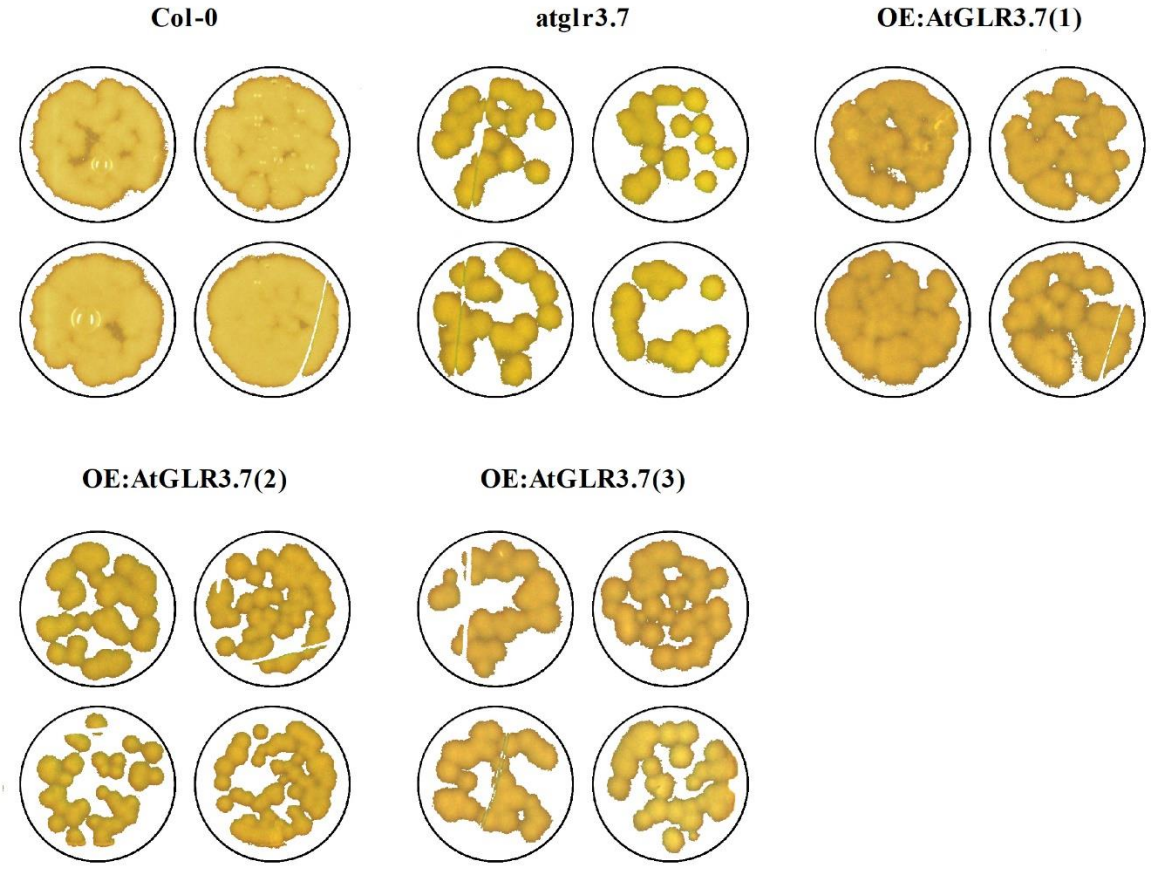

Figure 31. **Bacterial Growth of *Pseudomonas syringae* pv tomato DC3000 After Incubation in *Arabidopsis thaliana*.** Wildtype and transgenic *Arabidopsis thaliana* were grown on soil for four to five weeks before they were inoculated with *Pseudomonas syringae* pv tomato DC3000. After 48 h, plant tissue samples were taken and a bacterial titer was performed. Displayed are bacterial growth dilutions of 1:1000 after an extraction of the bacteria from grinded leaf tissue. Diameter of black rings represent 2 cm.

Plant immunity tests were conducted with the plant pathogen *Pseudomonas syringae* on adult transgenic and wildtype *Arabidopsis thaliana* in order to verify if there is an effect of the knockout or overexpression of *AtGLR3.7* on the plant's defence capabilities. A bacterial titer allowed for an evaluation of the plants' immune system and how it can cope with this kind of biotic stress. Growth assays of the virulent strain Pto DC3000 after inoculation in Arabidopsis leaves revealed significant deviations in sensitivities against this pathogen between transgenic and wildtype plants (Figure 31). While the bacterium showed a comparable growth in Col-0

and OE:AtGLR3.7(1), its growth was significantly reduced in OE:AtGLR3.7(2), -(3) and atglr3.7. In the latter plant line, the strongest reduction of bacterial growth was observed.

Quantitative analyses used two strains of *Pseudomonas syringae* (Pto DC3000 and Pto DC3000 hrcC) and evaluated their propagation capabilities in different *Arabidopsis thaliana* genotypes. After a 48-h incubation period, bacterial growth of the dissolved plant material was measured employing a bacterial titer. The growth of the non-virulent strain Pto DC3000 hrcC served as a control for the amount of collected plant material and the bacterial survivability in Arabidopsis. No deviations among the tested genotypes were detected in Arabidopsis plants inoculated with Pto DC3000 hrcC since a comparable bacterial growth of 3.57 ± 0.05 $\log_{10}(CFU/cm^2)$ was detected after inoculation in the respective plant lines (Figure 32).

The virulent strain Pto DC3000, however, showed significantly altered growth capabilities depending on the plant's genotype. All transgenic plant lines displayed a reduction in the bacterial titer compared to the wildtype Arabidopsis. OE:AtGLR3.7(1) showed a bacterial titer only slightly reduced by about -4% (5.56 ± 0.23 $\log_{10}(CFU/cm^2)$) compared to Col-0 with 5.82 ± 0.18 $\log_{10}(CFU/cm^2)$. Also minor but still significant reductions of -7 and -6% in the bacterial titer were observed for OE:AtGLR3.7(2) (5.44±0.39 $\log_{10}(CFU/cm^2)$) and -(3) (5.48±0.21 $\log_{10}(CFU/cm^2)$), respectively. The *AtGLR3.7* knockout line displayed the lowest bacterial growth with a bacterial titer of 5.01 ± 0.18 $\log_{10}(CFU/cm^2)$ which equals a reduction of -14% compared to Col-0.

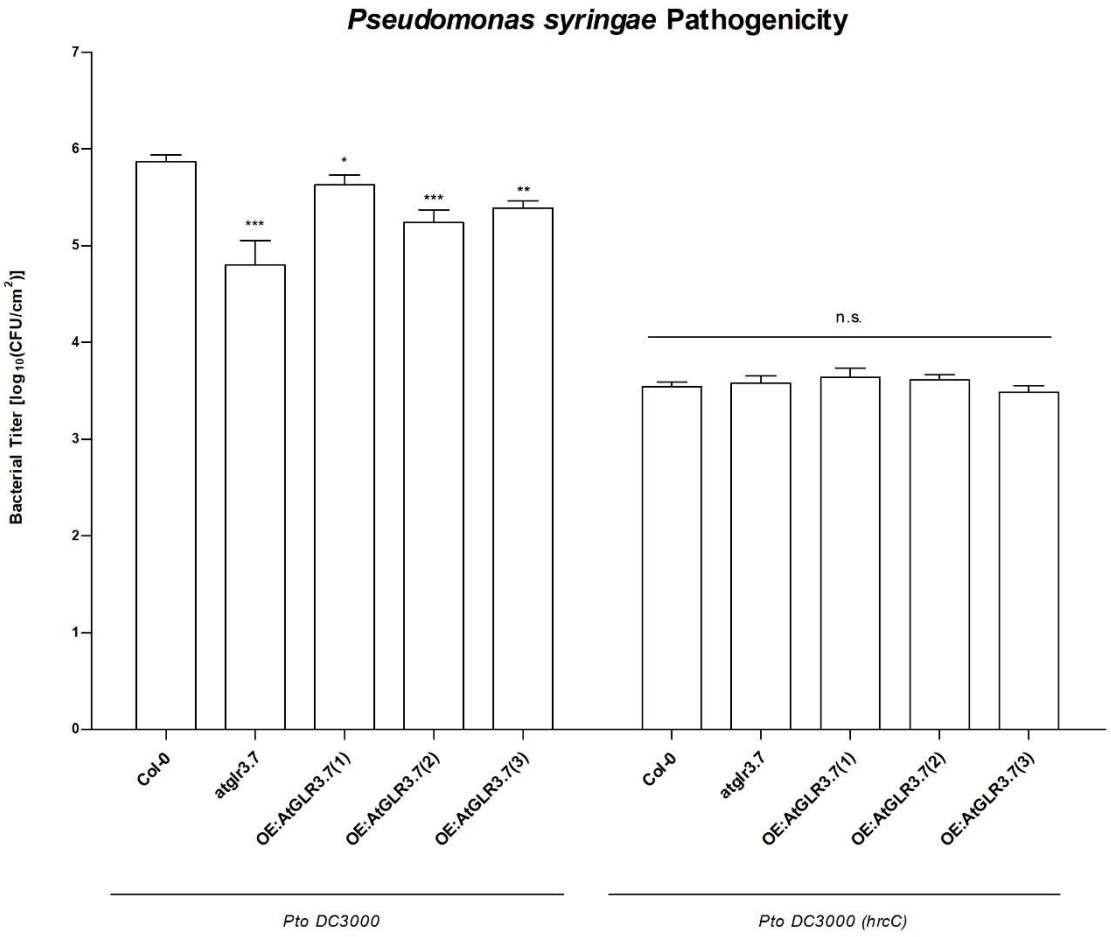

Figure 32. **Pathogenicity of Two Different Strains of *Pseudomonas syringae* via Bacterial Titer After Inoculation in *Arabidopsis thaliana*.** Bacterial titer of *Pseudomonas syringae pv. tomato* DC3000 (Pto DC3000) and a non-virulent mutant strain (Pto DC3000 hrcC) was conducted 48 h after bacterial incubation in four- to five-week-old wildtype and transgenic *Arabidopsis thaliana* grown in soil. Highly significant reductions in bacterial growth of Pto DC3000 were detected in all transgenic plant lines compared to Col-0 with the least bacterial growth occurring in the *AtGLR3.7* knockout line. Growth of the non-virulent strain Pto DC3000 hrcC was comparable in all tested plant lines. Statistical analyses among genotypes were conducted using a one-way ANOVA and Dunnett's *post hoc* test; n = 7-8. Asterisks indicate significant deviations from Col-0 with *$\rho < 0.05$, **$\rho < 0.01$ and ***$\rho < 0.001$. Error bars indicate SE.

4 Discussion

4.1 Varying *AtGLR3.7* Gene Expression Levels

In this work, three separate *Arabidopsis thaliana* overexpression lines were constructed in order to compare different gene expression levels of *AtGLR3.7* with wildtype plants as well as with the knockout line atglr3.7. All transgenic plant lines had Col-0 as a genotypic background allowing for an exclusive investigation of the AtGLR3.7-mediated effects on Arabidopsis plant development and physiology. The *AtGLR3.7* overexpression lines were chosen based on their divergent gene expression degrees in order to have an overexpression gradient and to exclude the effect of a potential insertion of the coding sequence into other functional genes within the genome of *Arabidopsis thaliana*. The latter could affect the plant phenotype aside from the desired alterations originating from an *AtGLR3.7* overexpression.

The three overexpression lines were labelled based on their *AtGLR3.7* overexpression levels as can be seen in Figure 5A, B. OE:AtGLR3.7(3) showed the highest *AtGLR3.7* gene expression level in both sqRT-PCR and qRT-PCR. Its gene expression was about eight times higher than in Col-0, followed by the *AtGLR3.7* expression level in OE:AtGLR3.7(2) and -(1) with an increase of about six and four times, respectively. This *AtGLR3.7* gene expression gradient allowed the investigation of an impact of a mild (OE:AtGLR3.7(1)), medium (OE:AtGLR3.7(2)) and strong (OE:AtGLR3.7(3)) gene overexpression on physiological characteristics such as plant growth rate and stress tolerance.

Interestingly, the *AtGLR3.7* knockout line exhibited a faint band during sqRT-PCR and a very low expression level of about 8% compared to Col-0 was detected employing qRT-PCR (Figure 5A, B). The knockout of *AtGLR3.7* was expected to result in a complete absence of the respective mRNA transcripts since a T-DNA fragment of about 4 kb was inserted into the gene coding sequence of *AtGLR3.7*. A verification of the insertion was conducted using primer pairs flanking the boarder at the end of the T-DNA fragment and the *AtGLR3.7* coding sequence (see section 7.3 ‘Verification of T-DNA Insertion in atglr3.7’).

It is possible that the insertion close to the end of the gene sequence at position 2698/2766 still allowed the transcription of a truncated version of *AtGLR3.7* which could probably become translated, too. The primer pairs used for the detection of the *AtGLR3.7* cDNA transcripts levels were situated near the beginning of the coding sequence so that a truncated *AtGLR3.7* version would have been detected in the presumed *AtGLR3.7* knockout line. On the other hand, the encountered cDNA levels were very low, and the functionality of a potentially curtailed protein

is cannot be expected. Further tests including an antibody labelling against the AtGLR3.7 protein in the respective knockout line could help to answer this question.

4.2 *AtGLR3.7* Positively Affects Plant Growth

4.2.1 Regulation of Seed Size

Seed development in *Arabidopsis thaliana* starts after the double fertilization of a central cell (twice haploid) and the egg cell (haploid) in the maternal ovule. The maternal integuments of the ovule develop into the seed coat whereas the fertilized central cell becomes the triploid endosperm and the fertilized egg cell forms a diploid embryo. The seed development itself takes place in two phases: (I) embryogenesis (syncytial stage) and (II) maturation.

During embryogenesis, high proliferation events of the endosperm and the integuments lead to multinucleated cells and an enlarged embryo sac/seed cavity, respectively. It is followed by further endosperm cellularization in which the multinucleated cells divide in a specific cytokinetic process (Sun *et al.*, 2010). Cell elongations, on the other hand, are characteristic for the maturation of the embryo where also storage compounds (lipids, proteins, etc.) are produced and compiled in organelles (Baud *et al.*, 2002). In this phase, most of the endosperm is replaced by the growing embryo until only a single cell layer remains in *Arabidopsis thaliana* (Berger, 2003). About ten days after pollination, the embryo reaches its final size and seed dormancy is established while its dry weight still increases due to further storage compound accumulations. The seed development is finalized when the seed desiccates about 20 days after pollination and both the embryo and the endosperm enter a developmental and metabolic quiescence until germination (Raz *et al.*, 2001).

The seed size itself is the product of a coordinated growth of the embryo and the endosperm as well as of the proliferation and the elongation of the integuments (Berger *et al.*, 2006). The initial growth of the integuments and the endosperm mostly determines the final seed volume since the embryo only replaces the already present endosperm (Sundaresan, 2013). Therefore, the regulation of these growth events is essentially affecting the final seed size.

The process of endosperm development is primarily made up of several mitotic cycles/nuclear divisions that lead to the formation of a syncytium. A comparison of the different seed sizes between wildtype and the transgenic Arabidopsis plant lines showed a marked increase in seed area for all *AtGLR3.7* overexpression lines while the *AtGLR3.7* knockout line exhibited a reduced seed extension (major, minor axis) and seed perimeter (Table 1). The

increase/reduction in seed size was strictly correlated to the *AtGLR3.7* mRNA/cDNA levels in which a gradual increase of *AtGLR3.7* expression levels as seen in the three overexpression lines caused larger seeds.

During endosperm development, an increase in mitotic cycles of the overexpression lines could have caused an enlargement of the endosperm that would become replaced by the growing embryo in later developmental stages. The reduced seed size in atglr3.7, on the other hand, could be a result of a premature endosperm cellularization leading to a reduced endosperm volume. In a study of Luo *et al.*, 2005, it was shown that the knockout of the LRR receptor kinase IKU2, which is solely expressed in the endosperm, caused a reduction in seed size.

LRR receptor kinases in general are known to be involved in developmental processes and as such their regulation is at least indirectly dependent on a proper calcium signalling (Torii, 2004). AtGLR3.7 as a putative calcium channel could function upstream of IKU2 as well as IKU1 which is also involved in seed size control (Wang *et al.*, 2010). In this way, an excess of AtGLR3.7 in the overexpression lines could lead to enhanced calcium fluxes and an amplified activation of theses receptor kinases.

An alternative explanation for the observed *AtGLR3.7*-mediated phenotype could be based on an increase in cell divisions of the integuments. An intensification of cell division activity of these compartments would create a larger space for a development of the endosperm and the embryo. The integument growth increase could also be transduced to other seed compartments where it would induce intensified growth of the endosperm or embryo, directly. APETALA 2 and auxin response factor 2 (ARF2) are two TFs known to affect the integument growth, which has repercussions also on the growth of other seed compartments (Schruff *et al.*, 2006; Ohto *et al.*, 2009). A possible involvement of ARF2 would indicate a much broader involvement of *AtGLR3.7* where this glutamate receptor could affect plant growth in general due to its effects exerted on the auxin signalling pathway.

A thorough analysis of the different seed compartments such as the integuments/seed coat, the endosperm and the embryo as well as their development during seed maturation are needed for a better understanding of the developmental processes affected by varying *AtGLR3.7* quantities. An estimation of the cell number in the integuments would clarify if this tissue is affected by the *AtGLR3.7*-mediated regulation of the final seed size. Cellular analyses could reveal if an increase in cell divisions occurs in the endosperm or the developing embryo and nuclear

duplication events could be investigated by determining the cellular DNA content. Moreover, gene expression analyses of the aforementioned TFs could help to pinpoint the exact mechanism in which an overexpression of *AtGLR3.7* leads to the observed enlarged seed size.

4.2.2 Accelerated Root Development

4.2.2.1 Root Architecture

The root system of *Arabidopsis thaliana* is typical for a dicot plant where at the beginning of the root development a pronounced primary root grows out of the embryo. The primary root is afterwards accompanied by several lateral roots that emerge from the root's pericycle. Eventually, adventitious roots are formed during the final stages of the plant development (Hochholdinger and Zimmermann, 2008). The growth of the root is regulated by intrinsic factors active during ontogenesis and shoot-derived signals adjusting root elongation and branching in response to above-ground events. Furthermore, the root architecture is reshaped also by an availability of inorganic (metals ions, phosphorus, nitrogen, etc.) and organic (amino acids, protein-derived substances, molecules of other organisms, etc.) compounds within the soil (Malamy, 2005).

Plants are capable of modifying their root development in two ways: (I) enhancing/reducing root growth or (II) determining the number of lateral roots (López-Bucio *et al.*, 2003). In order to accelerate the penetration of the soil as part of a foraging mechanism, plants can either increase the rate of cell divisions or alter cell elongations in a predefined range. These performances are found both in the primary root as well as in lateral roots.

Observations of the root growth in *AtGLR3.7* knockout, overexpression and wildtype plant lines revealed strong variations of the primary root length. The overexpression lines showed an increase in primary root length that was correlated to their *AtGLR3.7* gene expression levels (Figure 5; Table 2). OE:AtGLR3.7(1) was characterized by a root phenotype comparable to Col-0 in all tested parameters, i.e. primary root length/diameter, lateral root density and beginning of root hair zone (Table 2). OE:AtGLR3.7(3) and -(2) exhibited the longest primary roots with significantly increased root diameters while OE:AtGLR3.7(3) exhibited a boost in growth throughout the time course (Figure 8B). In contrast, the knockout line atglr3.7 displayed a shortened primary root and a significant reduction in daily root growth especially on 7 DAI (Figure 8B). These findings are in accordance with the observations regarding differences in

primary root length which were most pronounced in early plant development stages. The measured deviations were mitigated in later growth stages in which OE:AtGLR3.7(3) showed an almost similar daily growth as Col-0.

The root architecture, apart from the primary root growth/length, however, was alike in all tested plant lines (Table 2). The frequency of lateral root formation correlated with the effective primary root length. Here, a longer root harboured more secondary roots but the density of additional roots on the primary root was comparable in the different Arabidopsis genotypes. However, the *AtGLR3.7* knockout line was characterized by a minor increase in secondary root density that was likely due to the reduction in primary root growth rate. It seems that the formation of new lateral roots did not parallel the growth process of the primary root in this genotype.

Nonetheless, this mismatch between primary root length and lateral root formation could be an indication for an impaired signal transduction pathway among the cellular determinants regulating and linking both processes. Auxin is well-known as a key regulator of plant growth in both shoot and root tissues. While high auxin concentrations promote growth in the above-ground tissue, i.e. meristems such as the SAM, equal concentrations applied to the root inhibit primary root growth and promote the formation of adventitious roots (Benjamins and Scheres, 2008; Vernoux *et al.*, 2011).

Auxin seems to affect several cellular aspects in this context and it has been shown that cell elongation and divisions in the root are heavily influenced by this phytohormone through the formation of actin filaments within root cells (Rahman *et al.*, 2007). Additionally, auxin plays an important role in the formation of lateral roots where it is involved in the processing of endogenous signals and their transmission into an adaptive lateral root development (Lavenus *et al.*, 2013).

An investigation of auxin distributions in all tested plant lines would help to elucidate a possible role for this hormone in the observed alterations of root growth. Whatever the exact mechanism in which primary root growth was altered in the transgenic Arabidopsis plants, there are only two ways in which root growth can be promoted: (I) enhanced cell elongation or (II) an increase of cell divisions within the meristem. Therefore, the final length of cells in the differentiation zone of the root and the meristematic activity of the RAM were investigated in order to isolate the pathways which were affected by the varying *AtGLR3.7* gene expressions.

4.2.2.2 Enlargement of the Root Apical Meristem due to AtGLR3.7 *Overexpression*

An explanation for the enhanced root growth observed in the *AtGLR3.7* overexpression lines as well as the slightly reduced growth in the *AtGLR3.7* knockout line was sought by investigating the possibility of alterations in cell morphology or cellular activity within the RAM. This meristem is a key regulator of root growth due to its capability of supplying new cells in the MZ of the root. The adjustment of cell division events is the basis for adaptive root growth since only by the addition of renewed cells, and their subsequent and eventual asymmetrical elongation, the plant root can penetrate the soil in a guided and controlled manner. For that reason, the size of the RAM was measured in all tested plant lines as a first indicator of altered root growth velocities. Reduced or enlarged RAM sizes/lengths have been reported to be directly associated with an impeded or accelerated growth (Meng *et al.*, 2012).

The overexpression lines exhibited an *AtGLR3.7* gene expression-dependent enlargement of the MZ within the RAM (Figure 19). A detailed analysis of the epidermal and cortical cells/rows revealed highly significant extensions of the cell division zone of about 10 to 15% for both cell types in OE:AtGLR3.7(2) and -(3) while OE:AtGLR3.7(1) was characterized by only a minor expansion of about 5% of these tissues (Figure 20). The knockout line atglr3.7, on the other hand, displayed a shortened MZ with a reduction of about -5% compared to Col-0 (Figure 20). These observations clearly indicate a connection between the expression level of *AtGLR3.7* and the size of the RAM in all transgenic plant lines.

Auxin gradients and maxima within the root tip have been found to be associated with cell divisions and elongations (Grieneisen *et al.*, 2007). A possible explanation for the extended MZ could be based on a change in those auxin gradients near the root apex. Here, the relocation of auxin efflux carriers like the PIN proteins or members of the AUX1/LAX family could prolongate the zone of auxin concentrations in the *AtGLR3.7* overexpression lines while this zone would be shortened in atglr3.7. Another explanation could be an increase in auxin biosynthesis within the root tip. It has been shown that dividing cells of the RAM are capable of synthesizing auxin by themselves to a limited extent rather than only responding to extracellular auxin gradients (Petersson *et al.*, 2009). Genes belonging to the tryptophan-dependent indole-3-acetic acid biosynthesis pathway play an important role in local auxin production (Ljung *et al.*, 2005). In this scenario, *AtGLR3.7* could be involved in calcium signalling events close to or within the meristematic tissue causing indole-3-acetic acid biosynthesis gene upregulation. Here, a crossing of the transgenic *AtGLR3.7* Arabidopsis with

plant lines expressing auxin reporters such as DR5 would help to elucidate if higher or broader auxin maxima along the root axis are involved in the observed root growth alterations.

4.2.2.3 Enhanced Meristematic Activity in AtGLR3.7 *Overexpression Plant Lines*

Kinematic models permit access to an array of key factors determining plant growth. The root of *Arabidopsis thaliana* provides an ideal system in which the indeterminate growth of the root tip, i.e. the continuous activity of the RAM, as well as its repetitive and straightforward cellular organization allow observations of fundamental parameters defining root development including meristem size, CN within the meristem, mature CL and overall growth rate. Applying equations established by Fiorinani and Beemster (2006), it was possible to compute the meristematic activities of all tested plant lines (Figure 22).

The measured decrease in root growth in atglr3.7 is only partially explained by the minor reduction in MZ expansion (Figure 20). The mature/differentiated cells displayed a comparable CL in Col-0 and atglr3.7 (see further below). Therefore, the diminished root growth measured in the *AtGLR3.7* knockout line can originate only in a reduction in CPM which was lowered in atglr3.7 due to a reduction in ADR and an extension of CCD (Figure 22). Moreover, cells of atglr3.7 appeared to remain longer within the RAM (see RTP) than cells of the other plant lines. The *AtGLR3.7* overexpression lines, on the other hand, were characterized by an *AtGLR3.7*-dependent increase in CPM (Figure 22A). It is intriguing that ADR as well as CCD were not affected by an overexpression of *AtGLR3.7* (Figure 22B). Therefore, the enhanced root growth in all three overexpression lines was not caused by faster dividing cells underlining the fact of a minimum time required for cells to duplicate (Richard *et al.*, 2001). These results are in accordance with comparable RTPs in Col-0, OE:AtGLR3.7(1), -(2) and –(3) (Figure 22C, D).

Taken together, the data suggest an involvement of *AtGLR3.7* in root growth by extending the cell division zone/MZ as well as the meristematic activity of the root in *AtGLR3.7* overexpressing plants while the knockout of *AtGLR3.7* seems to reduce the rate of cell divisions within the RAM and/or prolong the duration of the plant cell cycle. Both phenomena could be explained by a variation of the auxin gradient at the root tip. Under this premise, the extension of MZ as well as an elevation of CPM would coincide with a broadened auxin maximum close to the QC in the *AtGLR3.7* overexpression lines while a reduction of the auxin concentration in this region would lead to fewer cell divisions as was observed in atglr3.7.

Interestingly, the observed extension of the cell cycle in atglr3.7 could be the origin of the measured elevated nuclear DNA content associated with a presumable increase in endoreduplication (see section 4.4.2.2 Endopolyploidy Levels). In this respect, endoreduplicating cells would 'migrate' more slowly along the developmental trajectory of the root axis since additional rounds of DNA replication could already take place within the RAM.

4.2.2.4 Similar Cell Morphologies in All Tested Plant Lines

An investigation of the cell morphology in the meristematic tissue and the DZ was conducted in order to determine if cell elongations/enlargements could have caused the observed alterations in root growth. A characterization of meristematic cells within the RAM showed that the cell features (CL, CW_r and CW_t) were comparable among the tested plant lines (Table 7 and Table 8). However, CS appeared to be increased in both epidermal and cortical cells in OE:AtGLR3.7(3) and to a lesser extent in OE:AtGLR3.7(2) (Table 5 and Table 6). This increase in CS of meristematic cells was, nonetheless, only subtle and originated from relatively weak augmentations in CW_r and CW_t while CL remained unaffected.

The observed enlargement of the cells could have been a side effect of the methods used to determine these cell parameters. As described in section 2.3 'Characterization of the Root Apical Meristem', the cell parameters were mean values of all cells added up starting from the QC to the beginning of the EZ. The proposed hypothesis for the observed root growth phenotype in the transgenic Arabidopsis plant lines is founded on the assumption that cell division events within the meristematic tissue are augmented as it is indicated by an increase in CN within this tissue in the *AtGLR3.7* overexpression lines while CN was reduced in atglr3.7 (Table 5 and Table 6). Here, additional cell division events could lead to a potential cytokinesis of cells that would have already started to expand under standard conditions like in Col-0. The resulting daughter cells would emerge from a previously comparatively large cell. These relatively sizable daughter cells would cause a shift in the mean cell values of all mitotic cells observed, especially in OE:AtGLR3.7(3), which was characterized by the longest MZ and the highest mitotic cell number in the RAM. In this way, the average CS would be distorted by these larger cells that would belong to the EZ in Col-0. Therefore, the possibility of an increase in cell elongation within the root as a cause for the measured root growth accelerations was ruled out.

4.2.3 Increase in Aerial Tissue

Observations of the *AtGLR3.7* overexpression lines showed a growth-stimulating effect for all above-ground tissues apart from the already described enhanced root growth. As a rough estimation, the total plant biomass increased significantly depending on the *AtGLR3.7* expression level in all three overexpression lines while it was reduced in *AtGLR3.7* knockout line (Figure 12A). Since the changes in FW were not associated with alterations of RWC (Figure 12B), a genuine effect on plant biomass accumulation including all biomolecules should be assumed in the transgenic Arabidopsis plants.

Detailed measurements revealed an overall growth boost of the rosette-forming leaves in terms of absolute rosette area and radial expansion in OE:AtGLR3.7(2) and to a lesser extent also in OE:AtGLR3.7(3) and -(1) (Figure 9A and Table 3). Interestingly, all three overexpression lines displayed an accelerated rosette growth in early developmental stages but this enhanced growth was only steady in OE:AtGLR3.7(2) whereas OE:AtGLR3.7(3) appeared to suffer from growth impairments at an advanced plant age. These observations were similar to the investigated stem growth where OE:AtGLR3.7(2) displayed a steady growth acceleration while the initial growth boost in the other two overexpression lines abated over time until the final stem length was comparable to Col-0 (Figure 10 and Table 4). The slightly enhanced growth characteristics in OE:AtGLR3.7(1) as well as the minor growth retardations in atglr3.7 were in accordance with the established *AtGLR3.7* expression gradient hypothesis.

However, following this proposition, it would have been expected that OE:AtGLR3.7(3) (with the highest *AtGLR3.7* gene expression level) exceeded all other plant lines in the growth of aerial parts. The results collected here contradict this assumption since OE:AtGLR3.7(3) exhibited an impaired rosette and stem growth in late developmental stages compared to the other overexpression lines. Looking at rosettes and stems characteristics (Table 4), the overexpression lines were characterized by an unsteady and non-linear growth boost. They developed more side bolts close to the rosette than Col-0 or atglr3.7 while at the same time fewer branches emerged on the main bolt.

Therefore, it can be speculated that an accelerated growth of the rosette and the stem negatively affects the formation of lateral shoot primordia on the main bolt. Furthermore, the growth limitations seen in OE:AtGLR3.7(3) could indicate a physiological *AtGLR3.7* gene expression threshold above which cell proliferation/production cannot be further accelerated but, on the contrary, appears to become impaired and causes developmental retardations.

The data regarding the growth of the above-ground tissue in the transgenic *Arabidopsis thaliana* could be connected to alterations and/or disturbances of the auxin distribution along the growth zones in the aerial parts of the plant. Auxin maxima are found within the SAM but also along the hypocotyl/stem located at newly forming plant organs such as leaves and side bolts (Reinhardt *et al.*, 2003). The presence of auxin in these tissues induces various signalling cascades and involves the activation of several cell proliferation promoting factors. One example is the plant-specific protein AUXIN-REGULATED GENE INVOLVED IN ORGAN SIZE (ARGOS) which is localized within the ER (Hu *et al.*, 2003). Its expression is clearly regulated by auxin and an overexpression of this gene causes larger above-ground organs while a reduced expression has the opposite effect and leads to the development of smaller leaves and shoots (Hu *et al.*, 2003). Here, it seems that this protein augments cell division events by increasing the duration of the cell proliferation phase in newly formed organs through a stimulation of CYCD3;1. The activation of ARGOS entails the recruitment of the APETALA 2-like ethylene-responsive transcription factor ANT, a member of the APETALA 2/ERF family, which in turn upregulates the cell cycle regulator CYCD3;1. A loss of CYCD3;1 together with the other two CYCDs causes a premature termination of the cell proliferation phase and provokes an untimely onset of the endocycle (Dewitte *et al.*, 2007).

It would be conceivable for AtGLR3.7 to influence the distribution/concentration of auxin maxima within the shoot and, in that way, prolong and/or extend the cell proliferation activity within the organ primordia. AtGLR3.7, as a potential calcium channel, could affect the localization of auxin efflux or influx carrier such as PIN1 or AUX1, respectively. It is well established that the subcellular localization of these transporters greatly affects auxin fluxes and concentrations in distinct regions of the plant (Benková *et al.*, 2003; Reinhardt *et al.*, 2003). Modifications of these proteins by protein kinases or phosphatases would strongly affect their subcellular localization and/or function. The phosphorylation status of PIN1 has been found to be controlled by the kinase PINOID and the phosphatase PP2A and it is reasonable to speculate about an AtGLR3.7-mediated calcium signalling which could affect the activity of such enzymes (Michniewicz *et al.*, 2007).

The alteration of auxin maxima by AtGLR3.7 would present a suitable explanation for the observed phenotype in the transgenic *Arabidopsis thaliana*. Gentle auxin concentration transitions could explain the smooth growth alterations in the *AtGLR3.7* overexpression lines. Under the light of these shifted auxin gradients, the observed phenotype of OE:AtGLR3.7(3) which was characterized by growth impairments, could be caused by mismatched Ca^{2+} signals

originating in an excess of the putative calcium channel AtGLR3.7 within the cellular membranes. Since this plant line displayed the highest *AtGLR3.7* expression level, a proper and carefully regulated AtGLR3.7 concentration seems to be crucial for a proper functioning of meristematic cell divisions and plant growth in general.

4.2.4 Modified Plant Growth

4.2.4.1 Etiolated Root and Hypocotyl Growth

The parameters of hypocotyl elongation and root growth under dark conditions (skotomorphogenesis) were measured in *Arabidopsis thaliana* wildtype and transgenic plants in order to investigate the associated, particular growth characteristics. The process of plant growth in darkness causes a distinct phenotype that is clearly different from plants grown in light or light-dark cycles. Specific growth adaptations allow the young plant to allocate its resources from the development of the root and photosynthetic apparatus to the exploration of its surroundings in order to find a suitable light source. Under natural conditions, seedlings are covered under foliage or within the soil and must penetrate the substrate to reach the sunlight. These so-called etiolated seedlings exhibit a reduced root growth, a noticeably elongated hypocotyl as well as a characteristic apical hook to pierce the overlaying stratum while at the same time protecting their closed cotyledons and the SAM (Josse and Halliday, 2008).

Root growth is unaffected by AtGLR3.7 *knockout during skotomorphogenesis*

The skotomorphogenic phenotype of all tested plant lines showed no deviations from Col-0 (Figure 13). All plant lines were characterized by an elongated hypocotyl and the presence of an apical hook. Detailed measurements of root growth and hypocotyl elongation showed alterations only in the final root length (Figure 14). These differences were comparable to the already described findings in which the *AtGLR3.7* overexpression lines exhibited an accelerated root growth.

Interestingly, the previously monitored root length reduction seen in atglr3.7 when grown under a standard light/dark cycle was absent in seedlings grown in darkness. Arabidopsis roots grown on MS agar plates normally experience light stress that prompts escape responses within the plant leading to an increased root growth in order to reach darkness/soil (Yokawa *et al.*, 2014). Therefore, it can be assumed that under the standard light cycle the transgenic as well as the

wildtype *Arabidopsis thaliana* were provoked to maximize their root growth and that only these conditions revealed the impairments in meristematic activity in the *AtGLR3.7* knockout line. A lack of light stress during skotomorphogenesis eliminated the need for an accelerated root growth, which ultimately led to comparable growth characteristics in atglr3.7 and Col-0 due to the normal growth rate of the root. However, the enhanced meristematic activity in the *AtGLR3.7* overexpression lines appeared to boost root growth even under these light-stress-free conditions.

Taken together, this could imply that the knockout of *AtGLR3.7* diminishes the ability for a faster than normal root growth (as seen under light stress) while the overall root growth development appears to be unaffected. An overexpression of *AtGLR3.7*, on the other hand, seems to cause enhanced root growth independent of the light/dark conditions (compare Figure 14B and Table 2), arguing for an in general increase in mitotic activity of the RAM in these transgenic plant lines.

Comparable hypocotyl elongation in transgenic and wildtype plant lines

Etiolated hypocotyl elongation is mainly driven by cell elongations along the hypocotyl while the contribution of cell proliferation appears to be negligible during this process (Gendreau *et al.*, 1997). Comparable etiolated hypocotyl lengths (see Figure 14A) among the tested plant lines indicate that cell elongation seems to be unaffected by an *AtGLR3.7* knockout or overexpression. Previous investigations of mature root cell morphologies have already shown that the final cell size/length was similar among the transgenic and wildtype Arabidopsis plant lines (see section 4.2.2.4 ‘Similar Cell Morphologies’). Both findings regarding the cell elongation exclude the possibility of an effect of AtGLR3.7 on the cell size via elongation or expansion further supporting the hypothesis of an involvement of *AtGLR3.7* in cell proliferation.

4.2.4.2 Inducible AtGLR3.7 *Overexpression*

The expression of *AtGLR3.7* under control of an inducible 17-β-estradiol promoter showed a characteristic phenotype similar to the one observed in the constitutively overexpressing OE:AtGLR3.7(1), -(2) and -(3) (Figure 15). The promoter used here was chosen due to its high sensitivity even at very low 17-β-estradiol concentrations with an effective range between 0.008 and 5 µM. The maximum gene expression of this inducible promoter can be up to eight times

greater than that of a gene under control of the 35S promoter within 24 h while first gene inductions can be observed within a short timeframe, starting from 30 min onwards after 17-β-estradiol application (Zuo *et al.*, 2000). The employed experimental setup for the induction of the *AtGLR3.7* overexpression covered ten days of growth under sterile conditions on ½ MS-agar plates which allowed for not only a sufficient time for an activation but also a period for an adjustment of the gene expression (down- and/or upregulation).

I:AtGLR3.7(1), one of two tested inducible overexpression lines, displayed a similar phenotype to OE:AtGLR3.7(2) and –(3) which differed significantly from Col-0 in terms of root length, number of secondary roots and rosette growth (Figure 15). Notably, the growth alterations were more pronounced when the roots grew within the agar instead of on its surface. The enhanced exposure of these root to the surrounding 17-β-estradiol-containing agar could have caused an amplified *AtGLR3.7* gene expression with the associated phenotype. The rosette growth was especially affected where the difference between roots grown within the agar and roots grown on its surface accounted for an increase in rosette size of about 30%.

The characterization of an induction of the *AtGLR3.7* overexpression further underlines the previous observations regarding the growth-stimulating effect of elevated *AtGLR3.7* expression levels. Comparisons between induced and non-induced *AtGLR3.7* plant lines showed a significant effect on root and rosette growth. However, the observed root growth phenotype was less pronounced than in the constitutively overexpression lines such as OE:AtGLR3.7(3). Speculations about either a subsequent downregulation of an induced *AtGLR3.7* overexpression or later impairments in growth due to an excess of *AtGLR3.7* transcript levels as it has been observed in the strong overexpression line OE:AtGLR3.7(3) (see section 4.2.3 ‘Increase in Aerial Tissue’), should be further investigated by determining the exact gene expression levels of *AtGLR3.7* via qRT-PCR during the course of a 17-β-estradiol treatment. The correlation between gene expression levels and plant phenotype could be further investigated by this method.

4.2.4.3 Divergent Effects of L-Glutamate on Root Growth in Transgenic Plant Lines

Glutamate as a potential major activator of GLRs was externally applied to transgenic and wildtype Arabidopsis plants in order to measure its effect on primary root growth. Here, significant variations have been detected between Col-0, atglr3.7 and OE:AtGLR3.7(2) (Figure 17). Increasing L-glutamate concentrations had the tendency to slow primary root growth where a low amino acid concentration-dependent reduction was confirmed in all concentrations except at 250 µM in wildtype plants (Figure 17A, B). The ability of glutamate to inhibit root growth was already described by Walch-Liu *et al.* (2006) where a concentration of 1,000 µM L-glutamate diminished primary root length significantly. Although concentrations as high as 1,000 µM were used in the experimental setup for this work, only minor reductions in daily root growth were observed and the more pronounced inhibition of daily root growth begun relatively late on 13 to 14 DAI in wildtype Arabidopsis.

However, L-glutamate exerted a much stronger inhibitory effect on primary root growth in OE:AtGLR3.7(2) (Figure 18). The lowest tested concentration (50 µM) reduced the final root length by about -12% compared to a mock treatment (Figure 16B). The enhanced sensitivity to the inhibiting effect of increasing L-glutamate concentrations was more obvious at higher concentrations of 250 and 1,000 µM where reductions of -25 and -45%, respectively, were detected. Furthermore, an investigation of the daily root growth in response to increasing L-glutamate concentrations revealed that OE:AtGLR3.7(2) responded much earlier with a root growth inhibition than Col-0 (Figure 17E, F). Both observations argue for a higher susceptibility of this transgenic plant line probably due to an excess of *AtGLR3.7* within the plant.

Since L-glutamate caused a suppression of root growth in Col-0 as well as in OE:AtGLR3.7(2) and considering the enhanced susceptibility to this inhibitory effect in the overexpression line, the *AtGLR3.7* knockout line was expected be insensitive to the L-glutamate-mediated reductions in primary root growth. However, increasing amino acid concentrations led to a concentration-dependent increase in primary root growth in atglr3.7 (Figure 16B). Detailed analysis of the daily root growth and a relative root growth comparing the initial root length before the transfer to glutamate-containing agar plates, showed a strong increase in root growth especially at higher concentrations of 250 and 1,000 µM (Figure 17C, D).

Interestingly, a concentration of 250 µM L-glutamate led to a restoration of the primary root growth phenotype in the *AtGLR3.7* both knockout and overexpression line (Figure 18E, F). This finding could indicate a physiologically effective concentration of L-glutamate within the

apoplast of plants participating in root growth regulations. It has already been established that naturally-occurring Arabidopsis ecotypes show different sensitivities to L-glutamate-mediated inhibitions of their primary root (Walch-Liu *et al.*, 2006). It is possible that these variations in glutamate susceptibility have their origin in varying expression levels of glutamate receptors such as AtGLR3.7 as it appears in this work where an excess of *AtGLR3.7* conferred a higher sensitivity against L-glutamate than in Col-0.

The mechanism in which elevated L-glutamate concentrations reduce root growth likely involves a diminished RAM size associated with lowered auxin concentrations at the root tip (Walch-Liu *et al.*, 2006). Since *AtGLR3.7* seems to affect meristematic activities, too, it is conceivable that local auxin maxima could be affected by a misexpression of this glutamate receptor also in the here tested transgenic plant lines.

Gene expression data established earlier (see section 3.1 'AtGLR3.7 Expression Levels') showed that very little quantities of *AtGLR3.7* mRNA/cDNA transcripts are present in atglr3.7. Assuming the measured mRNA/cDNA quantities were truly negligible, AtGLR3.7 would have been removed as a regulating element for plant growth via an adjustment of meristematic activities. In this scenario, L-glutamate concentrations potentially affecting cell divisions within the root would no longer be active in atglr3.7. This, however, would imply a permanent lack of cell division regulation which would either cause an upregulation of cell proliferation due to a lack of the cell division repressor L-glutamate or it would lead to a severe growth arrest. However, neither of these scenarios was observed in the *AtGLR3.7* knockout line.

Another theory implies that atglr3.7 is only a knockdown plant line where still minor quantities of *AtGLR3.7* would be translated. In this case, exogenously applied L-glutamate concentrations in the apoplast would compensate the deprivation of AtGLR3.7 at the PM by increasing the ligand:receptor ratio. An application of additional L-glutamate to the root would translate into an imbalance of this system causing root growth reductions in Col-0 and more severely in plants overexpressing *AtGLR3.7* while the same elevated L-glutamate concentrations could compensate the quantitative reduction of AtGLR3.7 in atglr3.7. The normal root growth phenotype could be restored in this plant line by the necessary concentration of exogenously applied L-glutamate.

Following this hypothesis, a strictly regulated balance of available and responsive AtGLR3.7 as well as precise concentrations of L-glutamate within the apoplast would govern the

meristematic activities within the root tip. Here, a rerouting of auxin fluxes would result in shifted auxin maxima and in this way extend or contract cell proliferation zones in order to fine-tune root growth. Further experiments investigating gene expression levels of *AtGLR3.7* in different Arabidopsis ecotypes coupled with examinations of auxin maxima within the root under normal conditions as well as with externally applied L-glutamate could help to elucidate the exact mechanism in which AtGLR3.7 shapes plant growth.

4.3 Cell Cycle Gene Expression and Endoreduplication

The data collected about the meristematic activity of the RAM in the tested plant lines indicated an increase in cell proliferation in the *AtGLR3.7* overexpression lines and a reduced cell division rate in atglr3.7. An investigation of alterations of cell cycle gene expressions was conducted with the aim of discovering essential up- or downregulations of key cell cycle regulators. Initial results based on sqRT-PCR suggested possible deviations of M-phase and S-phase genes (Table 9 and see below). These findings prompted an analysis of endoreduplication events in transgenic and wildtype *Arabidopsis thaliana* by an assessment of the nuclear DNA content of cells from the respective plant lines (Figure 25).

4.3.1 Enhanced Endoreduplication in Transgenic *AtGLR3.7* Plant Lines

Investigations of the nuclear DNA content revealed a much higher proportion of cells with >4C in atglr3.7 and a lesser but still noticeable increase of these C-values in OE:AtGLR3.7(1), -(2) and -(3) compared to Col-0 (Figure 26A). A rise of cells with >4C indicated an increased endocycling in both the *AtGLR3.7* knockout and overexpression lines, and additionally, the higher C-values in atglr3.7 suggested a much stronger endoreduplication than in the overexpression lines.

Interestingly, the ratio of 4C:2C cells is comparable among the transgenic plant lines and this ratio is almost twice as high as in the wildtype plants (Figure 26B). Considering cells with a 2C content as cells before DNA duplication due to either proliferation or the first round of endoreduplication and regarding cells with a 4C content as either proliferating or endoreduplicating cells, the similar 4C:2C ratios in the transgenic plant lines suggest an equal increase in DNA synthesis. However, looking at the >2C:2C ratio (Figure 26C), it becomes obvious that the rise of DNA biosynthesis appears to have different origins and objectives. This ratio takes into account all non-dividing and non-endocycling cells (2C) and their relation to

cells which undergo/underwent DNA-synthesis either due to cell proliferation or additional rounds of endoreduplication (>2C). Under normal conditions as they are present in Col-0, this ratio is one. The knockout of *AtGLR3.7* increased this ratio to four while the overexpression of *AtGLR3.7* caused a ratio of about two in all three tested overexpression lines.

The strong increase in C-values in atglr3.7 coincided with reduced CPM and a prolonged RTP, while the weakened (relative to atglr3.7) increase in C-values in the overexpression lines concurred with a higher cell division rate in the meristem (see section 3.3.3 'Meristematic Activity and Cell Cycle Progression'). Taken together, the data suggest a general increase in DNA synthesis due to either lowered and elevated *AtGLR3.7* gene expression and that these misexpressions probably cause a change of the plant cell cycle.

AtGLR3.7 could be a key regulator mediating calcium signals intended on integrating stimuli that are affecting the meristematic activity. Although down- or upregulation of *AtGLR3.7* appears to influence the S-phase of the cell cycle in a similar way, the outcome for the whole plant seems to be contrary when looking at the growth rates. Here, the knockout of *AtGLR3.7* caused minor growth impairments whereas its overexpression led to an acceleration of growth. Looking at the cellular level, atglr3.7 exhibited enhanced polyploidy levels which could be based on impairments of mitosis, i.e. only the M-phase of the cell cycle, rather than a slowed or otherwise hampered cell cycle progression in general. In this scenario, cells of atglr3.7 would undergo several rounds of endocycles instead of a complete cell cycle including the M-phase that normally occurs within meristematic tissues.

Since the mitotic cell cycle differs from the endocycle only by the presence of the M-phase, a model proposed by Edgar *et al.* (2014) distinguishes between S- and M-phase CDKs (S-CDK and M-CDK, respectively) whose presence/activity determines if cells undergo proliferation or endoreduplication. In both cases, CDK activities are oscillating in order to pass from one phase of the cell cycle to another whereas there are peaks of S-CDK activities (mainly CDKA;1) within the S-phase and peaks for M-CDK activities (CDKBs) during the M-phase. Following this model, omitting the M-phase by deregulating/inactivating M-CDKs would cause cells to undergo repeated endocycles in which phases of DNA biosynthesis (S-phase) are separated only by gaps (G1) necessary for cell growth and a renewal of DNA-licensing.

The fact that cells of atglr3.7 remained longer in the meristem could be also interpreted as a lowered potential of the cells to divide. At the same time, these cells would undergo several

rounds of DNA biosynthesis/endoreduplication thereby causing the observed increase in polyploidy levels. Therefore, the *AtGLR3.7* knockout phenotype could be described as (I) a rise in DNA biosynthesis due to increased activities of S-CDKs and (II) an impairment of M-CDKs leading to reduced cell division events and in return increasing the nuclear DNA content/endopolyploidy level due to various rounds of endoreduplication.

Following this explanation where a knockout of *AtGLR3.7* negatively affects M-CDKs, an overexpression of *AtGLR3.7*, on the other hand, would increase the presence/activity of M-CDKs. All three overexpression lines were characterized by an accelerated plant growth rate due to an increase in meristematic activity. The underlying mechanism in these plant lines could be an overstimulation of M-CDKs within the meristem and/or an enlargement of the whole MZ. Therefore, the phenotype of the *AtGLR3.7* overexpression lines could be described as (I) an increased DNA biosynthesis due to intensified activities of S-CDKs similar to atglr3.7 and (II) a stimulation of M-CDK activities causing additional cell divisions given that an extension of the MZ within the root and ectopical cell divisions close to the RAM was observed.

The model proposed here is supported by the cell cycle gene expression analysis that indicates an upregulation of genes essential for DNA biosynthesis.

4.3.2 Deviations in Cell Cycle Gene Expression in Transgenic Plants

The *AtGLR3.7* knockout line showed a tendency for gene upregulation among the selected cell cycle regulators while a similar, but weakened trend, was observed for the overexpression line OE:AtGLR3.7(2) (Table 9). However, cell cycle regulators involved in the potency of cell to divide, namely RBR1 and OBP1, displayed comparable gene expression levels in all tested plant lines. The transcriptional repressor RBR1 determines the cell proliferation potential by repressing the E2F-DP pathway through binding and inhibiting E2Fs and it is further known to affect the cellular endoreduplication potential (Sabelli *et al.*, 2013; Harashima and Sugimoto, 2016). The TF OBP1 has been found to upregulate various cell cycle genes upon developmental stimuli and it prompts increased cell divisions within the plant body (Skirycz *et al.*, 2008). Similarly, two tested CDK inhibitors (KRP1 and KRP4) exhibited no major deviations in their gene expressions among wildtype and transgenic *Arabidopsis thaliana*.

Since these results reflect only data gathered on the gene expression level, it is still possible that posttranslational modifications such as phosphorylations could be altered in the transgenic plant lines. For instance, the CDKA;1-CYCD3;3 complex is known to phosphorylate RBR1 at the

G1-S-phase transition in order to activate the E2F-DP-pathway (Nakagami et al, 2002). An assessment of the phosphorylation status of such proteins as well as other key cell cycle regulators would be useful in order to comprehend in detail the potential cell cycle alterations in the transgenic Arabidopsis plants.

4.3.2.1 Cyclin-Dependent Kinases

There was still significant gene upregulation detected, especially for the three tested CDKs CDKA;1, CDKB1;1 and CDKB2;1. The CDKB genes were about 80% upregulated in both the *AtGLR3.7* knockout and overexpression line compared to Col-0. CDKA;1, on the other hand, showed an upregulation only in atglr3.7 while its mRNA/cDNA level in OE:AtGLR3.7(2) was similar to that of wildtype plants.

CDKA;1 was the only investigated CDK which was upregulated in atglr3.7 but not OE:AtGLR3.7(2). CDKA;1 has an important role in cell division competence due to its primary function in S-phase entry (Nowack *et al.*, 2012). Here, it mainly phosphorylates RBR1 in order to release this protein from the E2F-DP transcriptional activator complex thereby enabling DNA replication. The kinase's involvement in the M-phase, on the other hand, appears to be only subordinate since the control of cytokinesis is exerted in concert with CDKBs (Nowack *et al.*, 2012). The observation of an increased CDKA;1 transcript level in atglr3.7 is in accordance with its presumed role as an activator of DNA synthesis since the elevated levels of nuclear DNA found in the present study originated in enhanced DNA biosynthesis (see section 4.3.1 'Enhanced Endoreduplication'). An investigation of the phosphorylation status of RBR1 as well as determining the exact quantities of active CDKA;1 would further help to understand the effects of an altered *AtGLR3.7* gene expression on the plant cell cycle and why this gene showed an upregulation only in atglr3.7 but not in OE:AtGLR3.7(2) which was characterized by elevated endopolyploidy levels, too.

CDKB1s appear to be fine-tuning kinases which are involved together with CDKA;1 in the G2-M-phase transition (Nowack *et al.*, 2012). Their involvement in stomatal development indicates furthermore a more pronounced role in asymmetrical cell divisions (Boudolf *et al.*, 2004). It has been shown that an mRNA level reduction of CDKB1;1 by RNA interference causes enhanced rounds of endoreduplication hinting at a role for CDKB1s in the control of the endocycle onset (Boudolf *et al.*, 2004b). However, CDKB1;1 was upregulated in both transgenic *AtGLR3.7* plant lines which were further characterized by intensified

endoreduplications (see section 4.3.1 ‘Enhanced Endoreduplication’). The potential role for CDKB1;1 as described in the studies from Boudolf *et al.* appears to contradict the found connection between enhanced CDKB1;1 gene expression levels and an increased DNA content in the transgenic *AtGLR3.7* plant lines. Nonetheless, the possibility of posttranscriptional/-translational alterations seems to be plausible since observations made on the gene expression level can differ significantly from the actual protein features.

An expression of CDKB2s is in general limited to the plant apices where these proteins are involved in the organization of the RAM/SAM (Andersen *et al.*, 2008). Their enzymatic activity peaks at the G2-M-phase transition, and, it is noteworthy, that both their knockout as well as their overexpression impair cell divisions while at the same time an increase in cellular DNA content can be detected. These findings point to ongoing rounds of DNA synthesis without a proper cytokinesis in the transgenic CDKB2 lines (Andersen *et al.*, 2008). The fact that only a medium/normal gene expression allows a proper cell cycle progression in wildtype plants, argues for a tightly controlled and dose-dependent functionality for both CDKB2s. An upregulation of CDKB2;1 in the *AtGLR3.7* knockout and overexpression lines could lead to the observed increase in nuclear DNA (see section 4.3.1 ‘Enhanced Endoreduplication’).

Noteworthy, both CDKB1;1 and CDKB2;1 were upregulated in the *AtGLR3.7* overexpression and knockout lines. While the characterization of atglr3.7 resembled the described phenotypes for an over- or downregulation of CDKBs, OE:AtGLR3.7(2) exhibited a dissimilar appearance with a contrary RAM activity. Since both transgenic plants lines exhibit similar transcriptional activations of CDKBs but their phenotype differed strongly from each other, further experiments involving measurements of CDK activities and/or protein modifications including the phosphorylation status are needed to elucidate the discrepancy found here.

4.3.2.2 Cyclins

Cyclins play a fundamental role in cell cycle progression in plants and animals since they are essential co-activators of CDKs. Based on their sequence similarities, the three groups of A-, B and D-type cyclins are most likely involved strictly in the cell cycle (Wang *et al.*, 2004). Here, D-type cyclins are thought to regulate the G1-S-phase transition and A-type cyclins control the passage from S- to M-phase whereas both cyclins seem to be involved in the control of DNA biosynthesis. The cell proliferation phase, on the other hand, is controlled by B-type cyclins

whose expression peaks at the transition from G2 to M-phase and remains high during M-phase progression (Potuschak and Doerner, 2001).

The gene expressions of CYCA3;2 and CYCD3;1 were similar among all tested plant lines. However, there was a strong upregulation observed for CYCB1;2 and CYCD3;3 in both atglr3.7 and OE:AtGLR3.7(2) whereas a medium upregulation of CYCD4;1 was measured only in atglr3.7. It was shown that CYCB1;1, a close relative to CYCB1;2, is capable of binding and activating A- and B-type CDKs and that its overexpression promotes root growth in *Arabidopsis thaliana* (Doerner *et al.*, 1996; Weingartner *et al.*, 2004). CYCD3;3 is known to stimulate the entry into both S- and M-phase and is associated with CDKs active during these cell cycle phases (Nakagami *et al.*, 2002; Koroleva *et al.*, 2004). Together with the other two CYCD3s (CYCD3;1 and CYCD3;2), these cyclins seem to be involved in the control of cell proliferation the shoot meristem and in leaves in *Arabidopsis thaliana* where they promote the mitotic phase and delay the initiation of endocycles (Dewitte *et al.*, 2007). CYCD4;1 is also known to stimulate cell divisions by activating CDKB2;1 during the M-phase (Kono *et al.*, 2003).

There was a tendency for cyclin upregulations detected in both the *AtGLR3.7* knockout and overexpression lines (Table 9). Almost all cyclins that showed a change in gene expression relative to Col-0 were equally upregulated. These findings underline the hypothesis of a general increase in the activation level of cellular components belonging to the cell proliferation apparatus. However, no precise conclusions can be drawn from these data to the enhanced mitotic events in the *AtGLR3.7* overexpression lines. Three out of five tested cyclins were upregulated in both atglr3.7 and OE:AtGLR3.7(2). These cyclins are known to be involved in cell division and endocycle onset clearly indicating a promotion of DNA biosynthesis in the transgenic plants. The upregulation demonstrate here of cyclins involved in cell divisions appears to match the cellular requirements for additional DNA quantities either for the observed enhanced endoreduplication events in atglr3.7 (see section 4.3.1 ‘Enhanced Endoreduplication’) or the intensified cell proliferation in OE:AtGLR3.7(2). It is possible that the crucial component that affects conversely the transgenic plant lines can be found at the gene expression level, but further investigations at the protein level are required to answer that question.

4.3.2.3 E2Fs and DPs

The E2F-DP pathway is well-known for its initiation of the S-phase during the cell cycle. It is notable that, only the E2Fa/-b-DP dimer complex functions as an activator of S-phase genes (Harbour and Dean, 2000). A strong upregulation was detected for E2Fa and DPa in both the *AtGLR3.7* knockout and overexpression lines (Table 9). This data is in accordance with the observed phenotype of atglr3.7 in which enhanced polyploidy levels were observed, since E2Fa and DPa have been found to activate DNA biosynthesis genes when bound together as a complex (Harbour and Dean, 2000). The increased nuclear DNA content measured in the transgenic *AtGLR3.7* plant lines (see section 4.3.1 'Enhanced Endoreduplication') could have its origin in the upregulation of the E2Fa-DPa pathway not only in atglr3.7 but also in OE:AtGLR3.7(2). In addition, an increased meristematic activity as observed in the *AtGLR3.7* overexpression lines would require a stimulation of DNA biosynthesis as well.

The overexpression of E2Fa and DPa is already known to cause both ectopic cell divisions and increased endopolyploidy levels (Veylder *et al.*, 2002). However, the cellular factor which is responsible for either enhanced cell divisions or an intensified endoreduplication is still elusive, although CDKB1;1 was proposed as a decision maker in a study by Boudolf *et al.* (2004b). Enhanced levels of CDKB1;1 appear to have a tendency to promote cell division whereas a reduction of CDKB1;1 transcripts seems to promote endoreduplication, likely due to its function as a promoter of the M-phase (Boudolf *et al.*, 2004b). In the same work, it was established that an overexpression of the E2Fa-DPa dimer promotes the upregulation of CDKB1;1 by creating a positive feedback loop for cell division events.

However, the gene expression data collected for the *AtGLR3.7* knockout line contradicts this hypothesis because the phenotype of atglr3.7 was characterized by a reduced meristematic activity and an enhanced endopolyploidy levels. It is possible that CDKB1;1 is not the actual regulator of cellular proliferation and endoreduplication. Glutamate receptor AtGLR3.7, on the other hand, could be directly involved in the control of cell division and endocycle since it appears to have a stimulating effect on RAM and SAM activities in promoting cell divisions whereas its absence negatively affects cell proliferation and causes DNA duplications without cytokinesis ultimately enhancing the endopolyploidy level.

Interestingly, there was a clear upregulation of two other E2Fs (E2Fd and E2Ff) in atglr3.7 but not OE:AtGLR3.7(2). E2Fd and E2Ff are considered to be TFs influencing cell proliferation and cell expansion rates, respectively (Ramirez-Parra *et al.*, 2004; Sozzani *et al.*, 2010). Investigations on the cotyledon size of E2Fd mutants showed a reduction in size due to reduced

cell quantities in the leaf while an overexpression of E2Fd appears to upregulate E2Fa and E2Fb (Sozzani *et al.*, 2010). Indeed, the upregulation of E2Fd in the *AtGLR3.7* knockout line coincided with an upregulation of E2Fa. However, atglr3.7 showed a reduction in cell division events despite an upregulation of both E2Fs. OE:AtGLR3.7(2), on the other hand, displayed increased meristematic activity together with an upregulation of E2Fa with no co-upregulation of E2Fd observed. Similarly, the elevated levels of E2Ff in the *AtGLR3.7* knockout line are not accompanied by an increased cell expansion as it was shown on mature root cells and the hypocotyl elongation in darkness for atglr3.7 (see section 4.2.2.4 'Similar Cell Morphologies' and 4.2.4.1 'Etiolated Root and Hypocotyl Growth').

However, when considering the TFs E2Fd, E2Fe and E2Ff as true transcriptional inhibitors of M- or S-phase genes as proposed by some authors (Kosugi and Ohashi, 2002; Mariconti *et al.*, 2002; Vandepoele *et al.*, 2002), there could exist a separate role for E2Fd and E2Ff as suppressors of M-CDKs. They are capable of inhibiting gene translations because these E2Fs can bind as monomers on DNA due to their intrinsic structure unlike E2Fa- and E2Fb, which require a dimerization partner (Kosugi and Ohashi, 2002). This inhibitory effect could be exerted on M-phase genes in atglr3.7 and so far, untested cell cycle genes could be downregulated causing the reduction in cell proliferation.

Taken together, the regulation of cell divisions/endoreduplications during the S- and M-phase by AtGLR3.7 likely encompasses the whole cell cycle network. The selected genes represent only a small proportion of the involved cellular machinery which needs to be further investigated. In addition, the data collected in this work, appears to be inconclusive with results from the current relevant literature. Therefore, investigations of cellular events at the post-translational level are required to explain the exact involvement of AtGLR3.7.

4.3.2.4 MYB3Rs

MYB3R1 and MYB3R4 are known to be positive regulators of cytokinesis. Both proteins were found to stimulate the expression of genes active during the M-phase of the cell cycle such as CYCB2s and the syntaxin KNOLLE, and their knockout causes multinucleated cells due to a failure of cell plate formations (Haga *et al.*, 2007; 2011). The upregulation of MYB3R1 in OE:AtGLR3.7(2) is in accordance with its described role as an activator of M-phase genes and therefore as a promoter of cell proliferations. This is underlined by the observation of a simultaneous upregulation of M-phase-promoting genes including CYCB1;2 as well as the

observed enhanced meristematic activity in the *AtGLR3.7* overexpression lines. The upregulation of MYB3R1 in the *AtGLR3.7* knockout line, on the other hand, cannot be explained by this model alone, since atglr3.7 displayed a reduction in cell division events.

However, MYB3R1 has another redundant function as a transcriptional repressor of M-phase genes when expressed in complex with MYB3R3 and MYB3R5 (Kobayashi *et al.*, 2015). It could be that the observed upregulation of MYB3R1 is caused by a different pathway in atglr3.7 than in OE:AtGLR3.7(2). These distinguished pathways would lead to diverging phenotypes seen in the transgenic *AtGLR3.7* plant lines.

MYB3R4 was found in complex with E2Fb in proliferating cells, underlining its role as a cell division promoter (Kobayashi *et al.*, 2015). Its moderate upregulation in the *AtGLR3.7* knockout line could be the cause of either a different regulatory network in which MYB3R4 is not involved in M-phase gene expression or a simultaneous repression of the respective promoters by other cell cycle controllers such as E2Fd or E2Ff. Furthermore, MYB3Rs are additionally controlled at the protein level by CDK-dependent phosphorylations and proteasomal degradations (Araki *et al.*, 2004; Chen *et al.*, 2017). In this respect, there is also a possibility of posttranslational modifications occurring at MYB3R1 and -4 in the *AtGLR3.7* knockout line which could weaken their functionality and cause a different phenotype than in OE:AtGLR3.7(2).

4.3.2.5 Confirmation of sqRT-PCR Data by qRT-PCR

Three components of the E2F-DP pathway (CDKB1;1, E2Fa and DPa) as well as MYB3R4 as a transcriptional activator of M-phase genes were selected for qRT-PCR in order to confirm the collected results obtained by sqRT-PCR concerning the regulation of the cell cycle. The additional data confirmed previous results in which CDKB1;1, E2Fa and DPa were similarly upregulated in both the *AtGLR3.7* knockout and overexpression lines (Figure 24). All three genes were significantly upregulated, although their expression levels varied in atglr3.7 and OE:AtGLR3.7(2). E2Fa as a TF for S-phase genes as well as the M-phase kinase CDKB1;1 showed higher upregulations in atglr3.7 than in OE:AtGLR3.7(2) while the E2F-binding partner DPa was comparably upregulated in both plant lines compared to Col-0. MYB3R4 was slightly upregulated in the *AtGLR3.7* knockout line and showed a minor downregulation in the *AtGLR3.7* overexpression line. Taken together, the qRT-PCR data confirmed the results of the sqRT-PCR in all four tested genes supporting the reliability of the collected data (Table 9).

4.4 Plant Physiology

4.4.1 Plant Ion Content and Elevated Salinity

A possible role for AtGLR3.7 in ion uptake at the PM affecting the transgenic plant lines' salt tolerance is based on findings regarding the plants' performance under mild and medium salt stress (Figure 30) as well as the varying concentrations of Na^+ within atglr3.7 and OE:AtGLR3.7(2) (Figure 29). The enhanced tolerance of the *AtGLR3.7* knockout line could be based on a lower Na^+ uptake from the medium/soil. Even though the ion content measurements were collected from untreated plants, there was a significant variation among wildtype and transgenic *Arabidopsis thaliana* in Na^+ concentrations in whole plant samples. The observed reduction of Na^+ in atglr3.7 as well as its increase in OE:AtGLR3.7(2) would likely intensify within a salt stress environment, and further studies of the ion content of both transgenic plant lines under high salinity are needed to confirm this hypothesis.

Nonetheless, the increased salt tolerance of atglr3.7 is very likely linked to reduced quantities of AtGLR3.7 at the PM of root cells (Figure 30). In the study by Roy *et al.* (2008), *AtGLR3.7* was the only GLR gene expressed in all tested cell types which indicates an omnipresence of this particular glutamate receptor throughout plant tissues. It has already been shown that several GLRs are involved in non-selective cation fluxes supporting a potential function of AtGLR3.7 in mediating ion fluctuations (Tapken and Hollmann, 2008; Vincill *et al.*, 2012). A knockout of *AtGLR3.7*, as seen in atglr3.7, could therefore severely affect the ion uptake from the environment. Na^+ sequestration can be excluded because compartmentalization would likely keep the plant's total Na^+ concentration unaffected. Therefore, the results of plant growth under salt stress in combination with the Na^+ ion content measurements in atglr3.7 and OE:AtGLR3.7(2) clearly indicated Na^+ exclusions from or a rectified entry into the plant body, respectively.

In general, Na^+ and K^+ uptake from soil/medium exist as high- and low-affinity assimilation systems in plants while sodium and potassium absorption are managed by different types of transporters (Yao *et al.*, 2010). The respective systems have varying sensitivities against other cations and it was found that the presence of Ca^{2+} affects only low-affinity uptake of Na^+ in *Arabidopsis thaliana* (Essah *et al.*, 2003). The HKT family represents the most understood high-affinity system involved in Na^+ uptake in plants. While HKT subfamily I appears to be

mostly involved in Na^+ circulation within the plant body, members of subfamily II can operate as K^+/Na^+ symporter for Na^+ influxes in plant cells (Yao *et al.*, 2010; Maathuis, 2014).

Low-affinity uptake, on the other hand, is mostly conducted by ion channels such as GLRs, CNGCs and other non-selective cation channels (NSCC) (Demidchik and Tester, 2002; Newton and Smith, 2004; Tapken and Hollmann, 2008). In the latter case, voltage-insensitive NSCCs are likely the main class responsible for Na^+ uptake and, noteworthy, this group of ion channels is highly sensitive to exogenous Ca^{2+} indicating a regulation by Ca^{2+} signalling (Demidchik and Maathuis, 2007). Furthermore, cation channels such as CNGC10 were found to be involved in Na^+ fluxes across cell membranes and proteins like AtHKT1;1 and AtHAK5 are capable of mediating Na^+ uptake within the root (Jin *et al.*, 2015; Wang *et al.*, 2015).

It is highly likely that AtGLR3.7, as a potential ion channel, directly mediates Na^+ fluxes within the root of *Arabidopsis thaliana* through the receptor's ion pore region and that it is therefore part of the low-affinity Na^+ uptake in plants. This hypothesis is supported by the finding that the knockout of *AtGLR3.7* conferred an increased tolerance only against low (50 mM) and medium (75 mM) salt concentrations whereas a high NaCl concentration of 100 mM affected root growth in a similar fashion like in Col-0 (Figure 30). The highest tested salt concentration could already trigger high-affinity Na^+ pathways while minor concentrations were mediated by the low-affinity Na^+ uptake in the tested Arabidopsis plants. In this case, reductions in AtGLR3.7 transcript/protein levels in atglr3.7 could have caused a diminished Na^+ influx while an overexpression of *AtGLR3.7* and the associated enhanced protein quantities (likely at the PM) would lead to additional Na^+ influxes causing elevated Na^+ concentrations in OE:AtGLR3.7(2).

There is also the possibility of a more complex cellular network leading to the observed plant phenotypes in atglr3.7 and OE:AtGLR3.7(2) under salt stress as well as to their altered ion content under normal growth conditions. AtGLR3.7, as a potential glutamate-gated calcium channel, could be involved in the Ca^{2+} signalling related to the plant's salt stress response. Recently, it was shown that salt tolerance in Arabidopsis is associated with a MAPK6-mediated Ca^{2+} signalling. The disruption of this pathway by either a knockout of the kinase or an arrest of the respective calcium signals via Ca^{2+} chelators or Ca^{2+} channel blockers, greatly affects the plant's tolerance against salt stress by reducing Na^+ fluxes within the root (Han *et al.*, 2014).

This example demonstrates another explanation for the obtained results of this work where a Na^+ accumulation (OE:AtGLR3.7(2)) or deprivation (atglr3.7) could be the result of misregulated AtGLR3.7-mediated Ca^{2+} signalling. Here, the glutamate receptor could affect other potential Na^+ influx mediators including members of the HKT family or voltage-insensitive NSCCs.

A first step to reveal the exact mechanism by which AtGLR3.7 affects salt tolerance could be in measuring Na^+ concentrations during/after salt stress treatment in the transgenic *AtGLR3.7* plant lines. In addition, a screening for salt stress-responsive gene expressions and their respective protein modifications would help to pinpoint the participating pathways. Possible candidates could comprise AtHKT1;1 as a passive Na^+ flux mediator, the salinity-responsive TF SERF1 or the PM-bound Na^+-H^+ antiporter NHX7 (Qiu *et al.*, 2002; Munns *et al.*, 2012; (Schmidt *et al.*, 2013).

Another question to be addressed in further experiments would be the finding that only sodium but not potassium or calcium concentrations were affected in the transgenic *AtGLR3.7* plant lines. GLRs are known to be permeable to various monovalent and divalent cations including K^+ and Ca^{2+} (Demidchik *et al.*, 2004; Tapken and Hollmann, 2008). Either Ca^{2+} channels other than AtGLR3.7 maintain Ca^{2+} homeostasis within the cells of the transgenic plant lines or AtGLR3.7 is a particular glutamate receptor which is permeable to Na^+ but unable to mediate K^+ fluxes. Here, heterologous expression studies would help clarify the exact ion permeability properties of AtGLR3.7.

Eventually, an investigation of a possible involvement in Ca^{2+} signalling could be conducted using Ca^{2+}-chelating compounds like EGTA. Under these calcium deprivation conditions, a Na^+ accumulation/reduction within the respective plant line should remain unaffected only if AtGLR3.7 mediates Na^+ influxes, directly, while an alteration of Na^+ concentrations and plant growth in the presence of Ca^{2+} signalling blockers during a salt stress treatment would indicate a role for AtGLR3.7 in transmitting the necessary signals to confer salt tolerance in *Arabidopsis thaliana*.

4.4.2 Enhanced Defence Capacity against *Pseudomonas syringae*

The gram-negative bacterium *Pseudomonas syringae* pv. tomato DC3000 represents an excellent model system to study plant immune responses in *Arabidopsis thaliana* against this hemibiotrophic pathogen. Since the bacterium affects mainly areal parts such as leaves, and it does not spread out widely from its site of infection, observations concerning the plant's resistance capabilities are easily obtained (Hirano and Upper, 2000). Additionally, there are several mutated strains available which allow for specific investigations of the various elements of plant immunity such as distinguishing between the plant's PTI and ETI responses.

The two different strains used in this work are the wildtype strain with its natural pathogenic repertoire (Pto DC3000) and a second strain impaired in delivering pathogen effectors into the host cell's cytoplasm, directly (Pto DC3000 (hrcC)). A mutation in the latter bacterial strain affects genes encoding a part of the type III twin-arginine transport secretion system (T3SS), rendering Pto DC3000 (hrcC) non-virulent due to its deficiency in penetrating and injecting its virulence factors into the host cell (Büttner and He, 2009). Nonetheless, Pto DC3000 (hrcC) is capable of secreting phytotoxins such as syringofactins or the polyketide toxin coronatine into the plant apoplast and its extracellular structures are still recognized by the plant's PM-localized PRRs as part of the PTI (Bender *et al.*, 1999).

Both strains were used to infect wildtype and transgenic *AtGLR3.7* plant lines in order to test if the absence or overexpression of this glutamate receptors has an effect on the plant's immune system. An infection with the non-virulent strain Pto DC3000 (hrcC) led to a comparable bacterial propagation in all tested plant lines (Figure 32). Based on this result, it can be concluded that the following immune processes are unaffected in the transgenic plant lines: (I) stomatal opening or closing as part of the plant's defence strategy to prevent bacterial entry through the stomata, (II) susceptibility to phytotoxins secreted without an involvement of the T3SS and (III) plant PTI.

However, when using the wildtype strain Pto DC3000, there was a strong reduction in bacterial growth observed in atglr3.7 as well as moderate but still significant diminutions of the pathogen's propagation in the *AtGLR3.7* overexpression lines (Figure 31 and Figure 32). In contrast to the non-virulent strain, Pto DC3000 possesses a functional T3SS which enables a translocation of the pathogen's effectors into the host plant cell. Therefore, it can be assumed that the increased resistance against *Pseudomonas syringae* in transgenic *AtGLR3.7* plant lines has its origin in an element of the ETI in *Arabidopsis thaliana*.

4.4.2.1 Calcium and Auxin Signalling During Plant Defence Reactions

A disturbance of proper Ca^{2+} signalling or the activity of pathogen effectors like the cysteine protease AvrRpt2 or HopM1 affecting auxin signalling and/or distribution within the plant could explain the observed phenomena. Regarding the involvement of Ca^{2+} fluxes in defence responses, it is well known that Ca^{2+} signalling is a prerequisite for a proper immune response in plants (Lecourieux *et al.*, 2006). Early reactions to a pathogen attack include an increase in $[Ca^{2+}]_{cyt}$ as well as specific Ca^{2+} signatures upon activation of PTI or ETI (Garcia-Brugger *et al.*, 2006; Keinath *et al.*, 2015). This in turn leads to a stimulation of MAPKs, the production of reactive oxygen species as well as nitric oxide, and the upregulation of plant defence genes (Blume *et al.*, 2000; Kurusu *et al.*, 2005; Vandelle *et al.*, 2006). CNGCs and GLRs have already been proposed as mediators of these early Ca^{2+} fluctuations during plant immune responses while the subsequent cellular signal transduction appears to rely on calcium-dependent protein kinases (Boudsocq *et al.*, 2010; Seybold *et al.*, 2014).

AtGLR3.7 as a potential calcium channel could be involved in early Ca^{2+}-mediated immune reactions in *Arabidopsis thaliana*. Here, a knockout or overexpression of *AtGLR3.7* could affect initial responses against effectors from Pto DC3000 and would cause the observed resistance against this pathogen. However, the exact pathway in which AtGLR3.7 could be involved remains elusive and there are indications leading to an exclusion of this hypothesis, as discussed further below.

Apart from affecting Ca^{2+} signatures related to the plant's immune response, an altered auxin distribution could be also responsible for the enhanced resistance of the transgenic *AtGLR3.7* plant lines. Auxin was already proposed as a source for the altered plant growth characteristics (see section 4.2.2 'Accelerated Root Development' and 4.2.3 'Increase in Aerial Tissue') and besides its role in plant development, auxin is also known as a phytohormone involved in plant defence responses where it acts in concert with jasmonic acid against necrotrophic pathogens (Kazan and Manners, 2008).

On the other hand, there are studies showing that an elevated auxin biosynthesis during a pathogen attack supresses the expression of plant defence genes (Shinshi *et al.*, 1987; Jouanneau *et al.*, 1991). Related to this, the pathogen effector AvrRpt2 appears to promote the host's auxin production and plants constitutively expressing this cysteine protease are among others characterized by an enhanced susceptibility to *Pseudomonas syringae* (Chen *et al.*,

2007). Therefore, it seems more likely that the attacking pathogen exploits auxin elevations within the host. This hypothesis is supported by findings that the plant defence hormone, salicylic acid, acts antagonistically against auxin in terms of biosynthesis, perception, transport and/or auxin response genes expression (Wang *et al.*, 2007). The general antagonistic interaction between auxin and salicylic acid may originate from a balance of plant growth versus plant defence in which the plant's resources are allocated to one physiological feature at the expense of the other (Park *et al.*, 2007; Huot *et al.*, 2014).

Disturbing auxin transport is another way of pathogen interference with a host plant's auxin signalling. The effector HopM1 was found to inhibit proper vesicle trafficking by promoting proteasomal-degradation of the trafficking regulator MIN7 (Nomura *et al.*, 2006). Since this regulator is known to promote PIN1-mediated auxin efflux from the cell, it appears that HopM1 disturbs the normal auxin transport that in turn could lead to unnatural auxin accumulations within the plant body (Tanaka *et al.*, 2009). For that reason, ETI was found to include a suppression of HopM1-mediated degradation of MIN7 in order to enhance plant resistance against *Pseudomonas syringae* (Nomura *et al.*, 2011).

It appears that pathogens take advantage of the host's auxin homeostasis, which in turn depends on functional auxin signalling pathway. An already disturbed auxin distribution within the transgenic *AtGLR3.7* plant lines could diminish the effectivity of pathogen effectors such as AvrRpt2 or HopM1 and compromise a pathogen propagation by curtailing its invasion strategy. However, assuming a distorted auxin homeostasis within the transgenic plant lines, diverging responses would have been expected for atglr3.7, where a reduction of auxin maxima at the root tip are anticipated based on its growth phenotype, and the *AtGLR3.7* overexpression lines which could be characterized by an elevated auxin concentration in the root.

Taken together, the model of an altered auxin distribution cannot fully explain the elevated resistance against *Pseudomonas syringae* with the diverging growth phenotypes in atglr3.7 and the *AtGLR3.7* overexpression lines. Similarly, a disturbance of the calcium signalling due to a knockout or overexpression of *AtGLR3.7* would probably be represented by varying resistance phenotypes contrary to the measured tendency for a higher resistance in all transgenic plant lines. Therefore, another explanation employing the enhanced endoreduplication events in atglr3.7 and to a lesser extent in the *AtGLR3.7* overexpressing lines will be proposed as the most reasonable interpretation.

4.4.2.2 Endopolyploidy Levels Could Enhance ETI Reactions

Interestingly, the degree of pathogen resistance seems to correlate with the polyploidy level in wildtype and transgenic *Arabidopsis thaliana* (Figure 26A and Figure 32). Pathogens are generally prone to stimulate endoreduplications in its host cells as a way to enhance the host's metabolic and proteinogenic capacities. In doing so, the physiological needs of the pathogen are matched by the host, e.g. by an additional supply of organic compounds for biotrophic bacteria (Wildermuth, 2010). Therefore, enhanced endopolyploidy levels are rather a symptom of a pathogen attack in plants. In other instances, the augmentation of the nuclear DNA content within a plant cell is a prerequisite for a proper symbiotic relation with benefitting organisms such as mycorrhizal fungi (Bainard *et al.*, 2011). Also here, endoreduplication events are associated with proteinogenesis.

However, a pathogen attack employing effectors and triggering the plant's ETI, would have a severe disadvantage in hosts with an unusual, constitutively-high endopolyploidy levels before an attack. Considering the mode in which pathogen effectors are working and that their quantities are limited by the number of invading pathogens, it is possible that a preceding increase in polyploidy, as it was observed for the transgenic *AtGLR3.7* plant lines, renders the effector-based strategy to circumvent the plant immune system much less effective. An augmentation of nuclear DNA is thought to also increase protein production, or could at least multiply potential nucleotide targets of pathogen effectors. In both ways, the effector:target ratio would be markedly reduced and the intended rerouting or suppression of the host's cellular pathways by the effectors would be strongly impeded.

This proposition is supported by a concept called 'gene-balance-hypothesis', established by Birchler and Veitia (2010). The principle is based on the idea that the amount of a single element (protein or gene) of a multi-component system, such as in a multi-protein complex or an elaborated metabolic pathway, would be decisive due to the stoichiometric properties of this system. An alteration in stoichiometry could heavily influence system kinetics. Transferring this concept to the observed immune response of the transgenic *AtGLR3.7* plant lines, the effector AvrRpt2 employed by Pto DC3000 during its attack on Arabidopsis, could be a representative for such a crucial element involving ETI. AvrRpt2 was found to cleave the plant protein RIN4 and that this cleavage is in turn recognized by the R protein RPS2 as part of the ETI in *Arabidopsis thaliana* (Axtell and Staskawicz, 2003). Here, an increased number of RIN4 or RPS2 due to enhanced polyploidy levels would ultimately lead to an augmented proportion of cleaved RIN4 during a pathogen attack employing the T3SS-mediated delivery of AvrRpt2.

The enhanced quantities of cleaved RIN4 would raise the likelihood of its detection by its guard protein RPS2 and the following ETI activation. This in turn would increase the host resistance against the respective pathogen. Since transgenic *AtGLR3.7* plants were more resistant only to the T3SS-employing Pto DC3000 but not to the non-virulent Pto DC3000 (hrcC), it is highly likely that ETI-mediated plant immunity in the transgenic plant lines has an advantage as compared that of Col-0.

The above-outlined hypothesis is highly feasible and could explain the positive correlation of the transgenic plants' polyploidy levels and their resistance against Pto DC3000. To further investigate this assumption, protein levels of key components of ETI should be measured in transgenic and wildtype *Arabidopsis thaliana*. Here, potential candidates are the mentioned RIN4 or the hydrolase EDS1 which is recognized by the R protein RPS6 after been targeted by the effector HopA1 (Kim *et al.*, 2009).

4.5 Protein Modifications: AtMAPK3/-6 and Histone H3

4.5.1 Unaffected AtMAPK3/-6 Quantities and Phosphorylation Status

AtMAPK3 and -6 are part of a universal cellular signal transduction network in *Arabidopsis thaliana* where extracellular stimuli become transduced into intracellular responses through protein phosphorylation events. These consecutive phosphorylations of various kinases are called MAPK cascades and their outcome affects enzyme activities, subcellular protein localizations and protein-protein interactions (Rodriguez *et al.*, 2010). MAPKs are known to be involved in various processes including cytokinesis, the cell cycle, as well as plant immunity.

The activation of MAPKs during mitosis and their localization close to the cell division plane appear to be crucial for mediating further downstream protein phosphorylations (Bögre *et al.*, 1999). The knockout of several kinases impairs early stages of plant development such as embryogenesis (Bayer *et al.*, 2009). MAPKs have also been found to be involved in PTI where they transduce signals perceived by PRRs, as well as in ETI causing inducible immune responses (Jones and Dangl, 2006). For example, a triggering of the plant immune system by flg22 was found to transiently activate MAPK3/-6 (Asai *et al.*, 2002). Besides biotic stress, MAPK3/-6 are also known to be involved in the mediation of salt stress where the knockout of MAPK3 or -6 causes hypersensitivity to elevated salinity levels (Pitzschke *et al.*, 2014; Liu *et al.*, 2015a). Furthermore, the plant hormone auxin has been found to positively affect MAPK

activities within the root and that MAPK function is essential to mediate auxin responses on the gene expression level (Mockaitis and Howell, 2000).

Considering the almost ubiquitous involvements of MAPKs in various plant processes, a monitoring of the AtMAPK3/-6 protein quantities as well as their phosphorylation status was conducted in order to identify them as potential mediators of the observed phenotypes in the transgenic *AtGLR3.7* plant lines (i.e. enhanced resistance against *Pseudomonas syringae*, altered meristematic activities and salt tolerances). However, Western blot assays for the non-phosphorylated and phosphorylated AtMAPK3/-6 proteins revealed no significant variations among the three tested plant lines (Figure 28B, C). This result could imply that neither kinases are involved in the observed *AtGLR3.7*-mediated plant processes either in their active state (phosphorylation of Thr202/Tyr204) nor on a translational level (non-phosphorylated antibody labelling) since their protein quantities were similar in all plant lines.

There is the possibility that deviations in total protein quantities as well as in the amount of activated/phosphorylated AtMAPK3/-6 were too subtle to be recognized by the method used in this work since the protein extraction was done from whole plant seedlings. Instead of this, selected regions of the plant such as meristematic active parts like the tips of the root and shoot should be investigated separately. Furthermore, possible AtMAPK3/-6 gene upregulations or protein activations could be monitored through protein extractions after salt stress induction.

4.5.2 Unaffected Histone H3 Quantity and Methylation Status

Alterations of the intrinsic or extrinsic plant environment need to be matched by up- and downregulations of associated genes in order to adapt the plant to its new conditions. Therefore, gene accessibility for transcriptional activators and ultimately gene transcription is regulated on several levels. One of them is the physical openness of the respective region on the chromatin structure. The density of chromatin is determined among others by histone octamers around which DNA can be wrapped to various degrees. These agglomerates are called nucleosomes and they consist of four different histones (H2A, H2B, H3 and H4) arranged in pairs surrounded by the DNA. The DNA- and histone-binding capacities of individual histones are mainly determined by posttranslational adjustments at the N-terminal domain. Here, phosphorylations, ubiquitinations, acetylations and methylations are carried out by different enzymes and the actual histone status is again interpreted by other proteins. Those modifications generate either

an intensified compression or a loosing of the chromatin structure which is accompanied by enhanced or lowered transcriptional activity, respectively (Bannister and Kouzarides, 2011).

Histone H3 methylations of lysine residues at the N-terminus are well known for their involvement in epigenetic cell reprogramming due to developmental stimuli or changes in the plant's environment. Although both lysine and arginine residue methylations can be found, mono-, di- and trimethylations of lysine K4, K9, K27, and/or K36 on histone H3 are most frequent and they are associated with either gene repression (K9 and K27) or activation (K4 and K36) (Bannister and Kouzarides, 2011). The occurrence of concomitant methylations of different lysines were found to be an additional regulating element where various methyl-residues influence each other, causing unique genetic responses including regulations of the meristematic activity of the inflorescence (Yang *et al.*, 2014; Liu *et al.*, 2015b). Heterochromatin is often associated with a monomethylation of K27 on histone H3 (H3K27me1) whereas H3K27me2 is found in euchromatin (Jacob *et al.*, 2010; Roudier *et al.*, 2011). Single genes are often upregulated by selected H3K27me3 on distinct DNA regions (Sequeira-Mendes *et al.*, 2014). The latter pattern can be widely found, and it is related to developmental stage transitions during fertilization, gametogenesis, seed germination, flowering and pathogen defence-related gene expressions as well as to paternally epigenetic imprinting and epigenetic stress adaptation such as vernalization (Li *et al.*, 2013a; Crevillén *et al.*, 2014; Zhang *et al.*, 2014; Mozgova *et al.*, 2015).

These widespread involvements of H3K27me3 prompted an investigation of its status in the transgenic *AtGLR3.7* plant lines. However, the total histone H3 levels as well as the amount of tri-methylated H3K27 were comparable among all tested genotypes (Figure 28E, F). Based on these results, it appears that there is no connection between the H3K27me3-mediated alterations in chromatin structure and the observed phenotype in atglr3.7, OE:AtGLR3.7(1), -(2) and -(3).

Nevertheless, there is still the possibility that the employed method was not sensitive enough to detect variations occurring in restricted parts of the plant body, i.e. meristematic tissues, similar to the results regarding AtMAPK3/-6 abundance and their phosphorylation status. The detection of increased DNA-synthesis in both the *AtGLR3.7* knockout and overexpression lines could have been reflected in an altered DNA structure or nucleosome/histone quantities, especially due to the observed enhanced endopolyploidy levels.

Further investigations of selected plant tissues such as the root and shoot tip or protein extraction after biotic and abiotic stress inducement would be advisable in order to elucidate a

possible involvement of histone H3 methylations in the observed plant phenotypes. A more advanced investigation of the methylation status encompassing also the other lysine residues on histone H3 (K4, K9 and K36) as well as their quantitative state (mono-, di and tri-methylated) would help to determine the role of these structural DNA modifications as a part of the altered AtGLR3.7-mediated plant physiology.

5 Conclusion

A hypothetical pathway in which AtGLR3.7 affects the plant physiology, likely involves a glutamate receptor-transduced Ca^{2+} signalling and redistributions of auxin maxima within the plant (Figure 33). An interplay between calcium and auxin where $[Ca^{2+}]_{cyt}$ variations redirect auxin flows within the plant, have been well described and include subcellular relocalizations of auxin transporters through Ca^{2+}-mediated endo-/exocytosis influencing members of the PIN family or protein phosphorylations on ABCB transporters (Henrichs *et al.*, 2012; Vanneste and Friml, 2015).

In connection to this, local auxin biosynthesis within the apical meristems has been found to be at least partially involved in organogenesis, and regions of auxin production could be similarly affected through Ca^{2+} sensors/calcium-binding proteins like calmodulin and in turn activate calcium-dependent protein kinases (Pinon *et al.*, 2013). These calcium-responsive elements could be capable of upregulating genes involved in auxin biosynthesis such as the tryptophan aminotransferase TAA1 or members of the YUC family. TAA1 has been found to be involved in establishing local auxin gradients affecting organogenesis in response to developmental and environmental stimuli organ (Stepanova *et al.*, 2008). Similarly, several YUC genes encoding flavin monooxygenases are expressed in meristems and young primordia and their activity is connected to auxin biosynthesis and developmental processes, too (Cheng *et al.*, 2006).

The so-created auxin maxima are known to be crucial for meristem establishment, maintenance and function where they have an influence on either the WUSCHEL-CLAVATA feedback loop at the SAM or the auxin-induced PLETHORA genes known as key transcriptional regulators of the root tip (Sabatini *et al.*, 1999; Aida *et al.*, 2004; Su *et al.*, 2009). The cell cycle in these meristems is known to be controlled by varying auxin concentrations, and auxin has been found to affect cell cycle regulators including CDKA;1, CDKB1;1 and CDKB2;1 as well as CYCD3;1 and E2Fa (Himanen *et al.*, 2002; La Martínez-de Cruz *et al.*, 2015). These impacts on the plant cell cycle would connect the presumably upstream-located AtGLR3.7 activation to the observed growth phenotypes and to the detected enhanced immunity against pathogens due to elevated endopolyploidy levels in OE:AtGLR3.7(1), -(2), -(3) as well as in atglr3.7.

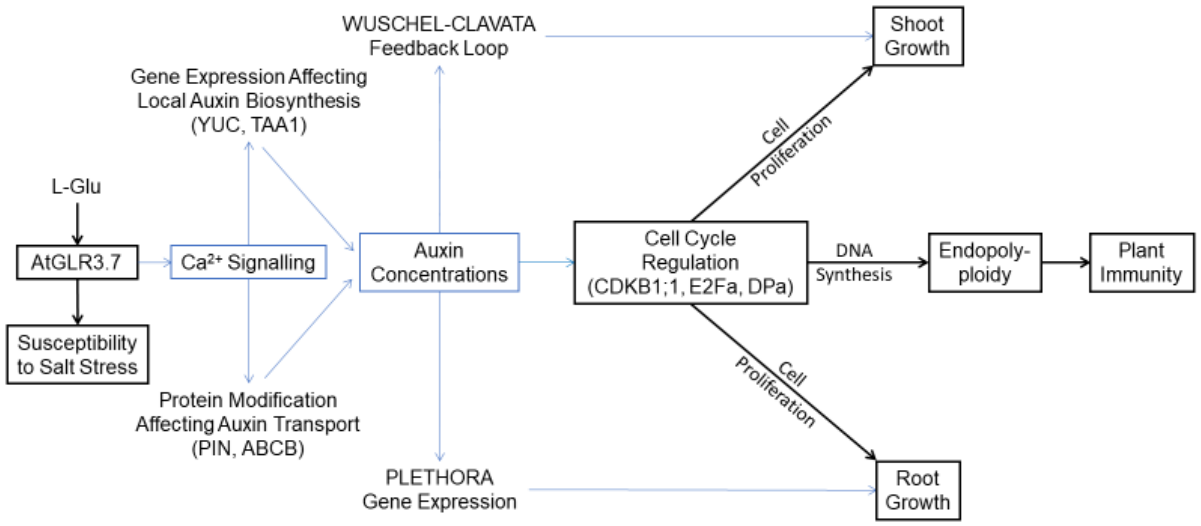

Figure 33. **Proposed AtGLR3.7 Signalling Pathway Affecting Plant Growth and Physiology.** Hypothetical involvements of calcium and auxin signalling (blue lines) in the here-described phenotypes of *AtGLR3.7* overexpression (OE:AtGLR3.7(1), -(2) and -(3)) and knockout (atglr3.7) *Arabidopsis thaliana* (black lines). The effects of *AtGLR3.7*-mediated alterations in root, rosette and shoot growth as well as in endopolyploidy/ endoreduplication are likely explained by the observed modifications of the plant cell cycle within the root and shoot apical meristems. Here, an up- or downregulation of *AtGLR3.7* was found to stimulate DNA biosynthesis and cause an augmentation or decrease, respectively, in cell proliferation affecting plant growth characteristics.

However, the hypothesis proposed here needs to be validated by further investigations of auxin distributions, gene expression profiles and protein modifications of potentially associated components of the entangled cellular pathways. Crossing transgenic *AtGLR3.7* plants with Arabidopsis lines harbouring cellular markers such as the auxin reporter DR5 would help to determine a potential involvement of the auxin signalling pathways, whereas the usage of proteinaceous Ca^{2+} sensors like aequorin could specify variations in Ca^{2+} signalling. DNA microarrays and RNA sequencing would be suitable to further investigate alterations on the gene expression level including a broader spectrum of cell cycle regulators and possibly other major controller of plant development as well. Chromatin immunoprecipitations as well as methods employing affinity purification and mass spectrometry would expand the study at the protein level. It could help to find interaction partner of AtGLR3.7 and identify protein-protein interactions in the affected pathways further downstream of an AtGLR3.7 signalling such as E2F-DP regulations. ChIP-sequencing could allow an investigation of protein-DNA interactions potentially occurring during plant defence involving effectors and nuclear targets as well as in detail studies of the cell cycle regulation where phase transitions are often associated with TF-induced gene upregulations.

6 References

Abas L, Luschnig C (2010) Maximum yields of microsomal-type membranes from small amounts of plant material without requiring ultracentrifugation. *Analytical Biochemistry* **401**, 217–227.

Acher FC, Bertrand H-O (2005) Amino acid recognition by Venus flytrap domains is encoded in an 8-residue motif. *Biopolymers* **80**, 357–366.

Ahuja I, Kissen R, Bones AM (2012) Phytoalexins in defense against pathogens. *Trends in Plant Science* **17**, 73–90.

Aichinger E, Kornet N, Friedrich T, Laux T (2012) Plant stem cell niches. *Annual Review of Plant Biology* **63**, 615–636.

Aida M, Beis D, Heidstra R, Willemsen V, Blilou I, Galinha C, Nussaume L, Noh Y-S, Amasino R, Scheres B (2004) The PLETHORA genes mediate patterning of the Arabidopsis root stem cell niche. *Cell* **119**, 109–120.

Allen GJ, Chu SP, Harrington CL, Schumacher K, Hoffmann T, Tang YY, Grill E, Schroeder JI (2001) A defined range of guard cell calcium oscillation parameters encodes stomatal movements. *Nature* **411**, 1053–1057.

Alvarez-Buylla ER, Benítez M, Corvera-Poiré A, Chaos Cador A, Folter S de, Gamboa de Buen A, Garay-Arroyo A, García-Ponce B, Jaimes-Miranda F, Pérez-Ruiz RV, Piñeyro-Nelson A, Sánchez-Corrales YE (2010) Flower development. *The Arabidopsis Book* **8**, e0127.

Alves MS, Dadalto SP, Gonçalves AB, Souza GB de, Barros VA, Fietto LG (2014) Transcription factor functional protein-protein interactions in plant defense responses. *Proteomes* **2**, 85–106.

Andersen SU, Buechel S, Zhao Z, Ljung K, Novák O, Busch W, Schuster C, Lohmann JU (2008) Requirement of B2-type cyclin-dependent kinases for meristem integrity in Arabidopsis thaliana. *The Plant Cell Online* **20**, 88–100.

Aouini A, Matsukura C, Ezura H, Asamizu E (2012) Characterisation of 13 glutamate receptor-like genes encoded in the tomato genome by structure, phylogeny and expression profiles. *Gene* **493**, 36–43.

Araki S, Ito M, Soyano T, Nishihama R, Machida Y (2004) Mitotic cyclins stimulate the activity of c-Myb-like factors for transactivation of G2/M phase-specific genes in tobacco. *The Journal of Biological Chemistry* **279**, 32979–32988.

Asai T, Tena G, Plotnikova J, Willmann MR, Chiu W-L, Gomez-Gomez L, Boller T, Ausubel FM, Sheen J (2002) MAP kinase signalling cascade in Arabidopsis innate immunity. *Nature* **415**, 977–983.

Axtell MJ, Staskawicz BJ (2003) Initiation of RPS2-specified disease resistance in Arabidopsis is coupled to the AvrRpt2-directed elimination of RIN4. *Cell* **112**, 369–377.

Bainard LD, Bainard JD, Newmaster SG, Klironomos JN (2011) Mycorrhizal symbiosis stimulates endoreduplication in angiosperms. *Plant, Cell & Environment* **34**, 1577–1585.

Baluška F, Mancuso S, Volkmann D, Barlow P (2009) The 'root-brain' hypothesis of Charles and Francis Darwin. *Plant Signaling & Behavior* **4**, 1121–1127.

Bannister AJ, Kouzarides T (2011) Regulation of chromatin by histone modifications. *Cell Research* **21**, 381–395.

Baud S, Boutin J-P, Miquel M, Lepiniec L, Rochat C (2002) An integrated overview of seed development in Arabidopsis thaliana ecotype WS. *Plant Physiology and Biochemistry* **40**, 151–160.

Bayer M, Nawy T, Giglione C, Galli M, Meinnel T, Lukowitz W (2009) Paternal control of embryonic patterning in Arabidopsis thaliana. *Science* **323**, 1485–1488.

Bender CL, Alarcón-Chaidez F, Gross DC (1999) Pseudomonas syringae phytotoxins. Mode of action, regulation, and biosynthesis by peptide and polyketide synthetases. *Microbiology and Molecular Biology Reviews (MMBR)* **63**, 266–292.

Benfey PN, Scheres B (2000) Root development. *Current Biology* **10**, R813-R815.

Benjamins R, Scheres B (2008) Auxin. The looping star in plant development. *Annual Review of Plant Biology* **59**, 443–465.

Benková E, Michniewicz M, Sauer M, Teichmann T, Seifertová D, Jürgens G, Friml J (2003) Local, efflux-dependent auxin gradients as a common module for plant organ formation. *Cell* **115**, 591–602.

Berger F (2003) Endosperm. The crossroad of seed development. *Current Opinion in Plant Biology* **6**, 42–50.

Berger F, Grini PE, Schnittger A (2006) Endosperm. An integrator of seed growth and development. *Current Opinion in Plant Biology* **9**, 664–670.

Birchler JA, Veitia RA (2010) The gene balance hypothesis. Implications for gene regulation, quantitative traits and evolution. *The New Phytologist* **186**, 54–62.

Block A, Alfano JR (2011) Plant targets for Pseudomonas syringae type III effectors. Virulence targets or guarded decoys? *Current Opinion in Microbiology* **14**, 39–46.

Blume B, Nürnberger T, Nass N, Scheel D (2000) Receptor-mediated increase in cytoplasmic free calcium required for activation of pathogen defense in parsley. *The Plant Cell Online* **12**, 1425–1440.

Blumwald E (2000) Sodium transport and salt tolerance in plants. *Current Opinion in Cell Biology* **12**, 431–434.

Blumwald E, Poole RJ (1985) Na/H antiport in isolated tonoplast vesicles from storage tissue of Beta vulgaris. *Plant Physiology* **78**, 163–167.

Bögre L, Calderini O, Binarova P, Mattauch M, Till S, Kiegerl S, Jonak C, Pollaschek C, Barker P, Huskisson NS, Hirt H, Heberle-Bors E (1999) A MAP kinase is activated late in plant mitosis and becomes localized to the plane of cell division. *The Plant Cell Online* **11**, 101–113.

Boller T, Felix G (2009) A renaissance of elicitors. Perception of microbe-associated molecular patterns and danger signals by pattern-recognition receptors. *Annual Review of Plant Biology* **60**, 379–406.

Bos JIB, Prince D, Pitino M, Maffei ME, Win J, Hogenhout SA (2010) A functional genomics approach identifies candidate effectors from the aphid species Myzus persicae (green peach aphid). *PLoS Genetics* **6**, e1001216.

Boudolf V, Barrôco R, Engler JdA, Verkest A, Beeckman T, Naudts M, Inzé D, Veylder L de (2004) B1-type cyclin-dependent kinases are essential for the formation of stomatal complexes in Arabidopsis thaliana. *The Plant Cell Online* **16**, 945–955.

Boudolf V, Vlieghe K, Beemster GTS, Magyar Z, Torres Acosta JA, Maes S, van der Schueren E, Inzé D, Veylder L de (2004b) The plant-specific cyclin-dependent kinase CDKB1;1 and transcription factor E2Fa-DPa control the balance of mitotically dividing and endoreduplicating cells in Arabidopsis. *The Plant Cell Online* **16**, 2683–2692.

Boudsocq M, Willmann MR, McCormack M, Lee H, Shan L, He P, Bush J, Cheng S-H, Sheen J (2010) Differential innate immune signalling via Ca(2+) sensor protein kinases. *Nature* **464**, 418–422.

Bray CM (1987) The cell division cycle in plants. *FEBS Letters* **219**, 492.

Brenner ED, Martinez-Barboza N, Clark AP, Liang QS, Stevenson DW, Coruzzi GM (2000) Arabidopsis mutants resistant to S(+)-β-methyl-α, β-diaminopropionic acid, a cycad-derived glutamate receptor agonist. *Plant Physiology* **124**, 1615–1624.

Büttner D, He SY (2009) Type III protein secretion in plant pathogenic bacteria. *Plant Physiology* **150**, 1656–1664.

Chae E, Tran DTN, Weigel D (2016) Cooperation and conflict in the plant immune system. *PLoS Pathogens* **12**, e1005452.

Chang C, Yu D, Jiao J, Jing S, Schulze-Lefert P, Shen Q-H (2013) Barley MLA immune receptors directly interfere with antagonistically acting transcription factors to initiate disease resistance signaling. *The Plant Cell* **25**, 1158–1173.

Chang I-F, Curran A, Woolsey R, Quilici D, Cushman JC, Mittler R, Harmon A, Harper JF (2009) Proteomic profiling of tandem affinity purified 14-3-3 protein complexes in Arabidopsis thaliana. *Proteomics* **9**, 2967–2985.

Chen GQ, Cui C, Mayer ML, Gouaux E (1999) Functional characterization of a potassium-selective prokaryotic glutamate receptor. *Nature* **402**, 817–821.

Chen P, Takatsuka H, Takahashi N, Kurata R, Fukao Y, Kobayashi K, Ito M, Umeda M (2017) Arabidopsis R1R2R3-Myb proteins are essential for inhibiting cell division in response to DNA damage. *Nature Communications* **8**, 635.

Chen Z, Agnew JL, Cohen JD, He P, Shan L, Sheen J, Kunkel BN (2007) Pseudomonas syringae type III effector AvrRpt2 alters Arabidopsis thaliana auxin physiology. *Proceedings of the National Academy of Sciences of the United States of America* **104**, 20131–20136.

Cheng Y, Dai X, Zhao Y (2006) Auxin biosynthesis by the YUCCA flavin monooxygenases controls the formation of floral organs and vascular tissues in Arabidopsis. *Genes & Development* **20**, 1790–1799.

Chiu J, DeSalle R, Lam HM, Meisel L, Coruzzi G (1999) Molecular evolution of glutamate receptors. A primitive signaling mechanism that existed before plants and animals diverged. *Molecular Biology and Evolution* **16**, 826–838.

Chiu JC, Brenner ED, DeSalle R, Nitabach MN, Holmes TC, Coruzzi GM (2002) Phylogenetic and expression analysis of the glutamate-receptor-like gene family in Arabidopsis thaliana. *Molecular Biology and Evolution* **19**, 1066–1082.

Cho D, Kim SA, Murata Y, Lee S, Jae S-K, Nam HG, Kwak JM (2009) De-regulated expression of the plant glutamate receptor homolog AtGLR3.1 impairs long-term Ca2+-programmed stomatal closure. *The Plant Journal for Cell and Molecular Biology* **58**, 437–449.

Churchman ML, Brown ML, Kato N, Kirik V, Hülskamp M, Inzé D, Veylder L de, Walker JD, Zheng Z, Oppenheimer DG, Gwin T, Churchman J, Larkin JC (2006) SIAMESE, a plant-specific cell cycle regulator, controls endoreplication onset in Arabidopsis thaliana. *The Plant Cell* **18**, 3145–3157.

Clough SJ, Bent AF (1998) Floral dip. A simplified method for Agrobacterium-mediated transformation of Arabidopsis thaliana. *The Plant Journal* **16**, 735–743.

Colcombet J, Hirt H (2008) Arabidopsis MAPKs. A complex signalling network involved in multiple biological processes. *The Biochemical Journal* **413**, 217–226.

Cosgrove DJ (2005) Growth of the plant cell wall. *Nature Reviews. Molecular Cell Biology* **6**, 850–861.

Coudreuse D, Nurse P (2010) Driving the cell cycle with a minimal CDK control network. *Nature* **468**, 1074–1079.

Crevillén P, Yang H, Cui X, Greeff C, Trick M, Qiu Q, Cao X, Dean C (2014) Epigenetic reprogramming that prevents transgenerational inheritance of the vernalized state. *Nature* **515**, 587–590.

Dangl JL, Jones JD (2001) Plant pathogens and integrated defence responses to infection. *Nature* **411**, 826–833.

Davenport RJ (2002) Glutamate receptors in plants. *Annals of Botany* **90**, 549–557.

Demidchik V, Essah PA, Tester M (2004) Glutamate activates cation currents in the plasma membrane of Arabidopsis root cells. *Planta* **219**, 167–175.

Demidchik V, Maathuis FJM (2007) Physiological roles of nonselective cation channels in plants. From salt stress to signalling and development. *The New Phytologist* **175**, 387–404.

Demidchik V, Tester M (2002) Sodium fluxes through nonselective cation channels in the plasma membrane of protoplasts from Arabidopsis roots. *Plant Physiology* **128**, 379–387.

Dennison KL, Spalding EP (2000) Glutamate-gated calcium fluxes in Arabidopsis. *Plant Physiology* **124**, 1511–1514.

Desvoyes B, Fernández-Marcos M, Sequeira-Mendes J, Otero S, Vergara Z, Gutierrez C (2014) Looking at plant cell cycle from the chromatin window. *Frontiers in Plant Science* **5**, 369.

Dewitte W, Scofield S, Alcasabas AA, Maughan SC, Menges M, Braun N, Collins C, Nieuwland J, Prinsen E, Sundaresan V, Murray JAH (2007) Arabidopsis CYCD3 D-type cyclins link cell proliferation and endocycles and are rate-limiting for cytokinin responses. *Proceedings of the National Academy of Sciences of the United States of America* **104**, 14537–14542.

Dingledine R, Borges K, Bowie D, Traynelis SF (1999) The glutamate receptor ion channels. *Pharmacological Reviews* **51**, 7–61.

Dodds PN, Lawrence GJ, Catanzariti A-M, Teh T, Wang C-IA, Ayliffe MA, Kobe B, Ellis JG (2006) Direct protein interaction underlies gene-for-gene specificity and coevolution of the

flax resistance genes and flax rust avirulence genes. *Proceedings of the National Academy of Sciences of the United States of America* **103**, 8888–8893.

Doerner P, Jørgensen JE, You R, Steppuhn J, Lamb C (1996) Control of root growth and development by cyclin expression. *Nature* **380**, 520–523.

Dolan L, Janmaat K, Willemsen V, Linstead P, Poethig S, Roberts K, Scheres B (1993) Cellular organisation of the Arabidopsis thaliana root. *Development (Cambridge, England)* **119**, 71–84.

Dolezel J, Göhde W (1995) Sex determination in dioecious plants Melandrium album and M. rubrum using high-resolution flow cytometry. *Cytometry* **19**, 103–106.

Donnelly PM, Bonetta D, Tsukaya H, Dengler RE, Dengler NG (1999) Cell cycling and cell enlargement in developing leaves of Arabidopsis. *Developmental Biology* **215**, 407–419.

Drisch RC, Stahl Y (2015) Function and regulation of transcription factors involved in root apical meristem and stem cell maintenance. *Frontiers in Plant Science* **6**, 505.

Dubos C, Huggins D, Grant GH, Knight MR, Campbell MM (2003) A role for glycine in the gating of plant NMDA-like receptors. *The Plant Journal* **35**, 800–810.

Edgar BA, Zielke N, Gutierrez C (2014) Endocycles. A recurrent evolutionary innovation for post-mitotic cell growth. *Nature Reviews. Molecular Cell Biology* **15**, 197–210.

Erickson RO, Silk WK (1980) The kinematics of plant growth. *Scientific American* **242**, 134–151.

Essah PA, Davenport R, Tester M (2003) Sodium influx and accumulation in Arabidopsis. *Plant Physiology* **133**, 307–318.

Fiorani F, Beemster GTS (2006) Quantitative analyses of cell division in plants. *Plant Molecular Biology* **60**, 963–979.

Forde BG, Cutler SR, Zaman N, Krysan PJ (2013) Glutamate signalling via a MEKK1 kinase-dependent pathway induces changes in Arabidopsis root architecture. *The Plant Journal for Cell and Molecular Biology* **75**, 1–10.

Fox DT, Duronio RJ (2013) Endoreplication and polyploidy. Insights into development and disease. *Development (Cambridge, England)* **140**, 3–12.

Frescatada-Rosa M, Robatzek S, Kuhn H (2015) Should I stay or should I go? Traffic control for plant pattern recognition receptors. *Current Opinion in Plant Biology* **28**, 23–29.

Friml J, Vieten A, Sauer M, Weijers D, Schwarz H, Hamann T, Offringa R, Jürgens G (2003) Efflux-dependent auxin gradients establish the apical-basal axis of Arabidopsis. *Nature* **426**, 147–153.

Fu H, Subramanian RR, Masters SC (2000) 14-3-3 proteins. Structure, function, and regulation. *Annual Review of Pharmacology and Toxicology* **40**, 617–647.

Furniss JJ, Spoel SH (2015) Cullin-RING ubiquitin ligases in salicylic acid-mediated plant immune signaling. *Frontiers in Plant Science* **6**, 154.

Furukawa H, Gouaux E (2003) Mechanisms of activation, inhibition and specificity. Crystal structures of the NMDA receptor NR1 ligand-binding core. *The EMBO Journal* **22**, 2873–2885.

Galletti R, Denoux C, Gambetta S, Dewdney J, Ausubel FM, Lorenzo G de, Ferrari S (2008) The AtrbohD-mediated oxidative burst elicited by oligogalacturonides in Arabidopsis is dispensable for the activation of defense responses effective against Botrytis cinerea. *Plant Physiology* **148**, 1695–1706.

Garcia-Brugger A, Lamotte O, Vandelle E, Bourque S, Lecourieux D, Poinssot B, Wendehenne D, Pugin A (2006) Early signaling events induced by elicitors of plant defenses. *Molecular Plant-Microbe Interactions : MPMI* **19**, 711–724.

Gendreau E, Traas J, Desnos T, Grandjean O, Caboche M, Hofte H (1997) Cellular basis of hypocotyl growth in Arabidopsis thaliana. *Plant Physiology* **114**, 295–305.

Geng Y, Wu R, Wee CW, Xie F, Wei X, Chan PMY, Tham C, Duan L, Dinneny JR (2013) A spatio-temporal understanding of growth regulation during the salt stress response in Arabidopsis. *The Plant Cell* **25**, 2132–2154.

Glazebrook J (2005) Contrasting mechanisms of defense against biotrophic and necrotrophic pathogens. *Annual Review of Phytopathology* **43**, 205–227.

Grieneisen VA, Xu J, Marée AFM, Hogeweg P, Scheres B (2007) Auxin transport is sufficient to generate a maximum and gradient guiding root growth. *Nature* **449**, 1008–1013.

Guo L, Yu Y, Law JA, Zhang X (2010) SET DOMAIN GROUP2 is the major histone H3 lysine corrected 4 trimethyltransferase in Arabidopsis. *Proceedings of the National Academy of Sciences of the United States of America* **107**, 18557–18562.

Ha CM, Jun JH, Fletcher JC (2010) Shoot apical meristem form and function. In 'Plant development' (Ed MCP Timmermans) pp. 103–140 (Academic Press: Amsterdam).

Haga N, Kato K, Murase M, Araki S, Kubo M, Demura T, Suzuki K, Müller I, Voss U, Jürgens G, Ito M (2007) R1R2R3-Myb proteins positively regulate cytokinesis through activation of KNOLLE transcription in Arabidopsis thaliana. *Development (Cambridge, England)* **134**, 1101–1110.

Haga N, Kobayashi K, Suzuki T, Maeo K, Kubo M, Ohtani M, Mitsuda N, Demura T, Nakamura K, Jürgens G, Ito M (2011) Mutations in MYB3R1 and MYB3R4 cause

pleiotropic developmental defects and preferential down-regulation of multiple G2/M-specific genes in Arabidopsis. *Plant Physiology* **157**, 706–717.

Hall D, Evans AR, Newbury HJ, Pritchard J (2006) Functional analysis of CHX21. A putative sodium transporter in Arabidopsis. *Journal of Experimental Botany* **57**, 1201–1210.

Han S, Wang C-w, Wang W-l, Jiang J (2014) Mitogen-activated protein kinase 6 controls root growth in Arabidopsis by modulating Ca2+ -based Na+ flux in root cell under salt stress. *Journal of Plant Physiology* **171**, 26–34.

Harashima H, Sugimoto K (2016) Integration of developmental and environmental signals into cell proliferation and differentiation through RETINOBLASTOMA-RELATED 1. *Current Opinion in Plant Biology* **29**, 95–103.

Harbour JW, Dean DC (2000) The Rb/E2F pathway. Expanding roles and emerging paradigms. *Genes & Development* **14**, 2393–2409.

Harmon AC, Gribskov M, Harper JF (2000) CDPKs - a kinase for every Ca2+ signal? *Trends in Plant Science* **5**, 154–159.

Hempel FD, Feldman LJ (1995) Specification of chimeric flowering shoots in wild-type Arabidopsis. *The Plant Journal* **8**, 725–731.

Henrichs S, Wang B, Fukao Y, Zhu J, Charrier L, Bailly A, Oehring SC, Linnert M, Weiwad M, Endler A, Nanni P, Pollmann S, Mancuso S, Schulz A, Geisler M (2012) Regulation of ABCB1/PGP1-catalysed auxin transport by linker phosphorylation. *The EMBO Journal* **31**, 2965–2980.

Himanen K, Boucheron E, Vanneste S, Almeida Engler J de, Inzé D, Beeckman T (2002) Auxin-mediated cell cycle activation during early lateral root initiation. *The Plant Cell Online* **14**, 2339–2351.

Hirano SS, Upper CD (2000) Bacteria in the leaf ecosystem with emphasis on Pseudomonas syringae-a pathogen, ice nucleus, and epiphyte. *Microbiology and Molecular Biology Reviews (MMBR)* **64**, 624–653.

Hochholdinger F, Park WJ, Sauer M, Woll K (2004) From weeds to crops. Genetic analysis of root development in cereals. *Trends in Plant Science* **9**, 42–48.

Hochholdinger F, Zimmermann R (2008) Conserved and diverse mechanisms in root development. *Current Opinion in Plant Biology* **11**, 70–74.

Horie T, Costa A, Kim TH, Han MJ, Horie R, Leung H-Y, Miyao A, Hirochika H, An G, Schroeder JI (2007) Rice OsHKT2;1 transporter mediates large Na+ influx component into K+-starved roots for growth. *The EMBO Journal* **26**, 3003–3014.

Horie T, Sugawara M, Okada T, Taira K, Kaothien-Nakayama P, Katsuhara M, Shinmyo A, Nakayama H (2011) Rice sodium-insensitive potassium transporter, OsHAK5, confers increased salt tolerance in tobacco BY2 cells. *Journal of Bioscience and Bioengineering* **111**, 346–356.

Hruz T, Laule O, Szabo G, Wessendorp F, Bleuler S, Oertle L, Widmayer P, Gruissem W, Zimmermann P (2008) Genevestigator v3. A reference expression database for the meta-analysis of transcriptomes. *Advances in Bioinformatics* **2008**, 420747.

Hu Y, Xie Q, Chua N-H (2003) The Arabidopsis auxin-inducible gene ARGOS controls lateral organ size. *The Plant Cell* **15**, 1951–1961.

Hua B-G, Mercier RW, Leng Q, Berkowitz GA (2003) Plants do it differently. A new basis for potassium/sodium selectivity in the pore of an ion channel. *Plant Physiology* **132**, 1353–1361.

Huot B, Yao J, Montgomery BL, He SY (2014) Growth-defense tradeoffs in plants. A balancing act to optimize fitness. *Molecular Plant* **7**, 1267–1287.

Ichihashi Y, Horiguchi G, Gleissberg S, Tsukaya H (2010) The bHLH transcription factor SPATULA controls final leaf size in Arabidopsis thaliana. *Plant and Cell Physiology* **51**, 252–261.

Jacob Y, Stroud H, Leblanc C, Feng S, Zhuo L, Caro E, Hassel C, Gutierrez C, Michaels SD, Jacobsen SE (2010) Regulation of heterochromatic DNA replication by histone H3 lysine 27 methyltransferases. *Nature* **466**, 987–991.

Jeon KW (ed) (2001) 'International review of cytology. Survey of cell biology' (Elsevier: Burlington).

Jeon KW (ed) (2004) 'International review of cytology. Survey of cell biology' (Academic Press: Boston, Amsterdam).

Jia W, Zhang J (2008) Stomatal movements and long-distance signaling in plants. *Plant Signaling & Behavior* **3**, 772–777.

Jiang Z, Zhu S, Ye R, Xue Y, Chen A, An L, Pei Z-M (2013) Relationship between NaCl- and H2O2-induced cytosolic Ca2+ increases in response to stress in Arabidopsis. *PloS one* **8**, e76130.

Jin Y, Jing W, Zhang Q, Zhang W (2015) Cyclic nucleotide gated channel 10 negatively regulates salt tolerance by mediating Na+ transport in Arabidopsis. *Journal of Plant Research* **128**, 211–220.

Jones JDG, Dangl JL (2006) The plant immune system. *Nature* **444**, 323–329.

Josse E-M, Halliday KJ (2008) Skotomorphogenesis. The dark side of light signalling. *Current Biology : CB* **18**, R1144-6.

Jouanneau JP, Lapous D, Guern J (1991) In plant protoplasts, the spontaneous expression of defense reactions and the responsiveness to exogenous elicitors are under auxin control. *Plant Physiology* **96**, 459–466.

Kang J, Mehta S, Turano FJ (2004) The putative glutamate receptor 1.1 (AtGLR1.1) in Arabidopsis thaliana regulates abscisic acid biosynthesis and signaling to control development and water loss. *Plant & Cell Physiology* **45**, 1380–1389.

Kang J, Turano FJ (2003) The putative glutamate receptor 1.1 (AtGLR1.1) functions as a regulator of carbon and nitrogen metabolism in Arabidopsis thaliana. *Proceedings of the National Academy of Sciences of the United States of America* **100**, 6872–6877.

Kang S, Kim HB, Lee H, Choi JY, Heu S, Oh CJ, Kwon SI, An CS (2006) Overexpression in Arabidopsis of a plasma membrane-targeting glutamate receptor from small radish increases glutamate-mediated Ca2+ influx and delays fungal infection. *Molecules and Cells* **21**, 418–427.

Kato A, Rouach N, Nicoll RA, Bredt DS (2005) Activity-dependent NMDA receptor degradation mediated by retrotranslocation and ubiquitination. *Proceedings of the National Academy of Sciences of the United States of America* **102**, 5600–5605.

Kazan K, Manners JM (2008) Jasmonate signaling. Toward an integrated view. *Plant Physiology* **146**, 1459–1468.

Keinath NF, Waadt R, Brugman R, Schroeder JI, Grossmann G, Schumacher K, Krebs M (2015) Live cell imaging with R-GECO1 sheds light on flg22- and chitin-induced transient Ca(2+)cyt patterns in Arabidopsis. *Molecular Plant* **8**, 1188–1200.

Kim SH, Kwon SI, Saha D, Anyanwu NC, Gassmann W (2009) Resistance to the Pseudomonas syringae effector HopA1 is governed by the TIR-NBS-LRR protein RPS6 and is enhanced by mutations in SRFR1. *Plant Physiology* **150**, 1723–1732.

Kim SA, Kwak J, Jae S-K, Wang M-H, Nam H (2001) Overexpression of the AtGluR2 gene encoding an Arabidopsis homolog of mammalian glutamate receptors impairs calcium utilization and sensitivity to ionic stress in transgenic plants. *Plant and Cell Physiology* **42**, 74–84.

Knight H, Trewavas AJ, Knight MR (1997) Calcium signalling in Arabidopsis thaliana responding to drought and salinity. *The Plant Journal* **12**, 1067–1078.

Kobayashi K, Suzuki T, Iwata E, Nakamichi N, Suzuki T, Chen P, Ohtani M, Ishida T, Hosoya H, Müller S, Leviczky T, Pettkó-Szandtner A, Darula Z, Iwamoto A, Nomoto M, Tada Y,

Higashiyama T, Demura T, Doonan JH, Hauser M-T, Sugimoto K, Umeda M, Magyar Z, Bögre L, Ito M (2015) Transcriptional repression by MYB3R proteins regulates plant organ growth. *The EMBO Journal* **34**, 1992–2007.

Kong D, Hu H-C, Okuma E, Lee Y, Lee HS, Munemasa S, Cho D, Ju C, Pedoeim L, Rodriguez B, Wang J, Im W, Murata Y, Pei Z-M, Kwak JM (2016) L-Met activates Arabidopsis GLR Ca2+ channels upstream of ROS production and regulates stomatal movement. *Cell Reports* **17**, 2553–2561.

Kong D, Ju C, Parihar A, Kim S, Cho D, Kwak JM (2015) Arabidopsis glutamate receptor homolog3.5 modulates cytosolic Ca2+ level to counteract effect of abscisic acid in seed germination. *Plant Physiology* **167**, 1630–1642.

Kono A, Umeda-Hara C, Lee J, Ito M, Uchimiya H, Umeda M (2003) Arabidopsis D-type cyclin CYCD4;1 is a novel cyclin partner of B2-type cyclin-dependent kinase. *Plant Physiology* **132**, 1315–1321.

Koroleva OA, Tomlinson M, Parinyapong P, Sakvarelidze L, Leader D, Shaw P, Doonan JH (2004) CycD1, a putative G1 cyclin from Antirrhinum majus, accelerates the cell cycle in cultured tobacco BY-2 cells by enhancing both G1/S entry and progression through S and G2 phases. *The Plant Cell Online* **16**, 2364–2379.

Kosugi S, Ohashi Y (2002) E2Ls, E2F-like repressors of Arabidopsis that bind to E2F sites in a monomeric form. *The Journal of Biological Chemistry* **277**, 16553–16558.

Krol E, Dziubinska H, Trebacz K, Koselski M, Stolarz M (2007) The influence of glutamic and aminoacetic acids on the excitability of the liverwort Conocephalum conicum. *Journal of Plant Physiology* **164**, 773–784.

Kumar MN, Jane W-N, Verslues PE (2013) Role of the putative osmosensor Arabidopsis histidine kinase1 in dehydration avoidance and low-water-potential response. *Plant Physiology* **161**, 942–953.

Kurusu T, Yagala T, Miyao A, Hirochika H, Kuchitsu K (2005) Identification of a putative voltage-gated Ca2+ channel as a key regulator of elicitor-induced hypersensitive cell death and mitogen-activated protein kinase activation in rice. *The Plant Journal* **42**, 798–809.

Kwaaitaal M, Huisman R, Maintz J, Reinstädler A, Panstruga R (2011) Ionotropic glutamate receptor (iGluR)-like channels mediate MAMP-induced calcium influx in Arabidopsis thaliana. *The Biochemical Journal* **440**, 355–365.

La Martínez-de Cruz E, García-Ramírez E, Vázquez-Ramos JM, La Reyes de Cruz H, López-Bucio J (2015) Auxins differentially regulate root system architecture and cell cycle protein levels in maize seedlings. *Journal of Plant Physiology* **176**, 147–156.

Lacombe B (2001) The identity of plant glutamate receptors. *Science* **292**, 1486b-1487.

Lafos M, Kroll P, Hohenstatt ML, Thorpe FL, Clarenz O, Schubert D (2011) Dynamic regulation of H3K27 trimethylation during Arabidopsis differentiation. *PLoS Genetics* **7**, e1002040.

Lam HM, Chiu J, Hsieh MH, Meisel L, Oliveira IC, Shin M, Coruzzi G (1998) Glutamate-receptor genes in plants. *Nature* **396**, 125–126.

Laohavisit A, Shang Z, Rubio L, Cuin TA, Véry A-A, Wang A, Mortimer JC, Macpherson N, Coxon KM, Battey NH, Brownlee C, Park OK, Sentenac H, Shabala S, Webb AAR, Davies JM (2012) Arabidopsis annexin1 mediates the radical-activated plasma membrane Ca^{2+}- and K+-permeable conductance in root cells. *The Plant Cell* **24**, 1522–1533.

Lavenus J, Goh T, Roberts I, Guyomarc'h S, Lucas M, Smet I de, Fukaki H, Beeckman T, Bennett M, Laplaze L (2013) Lateral root development in Arabidopsis. Fifty shades of auxin. *Trends in Plant Science* **18**, 450–458.

Lecourieux D, Ranjeva R, Pugin A (2006) Calcium in plant defence-signalling pathways. *The New Phytologist* **171**, 249–269.

Li G, Wu S, Cai L, Wang Q, Zhao X, Wu C (2013b) Identification and mRNA expression profile of glutamate receptor-like gene in quinclorac-resistant and susceptible Echinochloa crus-galli. *Gene* **531**, 489–495.

Li J, Zhu S, Song X, Shen Y, Chen H, Yu J, Yi K, Liu Y, Karplus VJ, Wu P, Deng XW (2006) A rice glutamate receptor-like gene is critical for the division and survival of individual cells in the root apical meristem. *The Plant Cell* **18**, 340–349.

Li T, Chen X, Zhong X, Zhao Y, Liu X, Zhou S, Cheng S, Zhou D-X (2013a) Jumonji C domain protein JMJ705-mediated removal of histone H3 lysine 27 trimethylation is involved in defense-related gene activation in rice. *The Plant Cell* **25**, 4725–4736.

Liu X, Zhou S, Wang W, Ye Y, Zhao Y, Xu Q, Zhou C, Tan F, Cheng S, Zhou D-X (2015b) Regulation of histone methylation and reprogramming of gene expression in the rice inflorescence meristem. *The Plant Cell* **27**, 1428–1444.

Liu Z, Li Y, Cao H, Ren D (2015a) Comparative phospho-proteomics analysis of salt-responsive phosphoproteins regulated by the MKK9-MPK6 cascade in Arabidopsis. *Plant Science : an International Journal of Experimental Plant Biology* **241**, 138–150.

Ljung K, Hull AK, Celenza J, Yamada M, Estelle M, Normanly J, Sandberg G (2005) Sites and regulation of auxin biosynthesis in Arabidopsis roots. *The Plant Cell* **17**, 1090–1104.

Lloyd AJ, William Allwood J, Winder CL, Dunn WB, Heald JK, Cristescu SM, Sivakumaran A, Harren FJM, Mulema J, Denby K, Goodacre R, Smith AR, Mur LAJ (2011) Metabolomic

approaches reveal that cell wall modifications play a major role in ethylene-mediated resistance against Botrytis cinerea. *The Plant Journal for Cell and Molecular Biology* **67**, 852–868.

López-Bucio J, Cruz-Ramírez A, Herrera-Estrella L (2003) The role of nutrient availability in regulating root architecture. *Current Opinion in Plant Biology* **6**, 280–287.

Lu G, Wang X, Liu J, Yu K, Gao Y, Liu H, Wang C, Wang W, Wang G, Liu M, Mao G, Li B, Qin J, Xia M, Zhou J, Liu J, Jiang S, Mo H, Cui J, Nagasawa N, Sivasankar S, Albertsen MC, Sakai H, Mazur BJ, Lassner MW, Broglie RM (2014) Application of T-DNA activation tagging to identify glutamate receptor-like genes that enhance drought tolerance in plants. *Plant Cell Reports* **33**, 617–631.

Lumba S, Cutler S, McCourt P (2010) Plant nuclear hormone receptors. A role for small molecules in protein-protein interactions. *Annual Review of Cell and Developmental Biology* **26**, 445–469.

Luo M, Dennis ES, Berger F, Peacock WJ, Chaudhury A (2005) MINISEED3 (MINI3), a WRKY family gene, and HAIKU2 (IKU2), a leucine-rich repeat (LRR) KINASE gene, are regulators of seed size in Arabidopsis. *Proceedings of the National Academy of Sciences of the United States of America* **102**, 17531–17536.

Maathuis FJM (2014) Sodium in plants. Perception, signalling, and regulation of sodium fluxes. *Journal of Experimental Botany* **65**, 849–858.

Macho AP, Zipfel C (2015) Targeting of plant pattern recognition receptor-triggered immunity by bacterial type-III secretion system effectors. *Current Opinion in Microbiology* **23**, 14–22.

Malamy JE (2005) Intrinsic and environmental response pathways that regulate root system architecture. *Plant, Cell & Environment* **28**, 67–77.

Manzoor H, Kelloniemi J, Chiltz A, Wendehenne D, Pugin A, Poinssot B, Garcia-Brugger A (2013) Involvement of the glutamate receptor AtGLR3.3 in plant defense signaling and resistance to Hyaloperonospora arabidopsidis. *The Plant journal for Cell and Molecular Biology* **76**, 466–480.

Mariconti L, Pellegrini B, Cantoni R, Stevens R, Bergounioux C, Cella R, Albani D (2002) The E2F family of transcription factors from Arabidopsis thaliana. Novel and conserved components of the retinoblastoma/E2F pathway in plants. *The Journal of Biological Chemistry* **277**, 9911–9919.

Melaragno JE, Mehrotra B, Coleman AW (1993) Relationship between endopolyploidy and cell size in epidermal tissue of Arabidopsis. *The Plant Cell* **5**, 1661–1668.

Mendgen K, Hahn M (2002) Plant infection and the establishment of fungal biotrophy. *Trends in Plant Science* **7**, 352–356.

Meng L, Buchanan BB, Feldman LJ, Luan S (2012) CLE-like (CLEL) peptides control the pattern of root growth and lateral root development in Arabidopsis. *Proceedings of the National Academy of Sciences of the United States of America* **109**, 1760–1765.

Meyerhoff O, Müller K, Roelfsema MRG, Latz A, Lacombe B, Hedrich R, Dietrich P, Becker D (2005) AtGLR3.4, a glutamate receptor channel-like gene is sensitive to touch and cold. *Planta* **222**, 418–427.

Michard E, Lima PT, Borges F, Silva AC, Portes MT, Carvalho JE, Gilliham M, Liu L-H, Obermeyer G, Feijó JA (2011) Glutamate receptor-like genes form Ca2+ channels in pollen tubes and are regulated by pistil D-serine. *Science* **332**, 434–437.

Michniewicz M, Zago MK, Abas L, Weijers D, Schweighofer A, Meskiene I, Heisler MG, Ohno C, Zhang J, Huang F, Schwab R, Weigel D, Meyerowitz EM, Luschnig C, Offringa R, Friml J (2007) Antagonistic regulation of PIN phosphorylation by PP2A and PINOID directs auxin flux. *Cell* **130**, 1044–1056.

Miya A, Albert P, Shinya T, Desaki Y, Ichimura K, Shirasu K, Narusaka Y, Kawakami N, Kaku H, Shibuya N (2007) CERK1, a LysM receptor kinase, is essential for chitin elicitor signaling in Arabidopsis. *Proceedings of the National Academy of Sciences of the United States of America* **104**, 19613–19618.

Mockaitis K, Howell SH (2000) Auxin induces mitogenic activated protein kinase (MAPK) activation in roots of Arabidopsis seedlings. *The Plant Journal* **24**, 785–796.

Monaghan J, Zipfel C (2012) Plant pattern recognition receptor complexes at the plasma membrane. *Current Opinion in Plant Biology* **15**, 349–357.

Mousavi SAR, Chauvin A, Pascaud F, Kellenberger S, Farmer EE (2013) GLUTAMATE RECEPTOR-LIKE genes mediate leaf-to-leaf wound signalling. *Nature* **500**, 422–426.

Mozgova I, Köhler C, Hennig L (2015) Keeping the gate closed. Functions of the polycomb repressive complex PRC2 in development. *The Plant Journal for Cell and Molecular Biology* **83**, 121–132.

Munns R, James RA, Xu B, Athman A, Conn SJ, Jordans C, Byrt CS, Hare RA, Tyerman SD, Tester M, Plett D, Gilliham M (2012) Wheat grain yield on saline soils is improved by an ancestral Na^+ transporter gene. *Nature Biotechnology* **30**, 360–364.

Nagata T, Iizumi S, Satoh K, Ooka H, Kawai J, Carninci P, Hayashizaki Y, Otomo Y, Murakami K, Matsubara K, Kikuchi S (2004) Comparative analysis of plant and animal

calcium signal transduction element using plant full-length cDNA data. *Molecular Biology and Evolution* **21**, 1855–1870.

Nakagami H, Kawamura K, Sugisaka K, Sekine M, Shinmyo A (2002) Phosphorylation of retinoblastoma-related protein by the cyclin D/cyclin-dependent kinase complex is activated at the G1/S-phase transition in tobacco. *The Plant Cell Online* **14**, 1847–1857.

Nawrot R, Barylski J, Nowicki G, Broniarczyk J, Buchwald W, Goździcka-Józefiak A (2014) Plant antimicrobial peptides. *Folia Microbiologica* **59**, 181–196.

Newton RP, Smith CJ (2004) Cyclic nucleotides. *Phytochemistry* **65**, 2423–2437.

Ni J, Yu Z, Du G, Zhang Y, Taylor JL, Shen C, Xu J, Liu X, Wang Y, Wu Y (2016) Heterologous expression and functional analysis of rice GLUTAMATE RECEPTOR-LIKE family indicates its role in glutamate triggered calcium flux in rice roots. *Rice (New York, N.Y.)* **9**, 9.

Nomura K, Debroy S, Lee YH, Pumplin N, Jones J, He SY (2006) A bacterial virulence protein suppresses host innate immunity to cause plant disease. *Science* **313**, 220–223.

Nomura K, Mecey C, Lee Y-N, Imboden LA, Chang JH, He SY (2011) Effector-triggered immunity blocks pathogen degradation of an immunity-associated vesicle traffic regulator in Arabidopsis. *Proceedings of the National Academy of Sciences of the United States of America* **108**, 10774–10779.

Nowack MK, Harashima H, Dissmeyer N, Zhao X'A, Bouyer D, Weimer AK, Winter F de, Yang F, Schnittger A (2012) Genetic framework of cyclin-dependent kinase function in Arabidopsis. *Developmental Cell* **22**, 1030–1040.

Ohto M-a, Floyd SK, Fischer RL, Goldberg RB, Harada JJ (2009) Effects of APETALA2 on embryo, endosperm, and seed coat development determine seed size in Arabidopsis. *Sexual Plant Reproduction* **22**, 277–289.

Omasits U, Ahrens CH, Müller S, Wollscheid B (2014) Protter. Interactive protein feature visualization and integration with experimental proteomic data. *Bioinformatics (Oxford, England)* **30**, 884–886.

Otto F (1990) DAPI staining of fixed cells for high-resolution flow cytometry of nuclear DNA. *Methods in Cell Biology* **33**, 105–110.

Pacheco-Villalobos D, Hardtke CS (2012) Natural genetic variation of root system architecture from Arabidopsis to Brachypodium. Towards adaptive value. *Philosophical Transactions of the Royal Society of London. Series B, Biological Sciences* **367**, 1552–1558.

Palmer CM, Bush SM, Maloof JN (2001) Phenotypic and developmental plasticity in plants. In 'eLS' (John Wiley & Sons, Ltd).

Pandey N, Ranjan A, Pant P, Tripathi RK, Ateek F, Pandey HP, Patre UV, Sawant SV (2013) CAMTA 1 regulates drought responses in Arabidopsis thaliana. *BMC Genomics* **14**, 216.

Park J-E, Park J-Y, Kim Y-S, Staswick PE, Jeon J, Yun J, Kim S-Y, Kim J, Lee Y-H, Park C-M (2007) GH3-mediated auxin homeostasis links growth regulation with stress adaptation response in Arabidopsis. *The Journal of Biological Chemistry* **282**, 10036–10046.

Perilli S, Di Mambro R, Sabatini S (2012) Growth and development of the root apical meristem. *Current Opinion in Plant Biology* **15**, 17–23.

Petersson SV, Johansson AI, Kowalczyk M, Makoveychuk A, Wang JY, Moritz T, Grebe M, Benfey PN, Sandberg G, Ljung K (2009) An auxin gradient and maximum in the Arabidopsis root apex shown by high-resolution cell-specific analysis of IAA distribution and synthesis. *The Plant Cell* **21**, 1659–1668.

Pina C, Pinto F, Feijó JA, Becker JD (2005) Gene family analysis of the Arabidopsis pollen transcriptome reveals biological implications for cell growth, division control, and gene expression regulation. *Plant Physiology* **138**, 744–756.

Pinon V, Prasad K, Grigg SP, Sanchez-Perez GF, Scheres B (2013) Local auxin biosynthesis regulation by PLETHORA transcription factors controls phyllotaxis in Arabidopsis. *Proceedings of the National Academy of Sciences of the United States of America* **110**, 1107–1112.

Pitzschke A, Datta S, Persak H (2014) Salt stress in Arabidopsis. Lipid transfer protein AZI1 and its control by mitogen-activated protein kinase MPK3. *Molecular Plant* **7**, 722–738.

Polyn S, Willems A, Veylder L de (2015) Cell cycle entry, maintenance, and exit during plant development. *Current Opinion in Plant Biology* **23**, 1–7.

Potuschak T, Doerner P (2001) Cell cycle controls. Genome-wide analysis in Arabidopsis. *Current Opinion in Plant Biology* **4**, 501–506.

Price MB, Kong D, Okumoto S (2013) Inter-subunit interactions between glutamate-like receptors in Arabidopsis. *Plant Signaling & Behavior* **8**, e27034.

Price MB, Jelesko J, Okumoto S (2012) Glutamate receptor homologs in plants. Functions and evolutionary origins. *Frontiers in Plant Science* **3**, 235.

Qiu Q-S, Guo Y, Dietrich MA, Schumaker KS, Zhu J-K (2002) Regulation of SOS1, a plasma membrane Na+/H+ exchanger in Arabidopsis thaliana, by SOS2 and SOS3. *Proceedings of the National Academy of Sciences of the United States of America* **99**, 8436–8441.

Rahman A, Bannigan A, Sulaman W, Pechter P, Blancaflor EB, Baskin TI (2007) Auxin, actin and growth of the Arabidopsis thaliana primary root. *The Plant Journal* **50**, 514–528.

Ramirez-Parra E, López-Matas MA, Fründt C, Gutierrez C (2004) Role of an atypical E2F transcription factor in the control of Arabidopsis cell growth and differentiation. *The Plant Cell Online* **16**, 2350–2363.

Raz V, Bergervoet JH, Koornneef M (2001) Sequential steps for developmental arrest in Arabidopsis seeds. *Development (Cambridge, England)* **128**, 243–252.

Reinhardt D, Pesce E-R, Stieger P, Mandel T, Baltensperger K, Bennett M, Traas J, Friml J, Kuhlemeier C (2003) Regulation of phyllotaxis by polar auxin transport. *Nature* **426**, 255–260.

Richard C, Granier C, Inzé D, Veylder L de (2001) Analysis of cell division parameters and cell cycle gene expression during the cultivation of Arabidopsis thaliana cell suspensions. *Journal of Experimental Botany* **52**, 1625–1633.

Rodriguez MCS, Petersen M, Mundy J (2010) Mitogen-activated protein kinase signaling in plants. *Annual Review of Plant Biology* **61**, 621–649.

Rodriguez RE, Debernardi JM, Palatnik JF (2014) Morphogenesis of simple leaves. Regulation of leaf size and shape. *Wiley Interdisciplinary Reviews. Developmental Biology* **3**, 41–57.

Rojas CA, Eloy NB, Lima MdF, Rodrigues RL, Franco LO, Himanen K, Beemster GTS, Hemerly AS, Ferreira PCG (2009) Overexpression of the Arabidopsis anaphase promoting complex subunit CDC27a increases growth rate and organ size. *Plant Molecular Biology* **71**, 307–318.

Roudier F, Ahmed I, Bérard C, Sarazin A, Mary-Huard T, Cortijo S, Bouyer D, Caillieux E, Duvernois-Berthet E, Al-Shikhley L, Giraut L, Després B, Drevensek S, Barneche F, Dèrozier S, Brunaud V, Aubourg S, Schnittger A, Bowler C, Martin-Magniette M-L, Robin S, Caboche M, Colot V (2011) Integrative epigenomic mapping defines four main chromatin states in Arabidopsis. *The EMBO Journal* **30**, 1928–1938.

Roy BC, Mukherjee A (2017) Computational analysis of the glutamate receptor gene family of Arabidopsis thaliana. *Journal of Biomolecular Structure & Dynamics* **35**, 2454–2474.

Roy SJ, Gilliham M, Berger B, Essah PA, Cheffings C, Miller AJ, Davenport RJ, Liu L-H, Skynner MJ, Davies JM, Richardson P, Leigh RA, Tester M (2008) Investigating glutamate receptor-like gene co-expression in Arabidopsis thaliana. *Plant, Cell & Environment* **31**, 861–871.

Ruelland E, Kravets V, Derevyanchuk M, Martinec J, Zachowski A, Pokotylo I (2015) Role of phospholipid signalling in plant environmental responses. *Environmental and Experimental Botany* **114**, 129–143.

Rushton PJ, Somssich IE, Ringler P, Shen QJ (2010) WRKY transcription factors. *Trends in Plant Science* **15**, 247–258.

Sabatini S, Beis D, Wolkenfelt H, Murfett J, Guilfoyle T, Malamy J, Benfey P, Leyser O, Bechtold N, Weisbeek P, Scheres B (1999) An auxin-dependent distal organizer of pattern and polarity in the Arabidopsis root. *Cell* **99**, 463–472.

Sabelli PA, Liu Y, Dante RA, Lizarraga LE, Nguyen HN, Brown SW, Klingler JP, Yu J, LaBrant E, Layton TM, Feldman M, Larkins BA (2013) Control of cell proliferation, endoreduplication, cell size, and cell death by the retinoblastoma-related pathway in maize endosperm. *Proceedings of the National Academy of Sciences of the United States of America* **110**, E1827-36.

Sahi C, Singh A, Blumwald E, Grover A (2006) Beyond osmolytes and transporters. Novel plant salt-stress tolerance-related genes from transcriptional profiling data. *Physiologia Plantarum* **127**, 1–9.

Salinas GD, Blair LAC, Needleman LA, Gonzales JD, Chen Y, Li M, Singer JD, Marshall J (2006) Actinfilin is a Cul3 substrate adaptor, linking GluR6 kainate receptor subunits to the ubiquitin-proteasome pathway. *The Journal of Biological Chemistry* **281**, 40164–40173.

Salvador-Recatalà V (2016) New roles for the GLUTAMATE RECEPTOR-LIKE 3.3, 3.5, and 3.6 genes as on/off switches of wound-induced systemic electrical signals. *Plant Signaling & Behavior* **11**, e1161879.

Salvador-Recatalà V, Tjallingii WF, Farmer EE (2014) Real-time, in vivo intracellular recordings of caterpillar-induced depolarization waves in sieve elements using aphid electrodes. *The New Phytologist* **203**, 674–684.

Sayle R (1995) RASMOL. Biomolecular graphics for all. *Trends in Biochemical Sciences* **20**, 374–376.

Schmidt R, Mieulet D, Hubberten H-M, Obata T, Hoefgen R, Fernie AR, Fisahn J, San Segundo B, Guiderdoni E, Schippers JHM, Mueller-Roeber B (2013) Salt-responsive ERF1 regulates reactive oxygen species-dependent signaling during the initial response to salt stress in rice. *The Plant Cell* **25**, 2115–2131.

Schopfer P (2006) Biomechanics of plant growth. *American Journal of Botany* **93**, 1415–1425.

Schroeder JI, Raschke K, Neher E (1987) Voltage dependence of K channels in guard-cell protoplasts. *Proceedings of the National Academy of Sciences of the United States of America* **84**, 4108–4112.

Schroeder JI, Ward JM, Gassmann W (1994) Perspectives on the physiology and structure of inward-rectifying K+ channels in higher plants. Biophysical implications for K+ uptake. *Annual Review of Biophysics and Biomolecular Structure* **23**, 441–471.

Schroeder JI, Delhaize E, Frommer WB, Guerinot ML, Harrison MJ, Herrera-Estrella L, Horie T, Kochian LV, Munns R, Nishizawa NK, Tsay Y-F, Sanders D (2013) Using membrane transporters to improve crops for sustainable food production. *Nature* **497**, 60–66.

Schruff MC, Spielman M, Tiwari S, Adams S, Fenby N, Scott RJ (2006) The AUXIN RESPONSE FACTOR 2 gene of Arabidopsis links auxin signalling, cell division, and the size of seeds and other organs. *Development (Cambridge, England)* **133**, 251–261.

Schutter K de, Joubès J, Cools T, Verkest A, Corellou F, Babiychuk E, van der Schueren E, Beeckman T, Kushnir S, Inzé D, Veylder L de (2007) Arabidopsis WEE1 kinase controls cell cycle arrest in response to activation of the DNA integrity checkpoint. *The Plant Cell* **19**, 211–225.

Scofield S, Jones A, Murray JAH (2014) The plant cell cycle in context. *Journal of Experimental Botany* **65**, 2557–2562.

Sequeira-Mendes J, Aragüez I, Peiró R, Mendez-Giraldez R, Zhang X, Jacobsen SE, Bastolla U, Gutierrez C (2014) The functional topography of the Arabidopsis genome is organized in a reduced number of linear motifs of chromatin states. *The Plant Cell* **26**, 2351–2366.

Seybold H, Trempel F, Ranf S, Scheel D, Romeis T, Lee J (2014) Ca2+ signalling in plant immune response. From pattern recognition receptors to Ca2+ decoding mechanisms. *The New Phytologist* **204**, 782–790.

Shimotohno A, Umeda-Hara C, Bisova K, Uchimiya H, Umeda M (2004) The plant-specific kinase CDKF;1 is involved in activating phosphorylation of cyclin-dependent kinase-activating kinases in Arabidopsis. *The Plant Cell* **16**, 2954–2966.

Shinshi H, Mohnen D, Meins F (1987) Regulation of a plant pathogenesis-related enzyme. Inhibition of chitinase and chitinase mRNA accumulation in cultured tobacco tissues by auxin and cytokinin. *Proceedings of the National Academy of Sciences of the United States of America* **84**, 89–93.

Singh A, Kanwar P, Yadav AK, Mishra M, Jha SK, Baranwal V, Pandey A, Kapoor S, Tyagi AK, Pandey GK (2014) Genome-wide expressional and functional analysis of calcium transport elements during abiotic stress and development in rice. *The FEBS Journal* **281**, 894–915.

Singh SK, Chien C-T, Chang I-F (2016) The Arabidopsis glutamate receptor-like gene GLR3.6 controls root development by repressing the Kip-related protein gene KRP4. *Journal of Experimental Botany* **67**, 1853–1869.

Sivaguru M, Pike S, Gassmann W, Baskin TI (2003) Aluminum rapidly depolymerizes cortical microtubules and depolarizes the plasma membrane. Evidence that these Responses are Mediated by a Glutamate Receptor. *Plant and Cell Physiology* **44**, 667–675.

Skirycz A, Claeys H, Bodt S de, Oikawa A, Shinoda S, Andriankaja M, Maleux K, Eloy NB, Coppens F, Yoo S-D, Saito K, Inzé D (2011) Pause-and-stop. The effects of osmotic stress on cell proliferation during early leaf development in Arabidopsis and a role for ethylene signaling in cell cycle arrest. *The Plant Cell* **23**, 1876–1888.

Skirycz A, Radziejwoski A, Busch W, Hannah MA, Czeszejko J, Kwaśniewski M, Zanor M-I, Lohmann JU, Veylder L de, Witt I, Mueller-Roeber B (2008) The DOF transcription factor OBP1 is involved in cell cycle regulation in Arabidopsis thaliana. *The Plant Journal for Cell and Molecular Biology* **56**, 779–792.

Sobolevsky AI, Rosconi MP, Gouaux E (2009) X-ray structure, symmetry and mechanism of an AMPA-subtype glutamate receptor. *Nature* **462**, 745–756.

Sorrell DA, Menges M, Healy JM, Deveaux Y, Amano C, Su Y, Nakagami H, Shinmyo A, Doonan JH, Sekine M, Murray JA (2001) Cell cycle regulation of cyclin-dependent kinases in tobacco cultivar Bright Yellow-2 cells. *Plant Physiology* **126**, 1214–1223.

Sozzani R, Maggio C, Giordo R, Umana E, Ascencio-Ibañez JT, Hanley-Bowdoin L, Bergounioux C, Cella R, Albani D (2010) The E2FD/DEL2 factor is a component of a regulatory network controlling cell proliferation and development in Arabidopsis. *Plant Molecular Biology* **72**, 381–395.

Steeves TA, Sussex IM (1989) 'Patterns in plant development' (Cambridge University Press).

Stepanova AN, Robertson-Hoyt J, Yun J, Benavente LM, Xie D-Y, Dolezal K, Schlereth A, Jürgens G, Alonso JM (2008) TAA1-mediated auxin biosynthesis is essential for hormone crosstalk and plant development. *Cell* **133**, 177–191.

Stephens NR, Qi Z, Spalding EP (2008) Glutamate receptor subtypes evidenced by differences in desensitization and dependence on the GLR3.3 and GLR3.4 genes. *Plant Physiology* **146**, 529–538.

Su YH, Zhao XY, Liu YB, Zhang CL, O'Neill SD, Zhang XS (2009) Auxin-induced WUS expression is essential for embryonic stem cell renewal during somatic embryogenesis in Arabidopsis. *The Plant Journal for Cell and Molecular Biology* **59**, 448–460.

Sun X, Shantharaj D, Kang X, Ni M (2010) Transcriptional and hormonal signaling control of Arabidopsis seed development. *Current Opinion in Plant Biology* **13**, 611–620.

Sunarpi, Horie T, Motoda J, Kubo M, Yang H, Yoda K, Horie R, Chan W-Y, Leung H-Y, Hattori K, Konomi M, Osumi M, Yamagami M, Schroeder JI, Uozumi N (2005) Enhanced salt tolerance mediated by AtHKT1 transporter-induced Na unloading from xylem vessels to xylem parenchyma cells. *The Plant Journal* **44**, 928–938.

Sundaresan V (2005) Control of seed size in plants. *Proceedings of the National Academy of Sciences of the United States of America* **102**, 17887–17888.

Taj G, Agarwal P, Grant M, Kumar A (2010) MAPK machinery in plants. Recognition and response to different stresses through multiple signal transduction pathways. *Plant Signaling & Behavior* **5**, 1370–1378.

Tanaka H, Kitakura S, Rycke R de, Groodt R de, Friml J (2009) Fluorescence imaging-based screen identifies ARF GEF component of early endosomal trafficking. *Current Biology : CB* **19**, 391–397.

Tapken D, Anschütz U, Liu L-H, Huelsken T, Seebohm G, Becker D, Hollmann M (2013) A plant homolog of animal glutamate receptors is an ion channel gated by multiple hydrophobic amino acids. *Science Signaling* **6**, ra47.

Tapken D, Hollmann M (2008) Arabidopsis thaliana glutamate receptor ion channel function demonstrated by ion pore transplantation. *Journal of Molecular Biology* **383**, 36–48.

Tarczynski MC, Jensen RG, Bohnert HJ (1993) Stress protection of transgenic tobacco by production of the osmolyte mannitol. *Science* **259**, 508–510.

Teakle NL, Tyerman SD (2010) Mechanisms of Cl(-) transport contributing to salt tolerance. *Plant, Cell & Environment* **33**, 566–589.

Teardo E, Carraretto L, Bortoli S de, Costa A, Behera S, Wagner R, Lo Schiavo F, Formentin E, Szabo I (2015) Alternative splicing-mediated targeting of the Arabidopsis GLUTAMATE RECEPTOR3.5 to mitochondria affects organelle morphology. *Plant Physiology* **167**, 216–227.

Teardo E, Formentin E, Segalla A, Giacometti GM, Marin O, Zanetti M, Lo Schiavo F, Zoratti M, Szabò I (2011) Dual localization of plant glutamate receptor AtGLR3.4 to plastids and plasmamembrane. *Biochimica et Biophysica acta* **1807**, 359–367.

Teardo E, Segalla A, Formentin E, Zanetti M, Marin O, Giacometti GM, Lo Schiavo F, Zoratti M, Szabò I (2010) Characterization of a plant glutamate receptor activity. *Cellular Physiology and Biochemistry : International Journal of Experimental Cellular Physiology, Biochemistry, and Pharmacology* **26**, 253–262.

Tian H, Smet I de, Ding Z (2014) Shaping a root system. Regulating lateral versus primary root growth. *Trends in Plant Science* **19**, 426–431.

Timmermans MCP (ed) (2010) 'Plant development' (Academic Press: Amsterdam).

Torii KU (2004) Leucine-rich repeat receptor kinases in plants. Structure, Function, and Signal Transduction Pathways. In 'International review of cytology. Survey of cell biology' (Ed KW Jeon) pp. 1–46 (Academic Press: Boston, Amsterdam).

Traas J, Doonan JH (2001) Cellular basis of shoot apical meristem development. In 'International review of cytology. Survey of cell biology' (Ed KW Jeon) pp. 161–206 (Elsevier: Burlington).

Tracy FE, Gilliham M, Dodd AN, Webb AAR, Tester M (2008) NaCl-induced changes in cytosolic free Ca2+ in Arabidopsis thaliana are heterogeneous and modified by external ionic composition. *Plant, Cell & Environment* **31**, 1063–1073.

Traynelis SF, Wollmuth LP, McBain CJ, Menniti FS, Vance KM, Ogden KK, Hansen KB, Yuan H, Myers SJ, Dingledine R (2010) Glutamate receptor ion channels. Structure, regulation, and function. *Pharmacological Reviews* **62**, 405–496.

Turano FJ, Panta GR, Allard MW, van Berkum P (2001) The putative glutamate receptors from plants are related to two superfamilies of animal neurotransmitter receptors via distinct evolutionary mechanisms. *Molecular Biology and Evolution* **18**, 1417–1420.

Ulbrich MH, Isacoff EY (2008) Rules of engagement for NMDA receptor subunits. *Proceedings of the National Academy of Sciences of the United States of America* **105**, 14163–14168.

van den Berg C, Willemsen V, Hendriks G, Weisbeek P, Scheres B (1997) Short-range control of cell differentiation in the Arabidopsis root meristem. *Nature* **390**, 287–289.

van der Hoorn RAL, Kamoun S (2008) From guard to decoy. A new model for perception of plant pathogen effectors. *The Plant Cell* **20**, 2009–2017.

van Leene J, Hollunder J, Eeckhout D, Persiau G, van de Slijke E, Stals H, van Isterdael G, Verkest A, Neirynck S, Buffel Y, Bodt S de, Maere S, Laukens K, Pharazyn A, Ferreira PCG, Eloy N, Renne C, Meyer C, Faure J-D, Steinbrenner J, Beynon J, Larkin JC, van de Peer Y, Hilson P, Kuiper M, Veylder L de, van Onckelen H, Inzé D, Witters E, Jaeger G de (2010) Targeted interactomics reveals a complex core cell cycle machinery in Arabidopsis thaliana. *Molecular Systems Biology* **6**, 397.

Vandelle E, Poinssot B, Wendehenne D, Bentéjac M, Alain P (2006) Integrated signaling network involving calcium, nitric oxide, and active oxygen species but not mitogen-

activated protein kinases in BcPG1-elicited grapevine defenses. *Molecular Plant-Microbe Interactions : MPMI* **19**, 429–440.

Vandepoele K, Raes J, Veylder L de, Rouzé P, Rombauts S, Inzé D (2002) Genome-wide analysis of core cell cycle genes in Arabidopsis. *The Plant Cell Online* **14**, 903–916.

Vanneste S, Friml J (2013) Calcium. The Missing Link in Auxin Action. *Plants (Basel, Switzerland)* **2**, 650–675.

Vatsa P, Chiltz A, Bourque S, Wendehenne D, Garcia-Brugger A, Pugin A (2011) Involvement of putative glutamate receptors in plant defence signaling and NO production. *Biochimie* **93**, 2095–2101.

Verbelen J-P, Cnodder T de, Le J, Vissenberg K, Baluska F (2006) The root apex of Arabidopsis thaliana consists of four distinct zones of growth activities. Meristematic Zone, Transition Zone, Fast Elongation Zone and Growth Terminating Zone. *Plant Signaling & Behavior* **1**, 296–304.

Vernoux T, Brunoud G, Farcot E, Morin V, van den Daele H, Legrand J, Oliva M, Das P, Larrieu A, Wells D, Guédon Y, Armitage L, Picard F, Guyomarc'h S, Cellier C, Parry G, Koumproglou R, Doonan JH, Estelle M, Godin C, Kepinski S, Bennett M, Veylder L de, Traas J (2011) The auxin signalling network translates dynamic input into robust patterning at the shoot apex. *Molecular Systems Biology* **7**, 508.

Veylder L de, Beeckman T, Beemster GT, Krols L, Terras F, Landrieu I, van der Schueren E, Maes S, Naudts M, Inzé D (2001) Functional analysis of cyclin-dependent kinase inhibitors of Arabidopsis. *The Plant Cell* **13**, 1653–1668.

Veylder L de, Beeckman T, Beemster GTS, Almeida Engler J de, Ormenese S, Maes S, Naudts M, van der Schueren E, Jacqmard A, Engler G, Inzé D (2002) Control of proliferation, endoreduplication and differentiation by the Arabidopsis E2Fa-DPa transcription factor. *The EMBO Journal* **21**, 1360–1368.

Veylder L de, Beeckman T, Inzé D (2007) The ins and outs of the plant cell cycle. *Nature Reviews. Molecular Cell Biology* **8**, 655–665.

Veylder L de, Larkin JC, Schnittger A (2011) Molecular control and function of endoreplication in development and physiology. *Trends in Plant Science* **16**, 624–634.

Vincill ED, Bieck AM, Spalding EP (2012) Ca(2+) conduction by an amino acid-gated ion channel related to glutamate receptors. *Plant Physiology* **159**, 40–46.

Vincill ED, Clarin AE, Molenda JN, Spalding EP (2013) Interacting glutamate receptor-like proteins in Phloem regulate lateral root initiation in Arabidopsis. *The Plant Cell* **25**, 1304–1313.

Vodermaier HC (2004) APC/C and SCF. Controlling each other and the cell cycle. *Current Biology : CB* **14**, R787-96.

Walch-Liu P, Liu L-H, Remans T, Tester M, Forde BG (2006) Evidence that L-glutamate can act as an exogenous signal to modulate root growth and branching in Arabidopsis thaliana. *Plant & Cell Physiology* **47**, 1045–1057.

Wang A, Garcia D, Zhang H, Feng K, Chaudhury A, Berger F, Peacock WJ, Dennis ES, Luo M (2010) The VQ motif protein IKU1 regulates endosperm growth and seed size in Arabidopsis. *The Plant Journal for Cell and Molecular Biology* **63**, 670–679.

Wang D, Pajerowska-Mukhtar K, Culler AH, Dong X (2007) Salicylic acid inhibits pathogen growth in plants through repression of the auxin signaling pathway. *Current Biology* **17**, 1784–1790.

Wang G, Kong H, Sun Y, Zhang X, Zhang W, Altman N, DePamphilis CW, Ma H (2004) Genome-wide analysis of the cyclin family in Arabidopsis and comparative phylogenetic analysis of plant cyclin-like proteins. *Plant Physiology* **135**, 1084–1099.

Wang Q, Guan C, Wang P, Lv M-L, Ma Q, Wu G-Q, Bao A-K, Zhang J-L, Wang S-M (2015) AtHKT1;1 and AtHAK5 mediate low-affinity Na+ uptake in Arabidopsis thaliana under mild salt stress. *Plant Growth Regulation* **75**, 615–623.

Weiland M, Mancuso S, Baluska F (2015) Signalling via glutamate and GLRs in Arabidopsis thaliana. *Functional Plant Biology* **43**, 1-25.

Weingartner M, Criqui M-C, Mészáros T, Binarova P, Schmit A-C, Helfer A, Derevier A, Erhardt M, Bögre L, Genschik P (2004) Expression of a nondegradable cyclin B1 affects plant development and leads to endomitosis by inhibiting the formation of a phragmoplast. *The Plant Cell Online* **16**, 643–657.

Weinl S, Kudla J (2009) The CBL-CIPK Ca(2+)-decoding signaling network. Function and perspectives. *The New Phytologist* **184**, 517–528.

Weng H, Yoo CY, Gosney MJ, Hasegawa PM, Mickelbart MV (2012) Poplar GTL1 is a Ca2+/calmodulin-binding transcription factor that functions in plant water use efficiency and drought tolerance. *PloS one* **7**, e32925.

White DWR (2006) PEAPOD regulates lamina size and curvature in Arabidopsis. *Proceedings of the National Academy of Sciences of the United States of America* **103**, 13238–13243.

Wildermuth MC (2010) Modulation of host nuclear ploidy. A common plant biotroph mechanism. *Current Opinion in Plant Biology* **13**, 449–458.

Wildwater M, Campilho A, Perez-Perez JM, Heidstra R, Blilou I, Korthout H, Chatterjee J, Mariconti L, Gruissem W, Scheres B (2005) The RETINOBLASTOMA-RELATED gene regulates stem cell maintenance in Arabidopsis roots. *Cell* **123**, 1337–1349.

Yang H, Howard M, Dean C (2014) Antagonistic roles for H3K36me3 and H3K27me3 in the cold-induced epigenetic switch at Arabidopsis FLC. *Current Biology : CB* **24**, 1793–1797.

Yao X, Feng H, Yu Y, Dong A, Shen W-H (2013) SDG2-mediated H3K4 methylation is required for proper Arabidopsis root growth and development. *PloS one* **8**, e56537.

Yao X, Horie T, Xue S, Leung H-Y, Katsuhara M, Brodsky DE, Wu Y, Schroeder JI (2010) Differential sodium and potassium transport selectivities of the rice OsHKT2;1 and OsHKT2;2 transporters in plant cells. *Plant Physiology* **152**, 341–355.

Yogendra KN, Pushpa D, Mosa KA, Kushalappa AC, Murphy A, Mosquera T (2014) Quantitative resistance in potato leaves to late blight associated with induced hydroxycinnamic acid amides. *Functional & Integrative Genomics* **14**, 285–298.

Yokawa K, Fasano R, Kagenishi T, Baluška F (2014) Light as stress factor to plant roots - case of root halotropism. *Frontiers in Plant Science* **5**, 718.

Yoo JH, Park CY, Kim JC, Heo WD, Cheong MS, Park HC, Kim MC, Moon BC, Choi MS, Kang YH, Lee JH, Kim HS, Lee SM, Yoon HW, Lim CO, Yun D-J, Lee SY, Chung WS, Cho MJ (2005) Direct interaction of a divergent CaM isoform and the transcription factor, MYB2, enhances salt tolerance in arabidopsis. *The Journal of Biological Chemistry* **280**, 3697–3706.

Yoshida R, Mori IC, Kamizono N, Shichiri Y, Shimatani T, Miyata F, Honda K, Iwai S (2016) Glutamate functions in stomatal closure in Arabidopsis and fava bean. *Journal of Plant Research* **129**, 39–49.

Zhang M, Xie S, Dong X, Zhao X, Zeng B, Chen J, Li H, Yang W, Zhao H, Wang G, Chen Z, Sun S, Hauck A, Jin W, Lai J (2014) Genome-wide high resolution parental-specific DNA and histone methylation maps uncover patterns of imprinting regulation in maize. *Genome Research* **24**, 167–176.

Zhang X, Bernatavichute YV, Cokus S, Pellegrini M, Jacobsen SE (2009) Genome-wide analysis of mono-, di- and trimethylation of histone H3 lysine 4 in Arabidopsis thaliana. *Genome Biology* **10**, R62.

Zielke N, Kim KJ, Tran V, Shibutani ST, Bravo M-J, Nagarajan S, van Straaten M, Woods B, Dassow G von, Rottig C, Lehner CF, Grewal SS, Duronio RJ, Edgar BA (2011) Control of Drosophila endocycles by E2F and CRL4(CDT2). *Nature* **480**, 123–127.

Zipfel C, Felix G (2005) Plants and animals. A different taste for microbes? *Current Opinion in Plant Biology* **8**, 353–360.

Zipfel C, Kunze G, Chinchilla D, Caniard A, Jones JDG, Boller T, Felix G (2006) Perception of the bacterial PAMP EF-Tu by the receptor EFR restricts Agrobacterium-mediated transformation. *Cell* **125**, 749–760.

Zuo J, Niu QW, Chua NH (2000) Technical advance. An estrogen receptor-based transactivator XVE mediates highly inducible gene expression in transgenic plants. *The Plant Journal* **24**, 265–273.

7 Supplemental Material

7.1 List of Primer and PCR Conditions for RT-PCRs

Gene	Forward Primer (5' – 3')	Reverse Primer (5' – 3')
AtGLR3.7 (sqRT-PCR)	ATGGGACTGGGCATTGACC	CCGAAGAAAGAAGGGAAATTGGAGGG
AtGLR3.7 (qRT-PCR)	GACTGGTCCCACTTGACTCG	AGGGAGTTCGTCGACAATGG
CDKA;1	GGAATTGCGTATTGCCACTCTC	GGGATACCGAATGCTCTGGC
CDKB1;1	TTTGCTGAGATGGTTCGGAGG	GTAAACATGCCAGTCACGCAG
CDKB2;1	TTGGTGAAGGGACATACGGG	CGGAGAGTGGTGGAAGGAAC
CYCA3;2	TTGACGGAGATCGGGTCAAC	AATCTGTTTCGCCGGAGGAG
CYCB1;2	TGACAGTCCCGACTCAATACG	AAGCATGGAGGGACAGAACG
CYCD3;1	CACAATGGCGATTCGGAAGG	ACTTCTTCTCCTTCATCGTCCC
CYCD3;3	ATGCAACAACCCGCTAGTCC	AGCAGAAGCAGACACAACCC
CYCD4;1	AAGGAGAAGCAGCATTTGCC	ACTTCACAAGCCTTCCAAATCC
KRP1	AATCAAGCTCTGTCTCCGTCG	CGTACCCCGTCGATACGTC
KRP4	CTCTTCAACAACAACAACAACGC	CCACAATCGTTCATCTGCTGC
MYB3R4	TTGCATGGAGGCAAATGTCAG	GTAGACAGGACTGGCTTACCG
MYB3R1	GATGTAATGACGGTGGTGCTTC	GGTCTAGCTCGAGTCATACCAG
E2Fa	AAGGGAGTTGATGCGTGTCC	TCGCTCAGGTCTCTTAATCTTTCC
E2Fb	TGGCCAGATGAATACTGGAACC	TGGGCTCGATGGAGTTTGTG
E2Fc	CTCAGGCGAAGATCCGACTC	TCGGAAGCGATTGAGAGACTG
E2Fd (DEL2)	CTCGCTCCCCAGGTTTACAG	ATACGCCGACGTTCAACTCC
E2Fe (DEL1)	TGGTTGGGCTTGATGATGCT	CCTGGAATTGCGGAAAACCC
E2Ff (DEL3)	CTAGAGATCGAGGCCCTTGC	TCCGATCAACCTCTGCATACC
DPa	GACTCAAGGCCCAGCAGAAG	TGGACCGAGAAAGGTGTGC
DPb	AAGGTGATGATGCTGGTTCTCA	TGCTTTCCACCTTTTCACAAACTT
OBP1	CGACAACGACGAATGTTGGG	ACCGGAGACAAATCCACCAC
RBR1	CCTCAGGCTATGAGCGGATG	TGGGACACCGAACACAGTTAG
T-DNA Salk Line (LBa1)	TGGTTCACGTAGTGGGCCATCG	
T-DNA Insertion (atglr3.7)		CAATTCCTCGATGCCATGCGCAA

RT-PCRs were conducted following the manufactures' instructions. Semi-quantitative RT-PCRs employed 'DreamTaq DNA Polymerase' (ThermoFisher Scientific) with an annealing temperature between 58 and 68 °C and 25-35 cycles depending on the GOI. Quantitative RT-PCRs were conducted on a 'Rotor-Gene Q 5plex HRM' thermocycler (Qiagen) using a 'SsoAdvanced™ Universal SYBR® Green Supermix' (Bio-Rad Laboratories) with an annealing temperature of 60 °C and 45 cycles.

7.2 Antibodies for Protein Quantification and Qualification

Primary Antibodies	Origin	Target	Manufacturer	Working solution
Anti-Histone H3	Rabbit (polyclonal)	Histone H3	Abcam (Cat. No. ab1791)	1:1000
Anti-Histone H3 (tri methyl K27)	Mouse (monoclonal)	Histone H3 (tri-methylated)	Abcam (Cat. No. ab6002)	1:2000
Anti-AtMPK3	Rabbit (polyclonal)	AtMPK3	Sigma Aldrich (Cat. No. M8318)	1:2000
Anti-AtMPK6	Rabbit (polyclonal)	AtMPK6	Sigma Aldrich (Cat. No. A7104)	1:20000
Phospho-p44/42 MAPK (Erk1/2) (Thr202/Tyr204)	Rabbit (polyclonal)	phosphorylated Thr202/Thr185 and Tyr204/Tyr187 of human p44/p42 MAP kinase	Cell Signalling Technologies (Cat. No. 9101)	1:1000

Secondary Antibodies	Origin	Manufacturer	Working solution
Anti-Mouse IgG	Rabbit (polyclonal)	Abcam (Cat. No. ab97046)	1:2000
Anti-Rabbit IgG	Goat (polyclonal)	Abcam (Cat. No. ab6721)	1:3000

7.3 Verification of T-DNA Insertion in atglr3.7

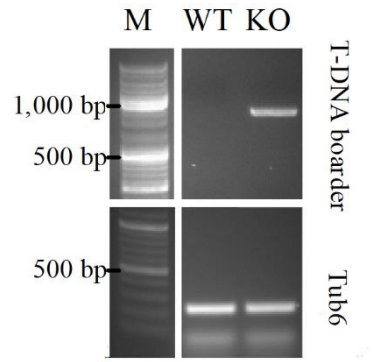

Figure 34. **Verification of T-DNA Insertion in Arabidopsis atglr3.7 with a Col-0 Background.** Wildtype and transgenic *Arabidopsis thaliana* were grown sterile in hydroponics and harvested on 14 DAI. Bulk RNA extractions and transcription into cDNA was followed by sqRT-PCR. Displayed images are representative for one to two repetitions. *Tubulin alpha-6 chain* (*Tub6*) served as a reference gene. Forward and reverse primer pairs were supposed to bind on DNA sequences of the T-DNA insertion and the C-terminal region of the gene encoding *AtGLR3.7*. A PCR product of about 1,000 bp was only attainable when the T-DNA insertion was present within the genome of the respective plant line. M: DNA ladder '50 bp DNA Ladder' (Bioland Scientific LLC, Cat. No. DM02-01) for T-DNA boarder region and 'GeneRuler DNA Ladder Mix' (Thermo Fisher Scientific) for *Tub6* as a control gene expression; WT - Col-0; KO - atglr3.7.

7.4 Mock Treatment of *AtGLR3.7* Inducible Overexpression Plants

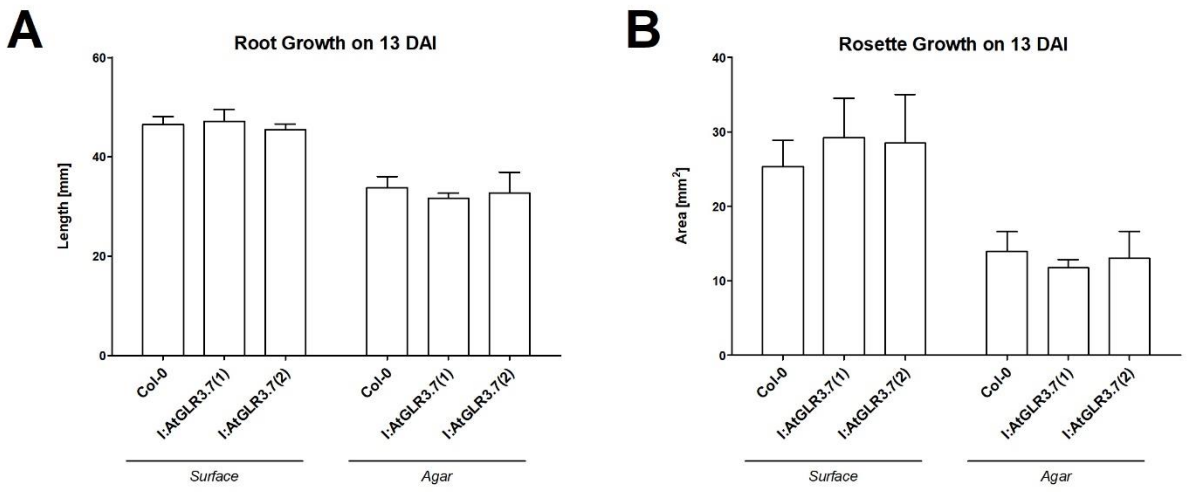

Figure 35. **Mock Treatment of I:AtGLR3.7 Arabidopsis Plant Lines.** Wildtype and transgenic *Arabidopsis thaliana* were grown in ½ MS agar without 17-β-estradiol until 13 DAI. Root length (A) and rosette size (B) were measured in the two transgenic plant lines (I:AtGLR3.7(1) and I:AtGLR3.7(2)) and Col-0 on 13 DAI. Error bars indicate SE.

7.5 D-Glutamate Treatment of Transgenic and Wildtype *Arabidopsis thaliana*

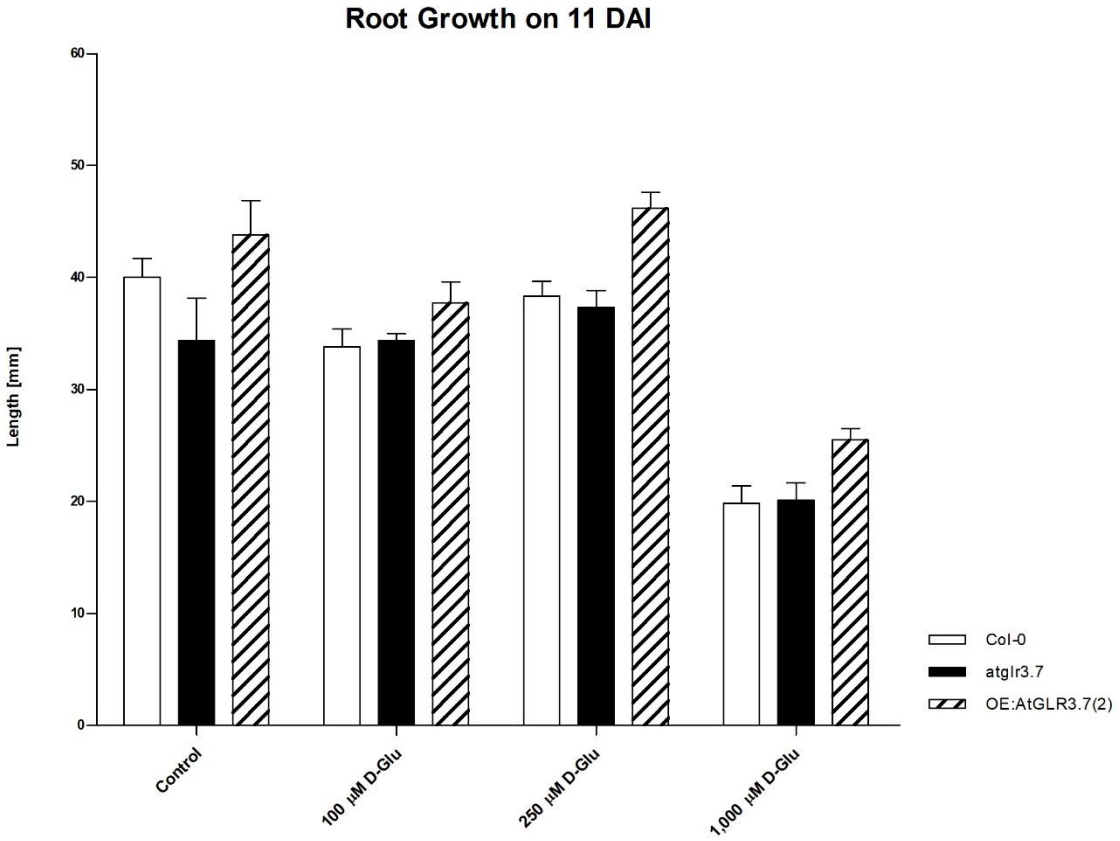

Figure 36. **Effect of D-Glutamate on Root Development on 11 DAI.** Wildtype and transgenic *Arabidopsis thaliana* were grown on ½ MS agar containing various D-glutamate concentrations (100, 250 and 1,000 µM) and a mock treatment (Control). Primary root length was determined for Col-0, atglr3.7 and OE:AtGLR3.7(2) on 11 DAI. Error bars indicate SE.

8 Appendices

Experimental data on DVD including:

- Files (Excel, Analyses software files)
- Images